MOLECULAR INTERACTIONS OF LATENT TRANSFORMING GROWTH FACTOR-β BINDING PROTEIN-2 (LTBP-2) WITH FIBRILLINS AND OTHER EXTRACELLULAR MATRIX MACROMOLECULES:

LTBP-2 COMPETES WITH LTBP-1 FOR BINDING TO FIBRILLIN-1 SUGGESTING THAT LTBP-2 MAY MODULATE LATENT TGF-β STORAGE

Rena M. Hirani

Discipline of Pathology
School of Medical Sciences, The University of Adelaide, Australia

MOLECULAR INTERACTIONS OF LATENT TRANSFORMING GROWTH FACTOR-β BINDING PROTEIN-2 (LTBP-2) WITH FIBRILLINS AND OTHER EXTRACELLULAR MATRIX MACROMOLECULES:

LTBP-2 COMPETES WITH LTBP-1 FOR BINDING TO FIBRILLIN-1 SUGGESTING THAT LTBP-2 MAY MODULATE LATENT TGF-β STORAGE

Rena M. Hirani

Submitted for the degree of Doctor of Philosophy (PhD) in August, 2006 with permission from the Faculty of Health Sciences, the University of Adelaide.

Supervisors: **Dr. Mark A. Gibson**
Dr. Eric Hanssen
Prof. Mark Bartold

ACADEMIC DISSERTATION

This work does not, to the best of my knowledge, contain any material previously published or written by another person except where due reference is given in the text and has not been previously presented as a component of any other academic course. This copy of my thesis may be made available by the University of Adelaide library for loan and photocopying.

Rena M. Hirani August 2006

Acknowledgements

There are many people to thank for the production of this thesis. It has been a long time in the making but I am grateful for the opportunity to complete this challenge. I extend a warm thanks to all my friends (they all know who they are) whom over the many years of my studies have kept me sane and shared all the great memories, pains and traditions of university life with me. I will hold many of you dear for life and sincerely hope that things go well for each and every one of you in all your future endeavours.

I thank the fantastic members, both past and present, of the Gibson lab and the discipline of Pathology who have been fantastic support to me every step of the way. You have all done so much and I have enjoyed every moment spent with you all. I would like to extend special thanks to Eric Hanssen for all his directional and supervisory advice; Betty Reinboth and Mahroo Parsi for their technical support, continual friendships and life-saving chocolate or ice-cream sessions; Emma Moore, Nigel Percy and Fan-Hing Hew for all their support, hard work and dedication during production of some of the recombinant fragments used during these studies and Ted Cleary for the many wonderful conversations and excellent insights he has given me throughout my candidature.

Finally, I would like to thank my principal supervisor, Dr. Mark Gibson for believing in my ability to conduct this PhD despite the many difficulties experienced by the lab during my candidature. I have enjoyed working with you immensely and I have learnt so much during my time in your lab. I thank you for all the fantastic guidance, advice, Friday night beer sessions and English football conversations through the years. I hope you continue to enjoy many more successes following the completion of my PhD.

I am also deeply in debt to my wonderful parents and family who have supported and encouraged me in every way possible. I would not have reached this stage of academia without them. I dedicate this thesis to my family as they have shaped all of my achievements and I cannot hope to pay them back in any way except to hope that the fantastic medical research that is currently conducted within various institutions in the world will help benefit them in every way possible.

Table of contents

Published Scientific Presentations

Poster and Oral presentation

2004 Matrix Biology Society of Australia and New Zealand (MBSANZ) annual scientific meeting, Perth, Western Australia.
Hirani, Rena M, Hanssen, Eric, Hew, Fan-Hing and Gibson, Mark
Binding studies of recombinant human LTBP-2 with elastic fibre components

Poster presentation

2005- Gordon Research Conference for Elastin and Elastic Fibres, Waterville Valley, New Hampshire, United States of America
Rena Hirani, Eric Hanssen and Mark A. Gibson
LTBP-2 competes with LTBP-1 for interaction with fibrillin-1

2005- Matrix Biology Society of Australia and New Zealand (MBSANZ) annual scientific meeting, Victor Harbor, South Australia
Rena Hirani, Eric Hanssen and Mark A. Gibson
LTBP-2 competes with LTBP-1 for interaction with fibrillin-1

2004 The Australian Society for Medical Research (AMSR) annual scientific meeting, South Australian Division, Adelaide
Rena Hirani, Eric Hanssen, Fan-Hing Hew and Mark A. Gibson
Binding studies of recombinant human LTBP-2 with elastic fibre components

2003 The Australian Society for Medical Research (AMSR) national scientific conference, Glenelg, South Australia
Rena Hirani, Eric Hanssen, Fan-Hing Hew and Mark A. Gibson
Mammalian expression of recombinant human LTBP-2 and specific binding to the N-terminal region of Fibrillin-1

2003 Matrix Biology Society of Australia and New Zealand (MBSANZ) annual scientific meeting, Acheron, Victoria, Australia
Hirani, RM, Hanssen, E and Gibson, MA
Mammalian expression of recombinant human LTBP-2

Awards arising from PhD candidature

2005/06- **Student representative** for the Matrix Biology Society of Australia and New Zealand

2005- **Dennis Lowther award** (student poster prize 2005) awarded by the Matrix Biology Society for Australia and New Zealand in Victor Harbor, South Australia

2005- **Travel Stipend** awarded by the Faculty of Health Sciences, the University of Adelaide to attend the Gordon Research Conference on Elastin and Elastic Fibres in New Hampshire, USA

2005- **Research Abroad Scholarship** awarded by the University of Adelaide to attend the Gordon Research Conference on Elastin and Elastic Fibres in New Hampshire, USA

2004/05- **Local organising committee** for the 2005 Matrix Biology Society of Australia and New Zealand (MBSANZ) South Australian meeting held in Victor Harbour

2004- **Travel award** awarded by the Sydney Tissue Engineering and Matrix (STEAM) organisation, New South Wales, Australia to attend the Matrix Biology Society of Australia and New Zealand (MBSANZ) annual meeting in Perth

Abbreviations

α-	alpha
β-	beta
Δ-	heat-deactivated (56^{o}C) or (in the case of DNA constructs) has meaning "with removal of"
8-Cys	8-cysteine containing motif, also known as TB (TGF-β binding protein like) domain and CR (cysteine-rich) domain
BCIP-	5-bromo-4-chloro-3-indolylphosphate toluidine salt
βIG-H3-	β-inducible gene-H3
BSA-	bovine albumin serum
BMPs-	bone morphogenetic proteins
C-	carboxy-terminus
Ca^{2+}-	calcium ions
$CaCl_2$-	calcium chloride
cbEGF-	calcium-binding epidermal growth factor-like
CCA-	Congenital Contractural Arachnodactyly
cDNA-	complementary deoxyribonucleic acid
Da-	Dalton
ddH_2O-	double distilled water
DMEM-	Dulbecco's Modification of Eagles Medium
DMSO-	dimethyl sulphoxide
DNA-	deoxyribonucleic acid
E-	embryonic day
ECM-	extracellular matrix
EDTA-	ethylenediaminetetraacetic acid (disodium salt)
EGF-	epidermal growth factor
EK-	enterokinase enzyme
ELISA-	enzyme-linked immunosorbent assay
EMILIN-	elastin-microfibril interface located protein
FBN-	fibrillin
FCS-	foetal calf serum
GAG-	glycosaminoglycan
GDFs-	growth and differentiation factors
HCl-	hydrochloric acid
HEK-	human embryonic kidney
his_6-tag-	6-histidine tag
hrs-	hours
IPTG-	Isopropyl β-D-1-thiogalactopyranoside
kb-	kilobase
kDa-	kiloDalton
LAP-	latency-associated protein
LLC-	large latent complex
LTBP-	latent TGF-β binding protein
m-	mouse
mRNA-	messenger RNA
MAGP-	microfibril-associated glycoprotein
MFAP-	small microfibril-associated protein
MFS-	Marfan syndrome
MMP-	matrix metalloprotease
N-	amino-terminus
NaCl-	sodium chloride
NBCS-	new born calf serum
NBT-	nitro-blue tetrazolium chloride
NEAA-	non-essential amino acids
Ni-	nickel
nm-	nanometers
NRS-	normal rabbit serum
OCT-	optimal cutting temperature compound

OMIM-	online Mendelian inheritance in man (http://www.ncbi.nlm.nih.gov/entrez/query.fcgi?db=OMIM)
PBS-	phosphate-buffered saline
PCR-	polymerase chain reaction
PO_4-	phosphate buffer
PVDF-	polyvinylidene difluoride
r-	recombinant
rb-	rabbit
RGD-	arginine-glycine-aspartic acid motif
RNA-	ribonucleic acid
RT-PCR-	reverse transcriptase-polymerase chain reaction
SCID-	severe combined immune deficiency
SDS-	sodium dodecylsulphate
SDS-PAGE-	sodium dodecylsulphate-polyacrylamide gel electrophoresis
SLC-	small latent complex
TGFBRI or II-	TGF-β type I and II receptors
TB-	TGF-β binding protein like domain, also known as 8-Cys (8-cysteine containing) motif and CR (cysteine-rich) domain
TBS-	tris-buffered saline
TGF-β-	transforming growth factor-β
TMB-	tetramethylbenezidine substrate
TTX-	tris/tween-20/triton X-100 buffer
U-	unit(s)
UTR-	untranslated region
V-	volts
v/v-	volume for volume
w/v-	weight for volume
WMS-	Weill-Marchesani Syndrome
x-	times
X-Gal-	5-bromo-4-chloro-3-indolylbeta-D-galactopyranoside

List of figures

1 Summary

Elastic fibres, a major component of many connective tissues, are composed of an amorphous elastin core surrounded by fibrillin-containing microfibrils. The function of these microfibrils appears to require the co-ordinated interactions of fibrillins with a range of extracellular matrix (ECM) macromolecules including, latent transforming growth factor-β (TGF-β) binding proteins (LTBPs). LTBPs share a high degree of structural similarity to fibrillins, since they both contain unique 8-cysteine motifs. Of the four members of the LTBP family, LTBPs-1, -3 and -4 covalently bind to latent forms of TGF-β. LTBP-1 has been shown to interact with the N-terminal domains of fibrillin-1 and –2 and LTBP-4 interacts with the N-terminal domains of fibrillin-1, suggesting that fibrillin-containing microfibrils may act as TGF-β stores and localise latent TGF-β complexes to the ECM. LTBP-2 differs from other members of the LTBP family since it does not covalently bind latent TGF-β. However, LTBP-2 strongly co-localises with fibrillin-containing microfibrils in a number of tissues suggesting that LTBP-2 could have a structural role associated with these elements presumably independent of TGF-β storage, or could act to mediate specific microfibril-ECM interactions. To understand more about the function of LTBP-2, this study involved screening for potentially important molecular interactions of LTBP-2 with fibrillins and a variety of ECM proteins.

Human recombinant LTBP-2 (r-LTBP-2) was cloned, expressed and purified using a mammalian cell culture system. Solid phase binding assays were used to screen for interactions between r-LTBP-2 and continguous fragments of fibrillin-1 and –2 as well as MAGPs, tropoelastin, collagens and proteoglycans. A cation dependant interaction was found between the C-terminal domains of LTBP-2 and the N-terminal domains of fibrillin-1, but not with the analogous region of fibrillin-2. Thus, LTBP-2 seems to have an exclusive role associated with fibrillin-1-containing microfibrils. Further studies found that the C-terminal region of LTBP-2 competes with LTBP-1 for binding to fibrillin-1, suggesting that the binding site for LTBP-2 on fibrillin-1 is the same or in close proximity to that for LTBP-1.

Immunohistochemical analysis of LTBP-1 and -2 within developing human aorta indicated that both LTBPs co-localised with fibrillin-1. However, the two LTBPs did have distinct distribution patterns in relation to each other, in that LTBP-2 was found throughout the medial layer whereas LTBP-1 was mainly located in patches of the outer medial layer. No regions of strong co-localisation of the two LTBPs were found. Thus, these findings suggest that LTBP-2 could indirectly modulate the presence of TGF-β upon the fibrillin-containing microfibrils by competing for binding with the LTBP-1/TGF-β complex to these structures.

Other binding studies showed a cation independent interaction between r-LTBP-2 and an as yet unidentified component of a crude bovine collagen-IV extract. Since collagen-IV is a major component of basement membranes, an interaction between r-LTBP-2 and a protein within this bovine collagen-IV preparation suggests LTBP-2 may have a further function involving a basement membrane component. It will be interesting to determine if LTBP-2 acts as a bridging molecule between basement membrane structures and fibrillin-containing microfibrils or if it has another function independent of these microfibrils.

2 The extracellular matrix (ECM) and its components

The extracellular matrix (ECM) of connective tissues is a complex composite material made up of insoluble fibres, microfibrils and a wide range of soluble proteins and glycoproteins that are capable of self-assembly. The ECM conveys mechanical and physiochemical properties to tissues and provides a scaffold for cell attachment and migration. The insoluble fibres resist tensile forces and the interfibrillar polymers inflate the fibrous network, thus providing resistance to compressive forces but still allowing diffusion of small molecules into and out of the tissue (reviewed by Bosman and Stamenkovic, 2003). The ECM exerts a regulatory role in promoting or maintaining cellular differentiation and phenotypic expression and also appears to serve as a reservoir for growth factor cytokines (reviewed by Rosso *et al.*, 2004).

Since different tissues have unique functional requirements, the composition of the ECM varies between tissues and is reflected by differential patterns of transcription, mRNA splicing and altered post-translational processing of the ECM macromolecules. The physical structure of a particular matrix has the potential to provide specific biological information to cells which in turn can impart regulatory information resulting in altered cell functions and can act as a mechanical scaffold for cell adhesion and migration (reviewed by Bateman *et al.*, 1996; Bissell and Barcellos-Hoff, 1987; Rosso *et al.*, 2004). The binding of growth factors to specific ECM components may also provide a mechanism for the local control of cellular behaviour, indicating that the role for each ECM molecule is sophisticated and highly specific (Yamaguchi *et al.*, 1990).

The major structural element of connective tissues and the most abundant insoluble proteins of the ECM are the collagen protein superfamily. Collagens-I and -III are the most abundant collagen proteins and form the long fibre bundles seen in many tissues (reviewed by Bateman *et al.*, 1996; Kielty and Grant, 2002). The various types of collagens share the same basic structural motif of three polypeptide chains wound around in a characteristic triple helical configuration. They differ in the way they form different supramolecular assemblies; collagens-I, -II, -III, -V and -XI are fibril-forming, collagens-IX (Piez *et al.*, 1963), -XII, -XIV and -XVI are fibril-associated collagens (Broek *et al.*, 1985). There are also non-fibrillar collagens like the short-chain collagens-VIII and –X (Yamaguchi *et al.*, 1991); anchoring fibril collagen-VII (Keene *et al.*, 1987) and collagen-VI (Chu *et al.*, 1988) which forms extensive microfibrils in the ECM of virtually all connective tissues. Collagen-VI has a short triple helical domain with very large terminal globular domains (reviewed by Timpl and Chu, 1994).

The primary structural element of basement membranes is collagen-IV, which is chemically and structurally distinct from the other collagens listed above (Kefalides, 1973). Basement membranes are sheet-like extracellular matrices, which underlay almost all epithelia and

endothelia, they surround many cell types including skeletal and smooth muscle cells. Basement membranes support and compartmentalise soft tissue structures and also serve as selective barriers to permeability (Keilty and Grant, 2002; Iozzo, 2005). Collagen-IV has six gene products that associate to form distinct networks but do not assemble into fibrillar structures (reviewed by Yurchenco and Schittny, 1990). A series of kinks occur within the triple helical domain, which arise due to imperfections in the Gly-X-Y sequence. The most abundant form of collagen-IV exists as heterotrimers with two α1(IV) and one α2(IV) chain (reviewed by Kielty and Grant, 2002; Hudson *et al.*, 1993).

Other important constituents that contribute to the functional and biological characteristics of individual connective tissues include; proteoglycans, hyaluronan, elastin, fibronectin, thrombospondin and microfibrillar-associated components. Extracellular proteoglycans provide tissues with elastic resilience against compressive forces and organise collagenous fibres and networks. Proteoglycans are a distinct subset of non-collagenous glycoproteins containing glycosaminoglycan (GAG) side chains. Some proteoglycans, such as decorin or biglycan, can be expressed as isoforms either with or without GAG chains (Johnstone *et al.* 1993). Many proteoglycans interact *via* their GAGs with soluble signalling molecules to facilitate appropriate cellular responses (reviewed by Aumailley and Gayraud, 1998). An example is the interaction between basic fibroblast growth factors to the GAG side-chains of heparan sulphate proteoglycans (reviewed by Ramirez and Rifkin, 2003). Binding of basic fibroblast growth factors to heparan sulphate increases the local concentration of these proteins to levels required for signalling, receptor dimerisation and signal transduction. Heparan sulphate also protects the growth factors from degradation by extracellular proteases (Bernfield *et al.*, 1999; Rapraeger, 2002; Schlessinger *et al.*, 2000). The GAG hyaluronan is important in tissues such as cartilage, vitreous and skin for regulating cell-matrix interactions and activation of chemokines, enzymes and growth factors (reviewed by Taylor and Gallo, 2006). Non-collagenous adhesive glycoproteins such as fibronectin, laminin, tenascin and entactin contribute to the stability of the ECM and may potentially function to bridge the ECM with neighbouring cells. The relative ratio of collagenous and proteoglycan components are generally considered to be key determinants of the mechanical properties needed by many tissues to fulfil their biological functions. A tissue such as tendon, which needs to be resistant to extension, is comprised primarily of tough collagen fibres, whereas tissues like cartilage must be resistant to compression and therefore contain at least 50% proteoglycan (reviewed by Wiesmann, 2002).

Fibronectin (Pytela *et al.*, 1985; Tamkun *et al.*, 1985), collagen (reviewed by Gullberg and Lundgren-Akerlund, 2002) and laminin (reviewed by Aumailley *et al.*, 2003), have been shown to act as ligands for various integrins and other cell surface receptors. Integrins mediate cell-matrix and cell-cell interactions and play important roles in many biological processes such as wound

healing, maintenance of tissue integrity, cell growth and survival. Integrins are heterodimeric transmembrane receptors consisting of α and β subunits. Eight β and seventeen α chains are currently known and the formation of differential α and β heterodimers enables a degree of ligand specificity for a range of cell types (reviewed by Hynes, 1992; Hynes, 2002).

Molecular interactions with the matrix are integral to connective tissue structure and function. Tissues that need to be rigid and resistant to deformation, such as bone, achieve this function by combining calcium salts and collagen fibres. Tissues such as aorta and lung, where elastic recoil is a crucial feature of their function, have collagen-containing fibrils accompanied by elastic fibres containing the protein elastin (reviewed by Rosenbloom and Abrams, 2002). Elastic fibres are composed of a number of extracellular matrix macromolecules and interactions between these various components are essential for elastic fibre function, which if disrupted have been shown to be implicated in several heritable connective tissue disorders.

2.1 Elastic fibres

2.1.1 Amorphous Elastin

Elastic resilience and the structural integrity of lungs, skin and large blood vessels of vertebrate animals is dependent on the correct assembly of elastic fibres. Elastic fibres contain the amorphous "rubber-like" protein, elastin, which is surrounded by a network of 10- to 12-nm glycoprotein-containing microfibrils (**figure 2.1**) (reviewed by Cleary and Gibson, 1996; Kielty *et al.*, 2002a; Kielty *et al.*, 2002b). Elastin is found only in the warm-blooded members of the vertebrate kingdom and has a characteristic chemical composition rich in glycine, proline and hydrophobic amino acids (Sandberg *et al.*, 1981).

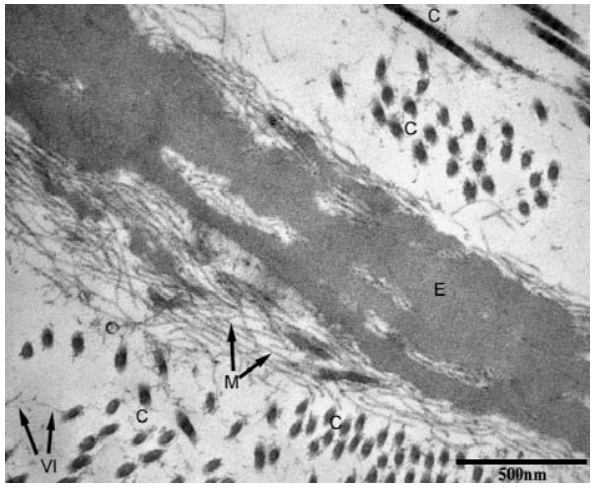

Figure 2.1. Electron micrograph of elastic fibre structure. The image was obtained using nuchal ligamentum tissue from a 210-day bovine. The amorphous elastin core (E) is surrounded by microfibrils (M); some microfibrils are interspersed within the amorphous core. Collagen type-VI microfibrils (VI) and interstitial collagen (C) type-I and -III fibrils are also visible. Scale bar 500nm. Image courtesy of Hanssen, E., 2003.

The 72kDa biosynthetic precursor of elastin, tropoelastin, exhibits a modular domain structure consisting of repeating hydrophobic sequences, which contribute to the elasticity of the molecule, and lysine-rich regions that are involved in intra- and intermolecular cross-linking (Indik *et al.*, 1989; Kozel *et al.*, 2003). Cross-linking of tropoelastin monomers into an elastic network is initiated when the ε-amino groups of lysine residues become oxidised by the copper-requiring enzyme lysyl oxidase (Kagan *et*

al., 1986; Pinnell and Martin, 1968). Subsequent non-enzymatic condensation of modified and unmodified lysines then forms cross-links specific to insoluble elastin. Correct cross-linking is essential for elastin function since the polymer requires properties that allow large extensions to be produced with the exertion of small forces (reviewed by Kozel *et al.*, 2003). The importance of cross-linking is further demonstrated by the weak and mechanically compromised elastic tissue associated with lathyrism, copper deficiency and Menkes syndrome (OMIM #309400). These conditions occur due to reduced amounts of, or the loss-of-activity of, lysyl oxidase (reviewed by Christiano and Uitto, 1994). Furthermore, two further inherited diseases, autosomal dominant cutis laxa (OMIM #219200) and supravalvular aortic stenosis (OMIM #185500), have been linked to mutations within the elastin gene that may alter the ability of the elastin precursor to undergo normal assembly (Milewicz *et al.*, 2000).

Regulation of the elastin gene during development is complex and sensitive to a number of growth factors, hormones, vitamins and cytokines, during processes such as tissue development, inflammation and wound healing. Some factors, such as transforming growth factor-β (TGF-β), have been found to stimulate elastin gene expression (Marigo *et al.*, 1993; Marigo *et al.*, 1994). The TGF-β signalling pathway, stimulates the activity of lysyl oxidase and appears to stabilise elastin mRNA through the activation of Smad-7, which controls downstream signalling after binding to serine/threonine kinase receptors (Kucich *et al.*, 2002; Shanley *et al.*, 1997; Smith-Mungo and Kagan, 1998). This intricate elastin deposition system is also further controlled by the presence of fibrillin-containing microfibrils where the proportion of microfibrils associated with elastic fibres is greatest during late foetal and early post-natal development and subsequently diminishes with age (Cleary and Gibson, 1983).

2.1.2 Microfibrils

In elastic tissues, such as lung, skin and aorta, preformed bundles of fibrillin-containing microfibrils are deposited before the amorphous elastin core of an elastic fibre. Thus, the microfibrils appear to act as a template for tropoelastin deposition during elastic fibre formation and are retained as an outer mantle of mature elastic fibres (**figure 2.2**) (Fahrenbach *et al.*, 1966; Greenlee *et al.*, 1966). The components and exact mechanisms involved with forming these complex elastic fibres is an active area of research. There has been evidence to suggest that microfibrillar components such as, fibrillins (Sakai *et al.*, 1991), heparin/heparan sulphate proteoglycans (Cain *et al.*, 2005), fibulin (Freeman *et al.*, 2005) and microfibril-associated glycoproteins (MAGPs) (Bashir *et al.*, 1994) are involved in elastic fibre formation and some of these components have been shown to interact with tropoelastin and/or have the potential for

forming a network of molecular bridges for elastin deposition (Brown-Augsburger *et al.*, 1994; Clarke and Weiss, 2004; Finnis and Gibson, 1997; Gibson and Cleary, 1987; Tsuruga *et al.*, 2005).

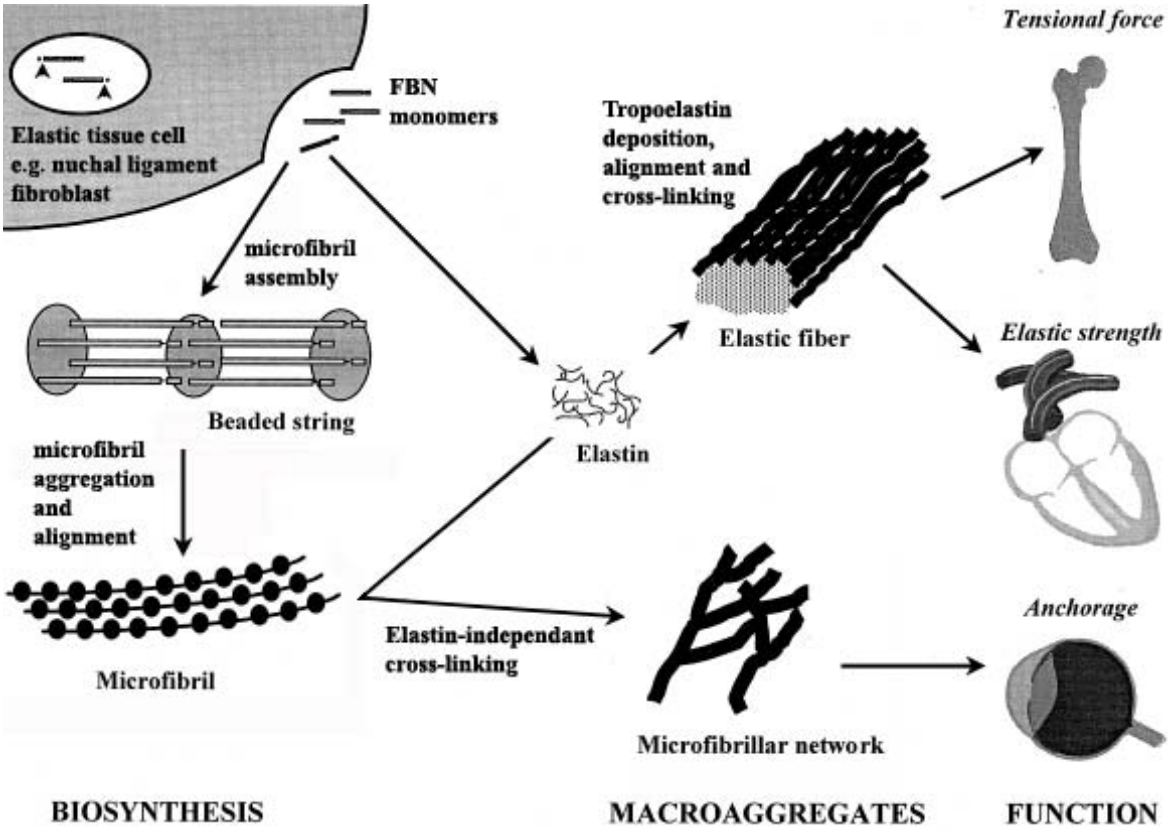

Figure 2.2. Schematic representation of the model for the formation of elastic fibres. Elastic tissue cells secrete microfibrillar components and the elastin precursor protein, tropoelastin. The microfibrils are synthesised, by mechanisms yet to be uncovered, into the 'beads-on-a-string' arrangement. Individual microfibrils are then aligned into bundles. Tropoelastin is deposited onto the microfibrils and a polymer is formed *via* the activity of the copper-requiring enzyme lysyl oxidase. Cross-linked elastin then functions within tissues such as the heart to provide elastic strength or within bone structures to provide tensional properties. Microfibrils can also form elastin-free networks, which function within some tissues such as the ocular ciliary zonules to anchor the lens of the eye in position. Diagram adapted from Ramirez and Pereira, 1999.

Microfibril arrays are also abundantly found in tissues devoid of elastin, such as the ocular ciliary zonules, which are structures that hold the lens in dynamic equilibrium (**figure 2.3**) (reviewed by Ashworth *et al.*, 2000). The precise role of microfibrils is not defined, but they may regulate the development of, and confer strength and elasticity to, connective tissues. The formation of elastin-associated fibrillin-containing microfibrils and elastin-free microfibrils required in specific tissues must be regulated by distinct molecular mechanisms that result in the differential spatiotemporal expression of elastic fibre related proteins during development.

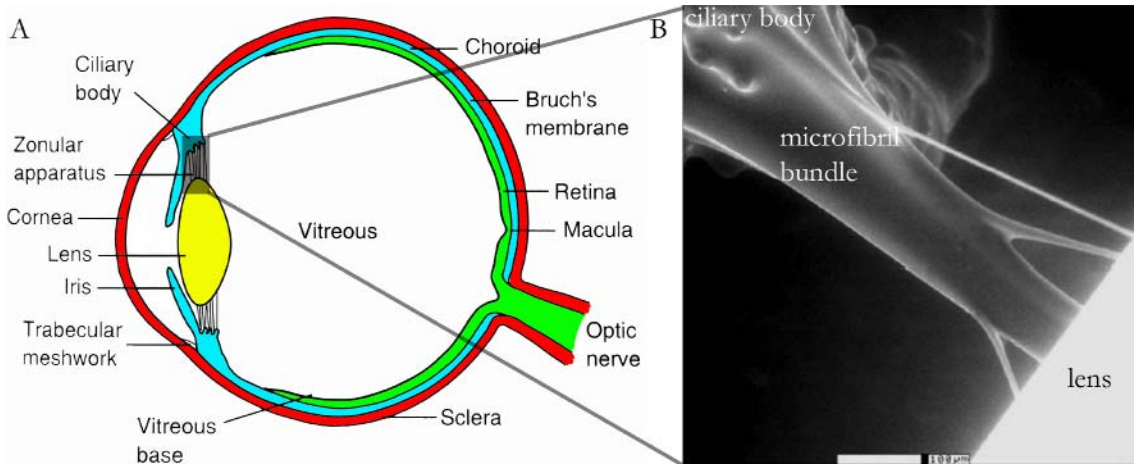

Figure 2.3. Elastin free microfibrils present within the zonular apparatus of the eye. *A,* Schematic representation of a human eye. The lens of the eye is held in suspension by the zonular apparatus, which extend out from the ciliary body. Elastin-free microfibrils formed within the ciliary body anchor the zonular apparatus to the lens allowing the lens to expand and contract as necessary. *B,* Zonular apparatus viewed using ESEM. The image is of hydrated ciliary zonule filaments composed of fibrillin-rich microfibrils. Zonular fibres are observed to branch prior to insertion into the lens capsule. Scale bars indicate 100µm. Images adapted from Mayne, 2002 and Sherratt *et al.*, 2001.

2.1.3 Fibrillins

Fibrillins have been identified as the ubiquitous component of the 10-12nm elastin-associated microfibrils found within connective tissues. Three members of the fibrillin family, fibrillins-1, -2 and -3, have been identified. Fibrillin-1 (350kDa) and a closely related glycoprotein fibrillin-2 are both extended linear molecules with a high cysteine content and have been identified with microfibrils as components of elastic fibres and in elastin-free bundles (Gibson *et al.*, 1989; Maddox *et al.*, 1989; Sakai *et al.*, 1991; Sakai *et al.*, 1986; Zhang *et al.*, 1994). Fibrillin-1 has widespread expression patterns within the extracellular matrices of a large range of tissues; including skin, lung, kidney, vasculature, cartilage, tendon, muscle, cornea, and ocular ciliary zonules during various stages of development (Sakai *et al.*, 1986). In contrast to fibrillin-1, fibrillin-2 has expression that is restricted to foetal tissues (Zhang *et al.*, 1994; Zhang *et al.*, 1995). Fibrillin-3 has high structural similarity to fibrillins-1 and -2, however, it has only recently been cloned and its function within elastic fibre biology is yet to be determined (Nagase *et al.*, 2001). *FBN3* gene orthologs have been identified in human, bovine and chick, but the gene appears to be inactivate in mouse and rat. It has been shown that *FBN3* expression, like that for fibrillin-2, is limited to foetal tissues such as developing skeletal elements (including digits, vertebrae, ribs and skull), skin, lung, kidney and skeletal muscle, and contrary to the other fibrillins, *FBN3* expression was shown to be highest in brain (Corson *et al.*, 2004).

Even though fibrillin-1 and -2 have distinct but overlapping spatiotemporal tissue distributions, it has been shown that these fibrillins can occur in the same individual microfibril in certain tissues and both fibrillins can copolymerise in the same fibroblast cultures (Charbonneau *et al.*, 2003). These findings indicate that the molecular information required to direct the formation of fibrillin-1- and fibrillin-2-containing microfibrils is similar for both fibrillins. Gene targeting experiments in mice demonstrate that neither fibrillin is essential for embryogenesis or development since both fibrillin-1 and –2 null mice are viable and fertile. In the absence of one fibrillin, microfibrils and elastic fibres are still assembled indicating that there exists a molecular basis for compensation of one fibrillin by the other during development (Atteaga-Solis *et al.*, 2001; Chaudhry *et al.*, 2001; Pereira *et al.*, 1997). It is also possible that the role for each fibrillin is still quite distinct where it has been suggested that fibrillin-1 may provide force bearing or structural support for tissues whereas fibrillin-2 may be involved with the initiation of elastinogenesis (Ramirez and Pereira, 1999).

The complex ultrastructure of fibrillin-containing microfibrils isolated from elastic tissues makes connecting their biomechanical function to their structural assembly difficult. Early microscopy studies highlighted some distinctive staining characteristics of microfibrils that indicated a strongly anionic nature (Cleary and Gibson, 1983; Cleary and Gibson, 1996). Rotary shadowing and negative staining, extensively used to examine isolated microfibrils, have since revealed a 'beads-on-a-string' arrangement with an average periodicity of around 56 nm and apparent diameter of 10-12 nm, indicating that fibrillin occurs as ordered aggregates within these structures (**figure 2.4**) (Keene *et al.*, 1991; Wallace *et al.*, 1991). It is unclear if fibrillin monomers are aligned in a register or staggered array within microfibrils, and the correlation between the molecular structure of fibrillin in relation to the beaded filament morphology is yet to be elucidated. It has been proposed that fibrillins form dimers prior to assembly into microfibrils and an association between the overlapping carboxy and amino termini of adjacent fibrillin molecules allows linear growth of the microfibril, stabilised by intramolecular crosslinks (Ashworth *et al.*, 1999a; Ashworth *et al.*, 1999b; Qian and Glanville, 1997; Trask *et al.*, 1999). This complex intramolecular folding of fibrillin molecules has been suggested to be driven by favourable hydrophobic and electrostatic interactions (Baldock *et al.*, 2001; Lu *et al.*, 2005). Antibody localisation has also suggested that a head-to-tail parallel unstaggered arrangement of fibrillin molecules occurs within

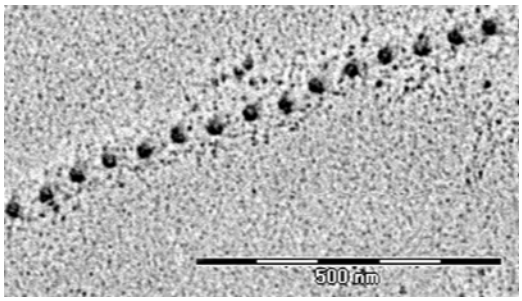

Figure 2.4. Electron micrograph image of a fibrillin-containing microfibril after rotary shadowing. The microfibril has a structure that resembles a 'beads-on-a-string' arrangement. Scale bar 500nm. Image courtesy of Hanssen, E. 2003

microfibrils (Baldock *et al.*, 2001; Reinhardt *et al.*, 1996a). Fibrillin polymers have been shown to form a structural scaffold of extensible microfibrils that are arranged into parallel bundles (Sakai *et al.*, 1986; Wright *et al.*, 1994). A one-third staggered arrangement could also be possible, which was proposed since electron microscopy and mass mapping of isolated microfibrils suggested eight molecules are present in a single cross-section slice of a microfibril (Baldock *et al.*, 2001; Davis, 1994; Lee *et al.*, 2004; Wallace *et al.*, 1991).

Fibrillin isoforms have highly homologous primary structures, being large glycoproteins composed of multiple domains dominated by 43 calcium-binding epidermal growth factor (cbEGF)-like binding domains, 4 non-calcium-binding EGF-like domains, 8-cysteine (8-Cys)-containing motifs and hybrid modules (**figure 2.5**) (Corson *et al.*, 1993; Downing *et al.*, 1996; Maslen *et al.*, 1991; Pereira *et al.*, 1993; Zhang *et al.*, 1994). In contrast to fibrillins-1 and -2, fibrillin-3 mRNA is alternatively spliced to remove the exon encoding cbEGF2 and has three alternate exons in the 5' untranslated region (UTR) (Charbonneau *et al.*, 2004; Corson *et al.*, 2004).

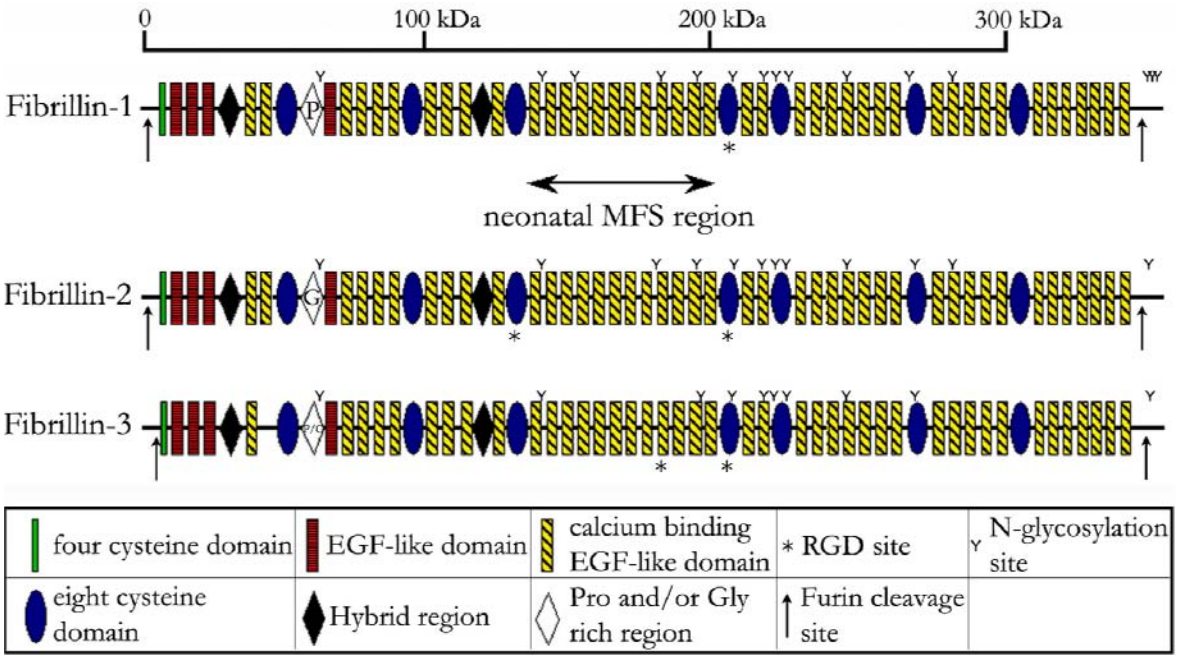

Figure 2.5. Schematic representation of domain modules found in fibrillin. These proteins contain many calcium-binding EGF-like (cbEGF) repeats interspersed with seven 8-cysteine containing motifs. Fibrillin-3 differs from fibrillin-1 and -2 in that cbEGF2 is not present and it has a mixture of proline and glycine residues within its 'hinge-like' region. The arrow indicates the region of fibrillin-1 that has been found to contain sequences, which if mutated, often result in neonatally lethal Marfan syndrome.

The 47 EGF-like domains distributed throughout the fibrillin molecules have a degree of homology to motifs found within the EGF precursor (Corson *et al.*, 1993; Pereira *et al.*, 1993). EGF-like domains are commonly found in many other extracellular matrix components, blood coagulation factors (for example, factor IX) (Giannelli *et al.*, 1998) and developmentally important proteins (for example, Notch) (Kidd *et al.*, 1986). They are independently folding modules characterised by six highly conserved cysteine residues and connected by disulphide bonds in a 1-3, 2-4, 5-6 arrangement which stabilise the folding of the domain (**figure 2.6**) (Handford *et al.*, 1991). The calcium-binding EGF motifs are arranged in tandem arrays and contain consensus sequences for hydroxylation of a specific asparagine or aspartate residue and calcium binding (Corson *et al.*, 1993; Pereira *et al.*, 1993; Smallridge *et al.*, 1999).

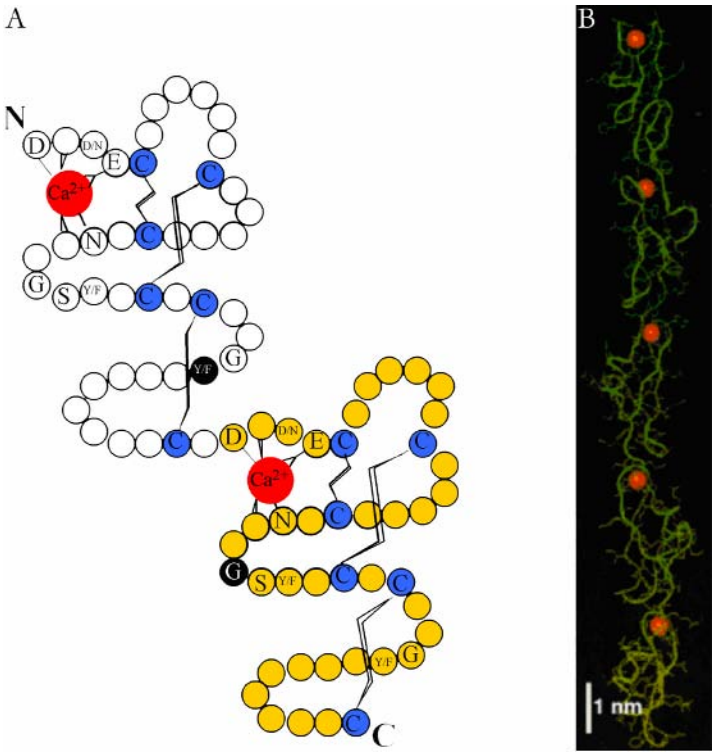

Figure 2.6. Diagrammatic representation of fibrillin calcium binding EGF-like domains. *A,* This two dimensional schematic represents two cbEGF-like domains, highlighting the residues that interact with the calcium ions or form the disulphide bonds to determine the spatial conformation of the domains. The calcium ions are represented in red and the cysteine residues are in blue. *B,* Three-dimensional representation of a row of five cbEGF domains. The domains have a linear conformation and provides the rod-like structural arrangement of the fibrillins. The calcium ion is represented in red (scale bar 1nm). Images adapted from Downing *et al.*, 1996.

The bound calcium appears to be essential to perform key structural roles, including restricting interdomain flexibility, facilitating protein-protein interactions and protecting modules against proteolytic cleavage (Downing *et al.*, 1996; Handford *et al.*, 1991; Reinhardt *et al.*, 1997; Werner *et al.*, 2000). The middle of the fibrillin molecules contains the longest stretch of 12 cbEGF repeats which forms a rigid rod-like conformation that has been confirmed by rotary shadow analysis and is predicted to have an important role in microfibril assembly (Reinhardt *et al.*, 1997; Sakai *et al.*, 1991). Crystal structures have revealed that the integrin-binding fragment, cbEGF22-8-Cys4-cbEGF23, of human fibrillin-1 is a Ca^{2+} ion-dependant rigidified pyramid and it is possible that other cbEGF pairs could form similar structures (Lee *et al.*, 2004). Mutations in fibrillin-1 or -2 that affect calcium binding may increase protein susceptibility to proteolytic

degradation, since the reduced level of calcium binding could introduce conformational changes that expose protease cleavage sites. Mutations found to affect the integrity of cbEGF domains appear to have significance in the human syndromes including; Marfan syndrome and congenital contractural arachnodactyly (Reinhardt *et al.*, 1997; Suk *et al.*, 2004).

The cbEGF domains of the fibrillins are interspersed with a single motif containing 9-cysteine residues (unique to fibrillins), two hybrid domains and seven examples of 8-cysteine-containing motifs (8-Cys), found exclusively in fibrillins and a family of related proteins known as the latent transforming growth factor-β binding proteins (LTBPs) (see section 2.3.6). The 8-Cys motifs, also known as TGF-β-binding (TB) modules, are structurally similar to the 9-cysteine motif, however they contain a unique triple cysteine peptide (CCC) sequence (Kanzaki *et al.*, 1990; Sinha *et al.*, 2002). 8-Cys motifs fold to form a globular conformation, where the cysteine residues appear to stabilise and strengthen the protein (**figure 2.7**) (Hubmacher *et al.*, 2005; Hutchinson *et al.*, 2005; Yuan *et al.*, 1997). A single RGD integrin recognition sequence is found in one of the 8-Cys motifs of fibrillins-1 and -3 but there are two 8-Cys motifs within fibrillin-2 with RGD sequences (Corson *et al.*, 1993; Lee *et al.*, 1991). The RGD sequence present in the fourth 8-Cys motif of fibrillin-1 appears to mediate interactions of fibrillin-1 with the integrins α5β1 and αvβ3. It has been proposed that through such interactions with integrins, fibrillin proteins may influence cell behaviour and mediate cell-to-matrix interactions (Bax *et al.*, 2003; Sakamoto *et al.*, 1996).

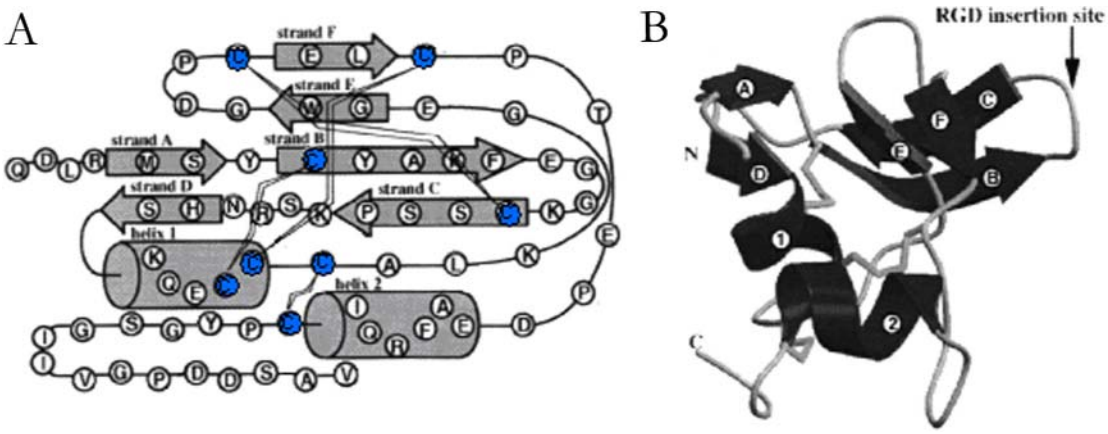

Figure 2.7. Diagrammatic representation of the 8-Cys domains found exclusively in fibrillin and LTBPs. *A,* Two-dimensional diagram of the 8-Cys domain with disulphide bonds positioned to form the globular conformation. The eight cysteine residues are represented in blue. *B,* Three-dimensional protein structure model of the 8-Cys domain. The letters represent the β-sheets whereas the numbers are the α-helices present within the structure. The RGD sequence used for cell interactions and glycosylation of the protein is also indicated. Diagram adapted from Yuan *et al.*, 1997.

Fibrillin-1 has a unique 58 amino acid proline-rich region towards the amino terminus, which is thought to act as a 'hinge-like' region. In contrast, this motif in fibrillin-2 is replaced by a glycine-rich sequence and in fibrillin-3 it contains a mixture of proline and glycine residues (Corson *et al.*, 2004; Lee *et al.*, 1991). The 'hinge-like' region of fibrillin-1 is sensitive to protease digestion since it contains this larger number of proline and positively charged residues but since this region of fibrillin-2 contains multiple glycine residues it is not as sensitive to pepsin digestion. Thus, the sensitivity of different fibrillin-containing microfibrils to proteolytic degradation could be important for their function (Maddox *et al.*, 1989; Zhang *et al.*, 1994).

The hinge region may also be important for the formation of fibrillin dimers during microfibril assembly. Studies have shown that the N-terminal region of fibrillin-1 readily aggregates *in vitro* forming homodimers, which become stabilised with covalent disulphide linkages (Reinhardt *et al.*, 2000; Trask *et al.*, 1999). Recombinantly expressed N-terminal fragments of fibrillin-1 tend to dimerise in solution and the N- and C-terminal regions of fibrillin-1 interact strongly with each other, but no other homotypic interactions have been detected (Ashworth *et al.*, 1999a; Lin *et al.*, 2002; Marson *et al.*, 2005; Trask *et al.*, 1999). In contrast, the N- and C-terminal regions of fibrillin-2 do not appear to interact with each other. Thus, it may be that fibrillins can directly interact in an N- to C-terminal fashion to form homotypic fibrillin-1 or heterotypic fibrillin-1/fibrillin-2 microfibrils but not homotypic fibrillin-2-containining microfibrils (Ashworth *et al.*, 1999b; Lin *et al.*, 2002). It is possible that fibrillin-2 can assemble into an as yet unidentified form of supramolecular aggregate or form homotypic microfibrils by alternative mechanisms using molecular adapters, or fibrillin-2 may form heterotypic microfibrils with fibrillin-3, which is also expressed within foetal tissues (Lin *et al.*, 2002; Nagase *et al.*, 2001; Quondamatteo *et al.*, 2002; Zhang *et al.*, 1994).

Subtle differences in the composition of fibrillin-containing microfibrils appear to influence the roles of these structures in different elastic tissues. The N-terminal region of fibrillin-1 is highly interactive and has been shown to bind fibulin-2 (Reinhardt *et al.*, 1996b), LTBPs-1, and -4 (Isogai *et al.*, 2003), microfibril-associated glycoprotein-1 and -2 (MAGP-1 and -2, (Hanssen *et al.*, 2004; Jensen *et al.*, 2001) and tropoelastin (Rock *et al.*, 2004) (see below for further details). The importance of the correct formation of fibrillin-containing microfibrils is further highlighted since mutations found to occur in the genes for human fibrillin-1 (*FBN1*) (15q21.1) and -2 (*FBN2)* (5q23-q31) have been linked to the human congenital disorders, Marfan syndrome (MFS) and congenital contractural arachnodactyly (CCA), respectively (Dietz *et al.*, 1991; Lee *et al.*, 1991; Magenis *et al.*, 1991; Maslen and Glanville, 1993; Putnam *et al.*, 1995). Further detail on human conditions linked to fibrillin-containing microfibrils and their function is given in the following section.

2.2 Heritable connective tissue disorders linked to fibrillin function

2.2.1 Marfan Syndrome (MFS) and Congenital Contractural Arachnodactyly (CCA)

Marfan syndrome (MFS) (OMIM #154700) is an inherited, autosomal dominant disorder that affects the skeletal, ocular and cardiovascular systems. This systemic connective tissue disorder occurs with a frequency of at least one person in ten thousand live births. However, since a number of cases remain undiagnosed or misdiagnosed, the prevalence of MFS remains difficult to determine precisely. The disease displays high penetrance and wide clinical variability both within and between families, therefore a patient may have mild to severe symptoms that may or may not correlate with other affected family members. The skeletal abnormalities are the most readily recognisable phenotype of the disease. There is long bone overgrowth resulting in an unusually tall, thin individual with disproportionately long extremities and weakened musculatures. Arachnodactyly, or long fingers and toes, are hallmarks of MFS patients. A number of overgrowths can also occur within the ribs (**figure 2.8**) (Pyeritz and Dietz, 2002).

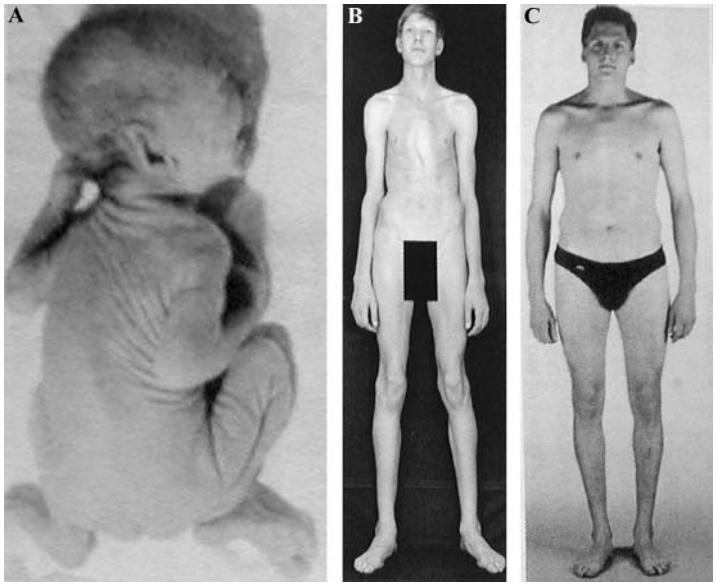

Figure 2.8. Examples of Marfan syndrome phenotypes. *A,* A week old baby displaying severe neonatal forms of MFS. Note the wrinkled appearance and the large soft ears alongside contractures of the hip, elbow, wrist and knee joints. *B,* A 15-year-old boy displaying classic MFS phenotypes of unusually tall stature, older facial appearance, long limbs, poorly developed musculature and asymmetric pigeon breast. *C,* 28-year-old man with no apparent external signs of MFS, however the patient has aortic dilation and both eye lenses are luxated. Images adapted from Pyeritz and Dietz, 2002.

MFS can severely affect the eyes resulting in the dislocation of the ocular lens (ectopia lentis) and a tendency for retinal detachment. Ectopia lentis occurs due to weakened suspensory ligaments that hold the lens in dynamic equilibrium. These ligaments are comprised of ciliary

ocular zonules containing elastin-free bundles of fibrillin-1-containing microfibrils (**figure 2.3** and **2.9**) (reviewed by Ashworth *et al.*, 2000).

The deadliest aspect of the MFS disease arises from cardiovascular defects. Progressive dilatation of the aorta can occur resulting in premature death from the rupture of an aortic aneurysm. Untreated, the disease can mean that a patient's life span is reduced by 30-40%. Treatments range from the prophylactic use of β-blockers to reduce the risk of aortic aneurysms, to surgical intervention for severe cases.

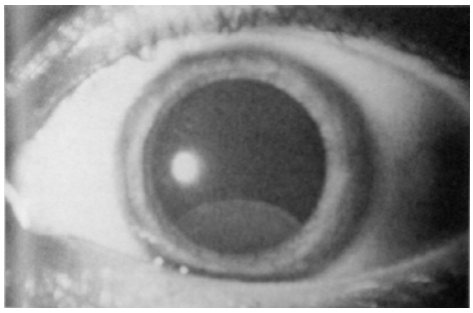

Figure 2.9. An example of Ectopia lentis. There is downward dislocation of the lens. Image obtained from Pyeritz and Dietz, 2002.

In the early 1990s, the MFS disease gene was mapped to the same chromosomal position as the *FBN1* gene. Genetic linkage between *FBN1* and the Marfan phenotype was established, and a number of MFS patients were shown to have mutations within *FBN1* (reviewed by Judge and Dietz, 2005). The pleiotropic nature of Marfan syndrome, where a single gene defect results in multiple system failure, has been of great interest to researchers. Evidence presented to date suggests that the one potential pathogenic mechanism could be a dominant negative effect of a mutant fibrillin-1 protein on microfibril assembly. As mentioned previously, the biochemical pathway of fibrillin-1 assembly into microfibrils is poorly understood, and as a consequence the mechanism by which mutations in *FBN1* result in disease is unclear. It has been suggested that a critical threshold of native fibrillin-1 protein is required to form functioning microfibrils within elastic tissues. In addition, if mutations are introduced within *FBN1* that result in mutant fibrillin protein being integrated into microfibrils, then the function of these microfibrils within the extracellular matrix could be compromised. This requirement of a critical level of native fibrillin-1 has been further demonstrated using mice that were engineered to express reduced levels of native fibrillin-1. These fibrillin-1 deficient mice demonstrated MFS-like phenotypes (Pereira *et al.*, 1997; Pereira *et al.*, 1999; Ramirez *et al.*, 1999).

Many of the mutations causing MFS are missense mutations that affect the conserved cysteine residues within the cbEGF domains and the 8-Cys motifs, and these mutations are predicted to cause misfolding of these domains resulting in protein instability. Substitution of other key structural residues, such as the highly conserved glycines, may also cause a misfold in the cbEGF and 8-Cys domains resulting in overall protein instability. A genotype-phenotype correlation has not been established between MFS and the fibrillin-1 gene, apart from a cluster of mutations in a region corresponding to exons 24-32 of *FBN1*, encoding an 8-Cys motif and cbEGF domains 11-18. Mutations in these regions are associated with the severe neonatal form

of MFS (**figure 2.5**) but they may also result in milder phenotypes including classic MFS (Kainulainen *et al.*, 1994; Putnam *et al.*, 1996; Tiecke *et al.*, 2001).

Some cysteine and glycine mutations have been studied in great detail as they have been found to be some of the most prominent mutations in MFS patients. Recombinant fragments of fibrillin-1 containing the missense mutations C1117Y and C1129Y accumulate within the cell, indicating that these mutations affect trafficking of the fibrillin-1 protein from the fibroblast cells to extracellular sites for microfibril assembly (Whiteman and Handford, 2003). Fibrillin protein containing these mutations undergo minimal levels of glycosylation and lack the complex glycosylation observed in the secreted wild-type molecules, suggesting the mutant protein remains retained in the endoplasmic reticulum. This suggests that disease associated with these missense mutations is caused either by an intracellular dominant negative effect or haploinsufficiency (Whiteman and Handford, 2003). In contrast, another missense mutation, G1127S, causes a moderate change in the folding of a cbEGF domain but does not affect protein trafficking or glycosylation in any way that is distinguishable from the wild-type fragment. Since expression of the recombinant fragments with this mutation does not disrupt the secretion of endogenous fibrillin-1 by the cell, it is suggested that G1127S causes disease *via* an extracellular dominant negative effect (Whiteman and Handford, 2003). Furthermore, it has been shown that human dermal fibroblasts incubated with recombinant fibrillin-1 fragments containing the integrin-binding RGD motif, induces up-regulation of matrix metalloproteinases (MMP)-1 and -3. Thus, fibrillin fragments themselves could have pathogenic effects leading to the up-regulation of MMPs, which may induce progressive breakdown of microfibrils, resulting in MFS (Booms *et al.*, 2005).

Recently, it has also been shown that the loss of fibrillin-1-containing microfibrils in MFS leads to multiple phenotypic features that may result from TGF-β activation. Specifically it was shown that mice deficient in fibrillin-1 show marked dysregulation of TGF-β activation and signalling, resulting in apoptosis within the developing lung (Neptune *et al.*, 2003). This aberrant TGF-β activation could occur since LTBPs-1, -3 and -4 are covalently bound to latent inactive forms of TGF-β. TGF-β-bound LTBPs have been shown to interact with fibrillins, where this interaction has been suggested to influence the activation of TGF-β (Isogai *et al.*, 2003). If the fibrillins are mutated such that there is a loss of interaction between the fibrillins and LTBP, this may result in aberrant TGF-β activation.

Further evidence to support the theory for the importance of TGF-β in MFS has recently been demonstrated within a subset of MFS patients, who have negative *FBN1* gene screening, but have been shown to have defects in the TGF-β binding receptor II (*TGFBRII*) gene (Disabella *et al.*, 2006). TGFBRII belongs to the serine–threonine kinase family of cell surface receptors, which regulate several cellular processes, including proliferation, cell cycle arrest,

apoptosis, differentiation and formation of the ECM (Disabella *et al.*, 2006; Mizuguchi *et al.*, 2004; Ng *et al.*, 2004). The version of MFS caused by TGFBRII defects is currently known as MFS2 (OMIM #154705). These patients display autosomal dominant MFS with major cardio-skeletal signs, including thoracic aortic aneurysms and dissection but appear to lack ectopia lentis. The genotyped cases studied to date are too low for exact confirmation that ectopia lentis is absent in MFS2 patients, however this study does highlight the importance for correct localisation and function of TGF-β in MFS cases (Disabella *et al.*, 2006).

There are several genetic disorders with related phenotypic characteristics to MFS. Congenital contractural arachnodactyly (CCA) (OMIM #121050) is the autosomal condition initially described in 1896 by a Parisian Professor of Paediatrics, Antoine-Bernard Marfan (Marfan, 1896). Marfan syndrome was mistaken for Marfans' original description since both disorders have striking similarities in skeletal abnormalities and display considerable clinical variability (**figure 2.10**). However, patients with CCA feature congenital joint contractures and deformed ears, which are not found in MFS and do not exhibit the ocular and cardiovascular abnormalities that are associated with MFS (**figure 2.10**) (Anderson *et al.*, 1984; Beals and Hecht, 1971; Hecht and Beals, 1972; Ramos-Arroyo *et al.*, 1985). In the early 1990s, CCA was linked to a gene on chromosome 5, which was later found to be the *FBN2* gene (5q23-q31) (Lee *et al.*, 1991; Putnam *et al.*, 1995). Interestingly the CCA mutations were found to mainly occur in exons 24-34 of *FBN2* (Gupta *et al.*, 2002; Park *et al.*, 1998). The generation of fibrillin-2 (*FBN2*)-null mice using gene targeting was found to result in a phenotype analogous to that seen in patients with CCA. A limb-patterning defect in the form of bilateral syndactyly and digit fusion was found in both soft and hard tissues. These defects are associated with a disorganised matrix (Atteaga-Solis *et al.*, 2001). Heterozygous *FBN2* mice were found to have contractures of the small and large joints that resolved a few days after birth (Atteaga-Solis *et al.*, 2001).

It is likely that the mechanism for the cause of CCA phenotypes is similar to MFS, but with a less severe and more limited effect due to the restricted spatiotemporal expression of fibrillin-2. For example, ocular lens dislocations are not found in patients with CCA since fibrillin-2 is not expressed within zonular structures of the eye, whereas fibrillin-1 is highly expressed in these structures and when mutated in MFS patients results in ectopia lentis (Sherratt *et al.*, 2001; Wright *et al.*, 1994).

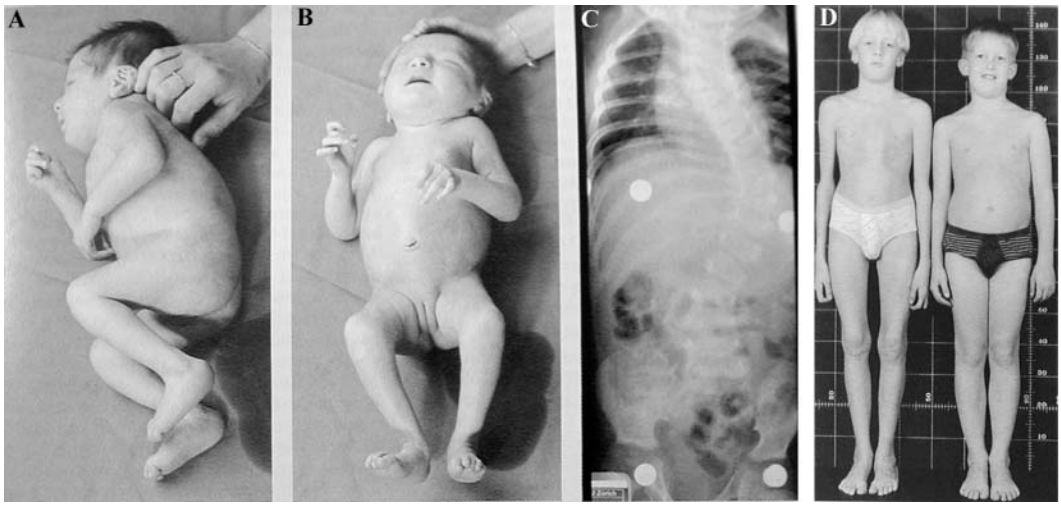

Figure 2.10. Examples of patients affected by the connective tissue disorder, congenital contractural arachnodactyly (CCA). A baby girl suffering from CCA just after birth where crumpled ears, joint contractures, arachnodactyly and scoliosis were noted. *A* and *B*, baby girl after 10 days of corrective procedures, contractures of the knees, hips, elbows and fingers with crumpled ears still present. *C,* Radiograph at four months showing severe scoliosis despite bracing. *D,* 9-year-old boy with CCA (left), and his healthy dizygotic twin brother (right). The patient exhibits an asymmetric rib cage and contractures of the fingers and elbows. Images adapted from Pyeritz and Dietz, 2002.

2.2.2 Homocystinuria

Homocystinuria (OMIM #236200) is an autosomal recessive inborn error of methionine metabolism, which results in raised serum levels of the highly reactive thiol-containing amino acid homocysteine. Cystathionine β-synthase catalyses the vitamin B6-dependent conversion of homocysteine to cystathionine in the trans-sulphuration pathway for the synthesis of cysteine. Cystathionine β-synthase deficiency is the most common cause of homocystinuria and homocystinurics often display phenotypic abnormalities similar to MFS patients. Since the phenotypes between these two diseases are similar it has been suggested that alterations in the function of fibrillin-1 could result in homocystinuria (Majors and Pyeritz, 2000). Indeed when arterial smooth muscle cells were cultured under conditions of cysteine deficiency, it was found that fibrillin-1 deposition into the ECM was diminished. However, when cysteine levels were returned to normal, the smooth muscle cells began to accumulate a matrix rich in fibrillin-1 (Majors and Pyeritz, 2000).

Studies have shown that the increased levels of homocysteine cause the cysteine bonds within the cbEGF domains of fibrillin-1 to be reduced using *in vitro* assays. This cysteine disruption causes misfolding of the cbEGF domains and makes it more susceptible to proteolytic attack and prevents deposition of fibrillin-1 into the ECM (Hubmacher *et al.*, 2005). Further studies indicated that disruption of the cysteine bonds prevents calcium binding to the cbEGF domains. Calcium is required for stabilisation and protection against homocysteine attack. The

effects of homocysteine may not be unique to fibrillin-1, and other cbEGF-containing proteins, such as LTBPs, could be implicated in pathogenic mechanisms underlying homocystinuria (Hubmacher *et al.*, 2005; Hutchinson *et al.*, 2005).

2.2.3 Weill-Marchesani Syndrome (WMS)

Weill-Marchesani syndrome (WMS) is a connective tissue disorder characterised by short stature, brachydactyly, joint stiffness, and characteristic eye anomalies including microspherophakia, ectopia of the lenses (the lens is usually round and abnormally small), severe myopia, and glaucoma (Faivre *et al.*, 2002). The autosomal dominant disease locus had consistent linkage to chromosome 15q21.1 (OMIM #608328). In a WMS patient, the fibrillin-1 gene was sequenced and an in-frame deletion within the sequence encoding for the LTBP-1 binding site within the fibrillin-1 gene was discovered. This suggests that autosomal dominant WMS and MFS are allelic conditions at the fibrillin-1 locus (Faivre *et al.*, 2003). The recessive disease locus was mapped to chromosome 19p13.3-p13.2 (OMIM #277600), a region where fibrillin-3 was also mapped. Fibrillin-3 is abundant within the eye and skeletal regions, thus fibrillin-3 could be a candidate gene for WMS (Corson *et al.*, 2004; Faivre *et al.*, 2002). In further support of the hypothesis of fibrillin-3 being a candidate gene in WMS, studies were conducted to determine if MFS-causing mutations were present within exons of the fibrillin-3 gene (*FBN3*) (Uyeda *et al.*, 2004). The MFS patients studied to date do not appear to have mutations within *FBN3*, thus if MFS-causing mutations were to be found within the fibrillin-3 gene they would be extremely rare (Uyeda *et al.*, 2004).

The above findings indicate that fibrillins perform regulatory roles important for skeletal growth, however an interesting question does arise with regard to MFS patients having tall stature and arachnodactyly but WMS patients having short stature and brachydactyly. If fibrillin-1 is involved with both syndromes, then how is it that the symptoms differ to such contrasts. It is possible that differences in the macromolecular composition of microfibrils in specific tissues could result in different physical manifestations. The macromolecular composition of microfibrils is an area of current research and a number of candidate microfibril-associated proteins have been studied. It is possible that these molecules could contribute to the manifestation of human syndromes linked to fibrillin-containing microfibrils and details on these candidate molecules is given below.

2.3 Other microfibril associated components

Fibrillin-containing microfibrils isolated from elastic tissues have been found to have a complex ultrastructure suggesting that they may be composed of several macromolecules (**figure**

2.4) (Keene *et al.*, 1991). This myriad of proteins may function to provide structural support for formation of the microfibrils; mediate interactions between adjacent microfibrils within microfibril bundles; assist in the assembly of elastin onto the surface of microfibrils; act as an interface between the microfibrils and other extracellular matrix elements and modulate interactions of microfibrils with cells to influence deposition; orientation and organisation of fibrillin-containing microfibrils and elastic fibres in different tissue environments or allowing specific interactions between other types of microfibrils (e.g. collagen-VI microfibrils) or enzymes such as lysyl oxidase (reviewed by Gibson, 2004). Several candidate extracellular matrix macromolecules have been found to be associated with, or influence the function of, fibrillin-containing microfibrils and a brief outline of a select few have been given below, with specific focus on latent transforming growth factor-β binding proteins (LTBPs), which form the basis of this research project.

2.3.1 Microfibril-Associated Glycoproteins (MAGPs)

The first of several candidate microfibrillar proteins to have been isolated, characterised and cloned, was the small molecular weight (31kDa) microfibril-associated glycoprotein-1 (MAGP-1) (Gibson *et al.*, 1986; Gibson *et al.*, 1991). MAGP-1 was first identified as a component of an elastic fibre rich tissue, bovine nuchal ligament. MAGP-1 contains two structurally distinct regions; the amino terminal half of the protein is rich in glutamine, proline and acidic amino acids, whereas the carboxyl-terminal half contains 13 cysteine residues and most of the basic amino acids (Frankfater *et al.*, 2000; Gibson *et al.*, 1996; Gibson *et al.*, 1991; Hatzinikolas and Gibson, 1998; Segade *et al.*, 2000). MAGP-1 localises to microfibril beads and is probably disulphide bonded to microfibrils since reduction is required for its extraction (Gibson *et al.*, 1986; Henderson *et al.*, 1996)

A structurally related molecule, MAGP-2 (approximately 25kDa) was also later identified (Gibson *et al.*, 1996). MAGP-2 is rich in serine and threonine residues and contains an RGD cell-binding motif through which it binds to a number of cell types *via* the integrin αvβ3 (Gibson *et al.*, 1999). However, MAGP-2 does have a more limited spatiotemporal tissue expression than MAGP-1 since MAGP-2 does not appear to be associated with microfibrils from the ocular zonules, medial layer of the aorta and within other tissues thus suggesting MAGP-2 has a function related to cell signalling during microfibril assembly and elastinogenesis (Gibson *et al.*, 1998; Gibson *et al.*, 1999; Hanssen *et al.*, 2004; Henderson *et al.*, 1996; Jensen *et al.*, 2001; Kitahama *et al.*, 2000; Trask *et al.*, 2000; Weber *et al.*, 2004; Werneck *et al.*, 2004).

MAGPs have been found to be an integral component of some populations of fibrillin-containing microfibrils. It has been suggested that the MAGPs may act as a

tropoelastin-binding protein present on the surface of microfibrils and may function as molecular cross-linkers and stabilise fibrillin monomers in folded conformation within or between the microfibrils (Brown-Augsburger *et al.*, 1994; Tsuruga *et al.*, 2005). MAGPs have also been found to interact with fibrillins and the tissue distribution patterns of both MAGPs are very similar to those of fibrillins in a number of tissues (Hanssen *et al.*, 2004). MAGPs have periodic distribution along the beaded microfibril structure, indicating MAGPs have a structural role within fibrillin-containing microfibrils.

MAGPs also appear to be involved in a number of other roles that may be distinct from, or complement, its role as a microfibrillar structural protein. Yeast-2-hybrid and co-immunoprecipitation experiments indicated a strong interaction between MAGP-2 and the EGF-like repeats of Jagged1, which activates the Notch signalling pathway enabling cellular differentiation (Nehring *et al.*, 2005). Further demonstration of the importance of MAGPs in the Notch signalling pathway was found when the C-terminal domains of MAGPs-1 and -2 interacted with the EGF-like repeats of Notch1, which led to both cell surface release of the Notch1 extracellular domain and activation of the intracellular Notch signalling pathway (Miyamoto *et al.*, 2006). More recently, MAGP-1 could have an important vascular development role. Altered expression of MAGP-1 in *magp1* morphant zebrafish embryos results in these morphant embryos exhibiting vessel dilation and altered vessel wall architecture and vein branching (Chen *et al.*, 2006). The authors suggest that a specific level of MAGP protein is critical for correct vascular development and if this level is not present then the associated integrin function is compromised, with the resultant reduction in integrin/matrix interactions being the main mechanism for vascular defects in these *magp1* morphants (Chen *et al.*, 2006).

2.3.2 Small Microfibril-Associated Proteins (MFAPs)

Other small microfibril components that have been identified and named microfibril-associated proteins (MFAPs). There are 5 MFAP proteins, of which, MFAP-2 is also known as MAGP-1 and MFAP-5 is MAGP-2 and have already been discussed in detail above (Faraco *et al.*, 1995; Gibson *et al.*, 1986; Strausberg *et al.*, 2002).

MFAP-1, a 54kDa protein was localised to microfibrils in several tissues, including the zonule fibres. The human gene for MFAP-1 has been characterised and mapped close to the fibrillin-1 gene locus on chromosome 15 (15q15-q21) (Lui *et al.*, 1997; Yeh *et al.*, 1994). MFAP-1 has a large amount of glutamic acid residues (~22%) that may serve as sites for interaction with tropoelastin (Horrigan *et al.*, 1992; Yeh *et al.*, 1994).

MFAP-3, a 31kDa serine rich protein is localised to zonular microfibrils and developing nuchal ligament. Northern blotting has indicated that the protein is also expressed in foetal aorta

and lung tissues (Abrams *et al.*, 1995). The gene contains only two exons and is mapped to chromosome 5q32-q33.2, which is close to the locus for the fibrillin-2 gene, *FBN2*. It is unknown if the similar chromosomal and tissue localisations of MFAP-1 and -3 to the fibrillins are functionally significant, and further studies will be required to establish their exact roles in microfibril assembly.

MFAP-4, a 29kDa protein showed ultrastructural localisation to microfibrils surrounding elastin fibres in aorta, skin and spleen. The protein appears not to be associated with elastin-free microfibrils in the ocular zonule and kidney (Kobayashi *et al.*, 1994; Kobayashi *et al.*, 1989; Toyoshima *et al.*, 2005; Toyoshima *et al.*, 1999; Zhao *et al.*, 1995). Cell adhesive proteins often contain the peptide sequence Arg-Gly-Asp-Ser or Arg-Gly-Asp-Ala (Chen and Doolittle, 1971; Pierschbacher and Ruoslahti, 1984). The amino acid sequence Arg-Gly-Asp-Ala is included in the N-terminal region of MFAP-3, thus suggesting that MFAP-3 is an adhesive protein that mediates cell-to-cell and cell-to-matrix interactions (Kobayashi *et al.*, 1989; Lawler and Hynes, 1986; Pierschbacher and Ruoslahti, 1984).

2.3.3 Proteoglycans

A number of proteoglycans have been identified that are associated with developing elastic fibres in tissues such as skin, aorta and ocular zonule microfibrils (Baccarani-Contri *et al.*, 1985; Baccarani-Contri *et al.*, 1990; Bartholomew and Anderson, 1983; Chan and Choi, 1995; Chan *et al.*, 1997; Fornieri *et al.*, 1987; Pasquali-Ronchetti and Baccarani-Contri, 1997). Immunohistochemical studies on human skin have suggested that two small dermatan sulphate proteoglycans, decorin and biglycan, are closely associated with the elastin component of elastic tissue (Baccarani-Contri *et al.*, 1990; Pasquali-Ronchetti and Baccarani-Contri, 1997). Decorin has been shown to bind tropoelastin *in vitro* suggesting that this proteoglycan may be involved in elastic fibre assembly (Reinboth *et al.*, 2000). It has also been proposed that decorin may direct assembly and co-ordination of individual microfibrils into bundles (Kielty *et al.*, 1996; Trask *et al.*, 2000).

The biglycan core protein has been shown to bind, using *in vitro* binding studies, to tropoelastin and MAGP-1 and it has been postulated that these three macromolecules could form a ternary complex *in vivo*. Biglycan may act to assist MAGP-1 in deposition of tropoelastin onto the surface of the microfibrils during elastinogenesis or stabilise the mature elastic fibre, perhaps by facilitating interactions between surrounding matrix elements (Reinboth *et al.*, 2002; Reinboth *et al.*, 2000). In contrast, decorin does not have the affinity to bind to MAGP-1. Thus this differential binding could point to decorin and biglycan fulfilling distinct functions during elastic fibre formation (Reinboth *et al.*, 2002).

Even though evidence suggests that decorin and biglycan play a significant role in microfibril and elastic fibre biology, decorin or biglycan null mice show no obvious elastic fibre abnormalities, but do present interesting new animal models for musculoskeletal diseases (Danielson *et al.*, 1997; Xu *et al.*, 1998; Young *et al.*, 2002). Decorin/biglycan double knockout mice resulted in viable animals with smaller stature, thinner skin and more severe osteopenia than the single biglycan or decorin knockout mice but also did not show major elastic fibre abnormalities (Young *et al.*, 2002). Since all these mice were viable with unaffected elastic fibres, the role of decorin and biglycan may have a degree of redundancy or substitution by other related macromolecules in their elastic fibre related functions.

The large chondroitin sulfate proteoglycan, versican, was found to ultrastructurally localise with fibrillin-containing microfibrils in skin (Zimmermann *et al.*, 1994). It was found the interaction between fibrillin-1 and versican was calcium dependant and the covalent binding to specific fibrillin-1 polypeptides occurred *via* the C-terminal lectin domains of versican (Isogai *et al.*, 2002). The potential binding site for versican appears to be between cbEGF domains 11 and 21 of fibrillin-1. Human mutations within this region can result in severe forms of neonatal MFS (Isogai *et al.*, 2002). This finding indicates that the association between this proteoglycan and fibrillin-containing microfibrils could be functionally important.

Heparin/heparan sulphate has been shown to have an essential role in the formation of fibrillin-containing microfibrils. Heparan sulphate is an anionic polymer composed of 50-200 disaccharide units covalently attached to specific proteins to form proteoglycans at the cell surface (e.g. syndecans) or in the ECM (e.g. perlecan) (reviewed by Kramer and Yost, 2003). Heparin is distinguished from heparan sulphate since it contains a large number of dissaccharides modified with *N*- and *O*-sulphation along its entire length, instead of being clustered as predominantly found in heparan sulphate. There are four heparin/heparan sulphate binding sites on fibrillin-1 and these binding sites were found to occur in regions commonly mutated in MFS patients (Cain *et al.*, 2005; Tiedemann *et al.*, 2001). It was shown using heparin oligosaccharides, which are analogous to the S-domains of heparan sulphate, that heparin does not inhibit fibrillin-1 N- and C-terminal interactions or RGD-mediated cell attachment but did compete with MAGP-1 for binding to the N-terminal region of fibrillin-1 and with tropoelastin for a central fibrillin-1 sequence (Cain *et al.*, 2005). Since heparin/heparan sulphate competes with MAGP-1 and tropoelastin for binding to fibrillin, the spatiotemporal regulation of each of these components in relation to each other may be a key factor during formation of fibrillin-containing microfibrils and elastic fibre assembly (Cain *et al.*, 2005).

2.3.4 Fibulins

The fibulin family consists of five distinct rod-like proteins containing multiple endothelial growth factor (EGF)-like repeat motifs and a globular C-terminal domain (Argraves *et al.*, 1990; Giltay *et al.*, 1999; Pan *et al.*, 1993). Each member of the fibulin family has a distinct distribution in tissues. Fibulin-1 (100kDa) is found in plasma and the ECM of a variety of tissues, where it is associated with several structures including the elastin core of elastic fibres (Kluge *et al.*, 1990; Roark *et al.*, 1995). Fibulin-1 has been located within the amorphous core of elastic fibres but not in fibrillin-containing microfibrils (Kostka *et al.*, 2001).

Fibulin-2 (195kDa) and the N-terminal region of fibrillin-1 interact and co-localise in skin (except adjacent to the dermal-epithelial junction), perichondrium, elastic intima of blood vessels and kidney glomerulus and does not appear to be present in ciliary zonules, tendon, lung alveoli and kidney tubules (Reinhardt *et al.*, 1996b). Fibulin-2 was found preferentially at the interface between microfibrils and the amorphous elastin core, suggesting the *in vivo* interaction between fibulin-2 and fibrillin-1 could be regulated by cellular expression and elastin deposition from other protein-protein interactions (Reinhardt *et al.*, 1996b). Fibulin-2 does not appear to have a role in microfibril integrity since it is absent from tissues subject to strong tensional forces (such as tendon and ciliary zonules). However, both fibulin-1 and -2 have been shown to bind to a range of matrix macromolecules, and have been shown to associate with tropoelastin and other elastic fibre components (Roark *et al.*, 1995; Sasaki *et al.*, 1999; Timpl *et al.*, 2003). It has also been suggested that fibulin-2 may have a role in attaching microfibrils to elastin and to basement membranes or in elastic fibre deposition and cell migration (Sasaki *et al.*, 1999; Tsuda *et al.*, 2001).

Fibulin-3 and -4 are similar to fibulins-1 and –2 in sequence and domain organisation. Fibulins-3 and –4 differ from fibulin-1 and –2 since they are prominently found in vessel walls of large elastic arteries to capillaries of several organs including; skeletal muscle and heart (Giltay *et al.*, 1999). Potential roles of fibulin-3 and -4 during elastic fibre assembly remain to be further investigated.

Fibulin-5 is a calcium-dependant, elastin-binding protein that localises to the surface of elastic fibres *in vivo* (Nakamura *et al.*, 2002; Yanagisawa *et al.*, 2002). Targeted disruption of the *fibulin-5* gene in mice has demonstrated that this fibulin is highly involved in elastic fibre assembly. The gene knockout resulted in severe disorganisation of the elastic fibre structures throughout the body. Fibulin-5 has been shown to interact with tropoelastin (Yanagisawa *et al.*, 2002), fibrillin-1 (Freeman *et al.*, 2005) and several integrins *in vitro* (Nakamura *et al.*, 2002), and it may have critical roles in the anchorage of elastic fibres to cells during elastic fibre development and/or in providing a link between tropoelastin and microfibrils in the pericellular space during elastic fibre assembly. Fibulin-5 also appears to be a gene target for TGF-β signalling (Schiemann

et al., 2002). Thus fibulin-5 may regulate cell growth and motility and may be a contributor to tumour development in humans.

2.3.5 Miscellaneous Proteins

The EMILIN family consists of two matrix glycoproteins, EMILIN-1 and -2 (Colombatti *et al.*, 2000). EMILIN-1 (115kDa) has been immunolocalised to the interface between the microfibrils and the elastin core of developing elastic fibres (Colombatti *et al.*, 1988). The molecule appears to form homotrimers and larger disulphide-bonded multimers (Doliana *et al.*, 1999). EMILIN-1 may have a role in elastic fibre formation, in anchoring smooth muscles cells to elastic fibres or in regulation of blood vessel assembly (Colombatti *et al.*, 2000). EMILIN-2 is similar in structure to EMILIN-1 and the two proteins have overlapping but distinct tissue localisations. EMILIN-1 has been shown to interact with EMILIN-2 *via* the C-terminal domains and to possess cell adhesive properties (reviewed by Colombatti *et al.*, 2000).

Mice deficient in EMILIN-1 have normal life spans, are fertile and don't exhibit gross morphological abnormalities. However, there are alterations in the structure of the elastic fibres and cell morphology in elastic arteries. It was shown that since EMILIN-1 binds elastin and fibulin-5 that the association of fibulin-5 with elastin is altered in the absence of EMILIN-1. The authors suggest that EMILIN-1 stabilises elastic fibres and influences cells behaviour (Zanetti *et al.*, 2004). More recently, studies conducted with the *Emilin1* knockout mice indicate that these mice display increased blood pressure, peripheral vascular resistance and reduced vessel size (Zacchigna *et al.*, 2006; Zanetti *et al.*, 2004). EMILIN-1 was found to inhibit TGF-β signalling by binding to the latent TGF-β and preventing its maturation by furin convertases in the ECM (Zacchigna *et al.*, 2006). Furthermore, genetic inactivation of *Emilin1* causes increased blood pressure due to increased TGF-β signalling in the vascular wall (Zacchigna *et al.*, 2006). Thus these findings indicate that EMILIN-1 may be a modulator of TGF-β function.

Other proteins that could be involved with the formation and function of microfibrils include the cross-linking enzyme lysyl oxidase and a 67kDa cell surface elastin-binding protein (Hinek, 1996; Smith-Mungo and Kagan, 1998). Lysyl oxidase (32kDa) has been localised very closely to the elastin-associated microfibrils in developing elastic tissues. This indicates a potentially important role of the interaction of lysyl oxidase with other microfibrillar components during tropoelastin deposition onto the microfibril scaffold (Kagan *et al.*, 1986). The activation and regulation of processing the lysyl oxidase pre-proprotein into the mature and active enzyme is influenced by TGF-β, indicating the importance of the role of TGF-β for influencing the synthesis and development of elastic fibres (Boak *et al.*, 1994; Roy *et al.*, 1996).

The cell surface associated elastin binding protein appears to have a role in tropoelastin secretion and assembly into elastic fibres (Hinek, 1996; Mecham *et al.*, 1991). The binding protein appears to be bound to tropoelastin intracellularly and then accompanies the elastin precursor to the extracellular side of the plasma membrane. It is then suggested that tropoelastin remains bound to the 67kDa protein until there is an interaction with a microfibril-associated galactoside sugar which induces the transfer of the tropoelastin onto an acceptor site on the microfibril (Mecham *et al.*, 1991). The identity of the microfibril component is unknown but there is potential for fibrillin-1 and/or MAGP-1 involvement as both proteins are rich in galactosamine and are known to bind to tropoelastin.

2.3.6 Transforming Growth Factor-β (TGF-β) and LTBPs

As mentioned previously, latent transforming growth factor-β binding proteins (LTBPs) share a high degree of structural similarity with fibrillins and since LTBPs form the basis of the research topic for this thesis they are discussed further here. LTBPs-1, -3 and –4 form covalent complexes with latent forms of TGF-βs, which are a potent multifunctional superfamily of cytokines consisting of more than 30 different genes. Distinctive subfamilies of the TGF-β superfamily include; TGF-βs, activins/inhibins, bone morphogenetic proteins (BMPs) and growth and differentiation factors (GDFs). These growth factor families exert a variety of effects on mammalian cells such as, growth, differentiation, wound healing, adhesion, migration and the capacity for matrix synthesis (Kingsley, 1994; Massague, 1990; Quaglino *et al.*, 1991).

The TGF-β superfamily consists of three mammalian isoforms (TGF-β1, TGF-β2 and TGF-β3), which are dimeric and multipotent growth modulators with numerous roles in tissue development, morphogenesis and homeostasis within a variety of mammalian cell types (Ignotz and Massague, 1986; Roberts *et al.*, 1986). The major sources of the TGF-β growth factor are platelets, bone and serum (reviewed by Massague, 1990). The effect of TGF-β varies between tissues since TGF-β can act as a growth promoting factor in some cells, such as smooth muscle cells and mesodermal cells, but can also act as a growth inhibitor in other cells, for example lung epithelial cells and keratinocytes (Massague, 1990; Nishio and Wantanabe, 1997; Siese *et al.*, 1999). Remodelling of the ECM may be associated with the release of matrix-bound growth factor signalling molecules, such as TGF-β, as well as the activation of specific matrix metalloproteases (MMPs) and serine proteases (reviewed by Wu and Werb, 2000). It has been shown that cell-surface localised matrix metalloproteinase-2 and -9 modify intracellular cell signalling for tissue remodelling by activating latent forms of TGF-β (Yu and Stamenkovic, 2000).

The importance of TGF-β isoforms is demonstrated by analysis of knockout mice. Half of the mice born with a TGF-β1 gene deficiency die before birth due to defects during

vasculogenesis and hematopoiesis where the remaining viable pups die shortly after weaning. It seems likely that a maternal supply of TGF-β1 is likely to contribute to the development of the postnatal mice (Christ *et al.*, 1994; Dickson *et al.*, 1995; Diebold *et al.*, 1995; Kulkarni *et al.*, 1993; Shull *et al.*, 1992). TGF-β2 deficiency in mice results in perinatal lethality and a number of developmental malformations in various organs, including the heart, lung, eye and urogenital system (Sanford *et al.*, 1997). Homozygous TGF-β3 deficient mice suffer from delayed pulmonary development and cleft palate and die soon after birth (Kaartinen *et al.*, 1995; Proetzel *et al.*, 1995). The null mice of the three TGF-β isoforms display a number of different phenotypes in a number of major developmental systems. Since there is such a varied response to the loss of each individual TGF-β isoform, this indicates the potential for the isoforms to have overlapping roles.

The secretion and activation of TGF-β dimers (**figure 2.11**) are regulated by their association with latency-associated proteins (LAPs) and latent transforming growth factor-β binding proteins (LTBPs) (**figure 2.12**). TGF-β isoforms are synthesised as pre-propolypeptides that are proteolytically processed in the Golgi apparatus to a mature growth factor and its LAP propeptide. Dimers of the mature TGF-β (**figure 2.11**) and LAP form the small latent complex (SLC), which has no biological activity. The SLC binds covalently to intracellular LTBP-1, -3 and -4 *via* a site in the third 8-Cys repeat by direct cysteine bridging, forming the large latent complex (LLC) (**figure 2.12**) (Kanzaki *et al.*, 1990; Miyazono *et al.*, 1991; Saharinen and Keski-Oja, 2000). The LLC is then secreted from the cell and targets TGF-β to specific locations in the ECM, therefore controlling the location of the biological activity of the growth factor (**figure 2.12**) (Flaumenhaft *et al.*, 1993; Gleizes *et al.*, 1996; Kanzaki *et al.*, 1990; Kojima *et al.*, 1993; Miyazono *et al.*, 1988; Miyazono *et al.*, 1991; Miyazono *et al.*, 1992; Nunes *et al.*, 1997; Saharinen *et al.*, 1996). LAPs are sufficient to render the mature homodimer inactive but removal of both LAPs and LTBP, by protease activity, is essential for the TGF-β isoforms to function.

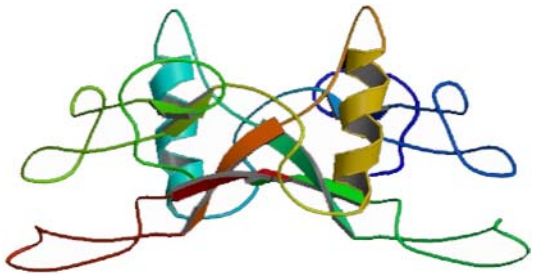

Figure 2.11. Ribbon diagram of mature TGF-β homodimer. Disulphide bonds hold the TGF-β monomeric units together. Image adapted from Hinck *et al.*, 1996, with data deposited into the protein database bank (image number 1klc), www.rcsb.org/pdb/Welcome.do.

The LTBP proteins of the large latent complex are structurally similar to fibrillins since both LTBPs and fibrillins are rod-like molecules consisting predominantly of tandem cbEGF 6-cysteine repeats interspersed with three or four 8-cysteine (8-Cys) motifs (**figure 2.13**) (Kanzaki *et al.*, 1990; Maslen *et al.*, 1991; Tsuji *et al.*, 1990). Since these 8-Cys motifs have only been found exclusively within the fibrillin and LTBP families, the two groups of proteins are considered to be

one superfamily (Öklü and Hesketh, 2000). The LTBP family consists of four proteins, LTBP-1 (with gene location, 2p22-p21) (Miyazono *et al.*, 1988; Stenman *et al.*, 1994), LTBP-2 (with gene location, 14q24.3) (Fang *et al.*, 1997; Gibson *et al.*, 1995; Morén *et al.*, 1994), LTBP-3 (with gene location, 11q12) (Penttinen *et al.*, 2002; Yin *et al.*, 1995) and LTBP-4 (with gene location, 19q13.1-q13.2) (Giltay *et al.*, 1997; Saharinen *et al.*, 1998).

The third 8-Cys motif of human LTBP-1 is the site for covalent disulphide bonding to the SLC (**figure 2.13**). This specific 8-Cys motif appears to increase surface hydrophobicity, and together with accessible sulphydryl groups, allows the formation of the covalent interaction with latent TGF-β. It is thought that upon forming this complex, latent forms of TGF-β can be secreted and localised to required structures in particular tissues prior to being activated (Corson *et al.*, 1993; Gleizes *et al.*, 1996; Saharinen *et al.*, 1996).

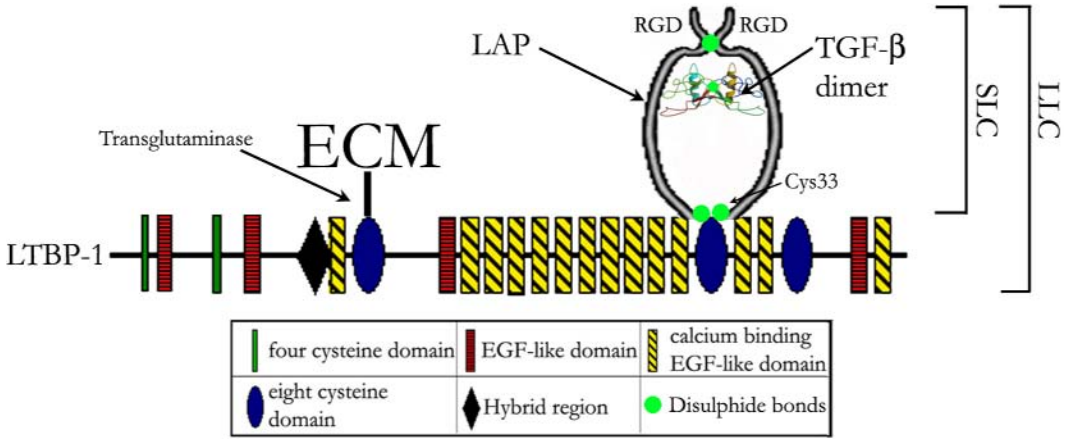

Figure 2.12. Schematic representation of the large latent complex. The disulphide bonded homodimer of the TGF-β growth factor is complexed non-covalently with a latency-associated protein to form the small latent complex. The LAP then covalently binds to LTBPs using cysteine residues in the third 8-Cys repeat. LTBPs contain an array of EGF-like domains, most of which bind to calcium. LTBPs are cross-linked into the ECM by transglutaminase. A region of the N-terminus is cross-linked to an unknown matrix protein(s). Removal of both the LAP and LTBP is required for function of the mature TGF-β growth factor. Image adapted from Hinck *et al.*, 1996 and Ramirez and Rifkin, 2003.

The most N-terminal 8-Cys motif, sometimes called a hybrid domain, may have derived from a former gene splicing event involving exons encoding an 8-Cys motif and an EGF-like domain resulting in a more divergent sequence than found for the other 8-Cys motifs. Between the second 8-Cys motif and the central core of repeating EGF-like domains is a sequence rich in basic amino acids and proline and is called the hinge domain because of its predicted flexibility (Kanzaki *et al.*, 1990; Rifkin, 2004). The long tandem array of cbEGF domains in the central region of the molecule is predicted to protect LTBPs from protease digestion (Colosetti *et al.*, 1993; Reinhardt *et al.*, 2000; Reinhardt *et al.*, 1997). It seems most probable that the cbEGF

domains bind Ca^{2+} ions which induces a structural conformation that protects the molecule from proteolysis as discussed for the fibrillin molecules in section 2.1.3.

Alternatively spliced forms of LTBP-1, -3 and -4 have been identified with the variations between isoforms mainly involving exons encoding the 8-Cys and cbEGF domains (reviewed by Öklü and Hesketh, 2000). Alternative promoters produce the two major isoforms of LTBP-1, defined as LTBP-1S and LTBP-1L, where LTBP-1L contains an additional 346 amino acids from the N-terminal region (Koski *et al.*, 1999). The alternative splicing to form LTBP-1S deletes the twelfth EGF-like domain and removes the eighth cysteine from the first 8-Cys motif. The removal of the eighth cysteine from an isolated 8-Cys motif of fibrillin-1 has been shown to affect intradomain disulphide bonding. If this residue is altered in fibrillin-1 through point mutations or exon skipping, subsequent destabilisation of disulphide bond formation has been shown and has been suggested as a contributing factor for Marfan syndrome (Dietz *et al.*, 1993; Liu *et al.*, 1997). The effect of the alternative splicing and consequential loss of the eighth cysteine residue on the function of LTBPs is currently unknown.

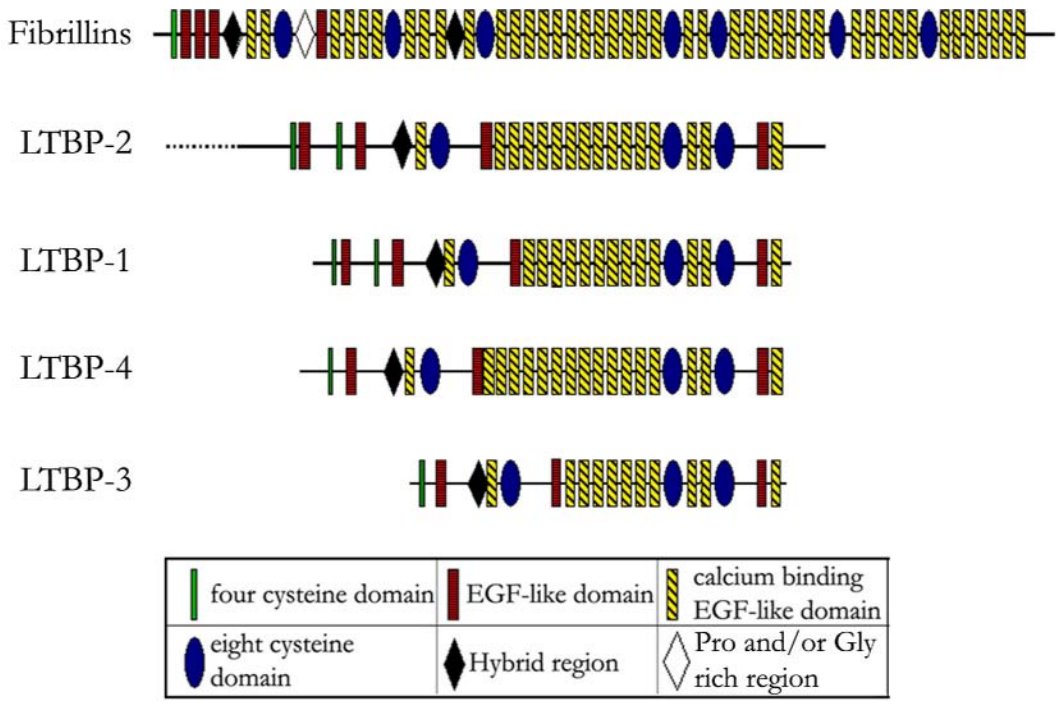

Figure 2.13. Schematic representation of the LTBP and fibrillin superfamily. LTBPs and fibrillins are the only proteins found to date that contain characteristic 8-cysteine-containing motifs. LTBPs, like the fibrillins, have a large number of calcium-binding EGF-like repeats. LTBP-2 is the largest member of the LTBP family and shares the highest homology to fibrillins.

Protein-protein interactions of LTBPs with ECM components could mediate the developmentally important signalling roles of LTBPs or TGF-β. Proteoglycans, specifically

biglycan and decorin, appear to be involved in the regulatory TGF-β feedback system of cell growth (Border *et al.*, 1990; Yamaguchi *et al.*, 1990). As mentioned previously in section 2.3.5, EMILIN-1 was found to inhibit TGF-β signalling by binding to the latent TGF-β complex, thus preventing activation of the mature growth factor cytokine (Zacchigna *et al.*, 2006). Other protein-protein interactions with ECM abundant molecules appear to function to activate TGF-β. TGF-β has been shown to have consensus sequences for furin convertase and can also be released in the presence of plasmin or thrombin (Dubois *et al.*, 1995; Taipale *et al.*, 1992). It has been shown that type-II transglutaminase is involved in the activation of TGF-β (Kojima *et al.*, 1993). Furthermore, since LTBP-1 has been shown to co-distribute with cell surface type-II transglutaminase this suggests type-II transglutaminase contributes to the binding of LTBP-1 to matrix proteins and thus controls matrix storage of latent TGF-β and since LTBP-1 also co-localises with fibronectin, it is possible that fibronectin may be one extracellular component to which LTBP-1 is cross-linked when type-II transglutaminase and LTBP-1 interact at the cell surface (Verderio *et al.*, 1999).

TGF-β activation also appears to be stimulated by integrins, which recognise Arg-Gly-Asp (RGD) motifs present within human LTBPs-1, -2, -4 and bovine LTBP-2. Thus LTBPs may have a role with integrin(s) in promoting transmembrane and cell adhesion signalling reviewed by Annes *et al.*, 2003. It has been shown that the small latent complex of TGF-β binds integrins αvβ1 (Munger *et al.*, 1998), αVβ6 (Annes *et al.*, 2002; Munger *et al.*, 1999), αvβ8 (Mu *et al.*, 2002) and α8β1 (Lu *et al.*, 2002) *via* an RGD sequence present on the LAP. However, the activation of TGF-β using αVβ6 and fibronectin requires LTBP-1 to be present (Fontana *et al.*, 2005; Annes *et al.*, 2004). In this situation it appears as though LTBP-1 cannot be substituted for by the other TGF-β-bound LTBPs and indicates a functional role for LTBP-1 in latent TGF-β activation and suggests that activation of specific latent complexes is determined by the LTBP isoform (Fontana *et al.*, 2005). In addition, further indication of the importance of αVβ6 during TGF-β activation is shown using β6-deficient mice, which have increased inflammation and decreased fibrosis, which are processes highly regulated by TGF-β (Huang *et al.*, 1996).

Furthermore, it has been shown that LTBP-1 and -2 can be secreted and deposited into the ECM without attachment to TGF-β, thus LTBPs could have additional functions independent of TGF-β complexes, such as structural components of the matrix (Saharinen, *et al.*, 2000; Hyytiäinen, *et al.*, 1998; Gibson, *et al.*, 1995; Unsöld, *et al.*, 2001). Studies have been conducted to determine if LTBPs function as architectural proteins for fibrillin-containing microfibrils, using microfibrils that were extracted from tissues and analysed by immunoblotting with specific antibodies. LTBP-1 was not detected upon the beads-on-a-string arrangement of isolated microfibrils, suggesting that at least LTBP-1 is not an integral structural component. However, in contrast, direct binding studies between LTBP-1 and fibrillins indicated an

interaction between the two protein families (Isogai *et al.*, 2003). The binding site was located to within three domains of the LTBP-1 C-terminus (the third 8-Cys motif, fourth EGF-like domain and the fourteenth cbEGF domain (**figure 2.13**)), and within four domains near the N-terminus of fibrillin-1 and -2 (the second and third EGF-like domains, hybrid motif and first cbEGF (**figure 2.13**)) (Isogai *et al.*, 2003). It has been suggested that LTBP-1 may be a fibrillin-associated protein present in select tissues at various stages of development (Dallas *et al.*, 2000; Kitahama *et al.*, 2000; Porst *et al.*, 2005). It is possible that in tissues where LTBP-1 is not found LTBP-4 may substitute, since it has been shown that the C-terminus of LTBP-4 binds equally well to the N-terminal region of fibrillins-1 and -2 (Isogai *et al.*, 2003).

It has been proposed that an interaction between LTBP-1 and fibrillin-1 may stabilise latent TGF-β complexes within the extracellular matrix. If fibrillin-1 is not present the stabilisation would not occur and TGF-β would be activated. Studies using fibrillin-1 deficient mice support this concept of abberant TGF-β activation. These fibrillin-1 deficient mice exhibit phenotypic features similar to those patients with classic MFS, including aortic aneurysms, severe kyphosis and overgrowth of the ribs and other long bones (Pereira *et al.*, 1999). Furthermore, a distinct subgroup of MFS patients have distal airspace enlargement and emphysema. Fibrillin-1 deficient mice were analysed for TGF-β activation levels and it was found that these mice had marked dysregulation of TGF-β activation and signalling, resulting in apoptosis in the developing lung (Neptune *et al.*, 2003). Thus, the loss of fibrillin-1 indicates latent forms of TGF-β are activated irregularly and disrupt developing tissues. Perinatal antagonism of TGF-β attenuated apoptosis and rescued the defect in the developing lung (Neptune *et al.*, 2003).

Ltbp-3$^{-/-}$ null mice also show a decrease in TGF-β signalling in the lungs at days 4-6, which alters cell proliferation and correlates with inhibition of septation and developmental emphysema (Colarossi *et al.*, 2005). Mice deficient in LTBP-3 also develop cranio-facial malformations with a pronounced rounding of the cranial vault, extension of the mandible beyond the maxilla, and kyphosis, possibly caused by the loss of TGF-β in bone and cartilage, which leads to compromised osteoclast turnover and decreased bone regeneration (Colarossi *et al.*, 2005; Neptune *et al.*, 2003). The loss of LTBP-4 is associated with abnormal lung development, cardiomyopathy, and colorectal cancer (Chen *et al.*, 2003; Dabovic, *et al.*, 2002b; Dabovic *et al.*, 2005; Sterner-Kock *et al.*, 2002).

The fibrillin-LTBP interaction appears to be significant for sequestration of cytokines in the matrix, which is important for their regulation, activation and signalling. The nature of the exact interplay between fibrillins, LTBPs and TGF-β is unclear and it appears as though both fibrillins and LTBPs perform complex levels of regulation that may be spatiotemporally specific. Perturbation of these interactions has the potential to result in the manifestation of pathogenic diseases. The exact function of each member of the fibrillin and LTBP superfamily and their

intricate biochemical interactions still need to be elucidated. Further research into spatial and temporal regulation of these proteins is required before fibrillin/LTBP functions can be fully understood. Furthermore, the divergence of the roles of LTBPs and fibrillins is illustrated by LTBP-2, which differs completely from the other LTBPs in that, like fibrillins, it does not appear to form covalent binding with small latent complexes of TGF-β (Gibson *et al.*, 1995; Lack *et al.*, 2003; Saharinen and Keski-Oja, 2000). Since, LTBP-2 has been found to be associated strongly with elastic tissues and fibrillin-containing microfibrils there is potential for LTBP-2 to mediate the function of these structures but currently no studies have been conducted to investigate potential roles of LTBP-2 (Gibson *et al.*, 1995). This research project aims to analyse the role of LTBP-2 in the ECM and further detail on the known properties of LTBP-2 is discussed below.

2.4 LTBP-2

LTBP-2 was initially characterised as a cDNA from a human fibroblast cDNA library and later the human *LTBP-2* gene was localised to chromosome 14 (14q24) (Bashir *et al.*, 1996; Morén *et al.*, 1994). The *LTBP-2* gene encodes a 195-240kDa protein containing 20 cbEGF repeats, three 8-Cys motifs, and one hybrid 8-Cys motif interspersed with proline rich regions (**figure 2.13**). Single exons code for each of the EGF repeats while the 8-Cys repeats are each encoded by two exons. LTBP-2 is also the largest member of the LTBP family since it contains a number of unique regions including the 4-cysteine motifs and extended cysteine free domains (**figure 2.13**). LTBP-2 has a proline/glycine rich region alternating with clusters of cysteine-rich structural motifs (Fang *et al.*, 1997). As mentioned previously, LTBP-2 differs from other members of the LTBP family since it does not appear to have high affinity for binding latent forms of TGF-β. The third 8-Cys domains of LTBP-2 and fibrillins lack the required latent TGF-β binding consensus sequence (Lack *et al.*, 2003; Saharinen and Keski-Oja, 2000). Human and bovine LTBP-2 have been shown to contain the common integrin recognition sequence, RGD, at its N-terminus suggesting the ability for binding to specific integrins allowing for a possible role in cell adhesion or transmembrane signalling (Bashir *et al.*, 1996; Gibson *et al.*, 1995; Morén *et al.*, 1994).

Biochemical analysis of matrix-bound LTBP-2 has been conducted using several methods. In an early study tissue-extracted bovine LTBP-2 had a molecular mass of 290- and 310kDa, whereas a 260kDa species was released into the medium of cultured elastic tissue cells. 6M guanidine and dithiothreitol were required for LTBP-2 to be fully extracted from tissues indicating the protein was tightly bound in the ECM. No TGF-β was covalently attached to tissue-extracted LTBP-2 (Gibson *et al.*, 1995). LTBP-2 was localised to fibrillar structures and treatment of the cell layer with plasmin or elastase released a soluble 160kDa LTBP-2 fragment (Hyytiäinen *et al.*, 1998). Thus, it seems likely that only the full-length LTBP-2 can assemble into

the extracellular matrix and proteolytic cleavage is needed to release it (Taipale *et al.*, 1995; Taipale *et al.*, 1994). The cleavage sites were localised to proline-rich regions at the N-terminus of LTBP-2, suggesting that the extracellular matrix binding sites are located within the N-terminal 500 amino acids (Hyytiäinen *et al.*, 1998).

In studies on unfolded LTBP-2, chemical deglycosylation decreased the molecular weight indicating that the protein is glycosylated, which is thought to protect LTBP-2 from protease targeting (Hyytiäinen *et al.*, 1998). Carbohydrates were detected in the central, proteolytically stable core fragment of LTBP-2, which is predicted to form the rigid rod-like structure (Downing *et al.*, 1996; Hyytiäinen *et al.*, 1998). Regions of high proline and basic residue content seem to confer sensitivity to protease digestion. The domains preceding the cbEGF repeats have a high proline content, thus supporting the hypothesis of the presence of a proteolytically sensitive hinge domain between the extracellular binding N-terminal domain and the first 8-Cys domain (**figure 2.13**) (Hyytiäinen *et al.*, 1998; Taipale *et al.*, 1994).

Phylogenetic studies of the *LTBP-2* gene indicates that *LTBP-2* shares more homology with *LTBP-1* than *LTBP-3*, thus suggesting that *LTBP-2* diverged from the *LTBP-1* gene following the divergence of *LTBP-3* from *LTBP-1* (Bashir *et al.*, 1996). The *LTBP-2* gene is localised on a different chromosome of the human genome (14q24) to that of *LTBP-1* (2p12-q22). Thus, it seems likely that the differences between the two genes have arisen through gene duplication of a common ancestor followed by chromosomal rearrangements (Morén *et al.*, 1994). The *LTBP-2* gene shows most similarity to the fibrillin genes and since the human *FBN1* gene is found at 15q21.1 and the banding patterns of Chromosomes 14 and 15 are very similar, it has been suggested that these chromosomes could have arisen due to an ancient duplication event (Comings, 1972; Lee *et al.*, 1991). Preliminary studies have reported several distinct missense point mutations in the *LTBP-2* gene in patients exhibiting Marfan-like phenotypes including mitral valve prolapse, aortic dilatation and spinal scoliosis (Robinson and Godfrey, 2000). It is yet to be determined if these mutations have a causative role for the phenotypes. If a link were to be established then it would indicate an important role for LTBP-2 involving TGF-β activation or in the function and/or modulation of fibrillin-containing microfibrils in a variety of tissues.

The majority of information concerning potential roles of LTBP-2 within elastic fibres and developmental tissues comes from studies conducted in mice. The mouse *Ltbp-2* gene is 80% homologous to the human sequence and is located on chromosome 12 band D of the mouse genome, which is a conserved area of synteny with the human chromosome 14 region (Fang *et al.*, 1997). It was found, on microscopic analysis of a 16.5 day post coitum mouse, that *Ltbp-2* gene expression was restricted to ear cartilage and blood vessels. Other LTBP genes are more widely expressed in rodent tissues. Expression patterns of LTBP-2 in mice at later stages

of development show more localised expression than LTBP-1 and -3. LTBP-2 correlates highly in expression to that of tropoelastin in tissues such as, lung, dermis, large arterial vessels, epicardium, pericardium and heart valves at various stages of rodent embryonic development (Shipley *et al.*, 2000). LTBP-2 has highest expression in aorta, lung and skin and co-expression of LTBP-2 with tropoelastin seems to indicate a structural role for LTBP-2 in developing elastic tissues (Fang *et al.*, 1997).

There were areas of tropoelastin expression in the absence of LTBP-2, such as perichondrial regions throughout the head of the developing mouse. This is not surprising as elastic fibre composition varies between tissues and it has been suggested that not all elastic fibres have LTBP-2 in association (Shipley *et al.*, 2000). So far, the only tissue where LTBP-2 is found in the absence of tropoelastin was in the testes of the young adult mouse. TGF-β is highly expressed in the testes and studies were conducted to determine if LTBP-2 had spatiotemporally selective interactions with TGF-β in the testes. It was shown that neither TGF-β1, -β2 nor -β3 co-localised with LTBP-2 when examined using *in situ* hybridisation confirming that LTBP-2 had an unknown functional role within the testes which could be differential to its roles within elastic fibres (Shipley *et al.*, 2000; Skinner and Moses, 1989).

To investigate the importance of LTBP-2 during development, mice with a targeted disruption of the *Ltbp-2* gene were generated. *Ltbp-2*$^{-/-}$ mice die between embryonic day (E) 3.5 and E6.5, which is pre-implantation of the embryo into the uterine wall (Shipley *et al.*, 2000). LTBP-2 expression was not detected by *in situ* hybridisation in E6.5 embryos but was detected in E3.5 blastocytes by reverse transcription polymerase chain reaction (RT-PCR) (Shipley *et al.*, 2000). The result of the LTBP-2 knockout mouse is not consistent with the phenotypes of TGF-β knockout mice (Proetzel *et al.*, 1995; Rappolee *et al.*, 1988; Sanford *et al.*, 1997) or mice with knockouts of other major elastic fibre proteins (Li *et al.*, 1998; Pereira *et al.*, 1997; Pereira *et al.*, 1999). Mice homozygous for targeted disruptions of MAGP-1 and fibrillin-1 genes live into adulthood and LTBP-1 or tropoelastin knockout mice die shortly after birth from either vascular or pulmonary complications (Li *et al.*, 1998; Pereira *et al.*, 1997; Pereira *et al.*, 1999). However, since these mice can survive past birth it suggests that the lethal phenotype associated with LTBP-2 is not due to a function related to elastic fibres. LTBP-2 appears to have an essential role during very early developmental stages, perhaps in implantation that cannot be compensated for by the other members of the LTBP family.

These studies indicate that LTBP-2, unlike other LTBPs, has a role independent of sequestering and localising latent forms of TGF-β to ECM structures. Since, it has been shown that LTBP-2 is associated with elastic fibres and is co-expressed with fibrillin this indicates LTBP-2 has the potential to be involved with the function of elastic fibres. However, mice knockout studies also implies LTBP-2 could have an essential role during early stages of

embryonic development. To date, studies have not been conducted to examine potential functions of LTBP-2 in the ECM. The research project outlined below aimed to investigate molecular interactions of LTBP-2 with a selection of extracellular matrix macromolecules, including fibrillins, to obtain information on the potential biological function of LTBP-2 within elastic fibres.

3 Aims of the present study

LTBP-2 is a matrix protein of unknown function although since LTBP-2 has been shown to be co-expressed with fibrillin at similar stages of tissue development this implies that LTBP-2 could be directly or indirectly involved with the function of elastic fibres. LTBP-2 also appears to have an important developmental function since gene knockout studies in mice result in early embryonic lethality. LTBP-2 differs from other members of the LTBP family in that it does not covalently interact with latent forms of TGF-β and thus does not appear to have a direct role in TGF-β storage and activation. However, like LTBPs-1 and –4, LTBP-2 has been localised in the extracellular matrix of a number of tissues as a microfibrillar component of elastic fibres. Elastic fibres found within connective tissues consist of an amorphous elastin core surrounded by microfibrils rich in the structural protein, fibrillin. Recently it has been shown that LTBP-1 interacts with fibrillins-1 and –2 and LTBP-4 interacts with fibrillin-1, thus suggesting that fibrillin-containing microfibrils could act as tissue stores for latent forms of TGF-β. If the LTBP-fibrillin interaction was disrupted this could result in aberrant expression of TGF-β during development and manifest human diseases such as Marfan syndrome. Thus, LTBPs appear to have a role in elastic tissue function and extracellular matrix cytokine localisation. However thus far, few studies have not been conducted to analyse the potential roles for LTBP-2 in the extracellular matrix.

This research project focused primarily on the function of LTBP-2 within elastic fibre biology. In particular, it was aimed to determine if LTBP-2 interacts with fibrillins-1 and –2 and if such an interaction was found to determine if LTBP-2 could modulate the binding of other LTBPs, particularly LTBP-1, with fibrillins. It was also aimed to elucidate the localisation of LTBP-2 in tissues and determine if LTBP-2 and LTBP-1 have similar or distinct distributions in tissues important in human diseases, particularly developing human aorta, which has a major involvement in Marfan syndrome.

It is also an aim to characterise other molecular interactions of LTBP-2 with a range of extracellular matrix macromolecular components including; tropoelastin, MAGPs, proteoglycans and collagens. This thesis reveals and characterises some molecular interactions of LTBP-2 with extracellular matrix macromolecules to elucidate clues for the potential function of LTBP-2.

Specific aims

1) To express and purify human recombinant LTBP-2 (r-LTBP-2) using a mammalian expression system

2) To define and characterise molecular interactions of LTBP-2 with fibrillins and other extracellular matrix macromolecules

3) To determine if LTBP-2 challenges other members of the LTBP family for binding upon fibrillin-containing microfibrils

4) To compare the tissue distribution patterns of LTBP-2 in relation to fibrillins and other members of the LTBP family

4 Materials and Methods

4.1 General molecular biology protocols

The following molecular biology protocols were adopted to facilitate cloning of human LTBP and fibrillin cDNA sequences into mammalian expression vectors.

4.1.1 Reverse-Transcription-Polymerase Chain Reaction (RT-PCR)

Reverse transcription to obtain single stranded cDNA sequences was carried out as follows. Random hexamer primers (10μM) and 2μg of total RNA were mixed together and the reaction volume was made up to 15μL with ddH_2O. This mixture was heated to 70°C for 10 minutes prior to chilling on ice for 2 minutes then adding 2.5mM $MgCl_2$, 0.2mM of each dNTP, 10mM of DL-dithiothreitol (DTT) and 1x platinum *taq* DNA polymerase buffer (supplied by the manufacturer of platinum *taq* DNA polymerase as a 10x stock containing 200mM Tris-HCl (pH 8.4) and 500mM KCl (Invitrogen, Carlsbad, CA)). The reaction mixture was made up to 24μL with ddH_2O, mixed and incubated at 42°C for 2 minutes. 200U of superscript II reverse transcriptase (Invitrogen, Carlsbad, CA) was then added and the reaction was incubated at 42°C for 50 minutes followed by enzyme inactivation at 90°C for 5 minutes. RNA template was removed with digestion using 1U of RNaseH (Promega, Madison, WI) for 20 minutes at 37°C. PCR amplification of single-stranded cDNA was conducted as indicated above.

4.1.2 Polymerase Chain Reaction (PCR)

The polymerase chain reaction (PCR) was carried out using an Eppendorf mastercycler gradient PCR machine (Eppendorf, Hamburg, Germany) as previously described in (Kitahama *et al.*, 2000). Briefly, PCR reaction mix contained 2.5U of *Pfu* turbo DNA polymerase (Stratagene, La Jolla, CA), 1x PCR reaction buffer (supplied by Stratagene as a 10x stock containing 200mM Tris-HCl (pH 8.8), 20mM $MgSO_4$, 100mM KCl, 100mM $(NH_4)_2SO_4$, 1% Triton X-100 and 1 mg/ml nuclease-free BSA), 0.2mM of each dNTP and a template:primer ratio of 2:1, with primers used at 10μM each. Total reaction volume of 50μL was made up using ddH_2O. PCR cycles were conducted with a heated lid of 100°C, denaturation of the template and activation of the DNA polymerase occurred at 94°C for 3 minutes followed by 20-40 cycles with denaturation at 94°C for 1 minute, annealing temperature (specific for each set of primer pairs) for 1 minute, extension temperature of 72°C for 1 minute per kilobase of product to be amplified and a final extension step at 72°C for 10 minutes. All reactions were held at 4-12°C prior to long-term storage at -20°C.

4.1.3 Agarose Gel Electrophoresis and DNA Purification

The PCR product [cDNA] (usually 50-200ng) was mixed with 6x load buffer (**appendix B**) to the final concentration of 1x and was loaded into wells of a 1% (w/v) agarose gel (Invitrogen, Carlsbad, CA, catalogue number 15510-027) dissolved in 1x TAE buffer (**appendix B**). Electrophoresis was carried out at 120V for 1 hour with 1x TAE buffer in the chamber prior to post-staining in ethidium bromide (10mg/mL) (Boehringer Mannheim GmbH, Mannheim, Germany). Specific DNA bands of required size were excised from the agarose gel using a clean scapel blade and purified using the ultraclean gelspin filter kit (MoBio, Solana Beach, CA) exactly following manufacturers instruction. cDNA yields were typically 20-80µg/mL. Yields were calculated from A_{260} readings of 1:100 dilution of cDNA in ddH_2O in a UV-1601 spectrophotometer (Shimadzu, Kyoto, Japan). The cDNA fragment was "A"-tailed in preparation for ligation into pGEM-T-easy vector (Promega, Madison, WI).

4.1.4 "A"-tailing and Ligation

"A"-tailing of the cDNA PCR fragment insert was performed as follows, 50-200ng of PCR fragment was incubated at 70°C for 1 hour with 5U of platinum *taq* DNA polymerase, 1x platinum *taq* DNA polymerase buffer, 2.5mM $MgCl_2$ and 0.2mM dATP. The reaction volume was made up to 10µL using ddH_2O.

Ligation of the "A"-tailed PCR product into the pGEM-T-easy vector was performed using an insert:vector ratio of 3:1 was used which was incubated for 2 hours at 37°C with 3U of T4 DNA ligase and 1x ligation buffer (supplied by Promega as a 10x stock containing 300mM Tris-HCl (pH 7.8), 100mM $MgCl_2$, 100mM DTT and 10mM adenosine triphosphate (ATP)) and the reaction volume was made up to 10µL using ddH_2O.

Ligated DNA was purified using ethanol precipitation as follows; 2.5 volumes of ice-cold 100% ethanol, 0.1 volumes of 3M sodium acetate (pH 5.2) and 1µL of glycogen were incubated with the ligation reaction for 20 minutes at -20°C and was immediately (without thawing) centrifuged at room temperature for 25 minutes at 17,500x g. The DNA pellet was washed using ice-cold 70% ethanol and was centrifuged at 17,500x g for 10 minutes prior to carefully decanting the ethanol and allowing the pellet to air-dry. DNA was resuspended using 20µL of ddH_2O prior to use in transformation of JM109 competent cells (Promega, Madison, WI).

4.1.5 Transformation of Competent Cells

JM109 competent cells (10^7 colony forming units/µg) were heat-shocked as recommended by the manufacturer at 42°C with 20-50ng of the ligated and purified DNA (in a volume not greater than 10µL) for exactly 45 seconds and cells were recovered in SOC media

(**appendix B**). Dilutions of 1:10 and 1:100 of the transformed cells were coated onto solid agar plates containing luria broth (**appendix B**) and 100µg/mL ampicillin and coated with 0.5mM IPTG and 40µg/mL X-Gal. The presence of X-Gal and IPTG coated on agar plates allows for blue/white colony selection. White colonies indicate JM109 competent cells transformed with pGEM-T-easy vector containing the required cDNA insert. The presence of this cDNA insert interrupts transcription of the *LacZ* gene whose protein product metabolises X-Gal and IPTG into a blue compound. White colonies were selected and propagated in luria broth (**appendix B**) containing 100µg/mL of ampicillin for plasmid DNA purification. Plasmid DNA was purified from 3mL of luria broth culture using the high pure plasmid isolation kit (Roche Diagnostics GmbH, Mannheim, Germany), exactly following manufacturers instructions. The DNA was eluted from the spin column using ddH_2O and resulted in DNA yields of 50-300µg/mL. DNA yields were calculated at A_{260} using 1:100 dilution of stock DNA in ddH_2O.

4.1.6 DNA Sequence Analysis

To ensure DNA integrity and to determine the orientation of cDNA inserts, DNA sequencing was conducted using automated sequence analysis technology (Applied Biosystems, Foster City, CA). Big-Dye version 3.0 ready reaction mix (8µL) was incubated with 1µg of purified plasmid DNA, 1x Big-Dye sequencing buffer (supplied by the manufacturer Applied Biosystems as 5x stock) and 10µM sequencing primer (M13F or M13R (**appendix A**), unless otherwise indicated) with reaction volume made up to 20µL using ddH_2O. Sequencing was carried out using the following PCR conditions: sample heating step 96°C for 1 minute, then 25 cycles of 96°C for 10 seconds, 50°C for 5 seconds, 60°C for 4 minutes where the reactions were then held at 12°C prior to DNA precipitation with isopropanol. Briefly, 80µL of 75% isopropanol (made fresh for each use) was added to the sequencing reaction and vigorously agitated for a few seconds prior to incubation at room temperature for 1 hour to precipitate extension products. The sample was then centrifuged for 20 minutes at 17,500x g and the isopropanol was carefully removed. The pellet was washed with 250µL of 75% isopropanol, agitated briefly and was then centrifuged for 10 minutes at 17,500x g. The isopropanol was removed carefully to avoid disturbing the pellet and the pellet was dried at 90°c for 1 minute. The sample was then sent to the molecular pathology sequencing centre (Institute for Medical and Veterinary Science, Adelaide, Australia) for automated sequence analysis using the 3700 DNA analyser (Applied Biosystems, Foster City, CA). Glycerol stocks of error-free clones were made using a 7:3 ratio of luria broth culture:100% sterile glycerol and stored at -70°C.

4.1.7 Restriction Digests

Restriction digests were carried out using 5U of restriction enzyme in 1x restriction buffer (optimal buffers for each restriction enzyme are supplied by the manufacturer) with 200-500ng of DNA. The reaction volume was made up to 20μL using ddH_2O and the mixture was incubated for 1 hour at 37°C.

4.1.8 Dephosphorylation

Vector dephosphorylation was conducted using Shrimp alkaline phosphatase as recommended by the manufacturer (Boehringer Mannheim GmbH, Mannheim, Germany). Briefly, 50-500ng of vector DNA was incubated with 10U of shrimp alkaline phosphatase with 1x dephosphorylation buffer (supplied by the manufacturer (Boehringer Mannheim GmbH) as 10x stock containing 0.5M Tris-HCl (pH 8.5) and 50mM $MgCl_2$). The reaction volume was made up to 100μL using ddH_2O and was incubated for 1 hour at 37°C. The enzyme was deactivated for 15 minutes at 65°C and the dephosphorylated vector was recovered using ethanol precipitation as stated above.

4.1.9 Quikchange Mutagenesis

Quikchange mutagenesis was performed as directed by the manufacturer (Stratagene, La Jolla, CA). Briefly, mutagenic oligonucleotide primers were designed for each individual mutation and were in most cases 45 bases in length with the mutation in the middle and 10-15 bases of correct sequence on either side which annealed to the corresponding complementary sequences on opposite strands of the plasmid. DNA plasmid template (50ng) was mixed with 2.5U of *pfu* turbo DNA polyermase, 10μM of each primer, 2.5mM of each dNTP and 1x PCR reaction buffer (supplied by Stratagene as 10x stock). The reaction volume was made up to 50μL using ddH_2O and the mutagenic PCR was conducted under the following conditions:- initial denaturation for 30 seconds at 95°C followed by 18 cycles of 95°C for 30 seconds, 55°C for 1 minute, 68°C for 2 minutes/kilobase of plasmid length, and a final extension step for 10 minutes at 68°C. 10U of *Dpn*I (Promega, Madison, WI) was added to the completed PCR reaction to remove the parental DNA template prior to transformation into JM109 competent cells.

4.1.10 Gateway® Cloning

Gateway® cloning (Invitrogen, Carlsbad, CA) was performed as follows; the cDNA insert was PCR amplified with specifically designed primers to contain the required *att*B sites which efficiently recombine with the *att*P sites engineered into the Gateway® donor vector,

pDONR™201. pDONR™201 vector (75ng) was incubated with cDNA insert containing the *att*B sites (100ng) and the manufacturer supplied BP Clonase™ enzyme mix (2μL). The reaction mixture was made up to 10μL using TE buffer (pH 8.0) (**appendix B**) and then incubated for 3 hours at 25°C. Proteinase K solution (supplied by the manufacturer, Invitrogen) was added to the reaction and incubated for 10 minutes at 37°C prior to transforming chemically competent DH5α bacterial cells. Chemically competent DH5α cells (10^8 colony forming units/μg) were transformed using heat shock at 42°C exactly as stated above for JM109 competent cells, except they were plated on luria broth agar plates containing kanamycin selection at 50μg/mL. Selected colonies were propagated using luria broth cultures with 50μg/mL of kanamycin.

4.2 Cloning of human LTBP and Fibrillin cDNA sequences

The full-length human LTBP-2 clone was prepared by Dr. E. Hanssen and is described here briefly. LTBP-2 cDNA (Genbank™ accession number NM_000428) was obtained by RT-PCR from human fibroblast RNA using primer LTBP-2mRNA (**appendix A**) followed by PCR amplification with primers LTBP-2F and LTBP-2R (**appendix A**) for 35 cycles with an annealing temperature of 61°C. The LTBP-2 PCR product (6119bp) was purified from the agarose gel and "A"-tailed and ligated to the pGEM-T-easy vector. This pGEM-T:LTBP-2 construct was propagated in JM109 competent cells and purified plasmid DNA was sequenced to confirm no errors were present.

To enable enhanced expression of the human recombinant LTBP-2 protein within the mammalian cells, a cDNA sequence encoding the BM-40 signal peptide was added in place of the cDNA sequence encoding the LTBP-2 signal peptide (Nischt *et al.*, 1991). The cDNA sequence encoding the BM-40 signal peptide (Genbank™ accession number Y00755) was obtained by RT-PCR from human trabecular bone mRNA followed by PCR amplification with primers BM40F and BM40R (**appendix A**) for 35 cycles with annealing temperature of 58°C. The product was ligated to the pGEM-T-easy vector and the plasmid DNA was propagated within JM109 competent cells. This cDNA encoding for the BM-40 signal peptide was added to the 5' end of the LTBP-2 cDNA (replacing bases 212-494) using the splicing by overlap extension technique with primers BM40/LTBP-2F and BM40/LTBP-2R (**appendix A**) for 30 PCR cycles with annealing temperature of 68°C (Horton *et al.*, 1993). A 6-histidine (his_6)-tag was added to C-terminal end of the modified LTBP-2 sequence using quikchange mutagenesis to allow for the purification of the recombinant protein (**figure 5.1**). For this, primers BM40F and LTBP-2R/His (**appendix A**) were used for 10 cycles of PCR with annealing temperature of 68°C prior to ligation into the pGEM-T-easy vector and propagation in JM109 competent cells. Plasmid DNA was purified from individual colonies and the desired error-free clone of the pGEM-T:LTBP-2 plasmid was selected for using automated sequence analysis.

The LTBP-2:BM-40:his$_6$-tag insert was digested out of the pGEM-T-easy vector with the *Not*I restriction enzyme and was subcloned using T4 DNA ligase into the dephosphorylated *Not*I site of the pCEP-4 vector (Invitrogen, Carlsbad, CA) that had been modified by quikchange mutagenesis to remove the *Hin*dIII restriction site (pCEP-4Δ*Hin*dIII). The construct was propagated within JM109 competent cells, plasmid DNA was purified and the desired error-free clone (pCEP-4:LTBP-2) was selected by automated sequence analysis with primers pCEPF and pCEPR (**appendix A**) (for complete sequencing of the LTBP-2 insert internal sequencing primers were individually designed as required).

The following constructs were prepared during this PhD candidature:

To produce the recombinant carboxy-terminal fragment of LTBP-2 (LTBP-2CT(H)), bases 5089-5847 of the LTBP-2 cDNA were PCR amplified from the full length clone using the primers LTBP-2CT(H)F and LTBP-2CT(H)R (**appendix A**) with 29 PCR cycles and an annealing temperature of 61°C. The 756bp product was purified from a 1% (w/v) agarose gel and was digested with *Hin*dIII in preparation for subcloning into the dephosphorylated pGEM-T:BM-40:his$_6$-tag cassette vector. For preparation of the pGEM-T:BM-40:his$_6$-tag cassette vector, the full-length LTBP-2 insert was removed from the pGEM-T:LTBP-2 plasmid by *Hin*dIII restriction enzyme digest. The pGEM-T:BM40:his$_6$-tag vector and full-length LTBP-2 cDNA insert were separated using agarose gel electrophoresis. The pGEM-T:BM-40:his$_6$-tag vector band (of approximately 3500bp) was purified from the agarose gel and dephosphorylated prior to ligation with the *Hin*dIII digested LTBP-2CT(H) cDNA insert. JM109 competent cells were transformed with the ligation product and plasmid DNA from individual colonies was purified. The desired pGEM-T:LTBP-2CT(H) clone in the required orientation was selected using automated sequence analysis.

All of the plasmids constructed for this project contained DNA sequences encoding for the his$_6$-tag, however in some circumstances it could be advantageous to remove this histidine-tag from the expressed protein. To enable removal of the his$_6$-tag, a DNA sequence encoding the enterokinase (EK) protease site (Asp-Asp-Asp-Asp-Lys) was introduced into the pGEM-T:LTBP-2CT(H) plasmid between the *Hin*dIII site and the his$_6$-tag encoding sequence with quikchange mutagenesis using the primers LTBP-2CT(H)EKF and LTBP-2CT(H)EKR (**appendix A**; **figure 6.1**). The mutagenised pGEM-T:LTBP-2CT(H):EK plasmid was propagated within JM109 competent cells, the plasmid DNA was purified and the desired clone containing the correct sequence was confirmed by automated sequence analysis.

The LTBP-2CT(H):BM-40:his$_6$-tag:EK insert was removed from the pGEM-T:LTBP-2CT(H):EK mutagenised plasmid using restriction digest with *Not*I and was subcloned using T4 DNA ligase into the dephosphorylated *Not*I site of the pCEP-4Δ*Hin*dIII

vector. For this, the full-length LTBP-2 insert was removed from the pCEP-4:LTBP-2 plasmid by digestion with the *Not*I restriction enzyme. The pCEP-4 vector and full-length LTBP-2:BM-40:his_6-tag cDNA insert were separated using agarose gel electrophoresis and the pCEP-4 vector band (approximate size of 10500bp) was purified from the agarose gel and dephosphorylated prior to ligation with the *Not*I digested LTBP-2CT(H):BM-40:his_6-tag:EK cDNA insert. JM109 competent cells were transformed with the ligation product, the plasmid DNA from individual colonies was purified and the desired clones containing the pCEP-4:LTBP-2CT(H) plasmid in the correct orientation were selected using automated sequence analysis with the pCEPF and pCEPR primers (**appendix A**).

Carboxyl-terminal human cDNA for LTBP-1CT(H), corresponding to bases 3681-4317 (Genbank™ accession number NM_000627), was obtained by reverse transcription of human breast cancer cell RNA using the LTBP-1CT(H)F primer (**appendix A**). PCR amplification of the 636bp single stranded cDNA product was conducted using LTBP-1CT(H)F and LTBP-1CT(H)R primers (**appendix A**) for 25 cycles with an annealing temperature of 60°C. The cDNA product was prepared for Gateway® cloning technology with the addition of *attB* sites using primers LTBP-1CT(H)gateF and LTBP-1CT(H)gateR (**appendix A**) with 12 PCR cycles and an annealing temperature of 55°C. DH5α cells were transformed with the recombination product and the pDONR:LTBP-1CT(H) plasmid DNA from individual colonies was purified using the high pure plasmid isolation kit as described in section **4.1**.

The LTBP-1CT(H) cDNA sequence was excised from the pDONR:LTBP-1CT(H) plasmid by restriction enzyme digestion with the *Hin*dIII enzyme. This LTBP-1CT(H) insert was subcloned into the dephosphorylated *Hin*dIII restriction site of the pGEM-T:BM-40:his_6-tag:EK vector. For preparation of the pGEM-T:BM-40:his_6-tag:EK plasmid, the LTBP-2CT(H) cDNA insert was removed from the pGEM-T:LTBP-2CT(H) plasmid by restriction digest with the *Hin*dIII enzyme. The pGEM-T:BM-40:his_6-tag:EK vector and LTBP-2CT(H) cDNA insert were separated using agarose gel electrophoresis. The pGEM-T:BM-40:his_6-tag:EK vector band (of approximately 3500bp) was purified from the agarose gel and dephosphorylated prior to ligation with the *Hin*dIII digested LTBP-1CT(H) cDNA insert. JM109 competent cells were transformed with the ligation product and plasmid DNA from individual colonies was purified and the desired pGEM-T:LTBP-1CT(H) clone in the required orientation was selected by automated sequence analysis.

The LTBP-1CT(H):BM-40:his_6-tag:EK insert was removed from the pGEM-T:LTBP-1CT(H) plasmid using restriction digest with *Not*I and was subcloned using T4 DNA ligase into the dephosphorylated *Not*I site of the pCEP-4Δ*Hin*dIII digest, obtained as described above during cloning of the LTBP-2CT(H) construct. JM109 competent cells were transformed with the ligation product, the plasmid DNA from individual colonies was purified

and the desired clones containing the pCEP-4:LTBP-1CT(H) plasmid in the correct orientation were selected using automated sequence analysis with the pCEPF and pCEPR primers (**appendix A**).

All the recombinant pCEP-4 expression constructs needed to be highly purified for transfection into mammalian cells. The selected clones were propagated using luria broth cultures prior to plasmid purification using the QIAfilter® midi kit (Qiagen GmbH, Hilden, Germany). Luria broth cultures of 50mL were utilised following the instructions for low-copy number plasmids supplied by the manufacturer (Qiagen) except for a slight modification in the final elution step. Eluted DNA (8mL) was aliquoted equally into 8 eppendorf tubes with the manufacturer stated amount of isopropanol (2.5mL) divided between them, the DNA was centrifuged and the DNA pellet in each individual eppendorf tube was resuspended in ~20µL of ddH_2O overnight at room temperature (if a large pellet was visible a little more water was used). The DNA was then pooled together into two batches of at least 80µL each. This elution step was modified since an increase in the yield and concentration of the purified plasmid DNA was found. General yields of 0.5-1mg/mL were obtained, which was calculated from the absorbance reading (A_{260}) using a 1:100 dilution of stock DNA in ddH_2O.

The fibrillin cDNA clones were prepared as previously described (Hanssen *et al.*, 2004; Hanssen *et al.*, 2003) but these recombinant proteins were expressed and purified as described below.

4.3 Expression and purification of recombinant polypeptides

For expression and purification of recombinant proteins, 293-EBNA human embryo kidney (HEK) cells (Invitrogen, Carlsbad, CA) were propagated to confluence using Dulbecco's Modification of Eagles Medium (DMEM) (medium reconstituted from powder exactly as stated by manufacturer (Gibco, Carlsbad, CA)) supplemented with 1x non-essential amino acids (NEAA) (Thermo electron, Australia), 10% (v/v) heat deactivated (Δ) foetal calf serum (FCS) (Gibco, Carlsbad, CA) (alternatively, a 50:50 mixture of Δnew born calf serum (NBCS) (Gibco, Carlsbad, CA)/ΔFCS or ΔNBCS have also been used successfully for a number of transfections) and 250mg/L geneticin (used for selection of EBNA-1 containing cells (EBNA-1 sites and OriP within the vectors allows for extrachromosomal replication) (Gibco, Carlsbad, CA). Cells counted with trypan blue stain (using 1:1 ratio of trypan blue and cell solution) were plated at 2 x 10^5 cells/mL prior to transfection using 2µg/mL of plasmid DNA and 4µg/mL of LF2000 lipofectamine reagent (Invitrogen, Carlsbad, CA). Controls wells containing 4µg/mL of LF2000 lipofectamine reagent only (substitute volume of DNA with ddH_2O) and no transfection (where no LF2000 or DNA was added to wells) were also carried out.

Twenty-four hours after transfection, the medium was removed from the cells and these were gently washed with Dulbecco's PBS (**appendix B**) to remove remaining transfection reagent. Cells were removed from the surface of the well by agitating in the presence of 10-20mL Dulbecco's PBS and washed in 5mL DMEM (no supplements) and pelleted by centrifugation (260x g for 5 minutes). The cells were gently resuspended in 25mL DMEM/10% (v/v) ΔFCS/1x NEAA/geneticin (250mg/L) and were divided equally between 10 fresh wells. LF2000 only and no transfection controls each had only one fresh well plated instead of 10.

Forty-eight hours after transfection, fresh medium containing the selective antibiotic hygromycin (1.25mg/L) (Roche Diagnostics GmbH, Mannheim, Germany) was added to each well (medium recipe as follows; DMEM/10% (v/v) ΔFCS/1x NEAA/geneticin (25mg/L)/hygromycin (1.25mg/L)). Cells containing the required recombinant plasmid (pCEP-4 contains the hygromycin resistance gene) were selected through a number of culture medium changes and were then propagated to confluence. Since selection takes a number of days to occur, cells with no DNA or LF2000 added were used as indicators for gauging the selection process. Once these control cells had died in the selection medium then all remaining viable cells in the transfection wells were deemed to be successfully transfected with the required recombinant plasmid.

To enhance the propagation of transfected cells to confluence, several wells of hygromycin-selected cells were pooled together. Standard practice was to have 12x 175cm^2 flasks of propagating cells, 10 of which were placed into serum-free medium for protein production and 2 flasks that were passaged into 12 fresh flasks to continue cell propagation. Stocks of stably transfected cells (from 1x 175cm^2 flask) were slowly frozen at -70°C in a 25% (v/v) ΔFCS/7.5% (v/v) dimethyl sulphoxide (DMSO) (Unilab, Seven Hills, NSW, Australia)/67.5% (v/v) DMEM solution prior to transfer into liquid nitrogen (note: ΔNBCS was never used for freezing cell stocks). These frozen stocks of transfected cells were thawed for propagation and protein production if required by placing a vial of the 293-EBNA cells into a 37°C water bath until nearly thawed and then placing the cells into 10mL of DMEM (no supplements). The cells were incubated with the DMEM for 5 minutes at room temperature and were then centrifuged (260x g for 5 minutes). The cells were then resuspended in 1mL DMEM (no supplements) and placed into 80cm^2 propagation flasks with 10mL of culture media (DMEM/10% (v/v) ΔFCS/1x NEAA/geneticin (25mg/L)/Hygromycin (1.25mg/L)).

Cells at confluence were washed 3x in Dulbecco's PBS (**appendix B**) prior to the addition of serum-free medium of DMEM supplemented with 1x NEAA or in the case of the full-length LTBP-2 expressing cells, Excell 293 serum-free medium (media reconstituted from powder exactly as stated by manufacturer (JRH Biosciences, Lenexa, KS)) supplemented with 1x NEAA (selection antibiotics do not need to be added with serum-free medium since cells are no

longer dividing). Serum-free medium was incubated with cells for 3 days prior to harvest. In some instances, harvested flasks were incubated overnight with DMEM supplemented with ΔFCS followed by a second round of serum-free medium for an additional three days (this procedure was found not to be possible for flasks incubated with Excell 293 medium, since cell viability was reduced when using Excell 293 medium).

Collected serum-free medium was centrifuged (260x g for 5 minutes) to remove cells and then was centrifuged at 50,000x g for 30 minutes at 4°C using a Heraeus Biofuge stratos centrifuge (Kendro laboratory products GmbH, Hanau, Germany) and was then filtered through a 0.45μm bell filter (Pall Corporation, Pensacola, FL) to remove cell debris. To equilibrate medium for Ni-chelate chromatography 160mM phosphate (PO_4) buffer and 2M imidazole (BDH Chemicals, Carle Place, NY) (**appendix B**) was added to medium to a final concentration of 20mM PO_4 buffer and 10mM imidazole. Since imidazole has a similar chemical structure as histidine, the addition of a low concentration of imidazole (10mM) to the medium prior to incubation with Ni-sepharose resin reduces the amount of non-specific binding of contaminating proteins without competing with the his_6-tagged protein for binding to the sepharose beads.

For purification of recombinant proteins, a His-trap sepharose column was prepared exactly as stated by manufacturer (Pharmacia Biotech, Uppsala, Sweden). Briefly, for every 100mL of serum-free media collected, 500μL of Ni-chelate sepharose was usually prepared. However, for high expression proteins, like the LTBPs, a ratio of 1mL sepharose to 100mL medium was used. Beads were prepared by rinsing with ddH_2O to remove the storage ethanol solution, 1.5 column volumes of $NiSO_4$ (**appendix B**) was added and incubated with the uncharged Ni-chelate sepharose beads for at least 10 minutes. Residual nickel solution was removed by gravitational filtration. Successfully charged sepharose beads appeared sky-blue in colour. Beads were then equilibrated for incubation with medium using 2 column volumes of 10mM imidazole buffer (**appendix B**).

Ni-sepharose beads were incubated with the serum-free medium for 3-4 hours at room temperature or overnight at 4°C on a rotator wheel. Beads were collected by gentle centrifugation (no more than 260x g for 5 minutes) and transferred to a column using a pipette and the medium supernatant was stored at 4°C. Three rounds of purification were performed per batch of medium to remove all recombinant protein present. The Ni-sepharose column was washed 5x using 2 column volumes of 10mM imidazole buffer (**appendix B**). All washes were collected and stored at 4°C for reapplication to a fresh Ni-sepharose column since they usually contained some recombinant protein. Pure recombinant protein was eluted using 8 washes of 1x column volume of 500mM imidazole buffer (**appendix B**). The higher concentration of imidazole (500mM) displaces the his-tagged protein from the Ni-charged sepharose. Ni ions were then stripped from the chelating-sepharose beads using 20mM sodium phosphate, 0.5M

NaCl, 0.05M EDTA, pH 7.4. This was followed by incubation with 0.1M NaOH for at least 2 hours at room temperature to remove any precipitated proteins. The beads were washed extensively with ddH_2O prior to storage in 20% (v/v) EtOH at room temperature.

500mM imidazole elution fractions 1-3 were generally found to contain the highest concentration of recombinant protein. Thus these samples were pooled together and dialysed into tris buffered saline (TBS) for fibrillin fragments or TBS/0.5M NaCl for LTBP proteins (**appendix B**). 500mM imidazole was always removed from purified protein since it was found to interfere with a number of assays where anti-[his_6-tag] antibodies were to be used for protein detection. Dialysis was carried out using Spectrapor membrane of molecular weight range 6-8000Da (Spectrum Laboratories, Inc., Rancho Dominguez, CA), overnight at 4°C or for several hours at room temperature in several changes of buffer of volume 500mL-1L. The remaining fractions containing recombinant protein were pooled together into dialysis membrane and concentrated using aquacide 1-A (Calbiochem, Merck KgaA, Darmstadt, Germany) prior to dialysis into TBS or TBS/0.5M NaCl buffer.

Briefly for aquacide concentration, the elution fractions were placed into dialysis membrane that was tightly knotted on one side and clipped on the other, with a cushion of air added to prevent the bag collapsing during the aquacide process. The dialysis bag containing the protein was placed into a measuring cylinder (of approximately 50mL volume) and was covered with aquacide powder and left at room temperature for 1 hour. Loose aquacide powder was gently tapped away from around the dialysis bag and wet aquacide powder was removed and discarded by gently rubbing along the length of the dialysis membrane. If sufficient concentration was achieved then the dialysis membrane was transferred into a suitable buffer and dialysed as described above. If the volume was not reduced sufficiently, fresh aquacide powder was added around the dialysis membrane and incubated until the desired volume had been achieved. Dialysed proteins were aliquoted, snap frozen and stored at -70°C. Proteins were warmed at 37°C until just thawed prior to aliquoting into working amounts. A working aliquot was stored at 4°C for no more than 2 months.

Ammonium sulphate precipitation of protein from serum-free medium was conducted using 5mL of culture medium as follows. The medium was centrifuged for 20 minutes at 50,000x g. The supernatant was removed and ammonium sulphate powder was slowly added with gentle stirring to give 30% (w/v) saturation. The mixture was then incubated for 45 minutes on ice to allow precipitate to form and was then centrifuged for 20 minutes at 50000x g at 4°C. The supernatant was removed and placed into a fresh vial and the pellet was dissolved in sample loading buffer (**appendix B**). To the supernatant additional ammonium sulphate was added to give 35% (w/v) saturation and the above procedure was repeated. Further precipitations of 40% (w/v), 45% (w/v) and 50% (w/v) saturation of ammonium sulphate were also conducted. The

pellets in sample loading buffer were then dialysed into fresh sample loading buffer overnight at 4°C to remove any residual ammonium sulphate. The final samples were then reduced using 2% β-mercaptoethanol and were analysed using SDS-PAGE and western immunoblotting as described below.

4.4 SDS-PAGE and western immunoblot analysis

Purified proteins (at least 0.5µg of protein per lane) were analysed using microslab SDS-PAGE, and the discontinuous buffer system of Laemmli with a separating gel of acrylamide concentrations ranging from 5-12% (v/v) and a stacking gel concentration of 3% (v/v) acrylamide (**appendix B**) (Sigma-Aldrich, St. Louis, MO) (Laemmli, 1970; Matsudaira and Burgess, 1978). LTBP-2, and in most cases the fibrillin-fragments, were separated using 6.5 or 8% SDS-PAGE and the LTBP C-terminal fragments and collagen-IV preparations were analysed on 12% polyacrylamide gels. Protein samples were precipitated at -20°C for at least 15 minutes with 10 volumes of cold 90% (v/v) acetone. Precipitated protein was pelleted by centrifugation at 17,500x g for 10 minutes, acetone supernatant was carefully decanted and the pellet was resuspended in sample loading buffer (**appendix B**) that contained 2% (v/v) β-mercaptoethanol (Sigma-Aldrich, St Louis, MO) when reducing samples and boiled for 1 minute. After loading into individual wells the samples were resolved at 150V in chamber buffer (**appendix B**) until the dye front was approximately 1mm from the bottom of the gel. Broad range molecular weight protein standards (Bio-Rad Laboratories, Hercules, CA) were run concurrently (to obtain 0.5µg/protein band, protein standard stock solution was diluted 1:20 using reduced sample loading buffer).

To visualise and quantitate proteins bands, SDS-PAGE gels were stained with Coomassie Blue (**appendix B**) for 1 hour with gentle shaking. The gel was destained by rinsing in 40% (v/v) methanol destain solution (**appendix B**) and incubating with gentle shaking in fresh 40% (v/v) methanol destain for 20 minutes followed by 7.5% (v/v) methanol solution (**appendix B**) for 30 minutes. The gel was washed in ddH_2O prior to drying overnight between cellophane sheets. Protein was quantitated using the Image J program (version 1.29, http://rsb.info.nih.gov/ij/).

In some instances silver staining of gels was employed (method obtained from Wilson, R. of Murdoch Childrens Research Institute and Department of Paediatrics, University of Melbourne, Australia) which was conducted as follows: after electrophoresis the gel was fixed in 50% (v/v) methanol, 12% (v/v) acetic acid, 0.05% (v/v) formalin (40% (v/v) formaldehyde solution) with gentle shaking for 30 minutes. This gel was then washed in 35% (v/v) ethanol for 3x 10 minutes, sensitised with 0.02% (w/v) sodium thiosulphate for 2 minutes and rinsed quickly in ddH_2O. The gel was stained using 0.2% (w/v) $AgNO_3$ (silver nitrate) containing 0.076% (v/v)

formalin for 20 minutes and was then rinsed very quickly in ddH_2O. The gel was rinsed twice very quickly and then developed using the developing solution (5% (w/v) $NaCO_3$, 0.05% (v/v) formalin, 0.008% (w/v) $Na_2S_2O_3$) until the desired signal strength was obtained. The development was stopped immediately using a 50% (v/v) methanol and 12% (v/v) acetic acid solution and the gel was rinsed several times in ddH_2O, prior to drying overnight between cellophane sheets.

For western and overlay immunoblots, the SDS-PAGE gels were used as above but instead of fixing and staining the proteins were transferred onto polyvinylidene difluoride membrane as follows. The gel was washed twice in immunoblot chamber buffer (**appendix B**) for 10-15 minutes. Bio-trace polyvinylidene difluoride (PVDF) (Pall Corporation, Pensacola, FL) membrane (0.45µm) was activated by rinsing in 100% (v/v) methanol for 1 minute, followed by rinsing in ddH_2O and immunoblot chamber buffer for 5 minutes each. The gel was sandwiched between the smooth side of the PVDF membrane and Whatman paper (3mm grade, Whatman international Ltd, Maidstone, England) prior to placing it into the wet transfer apparatus. Protein bands were transferred onto PVDF membrane using 60V in a negative to positive direction for 90 minutes with gentle stirring of the immunoblot chamber buffer using a magnetic stirrer. After transfer, the lane containing the Bio-Rad standard proteins was cut off and stained with Coomassie Blue. The remainder of the membrane was washed 2x 5-10 minute in TBS and placed into blocking solution (3% (w/v) non-fat skim-milk/TBS or if anti-[his_6-tag] antibody, tetrahis, was to be used for protein detection, 3% (w/v) bovine serum albumin (BSA) (Sigma-Aldrich, St Louis, MO) in TBS), for at least 1 hour at room temp with gentle agitation.

The blot was incubated in primary antibody for at least 2 hours at room temperature or 4°C overnight in 3% (w/v) milk/TBS at the designated concentration (**appendix C**) (anti-[his_6-tag] antibody, tetrahis, was diluted in 3% (w/v) BSA/TBS (**appendix C**)). The PVDF membrane was washed 2x 5 minutes in tris/tween-20/triton X-100 (TTX) solution (**appendix B**) and 5 minutes in TBS with gentle shaking. Secondary antibody conjugated with alkaline phosphatase (Bio-Rad Laboratories, Hercules, CA) diluted in 3% (w/v) non-fat skim-milk/TBS (3% (w/v) BSA/TBS for anti-[his_6-tag] antibody, tetrahis) (**appendix C**) was incubated with the membrane for at least 1 hour at room temperature. The membrane was then washed 3x 5 minutes in TTX prior to rinsing in substrate buffer (**appendix B**) and development using an nitro-blue tetrazolium chloride (NBT) (Boehringer Mannheim GmbH, Mannheim, Germany)/5-bromo-4-chloro-3-indolylphosphate toluidine salt (BCIP) (Diagnostic Chemicals Ltd, Charlottetown, PEI) colour solution (**appendix B**). Colour development was stopped in ddH_2O and the membrane was air-dried.

For blot overlay assays, 1µg/lane of purified recombinant protein was precipitated using 90% (v/v) cold acetone, resolved by SDS-PAGE and transferred onto PVDF membrane as

stated above. After blocking in 3% (w/v) non-fat skim-milk/TBS/2mM $CaCl_2$ for at least 1 hour at room temperature, the membrane was incubated with test recombinant protein (5µg/mL) in 0.05% (w/v) BSA/TBS/2mM $CaCl_2$ solution overnight at 4°C. After washing as stated above the appropriate primary mouse monoclonal or rabbit polyclonal antibodies specific to the liquid phase ligand were diluted in 3% (w/v) milk/TBS/2mM $CaCl_2$ to concentrations as stated in **appendix C**, and were incubated for at least 3 hours at room temperature. After washing, as stated for western blots above, a final incubation with alkaline phosphatase-conjugated secondary antibody diluted in 3% (w/v) low-fat dried milk/TBS/2mM $CaCl_2$ (**appendix C**) was carried out for at least 1.5 hours at room temperature. The blots were developed using the colour reaction as described above.

4.5 Mass spectrometric analysis

Mass spectrometric analysis was conducted by Dr. Chris Bagley (Adelaide proteomics institute, School of Molecular and Biomedical Sciences, University of Adelaide, Australia). All storage containers and gel apparatus were rinsed thoroughly with 5% (w/v) SDS solution and ddH_2O prior to use. Coomassie Blue stained gels were stored in 5% (w/v) SDS solution prior to analysis on the mass spectrophotometer. The required protein band for analysis was excised from SDS-PAGE gels stained with Coomassie Blue, washed three times in ammonium bicarbonate (100mM) containing 50% (v/v) acetonitrile (HPLC grade, Merck KgaA, Darmstadt, Germany) and again in 100% acetonitrile before drying completely under vacuum. 25µl of trypsin solution (made up as a stock containing; 500ng of modified porcine trypsin dissolved in acetic acid (2mM), ammonium bicarbonate (80mM) and 8% (v/v) acetonitrile) was then added to re-hydrate the spots. Proteolytic digestion was allowed to occur at 37°C for 16 hours. Tryptic peptides were reduced by the addition of tris(2-carboxyethyl)phosphine hydrochloride (0.1M) and the tryptic digestion was stopped by the addition of 1% (v/v) formic acid. The supernatant was collected and the protein was further extracted in 25µl of acetonitrile (100%). The combined extracts were reduced in volume to 10µL using a Speed-Vac system (Savant Instruments, Inc., Thermo electron corporation, Waltham, MA) prior to LC-MS/MS analysis.

The resulting peptides were desalted through a C18 reverse phase silica column (0.3 x 3mm, 5µm packing, LC-Packings, Sunnyvale, CA) and separated on an Atlantis dC18 analytical column (0.075 x 50mm, 3µm packing, Waters corps, Milford, MA) using an acetonitrile gradient (5-70% containing 0.1% formic acid) at a flow rate of 200nL/minute. Peptides were then ionised through a NanoSpray source with 3kV and were applied to a Micromass $QTOF_2$ mass spectrometer (Waters corps, Milford, MA). Automated MS/MS sequencing was carried out using data direct analysis and the spectrophotometer was calibrated against [Glu_1]-fibrinopeptide B. *De novo* sequence tag analysis were determined from the fragmentation data and used to search the

National Centre for Biotechnology information (http://www.ncbi.nlm.nih.gov) non-redundant protein database for protein identification matches. The sequences of matching peptides were validated by manual inspection.

4.6 Collagens and other matrix macromolecules

MAGPs (Finnis and Gibson, 1997), decorin (Reinboth *et al.*, 2000), biglycan (Reinboth *et al.*, 2000), tropoelastin (Brown *et al.*, 1992) and collagens (Abedin *et al.*, 1982) were prepared as described previously. Human fibronectin (catalogue number F6277), human laminin (catalogue number L6274) and native human placenta collagen-IV (catalogue number C5533, which was confirmed to be basement membrane collagen type-IV by the vendor) were purchased from Sigma-Aldrich (St. Louis, MO) and reconstituted as stated by the manufacturer.

4.7 Protein digestions

r-LTBP-2 was digested with N- and O-glycosidases as stated by manufacturer (Roche Diagnostics GmbH, Mannheim, Germany). Briefly, 500ng of protein was diluted in sodium phosphate buffer (**appendix B**) containing 1% (w/v) SDS and boiled for 5 minutes prior to adding 10% (v/v) nonidet P40 (LKB Produkter AB, Bromma, Sweden) and ddH_2O for a final volume of 100µL. N-glycosidase (0.5U) or O-glycosidase (0.5mU) was added to the reaction mixture, which was incubated for 16 hours at 37°C, prior to acetone precipitation and analysis by SDS-PAGE.

Recombinant enterokinase was used to digest the his_6-tag from recombinant LTBP C-terminal fragments. Digestion was carried out as stated by the manufacturer (Novagen, Madison, WI, catalogue number 69067-3). Briefly, 10µg of r-LTBP fragment was incubated with 0.2U of enzyme for 8-16 hours at room temperature. The enzyme was removed using the EKapture agarose and the spin filters provided in the capture kit (Novagen, Madison, WI), prior to analysis of the digested protein using SDS-PAGE and western immunoblotting. Western immunoblots were conducted using the anti-[his_6-tag] antibody, tetrahis to determine if the digestion was successful, since recombinant protein still containing the his_6-tag would immunoreact with this antibody. Controls for these digestion experiments included untreated LTBP fragment, LTBP fragment treated with Novagen EK kit components but without adding the enzyme and a control protein provided within the kit.

4.8 Antibodies

Anti-[fibrillin-1] mouse monoclonal antibodies MAB2502, MAB2499 and MAB1919 were purchased from Chemicon (Chemicon International, Temecula, CA). Anti-[fibrillin-1] peptide rabbit polyclonal antibody, Fib1A, was produced using methods as described previously (Gibson

et al., 1995) with the following synthetic peptide [VPRPPVEYLYPSREPPRVC] (Chiron Mimotopes Pty Ltd, Clayton, Victoria, Australia), which is an antigen specific for the hinge region of fibrillin-1. Mouse monoclonal anti-[fibrillin-2] antibody, 16E12, has been described previously (Hanssen *et al.*, 2004). Mouse monoclonal antibody to human LTBP-1CT(H), MAB388, was purchased from R&D Systems (Minneapolis, MN). Mouse monoclonal anti-[his_6-tag] specific antibody, tetrahis, was purchased from Qiagen (Valencia, CA). Collagen-IV antibody rabbit 29 was produced using methods as described previously (Gibson *et al.*, 1995) with native collagen-IV purchased from Sigma (catalogue #C5533) as the antigen (Sigma-Aldrich, St. Louis, MO). Rabbit polyclonal antibodies raised to MAGP-1 (rabbit 18) and MAGP-2 (rabbit 49) have been previously described (Gibson *et al.*, 1998; Gibson *et al.*, 1986; Henderson *et al.*, 1996).

Rabbit polyclonal anti-LTBP-2 antibody, FLP-E has been characterised previously (Gibson *et al.*, 1995). A further rabbit polyclonal anti-[LTBP-2 peptide] antibody, LTBP-2C, was produced using methods as described previously (Gibson *et al.*, 1995) with the following synthetic peptide DDLHYSIYGPDGAC (Auspep, Parksville, Australia) as a specific antigen for the carboxy-terminal 8-Cys motif of LTBP-2. Briefly, after coupling the peptide to the diphtheria toxoid carrier protein, the diphtheria toxoid/peptide antigen was injected into a rabbit with 10mL bleeds collected every 2 weeks for the duration of 6 months. Red blood cells were removed from serum by centrifugation (at 260x g for 20 minutes) then preservative (0.005% (w/v) thimerosal (Sigma-Aldrich, St. Louis, MO)) was added to the serum prior to aliquoting and freezing at -20°C.

Specific anti-[LTBP-2C peptide] antibody was affinity purified using a thiol sepharose column charged with the LTBP-2C peptide. The peptide column was prepared using as follows; 2.5mg of peptide (dissolved in dimethylformamide) was bound to 2mL of thiol sepharose with overnight incubation at room temperature on the rotator wheel. The column was drained and the unbound eluate was analysed on a UV-1601 spectrophotometer (A_{343}) (Shimadzu, Kyoto, Japan) to determine the number of moles of peptide coupled. The sepharose column was then washed twice with PBS/EDTA (**appendix B**) followed by three further washes in sodium acetate (**appendix B**). Residual reactive sites within the column were blocked using 0.8% (v/v) β-mercaptoethanol in acetate buffer for 20 minutes on rotator wheel.

For antibody purification, the 2mL peptide column was washed in acetate buffer and PBS/EDTA. 5mL of anti-[LTBP-2C peptide] antiserum was diluted in PBS/EDTA to a final volume of 10mL and incubated with the column at room temperature for 2 hours on a rotator wheel. The unbound serum solution was drained off and retained. The column was washed in 2mL of PBS/EDTA, which was collected and followed by 5x 10mL washes with PBS/EDTA. These washes were analysed using a spectrophotometer until a reading at A_{280} of zero was obtained to indicate no further protein was eluting. The column was washed with unbuffered NaCl (**appendix B**) prior to eluting the bound antibody with 10x 1mL fractions of glycine buffer

of pH 2.8 (**appendix B**). The fractions were immediately neutralised to pH 7.4 using Tris base (**appendix B**). The sepharose column was immediately re-equilibrated in PBS/EDTA prior to storage at 4°C for further antibody purifications. Appropriate fractions were pooled and analysed at A_{280} for accurate concentration measurement (antibodies of concentration 1mg/mL have A_{280} of 1.4). Ovalbumin at 50µg/mL was then added as a carrier protein. The purified antibodies were dialysed into PBS (**appendix B**), snap frozen at -70°C and stored at -20°C. Affinity purified anti-[LTBP-2C peptide] antibody was stored at a concentration of 500µg/mL. The specificity of the affinity purified and the serum anti-[LTBP-2C peptide] specific antibody was confirmed by enzyme-linked immunosorbent assay (ELISA) and western blotting against the recombinant polypeptides of LTBP-2 and LTBP-2CT(H).

4.9 Radiolabelling of recombinant polypeptides

For some experiments the recombinant fragments were radiolabelled with $Na^{125}I$ (GE healthcare, Chalfont St. Giles, United Kingdom) using IODO-BEADs (Pierce Biotechnology, Rockford, IL) as described previously (Finnis and Gibson, 1997). Briefly, 100µg of recombinant protein was reacted with an IODO-BEAD (that had been rinsed with TBS) and 1mCi of $Na^{125}I$ for 15 minutes in TBS (for fibrillin fragments) or TBS/0.5M NaCl (for LTBP fragments). Free radiolabel was removed from the protein by gel filtration through Sephadex PD-10 desalting column (GE Healthcare, Chalfont St. Giles, United Kingdom). The specific activities of the ^{125}I-labelled fibrillin fragments were 1.28 x 10^7 dpm/µg and of the ^{125}I-labelled LTBP proteins were 1.28 x 10^5 dpm/µg unless stated otherwise.

r-LTBP-2 was also biosynthetically labelled using TRAN^{35}S-label (containing 70% (w/v) L-Methionine) (MP Biomedicals, Irvine, CA). This procedure was conducted using 293 cells transfected with the LTBP-2 expression construct, LTBP-2:pCEP-4, which were grown to confluence in DMEM. The confluent cells were washed 3x in Dulbecco's PBS (**appendix B**) and once in Cysteine/Methionine free media (Gibco, Carlsbad, CA). Cysteine/Methionine free media (supplemented with 584mg/L of L-Glutamine (Sigma-Aldrich, St. Louis, MO) dissolved in 0.85% (w/v) NaCl/ddH_2O) containing 100µCi/mL of TRAN^{35}S-label was added and incubated with cells for 4 days. ^{35}S-labelled rLTBP-2 was purified using Ni-chelate chromatography and dialysed into TBS/0.5M NaCl exactly as stated for the unlabelled rLTBP-2 protein in section **4.2**. The specific activity was 1.8 x 10^5 dpm/µg unless otherwise stated.

4.10 ELISAs

Plastic flat-bottomed multiwell microtitre plates (Immuno-maxisorb modules (Nalge-Nunc International, Roskilde, Denmark) were coated with purified recombinant test polypeptides (usually 400ng in TBS/2mM $CaCl_2$ per well) at 4°C overnight in a humidity

chamber. Control wells were coated with the molar equivalent of BSA. All experiments were carried out using triplicate or quadruplicate wells. The wells were rinsed 3x with TBS/2mM $CaCl_2$, blocked for at least 1 hour at room temperature with gentle agitation in 5% (w/v) low-fat dried milk (Diploma instant, Rowville, Vic, Australia) in TBS/2mM $CaCl_2$, followed by rinsing 3x with TBS/2mM $CaCl_2$. The brand and concentration of milk powder was found to affect non-specific background binding. Some experiments conducted with 3% (w/v) low-fat dried milk in TBS/2mM $CaCl_2$ were found to have slightly higher background binding. The optimal blocking conditions of 5% diploma brand low-fat milk in TBS/2mM $CaCl_2$ were used in most cases unless stated otherwise within figure legends.

Primary antibody was then added to the wells at the required dilution (concentrations as stated in **appendix C**) in TBS/0.05% (v/v) tween-20/2mM $CaCl_2$ and these were incubated for at least 1.5 hours at 37°C in humidity chamber with gentle agitation. Wells were then washed 3x with TBS/0.05% (v/v) tween-20/2mM $CaCl_2$. Antibody titres were determined using a serial dilution of primary antibody.

Horseradish peroxidase conjugated secondary antibody (Bio-Rad Laboratories, Hercules, CA) was then added at the required dilution (**appendix C**) in TBS/0.05% (v/v) tween-20/2mM $CaCl_2$ and the wells were incubated for at least 1 hour at 37°C in a humidity chamber with gentle agitation. The wells were then washed 4x in TBS/0.05% (v/v) tween-20/2mM $CaCl_2$ and interactions were detected using 100µL of 3,3',5,5'-tetramethylbenzidine (TMB) substrate (Sigma). Colour was allowed to develop for up to 1 hour at room temperature with no agitation and the reaction was stopped using 0.5M H_2SO_4 (50µL per well). Absorbance was detected at 450nm, unless stated otherwise, using a Titertek Multiskan MC (Flow Laboratories, North Ryde, NSW, Australia).

4.11 Solid phase binding assays

Individual maxisorb modules were coated overnight at 4°C with the solid phase test protein as stated in section **4.8**. Control wells were coated with the molar equivalent of BSA. The wells were blocked in 3% low-fat skim milk powder in TBS and were then extensively washed in TBS/2mM $CaCl_2$. For initial screening, various extracellular matrix macromolecules were added in TBS/2mM $CaCl_2$ buffer to wells coated with 1 molar equivalent of the test protein and was incubated for 3 hours at 37°C. Control wells had molar equivalent amounts of BSA added in solution. Protein-protein interactions were detected using primary antibodies specific to the protein in liquid phase and detected using horseradish peroxidase-conjugated secondary antibody and TMB revelation as stated in section **4.8**.

For saturation curves, maxisorb modules were coated with uniform amounts of the solid phase test protein and blocked as stated in section **4.8**. Control wells were coated with molar

equivalents of BSA. A serial dilution of the liquid phase protein (in TBS/2mM $CaCl_2$) was added to the wells and incubated for at least 3 hours at 37°C in a humidity chamber with gentle shaking. Protein-protein interactions were detected using primary antibodies specific for the protein in the liquid phase and binding of the primary antibody was detected using horseradish peroxidase conjugated secondary antibody and TMB revelation as stated in section **4.8**. In some instances ^{125}I-labelled recombinant proteins were added in liquid phase in place of unlabelled proteins. In these cases, at least 50000dpm of labelled protein was added per well (unless stated otherwise), diluted in TBS/2mM $CaCl_2$ and incubated with the solid phase protein for 3 hours at 37°C in a humidity chamber with gentle shaking. The wells were then washed 3x in TBS/0.05 % (v/v) tween-20/2mM $CaCl_2$. Bound ^{125}I-labelled protein was directly measured using a 1261 Multi-γ counter at 80% efficiency (Wallac, Inc., Gaithersburg, MD).

To determine dissociation constants (K_d) for specific interactions, the method of Bidanset *et al.* was used (Bidanset *et al.*, 1992). Briefly, maxisorb modules were coated with the required recombinant test protein (usually 50ng/well) and then incubated with a serial dilution of ^{125}I-labelled protein in liquid phase for at least 3 hours at 37°C. Control wells were coated with a molar equivalent of BSA. Bound and unbound radiolabelled protein was measured in each well and following subtraction of the background binding of the corresponding BSA coated wells, a specific binding curve was plotted from which the K_d was calculated using GraphPad Prism version 4.00 for Windows (GraphPad Software, San Diego, CA, www.graphpad.com).

In some instances solid phase binding assays were conducted with ^{35}S-labelled r-LTBP-2 in liquid phase. Binding of ^{35}S-labelled protein was measured after the addition of 2mL of starscint scintillation fluid (Perkin-Elmer, Boston, MA) and counting for 5 minutes using a Beckman LS 3801 scintillation counter at 90% efficiency (Beckman Coulter, Inc., Fullerton, CA).

4.12 Competitive solid phase binding assays

Initial blocking experiments were conducted using ^{125}I-labelled Fib1(H)NT. Maxisorb modules were coated with recombinant LTBP proteins and blocked as described in section **4.8**. Control wells were coated with a molar equivalent of BSA. ^{125}I-labelled Fib1(H)NT was pre-treated with 10-fold molar excess of r-LTBP-2CT(H), r-LTBP-1CT(H) or BSA for 18 hours at 37°C without agitation in TBS/2mM $CaCl_2$, then added to triplicate wells and left to interact for 3 hours at 37°C without agitation. Unbound proteins were then removed using 3x washes with TBS/0.05% (v/v) tween-20/2mM $CaCl_2$. ^{125}I-labelled protein bound was measured using the 1261 multi-γ counter.

Competitive binding curves were conducted using unlabelled proteins. Maxisorb modules were coated with r-LTBP-1CT(H) (100ng/well) and r-LTBP-2CT(H) (140ng/well) and blocked as stated within section **4.8**. Control wells were coated with a molar equivalent of BSA.

Unlabelled Fib1(H)NT (280ng/well) was pre-treated with a serial dilution of r-LTBP-1CT(H) (0-0.5µg/well) or with a serial dilution of a molar equivalent of r-LTBP-2CT(H) (0-0.35µg/well) for 18 hours at 37°C without agitation in TBS/2mM $CaCl_2$ and was then added to triplicate wells and left to interact for a further 3 hours at 37°C without agitation. Binding of Fib1(H)NT was detected using anti-[fibrillin-1] specific antibody, MAB2502 (1:2000 dilution in TBS/0.005% (v/v) tween-20/2mM $CaCl_2$) followed by anti-[mouse] horseradish-peroxidase conjugated secondary antibody and colour development using TMB substrate exactly as stated in section **4.8**.

4.13 Tissue sectioning and immunofluorescence

Frozen sections (5µm thick) were cut using a cryostat 1720 (Leitz, Solms, Germany) from tissue blocks of third trimester human foetal thoracic aorta and bovine nuchal ligament from 210-230 day foetuses embedded in optimal cutting temperature (OCT) compound (Miles Inc., Elkhart, IN). The sections were air-dried and then incubated with antibodies specific for LTBP-1, -2 and fibrillin-1 (using concentrations as stated in **appendix C**) diluted in PBS (**appendix B**) overnight at 4°C in a humidity chamber. Sections were gently washed in PBS prior to the addition of secondary antibodies conjugated to flurophores, Alexa 488 (Invitrogen, Carlsbad, CA), FITC or Cy5 (Jackson Immunoresearch, West Grove, PA) (**appendix C**) for 1-2 hours at room temperature. Sections were washed and then mounted in anti-fade solution (90% (v/v) glycerol/10% (v/v) PBS and 0.1% p-phenylenediamine (Sigma-Aldrich, St. Louis, MO) prior to analysis using fluorescence (Gibson and Cleary, 1987) and/or laser confocal microscopy.

Specimens were examined using a Nikon Microphot-FXa microscope (Nikon, Japan) or a Bio-Rad MRC-1000 scanning laser confocal microscope (Bio-Rad Laboratories, Hercules, CA). The Nikon Microphot-FXa was equipped with 10x, 20x and 40x Nikon objectives, ISO setting of 3000 and FX-35DX digital camera (Nikon, Japan). The FITC flurophore was detected with the B-1E emission filter containing a dichroic mirror of 510, an excitation filter of 470-490 and a barrier filter of 520-560.

The Bio-Rad MRC-1000 scanning laser confocal microscope was equipped with a krypton-argon laser, a 40x objective with 1.5x zoom, kalman of 4, 0.4µm section thickness for z-series and slow scan speed. Further individual settings for each filter were as follows: emission filter 522/35 (to detect the alexa488 flurophore) was used with iris 3.0, gain 980 and black levels of -4 with 30% laser transmission. Emission filter 585LP (to detect elastin autofluorescence) was used with iris 3.0, gain 1000 and black levels of -4 with 30% laser transmission. Emission filter 680 DF32 (to detect the Cy5 flurophore) was used with iris 3.6, gain 1000 and black levels of -4 with 30-100% transmission. Confocal images were processed using Confocal Assistant software version 4.02 and all images were assimilated into figures using Adobe Photoshop version 6.0 (Adobe Software Ltd, San Jose, CA).

5 Binding interactions of human LTBP-2 with human fibrillin proteins

LTBP-2 is a unique member of the LTBP family since it does not form latent covalent complexes with the TGF-β cytokine and appears to have a unique developmental role as demonstrated since *Ltbp-2*$^{-/-}$ null mice die in pre-implantation stages of development. The function of LTBP-2 within the extracellular matrix has not yet been elucidated, however, since LTBP-2 is strongly associated with fibrillin-containing microfibrils during development in tissues such as aorta and elastic ligaments, LTBP-2 could have an important role within these structures (Gibson *et al.*, 1995). To determine potential roles for LTBP-2 within the ECM, binding partners of LTBP-2 need to be identified. This chapter describes the expression and purification of recombinant LTBP-2 protein and its subsequent use for investigations of direct protein-protein interactions.

Previous sources of LTBP-2 protein required solubilising the protein from bovine tissues by using a rigorous reductive treatment with 6M guanidine (Gibson *et al.*, 1995). Guanidine treatment has been shown to be specific for the extraction of proteins, including fibrillins and MAGPs, that are covalently linked to microfibrils by disulphide bonding thus indicating LTBP-2 is associated with microfibrillar structures (Gibson *et al.*, 1986; Sakai *et al.*, 1986). However, the use of reductive treatment for obtaining protein for direct interaction studies can be disadvantageous since solubilisation of the protein requires disruption of inherent disulphide bonds. If these bonds do not re-form correctly after solubilisation there may be disrupted protein integrity. It is also possible that reductive treatment could affect the integrity of post-translational modifications present upon the protein. Furthermore, bovine or murine sources of proteins would not be ideal for the proposed interaction studies since the majority of the recombinant test proteins to be used within these studies were of human origin. It is best to analyse direct protein-protein interactions between proteins of the same species in as many instances as possible, thus a source of human LTBP-2 protein would be required for these studies. In order to obtain human LTBP-2 using the methods described above, human tissues would be required, these are often difficult to acquire and would involve seeking permission from rare donor sources, introducing ethical complications. An alternative to tissue-extraction for obtaining human proteins would be to produce recombinant proteins. Bacterial expression systems could be used to express these recombinant human proteins. However, bacterial cells do not have the intracellular systems required for the complex post-translational modifications or surveillance systems to ensure accurate protein folding. Furthermore, in order to obtain the

required recombinant protein from the bacterial cells, the protein needs to be denatured and upon renaturation it cannot be guaranteed that the protein will refold authentically.

The most advantageous method for obtaining human LTBP-2 protein is to produce the recombinant protein using a mammalian cell-culture expression system. The use of a mammalian system allows for the expression of human cDNA to produce human proteins using cell lines which contain the required cellular 'machinery' for; a) authentic post-translational modifications and tertiary structures, b) production of a consistent defined product and c) purification of a high yield of the recombinant protein from the culture medium without cellular extraction and protein denaturation. 293-EBNA human embryonic kidney (HEK) cells, obtained commercially from Invitrogen, were selected for production of the recombinant human fibrillin and LTBP proteins for this project. This human cell line has been used successfully in a number of previous studies to produce recombinant human proteins (Colombatti *et al.*, 2000; Hanssen *et al.*, 2004; Isogai *et al.*, 2003; Kim *et al.*, 2002; Nehring *et al.*, 2005; Vollbrandt *et al.*, 2004).

5.1 Expression and purification of recombinant human extracellular matrix macromolecules

5.1.1 Recombinant Human Full-Length LTBP-2

Full-length human LTBP-2 cDNA was successfully cloned (details in section **4.2**) into the episomal expression vector pCEP-4 (**figure 5.1**). Vector pCEP-4 was chosen since it contains the cytomegalovirus (CMV) promoter for high-level transcription of recombinant genes, the Epstein-Barr Virus replication origin (oriP) and nuclear antigen (encoded by the EBNA-1 gene) to permit extrachromosomal replication in human, primate and canine cells. The pCEP-4 vector also carries an ampicillin resistance gene for the selection of transformed JM109 competent cells used for plasmid DNA purification. Purified plasmid DNA was used to transfect mammalian 293-EBNA cells and, since pCEP4 also carries the hygromycin B resistance gene, mammalian cells transfected with recombinant DNA can be selected as stable cell-lines. The amount of hygromycin-B required to select stably transfected cells differs for each cell line and for the 293-EBNA cells was optimised at 1.25mg/L.

To produce recombinant human LTBP-2 a number of amino acid changes were introduced compared with the published sequence (Genbank™ accession number NM_000428) and are listed in **appendix D**. The endogenous LTBP-2 signal peptide was substituted for the signal sequence of human basement membrane protein BM-40 (Genbank™ accession number Y00755) to allow for enhanced gene expression within the HEK cell-line (Nischt *et al.*, 1991), and a 6-histidine (his_6)-tag was added to the C-terminus to allow for protein purification (**figure 5.1**). The transfection and expression of the LTBP-2 construct within the mammalian cell expression system proved to be a challenging but ultimately successful process.

A number of transfections of 293-EBNA cells were attempted using various concentrations of plasmid DNA (0.8μg-4μg/mL) and the resultant recombinant LTBP-2 protein was purified from the serum-free DMEM medium using nickel-sepharose chromatography (see section **4.3** for details on experimental procedure). A ratio of 500μL of Ni-sepharose beads to every 100mL of collected medium was used for protein purification. However, the result of these purifications was an insignificant amount of low quality recombinant protein containing a large number of contaminating proteins (**figure 5.2*A***).

In an attempt to reduce non-specific binding of contaminating proteins, recombinant LTBP-2 (r-LTBP-2) was precipitated from the DMEM serum-free medium using 30-50% (w/v) saturation of ammonium sulphate (see section **4.3** for details on experimental procedure) and was then purified using Ni-chelate chromatography. However, this fractionation had little effect on reducing background contaminants (data not shown). The Ni-chelate columns were reacted with conditioned serum-free medium containing various concentrations of imidazole (1-10mM) and the sepharose:medium ratios were varied from 0.25-1mL of Ni-sepharose for every 100mL of medium. However, these variants had little effect on the quality of the protein purified.

It was also attempted to re-purify the 500mM imidazole eluants containing contaminated r-LTBP-2 by dialysing the eluants from the 500mM imidazole elution buffer into the 10mM imidazole incubation buffer and re-incubating with fresh Ni-charged sepharose. This technique did improve the purity slightly but the r-LTBP-2 was still not considered pure enough for use in binding assays. It was also attempted to concentrate the conditioned medium to reduce the volume to help r-LTBP-2 to compete with contaminants for binding to Ni-charged sepharose. The conditioned medium was concentrated from 100mL to 20mL using a centricon vacuum pump with Diaflo ultrafiltration cellulose membranes (YM10 of diameter 44.5mm; Amicon, Beverly, MA) prior to incubation with Ni-sepharose beads (100μL). Once again the above measures did not improve the yield of r-LTBP-2 (data not shown).

After a number of attempts to purify r-LTBP-2 from cells grown in DMEM, options for using an alternative serum-free medium to enhance recombinant protein expression were explored. Excell 293 serum-free medium, obtained commercially from JRH Biosciences, was tested as it is designed specifically for use with suspension cultures of 293 HEK cell lines. When confluent r-LTBP-2-expressing cells were incubated with Excell 293 medium in place of DMEM, a greatly improved yield of pure r-LTBP-2 protein was obtained (**figure 5.2**). When using the Excell 293 medium, r-LTBP-2 protein was readily expressed and could be purified free of major contaminants using Ni-sepharose chromatography. Recombinant protein was present so abundantly that it was found that an increase in the ratio of Ni-sepharose to serum-free medium from 500μL of Ni-sepharose per 100mL of medium to 1mL of Ni-sepharose for 100mL of medium was required. Three rounds of purification were performed for each batch of

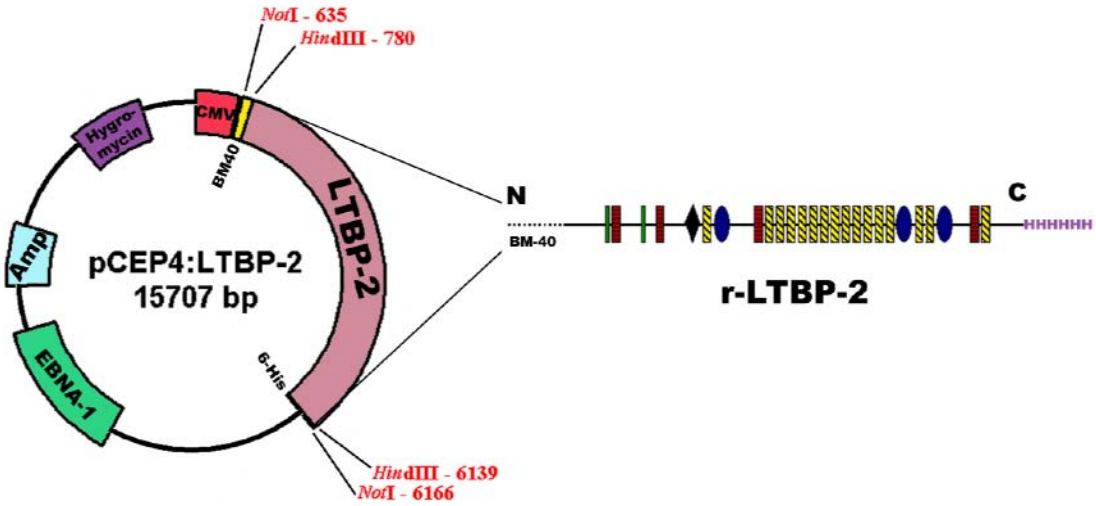

Figure 5.1. Schematic representation of the r-LTBP-2 expression vector and expressed recombinant protein. The modified pCEP-4:LTBP-2 expression vector (15707bp) contains resistance genes for a) ampicillin (allowing for selection of transformed bacterial cells), b) geneticin (EBNA-1 selection) and c) hygromycin (for selection of stably transfected mammalian HEK cells). The cDNA encoding for LTBP-2 was inserted using the *Not*I restriction site of the vector. The cytomegalovirus (CMV) promoter drives expression of the r-LTBP-2 protein modified to contain the sequence for the BM-40 signal peptide and 6-histidine tag. The domain structure of the expressed recombinant protein is shown. The N-terminus (*N*) of r-LTBP-2 contains the BM-40 signal peptide for enhanced protein expression (*dotted line*) and the C-terminus (*C*) region contains the his_6-tag (*purple*) to allow for protein purification. *green rectangles*, 4-cys motif; *red rectangles*, EGF-like domain; *black diamond*, hybrid region; *yellow cross-hatched rectangles*, calcium-binding EGF-like domains; *blue ovoid*, 8-Cys containing motif.

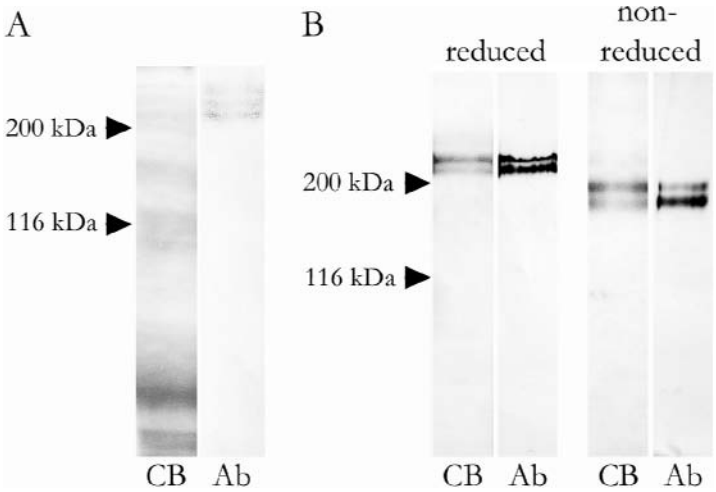

Figure 5.2. Analysis of purified r-LTBP-2 from cells cultured in DMEM and Excell 293 serum-free medium. *A,* r-LTBP-2 (500µg/lane) purified from DMEM serum-free medium and resolved using 8% SDS-PAGE and stained with Coomassie Blue (*CB*). Transfer onto PVDF membrane and probing with the anti-[tetrahis] antibody indicated the presence of three high molecular weight (220-260kDa) r-LTBP-2 bands (*Ab*). *B,* r-LTBP-2 (500µg/lane) purified from cells incubated with Excell 293 culture medium, resolved on 6.5% SDS-PAGE and stained with Coomassie Blue (*CB*). The two protein bands of molecular weight 210- and 219kDa reduced and 170- and 180kDa non-reduced, were immunoreactive to the anti-[tetrahis] antibody following transfer onto PVDF membrane (*Ab*). The *arrowheads* indicate the relative mobilities of concurrently run protein standards.

conditioned medium to extract all of the r-LTBP-2 present. Approximately 4mg of recombinant protein was produced per litre of Excell 293 media. One major disadvantage of using the Excell 293 media in place of DMEM was that the transfected cells were no longer viable after a 2-day incubation period under serum-free conditions, thus a large number of confluent flasks were required. Cell passage numbers also had to be carefully regulated since 6-10 cell passages was shown to result in the production of degraded recombinant protein.

Figure 5.2 illustrates the difference between using DMEM serum-free medium and Excell 293 medium for production of purified r-LTBP-2. The use of DMEM resulted in a number of protein bands (**figure 5.2*A***). When these bands were tested for reactivity to the anti-[tetrahis] antibody three closely spaced high molecular weight bands (210-260kDa) were detected which were presumably r-LTBP-2 (**figure 5.2*A***). These r-LTBP-2 protein bands were not present in high concentrations when compared to the other contaminating protein bands present within the fraction. Thus it was considered that the r-LTBP-2 was of insufficient purity since the contaminating proteins would interfere with subsequent binding studies.

In contrast, improved results were obtained with the Excell 293 medium. Two protein bands were detected in Excell 293 medium when analysed on 6.5% SDS-PAGE, with molecular weight sizes of 210 and 219kDa under reducing conditions and 170 and 180kDa under non-reducing conditions (**figure 5.2*B***). There was no evidence of contaminating protein bands. The molecular weight values of the recombinant LTBP-2 protein corresponded well to the predicted LTBP-2 polypeptide molecular weight (MW) of 195kDa and the size of tissue extracted LTBP-2, which migrates at 240-260kDa and 175-210kDa under reducing and non-reducing conditions respectively (Gibson *et al.*, 1995; Morén *et al.*, 1994). The lower apparent molecular weight of the recombinant protein under non-reducing conditions is consistent with the molecule being stabilised in a folded conformation with extensive disulphide bonding. Western immunoblots confirmed the purified protein was immunoreactive to the anti-[his_6-tag] antibody, tetrahis (**figure 5.2*B***) and the identity of the protein was confirmed as LTBP-2 with specific anti-[LTBP-2-peptide] antibodies, FLP-E (Gibson *et al.*, 1995) and LTBP-2C (**figure 5.3**).

LTBP-2 has 10 potential N-glycosylation sites (Hyytiäinen *et al.*, 1998) and since there was a discrepancy of 15kDa between the predicted MW of r-LTBP-2 (195kDa) and the observed MW of r-LTBP-2 (210kDa), it was thought that the differences in size and/or the multiple bands present may have been due to varying degrees of protein glycosylation. Incubation of the r-LTBP-2 with glycosidase enzymes showed that the r-LTBP-2 doublet was reduced in size by 15kDa in the presence of N-glycosidase but did not change dramatically when digested with O-glycosidase (**figure 5.4**). Incubation with both N- and O-glycosidases also showed a 15kDa difference, thus r-LTBP-2 was found to be extensively N-glycosylated but not significantly O-glycosylated. Glycosidase digestion did not consolidate the multiple bands seen during

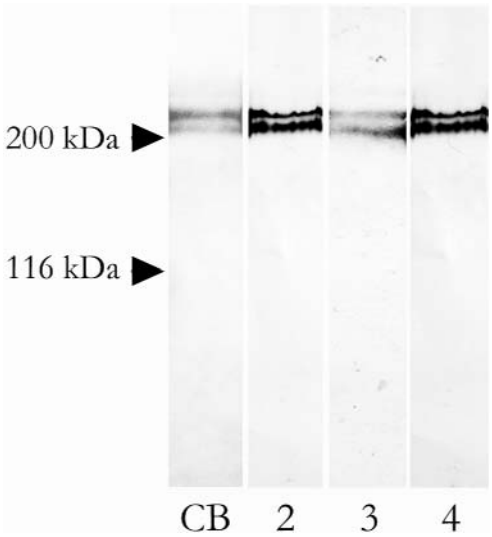

Figure 5.3. Confirmation of the identity of the purified r-LTBP-2 protein. Purified r-LTBP-2 protein was resolved using 6.5% SDS-PAGE and either stained with Coomassie Blue (*CB*) or was transferred onto PVDF membrane and incubated with the anti-[tetrahis] antibody (*lane 2*) or polyclonal serum anti-[LTBP-2 peptide] antibodies, FLP-E (*lane 3*) or LTBP-2C (*lane 4*). The *arrowheads* indicate the relative mobilities of concurrently run protein standards.

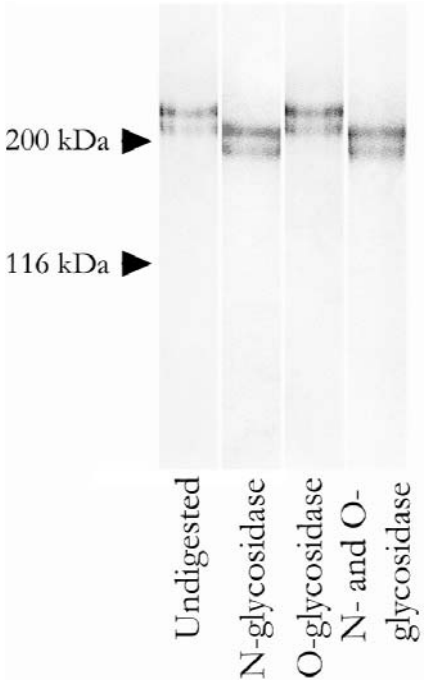

Figure 5.4. r-LTBP-2 has authentic post-translational modifications. r-LTBP-2 (undigested lane) was incubated with N- (0.5U) and O-glycosidases (0.5mU) for 16 hrs at 37^{o}C prior to resolving on 6.5% SDS-PAGE and staining with Coomassie Blue. Digestion with N-glycosidase resulted in reduction of protein size by 15kDa compared to the undigested sample. Digestion with O-glycosidase resulted in minimal size change. Double digestion with N- and O-glycosidase enzymes resulted in reduction of protein size by 15kDa when compared with the undigested sample. The *arrowheads* indicate the relative mobilities of concurrently run protein standards.

analysis of the protein, thus it is possible that other forms of post-translational modifications were occurring to the mature r-LTBP-2 protein.

Imidazole has a similar chemical structure to histidine and was found to interfere with preliminary interaction studies conducted between his_6-tagged recombinant proteins where anti-[his_6-tag] specific antibodies were used to detect binding (data not shown). Thus, the 500mM imidazole was removed from purified recombinant protein fractions. For this, r-LTBP-2 was initially dialysed into TBS with minimal losses using spectrapor dialysis membrane (**appendix B**). However, when r-LTBP-2 was analysed for solubility after a freeze/thaw cycle it was found that r-LTBP-2 had precipitated out of solution in TBS. It was found that the 0.13M sodium chloride concentration in TBS was not high enough to keep r-LTBP-2 soluble after the freezing process. Dialysis of purified r-LTBP-2 into a high salt storage buffer (TBS containing 0.5M sodium chloride) was found to prevent this precipitation. Solubility problems were also resolved if the recombinant protein was a) snap-frozen and stored at -70°C and b) was warmed quickly at 37°C until just thawed prior to aliquoting into amounts for daily use and re-freezing.

The yield of recombinant LTBP-2 produced was consistently around 4mg/L of conditioned media. Dialysed eluants containing 0.5M NaCl with high protein concentrations (over 100µg/mL) could be diluted into TBS for protein assays to give an overall salt concentration similar to those found at physiological levels. For eluants with low concentrations of protein present (less than 100µg/mL), it was found that concentrating the protein using aquacide prior to dialysis into TBS/0.5M NaCl enabled satisfactory concentrations of protein to be obtained. Concentration of proteins using aquacide was advantageous in comparison to other methods of concentrating proteins, such as freeze-drying, since aquacide allowed for the ionic strength of buffer solutions to be maintained. In addition, pooled protein samples with concentrations of 1-50µg/mL could be concentrated to 300µg/mL and dialysed into TBS/0.5M NaCl with minimal losses.

5.1.2 Human Recombinant Fibrillin Fragments

Recombinant fibrillin fragments (**figure 5.5**) were produced as described previously (Hanssen *et al.*, 2004). All fibrillin fragments were expressed using DMEM serum-free media and each recombinant protein was purified free of contaminating proteins using Ni-chelate chromatography with yields of 3-5mg/L per fragment. The recombinant fragments were analysed using 8% SDS-PAGE and western immunoblots to confirm protein identity and sizes (**figure 5.6**). The apparent molecular weights of the recombinant fibrillins fragments are as listed; Fib1(H)NT was 74.8kDa (expected 70-74kDa), Fib1N(H) was 124kDa (expected 100kDa), Fib1C(H) was 135kDa (expected 89kDa), Fib1(H)CT was 67kDa (expected 59-80kDa),

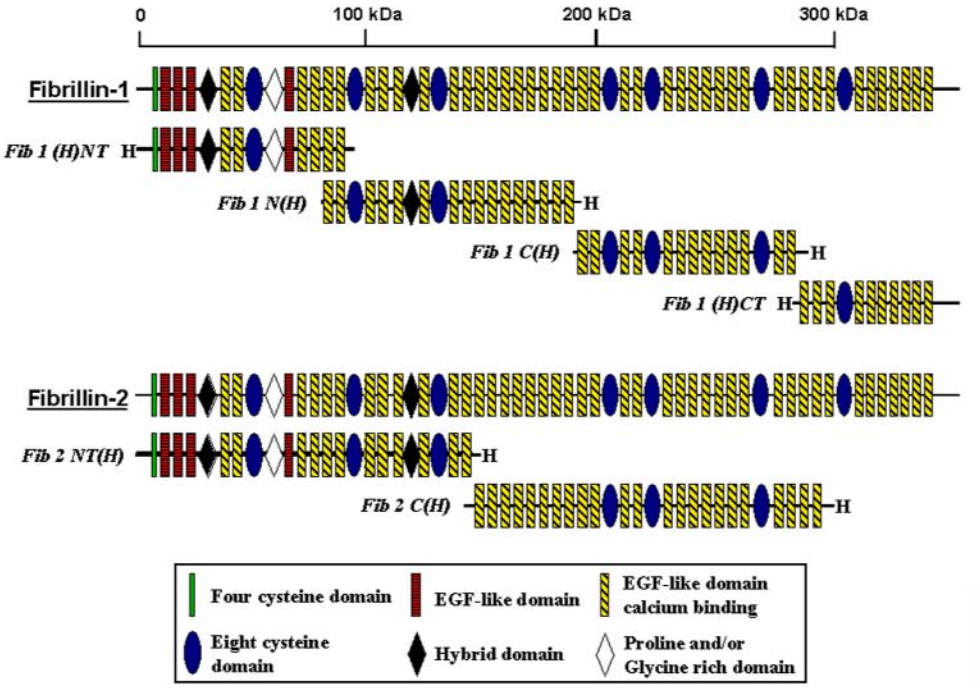

Figure 5.5. Schematic representation of recombinant fibrillin fragments. The domain structure of full length fibrillin-1 and -2 is shown. Four recombinant fragments spanning the length of fibrillin-1 were constructed, Fib1(H)NT, Fib1N(H), Fib1C(H) and Fib1(H)CT. Two recombinant fragments spanning most of fibrillin-2 were constructed; Fib2NT(H), Fib2C(H). *H*, indicates the positions of the his_6-tag for protein purification. Image adapted from Gibson, 1996.

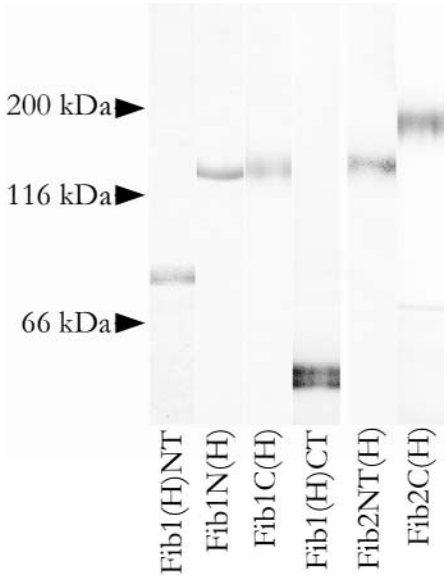

Figure 5.6. Recombinant fibrillin fragments analysed using SDS-PAGE. Recombinant fibrillin fragments were resolved on 8% SDS-PAGE and stained with Coomassie Blue. The four recombinant fragments spanning the length of fibrillin-1 are shown, Fib1(H)NT (74.8kDa), Fib1N(H) (124kDa), Fib1C(H) (135kDa) and Fib1(H)CT (50kDa). Two expressed recombinant fragments for fibrillin-2 are also shown, Fib2NT(H) (130kDa), Fib2C(H) (120kDa). The *arrowheads* indicate the relative mobilities of concurrently run protein standards.

Fib2NT(H) was 130kDa (expected 132kDa) and Fib2C(H) was 120kDa (expected 183kDa). These recombinant fragments were snap frozen and stored at -70°C in TBS and remained soluble in this solution. If necessary fibrillin fragments were concentrated with aquacide prior to dialysis. To remove any aggregated material fibrillin protein stocks were centrifuged at 17,500x g for 5 minutes prior to dilution into working solutions. Once thawed recombinant fibrillin stocks were kept at 4°C for daily use for up to 2 months (Reinhardt *et al.*, 2000; Trask *et al.*, 1999).

5.1.3 Antibody Detection of Recombinant LTBP-2 and Fibrillins

Prior to commencing interaction studies each antibody to be used for detecting the liquid phase test proteins was tested for reaction with the specific protein and for undesired cross-reaction with other recombinant or tissue-derived proteins. Checking for cross-reaction is particularly important for antibodies raised to specific LTBPs and fibrillins. These molecules share such a high degree of structural homology that it is possible some antibodies, particularly rabbit polyclonals, may cross-react with other members of this fibrillin superfamily. It was also useful to have an indication of the signal-to-background ratio and the sensitivity at optimal dilutions for each antibody, to ensure that a minimal amount of specifically bound protein would be detectable in each binding experiment.

Since r-LTBP-2 was engineered with a his_6-tag at its C-terminus, ELISA experiments were performed to determine the optimal dilution of the anti-[his_6-tag] antibody, tetrahis and clarify the least amount of r-LTBP-2 that will be detectable using that chosen dilution. It was established that the anti-[tetrahis] antibody could be used at a 1:2000 dilution with an excellent ratio of signal above background binding (**figure 5.7**). It was determined that at least 1.5ng of bound r-LTBP-2 could be detected above background levels (**figure 5.8**). The specificity of the anti-[tetrahis] antibody for his_6-tagged recombinant proteins was confirmed since no cross-reaction was detected with tissue-derived collagen-IV or type-7S, which do not contain a histidine tag (**figure 5.9**).

Rabbit polyclonal antibodies specific to LTBP-2 peptides, FLP-E (bovine) (made as described previously (Gibson *et al.*, 1995)) and LTBP-2C (human) (made during this PhD candidature, see section **4.8** for details on experimental procedure), were also tested for immunoreactivity to r-LTBP-2. FLP-E was found to react strongly with r-LTBP-2 and did not cross-react with fibrillin-1 or -2 or any other extracellular matrix macromolecules tested (**figure 5.10**). However, using this antiserum the signal-to-background ratio was lower than for the anti-[tetrahis] antibody (**figure 5.9**). Thus the antibody had to be used at a higher concentration (1:30) to obtain a similar positive signal, which contributed to higher levels of non-specific binding (**figure 5.10**).

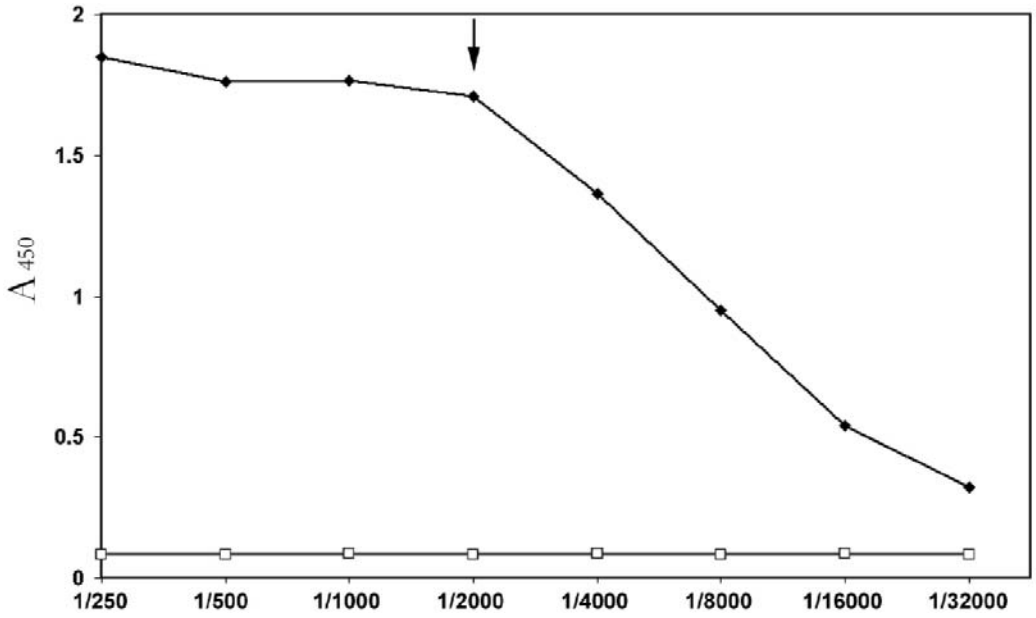

Figure 5.7. ELISA to show r-LTBP-2 was detectable using the anti-[tetrahis] antibody. Individual wells of microtitre plates were coated with r-LTBP-2 (100ng/well, *black diamonds*) in TBS buffer. Control wells were coated with a molar equivalent of BSA (31ng/well, *open squares*). After blocking with 3% BSA/TBS, a serial dilution of anti-[tetrahis] antibody (1:250 to 1:32000) was added to the wells and incubated for 3 hrs at 37^{o}C. After washing, specific binding of the anti-[tetrahis] antibody was detected at 450nm using peroxidase-conjugated secondary antibody and colour development for 5 minutes. *Arrow* indicates the optimal antibody working dilution of 1:2000.

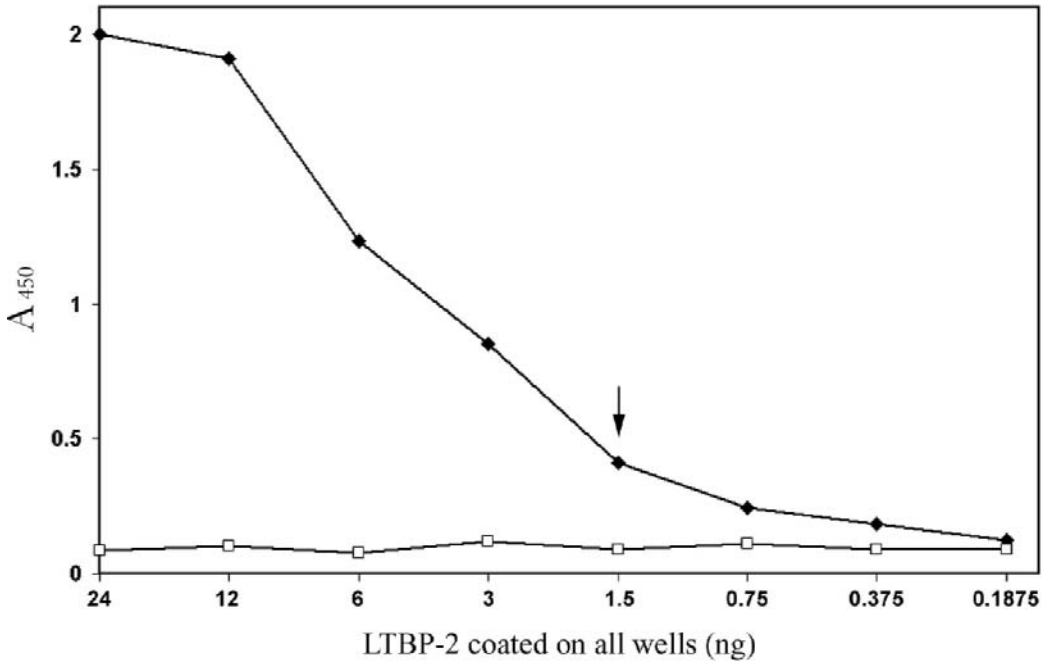

Figure 5.8. ELISA to show the minimum amount of r-LTBP-2 detectable with a 1:2000 dilution of the anti-[tetrahis] antibody. Individual wells of microtitre plates were coated with a serial dilution of r-LTBP-2 (0.1875-24ng/well, *black diamonds*) or a molar equivalent of BSA (*open squares*) using TBS buffer. After blocking with 3% BSA/TBS, anti-[tetrahis] antibody (1:2000 dilution) was added to each well and incubated for 3 hrs at 37^{o}C. After washing, specific binding of the anti-[tetrahis] antibody was detected at 450nm using peroxidase-conjugated secondary antibody and colour development for 60 minutes. *Arrow* indicates that 1.5ng of r-LTBP-2 was detectable using a 1:2000 dilution of the anti-[tetrahis] antibody.

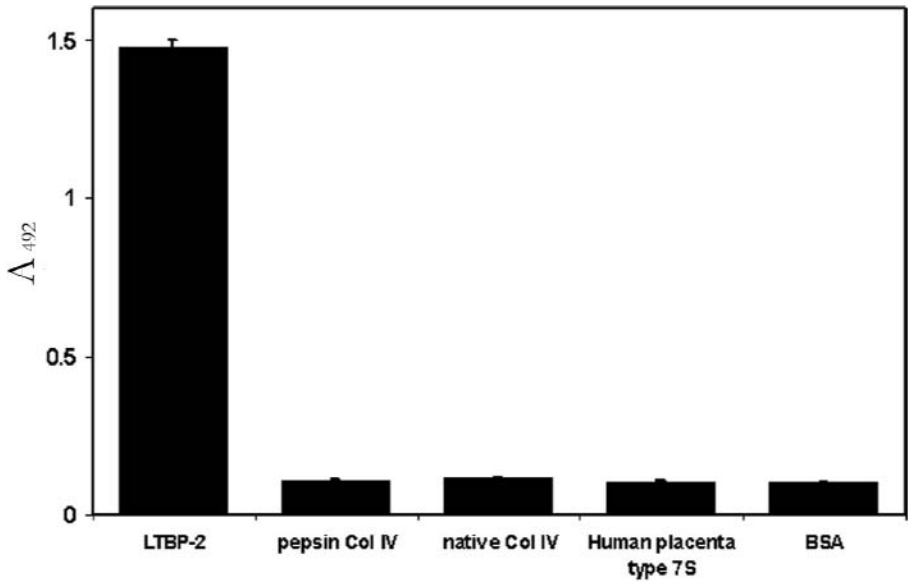

Figure 5.9. ELISA to screen for cross-reactivity of the anti-[tetrahis] antibody with collagens. Individual wells of microtitre plates were coated with collagen proteins (400ng/well), r-LTBP-2 (100ng/well) or BSA (100ng/well) in TBS buffer. After blocking with 3% BSA/TBS, anti-[tetrahis] antibody (1:2000 dilution) was added to each well and incubated for 3 hrs at 37^{o}C. After washing, specific binding of the anti-[tetrahis] antibody was detected at 492nm using peroxidase-conjugated secondary antibody and colour development for 30 minutes. Means ± S.D. and binding of triplicate determinations are shown.

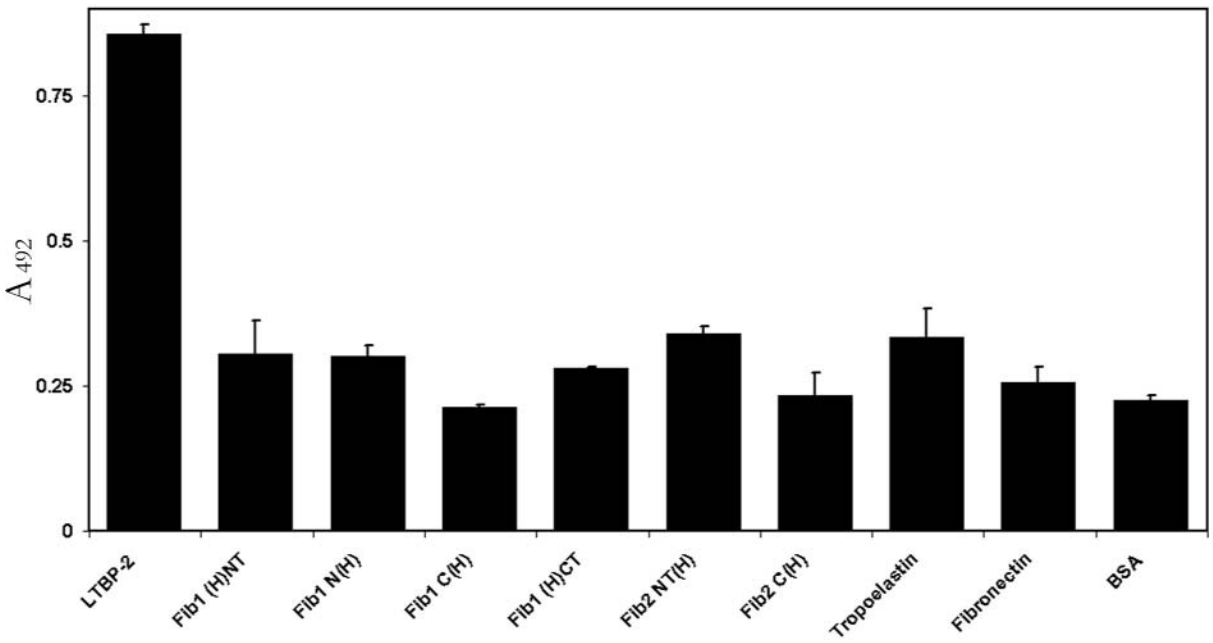

Figure 5.10. ELISA to screen for cross-reactivity of anti-[LTBP-2 peptide] antibody, FLP-E, with extracellular matrix macromolecules. Individual wells of microtitre plates were coated with r-LTBP-2 (200ng/well) or molar equivalents of other test proteins and BSA as a control in TBS buffer. After blocking with 3% milk/TBS, anti-[LTBP-2 peptide] antibody, FLP-E (1:30 dilution) was added to wells and incubated for 3 hrs at 37^{o}C. After washing, specific antibody binding was detected at 492nm using peroxidase-conjugated secondary antibody and colour development for 15 minutes. Means ± S.D. and binding of triplicate determinations are shown.

In contrast to the FLP-E antibody, the rabbit polyclonal antibody, LTBP-2C, made to recognise a peptide from the C-terminal region of the human LTBP-2, was strongly immunoreactive to r-LTBP-2 with a titre of at least 1:64000 (**figure 5.11**), although the antibody was more commonly used at dilutions of at least 1:10000 to ensure accurate volume measurements (**figure 5.11**). This antibody did not cross-react with any extracellular matrix macromolecules tested (**figures 5.12** and **5.13**). r-LTBP-2 was routinely screened for cross-reactivity to antibodies raised to other extracellular matrix macromolecules before each set of binding interaction studies as discussed in further detail below.

Monoclonal antibodies raised against the fibrillin fragments were used at concentrations previously determined within the laboratory and are listed in **appendix C**, these antibodies were routinely checked for cross-reaction to r-LTBP-2 during individual experiments as described below. However, for immunofluorescence analysis a polyclonal anti-[fibrillin-1] antibody, Fib1A was required for dual labelling experiments (see **chapter 8** for details). Antibody Fib1A was screened for cross-reaction to LTBPs and fibrillin-2. It was shown that the antibody had specificity to Fib1(H)NT as expected when used at a 1:500 dilution and did not cross-react with other fibrillin-1 fragments, LTBPs or fibrillin-2 (**figure 5.14**).

5.2 The analysis of LTBP-2 interactions with fibrillins

5.2.1 Solid Phase Binding Studies

It was decided to screen a selection of extracellular macromolecules for protein-protein interaction with r-LTBP-2 using the simple, high-throughput solid phase binding method. These assays function by coating a test protein onto individual wells of maxisorb microtitre plates, which has high affinity for proteins with both hydrophilic and hydrophobic domains. The remaining binding sites were blocked using a 3-5% low-fat dried milk or BSA solution. The second test protein is then added in solution and incubated for 3 hours at 37°C. Protein-protein interactions are detected by using either a) antibodies specific to the protein in solution followed by colour detection or b) γ-counting in cases where the test protein, in solution, has been radiolabelled. Control wells required for each experiment include a) replacing the liquid phase protein with the molar equivalent of BSA to detect any cross-reaction of the protein coated on the well with the antibody specific to the test protein in solution and b) replacing the protein coated on the well with the molar equivalent of BSA to determine the level of background binding of the liquid phase test protein to the well. If experimental wells showed significant binding above background wells, further studies such as overlay blot assays, were then conducted to confirm the protein-protein interaction. Kinetic dissociation constants were calculated from specific binding curves to determine the strength of each association.

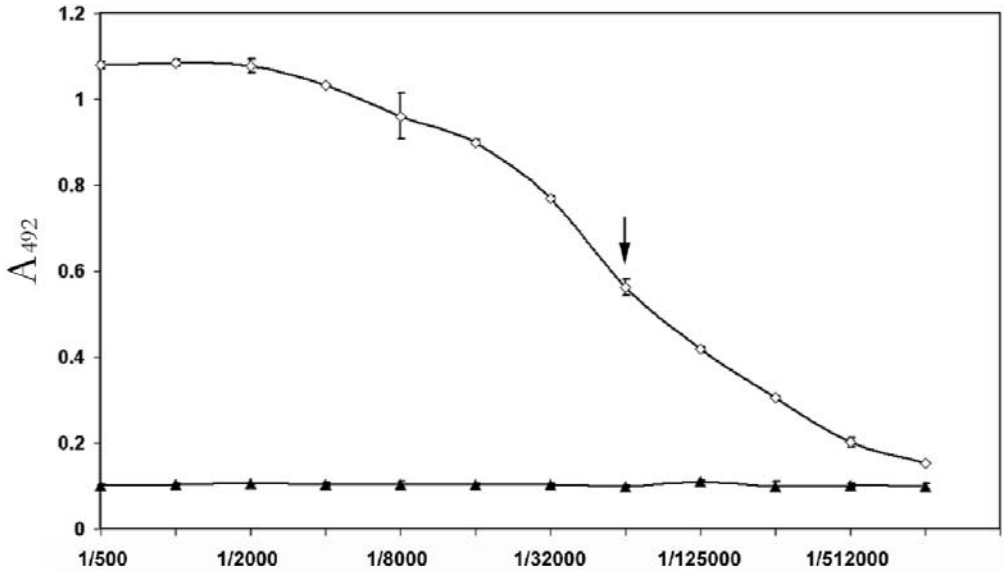

Figure 5.11. ELISA to determine the sensitivity of the polyclonal anti-[LTBP-2 peptide] antibody, LTBP-2C. Individual wells of microtitre plates were coated with r-LTBP-2 (50ng/well, *open diamonds*) in TBS buffer. Control wells were coated with a molar equivalent of BSA (16ng/well, *black triangles*). After blocking with 5% diploma milk/TBS, a serial dilution of anti-[LTBP-2 peptide] antibody, LTBP-2C (1:500 to 1:1024000) was added to the wells and incubated for 3 hrs at 37°C. After washing, specific binding of the LTBP-2C antibody was detected at 492nm using peroxidase-conjugated secondary antibody and colour development for 10 minutes. *Arrow* indicates the optimal titre of 1:64000. Means ± S.D. of triplicate determinations are shown.

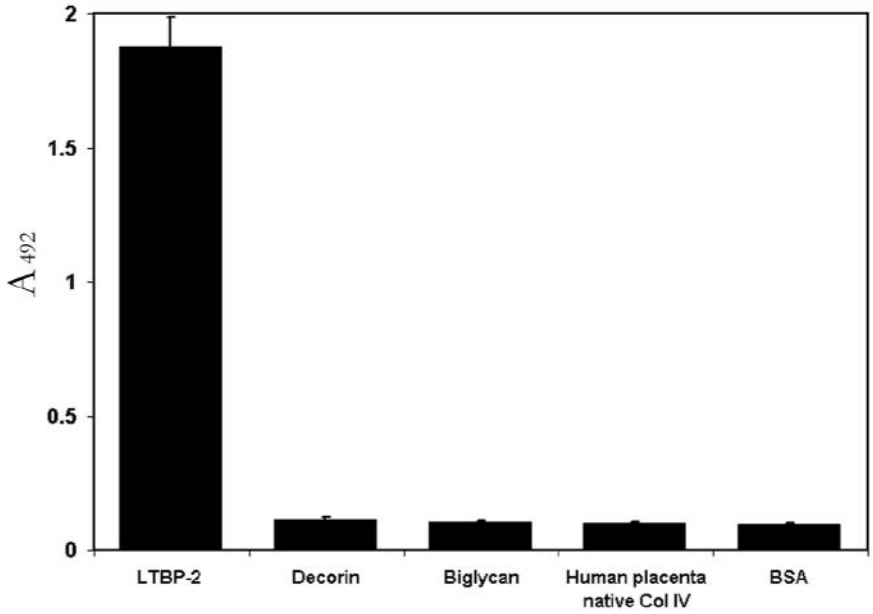

Figure 5.12. ELISA to determine cross-reactivity of anti-[LTBP-2 peptide] specific antibody, LTBP-2C with decorin, biglycan and collagen-IV. Individual wells of microtitre plates were coated with decorin (200ng/well), biglycan (200ng/well), collagen-IV (200ng/well), r-LTBP-2 (50ng/well) or BSA (400ng/well) in TBS buffer. After blocking with 5% diploma milk/TBS, antibody LTBP-2C (1:10000 dilution) was added to wells and incubated for 3 hrs at 37°C. After washing, specific binding of the LTBP-2C antibody was detected at 492nm using peroxidase-conjugated secondary antibody and colour development for 30 minutes. Means ± S.D. and binding of triplicate determinations are shown.

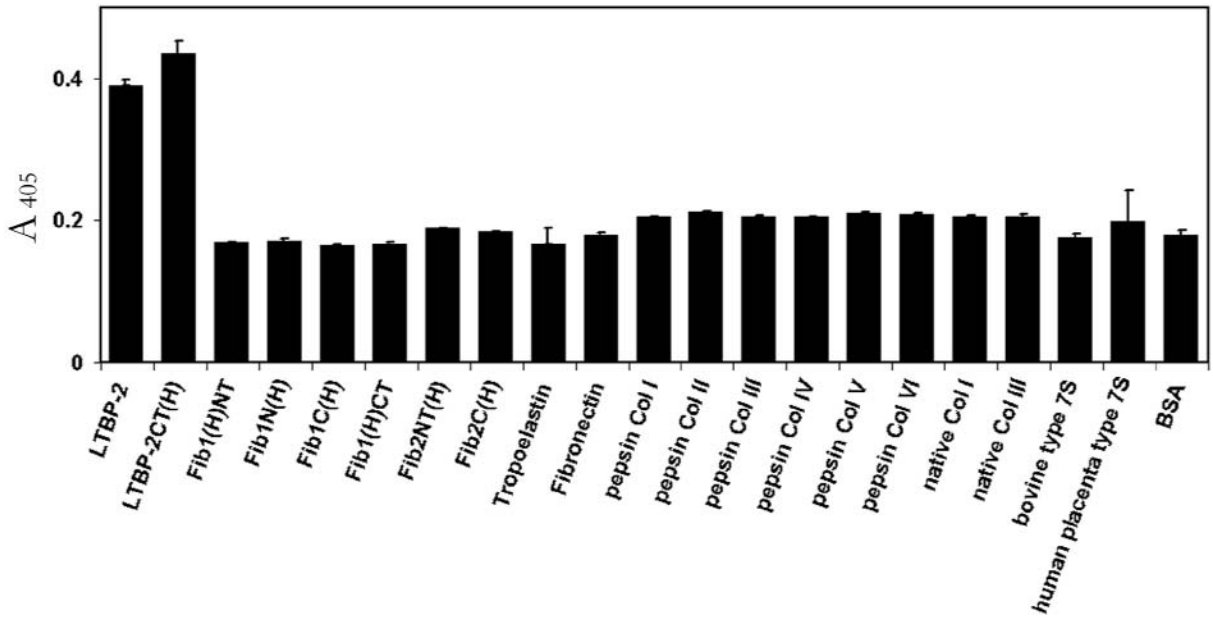

Figure 5.13. ELISA to test for cross-reactivity of anti-[LTBP-2 peptide] antibody, LTBP-2C with fibrillins, collagens and a range of other extracellular matrix macromolecules. Individual wells of microtitre plates were coated with extracellular macromolecules (200ng/well), LTBP-2 (50ng/well) or BSA (16ng/well) in TBS buffer. After blocking with 5% diploma milk/TBS, antibody LTBP-2C (1:10000 dilution) was added to each well and incubated for 3 hrs at 37°C. After washing, specific binding of the LTBP-2C antibody was detected at 405nm using peroxidase-conjugated secondary antibody and colour development for 30 minutes. Means ± S.D. and binding of triplicate determinations are shown.

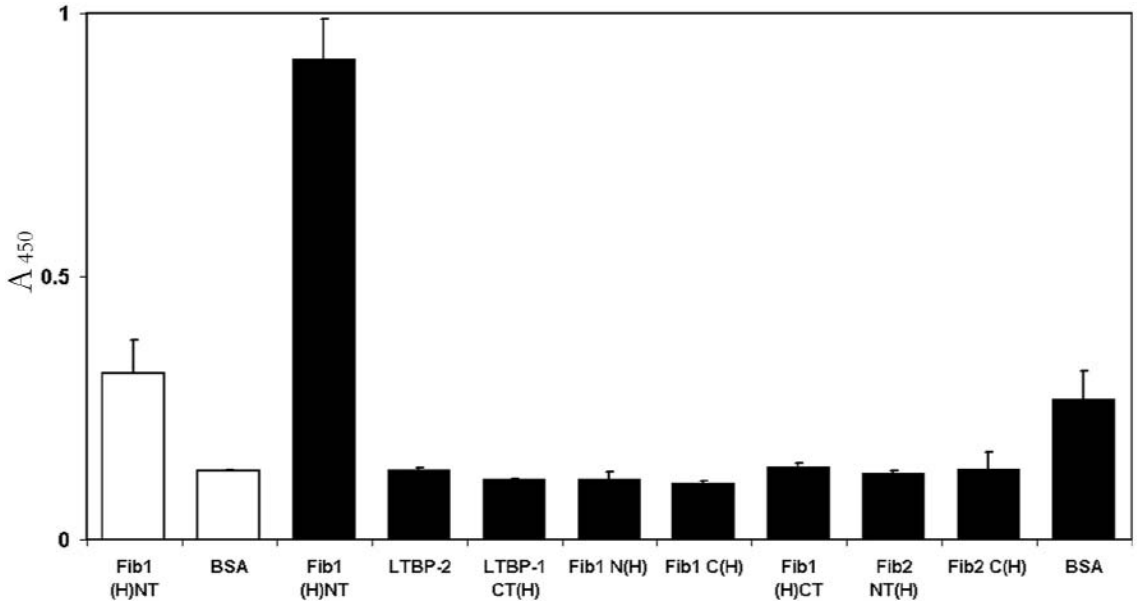

Figure 5.14. ELISA to determine reactivity of antibody Fib1A with fibrillins-1 and –2 and LTBPs. Individual wells of microtitre plates were coated with Fib1(H)NT (50ng/well) or a molar equivalent of all other LTBP or fibrillin test molecules in TBS/2mM $CaCl_2$. Control wells were coated with a molar equivalent amount of BSA (44ng/well). After blocking with 5% milk/TBS, mouse monoclonal anti-[fibrillin-1] antibody, MAB2502 (1:5000 dilution, *white columns*) or rabbit polyclonal anti-[fibrillin-1 peptide] antibody, Fib1A (1:500 dilution, *black columns*) was added to wells and incubated for 2 hrs at 37°C. After washing, specific binding of the MAB2502 and Fib1A antibodies were detected at 450nm using peroxidase-conjugated secondary antibody and colour development for 20 minutes. Means ± S.D. and binding of triplicate determinations are shown.

Prior to commencing solid phase binding assays the optimal blocking conditions had to be determined to prevent non-specific background binding of the protein to the plastic wells used for coating the test proteins. An example of a large degree of non-specific background binding could be found especially in the cases where r-LTBP-2 was used in solution (as an example see **figure 9.1** *(black columns)*). In most experiments 3% low-fat milk powder (dutch jug brand) or 3% BSA (for anti-[tetrahis] antibody) was being used for blocking. However, these blocking conditions were not optimal to minimise non-specific background binding of the liquid phase protein to the plastic wells. In order to reduce this non-specific background binding, it was decided to check different protein solutions and block concentrations, to optimise conditions prior to commencing interactions studies between r-LTBP-2 and fibrillins.

It was found that using 3% (w/v) ovalbumin (**figure 5.15**, *white columns*), 1% (v/v) tween-20 or 1% (w/v) collagen-I (**figure 5.16**) as block solutions did not reduce the non-specific background binding of r-LTBP-2 protein, added in the liquid phase, to the plastic wells. The addition of 2mM Ca^{2+} ions to buffer solutions did reduce background binding, especially in the case of wells blocked with BSA, which would be advantageous when anti-[his_6-tag] antibodies were used in assays (**figures 5.15** and **5.16**) and Ca^{2+} was added to all subsequent buffer solutions. Since milk seemed to be the best option for blocking non-specific binding of other antibodies, another brand of non-fat skim milk powder (diploma) was tested in an attempt to reduced background binding. It was found that in most cases, 5% (w/v) diploma skim milk solution was the best brand and concentration to use to give minimal background binding levels (**figure 5.17**).

5.2.2 LTBP-2 Interacts with the N-terminal Region of Fibrillin-1

An interaction between the N-terminal regions of fibrillin-1 and -2 with LTBP-1, and the N-terminal region of fibrillin-1 with LTBP–4 has recently been reported (Isogai *et al.*, 2003). In that study, LTBP-3 was found not to interact with fibrillin-1 and binding of LTBP-3 to fibrillin-2 was not investigated. Furthermore, that paper did not analyse the potential for interactions between LTBP-2 and fibrillins (Isogai *et al.*, 2003). A major aim of the experiments conducted within this thesis was to investigate the interaction of LTBP-2 with fibrillins. Using solid phase binding assays, r-LTBP-2 was tested for interaction with a number of ^{125}I-labelled recombinant fibrillin-1 and -2 fragments, which are shown schematically in **figure 5.5**. It was found that r-LTBP-2 interacts specifically with the N-terminal region of fibrillin-1 [Fib1(H)NT] but not with the analogous region of fibrillin-2 [Fib2NT(H)] (**figure 5.18** and **5.19**). Using ^{125}I-labelled fibrillin fragments in solution it was shown that a significant interaction occurred between the r-LTBP-2 coated on the well and the ^{125}I-labelled Fib1(H)NT fragment in solution, when compared with the background signal (**figure 5.18**, *white columns*). No significant interactions occurred with the

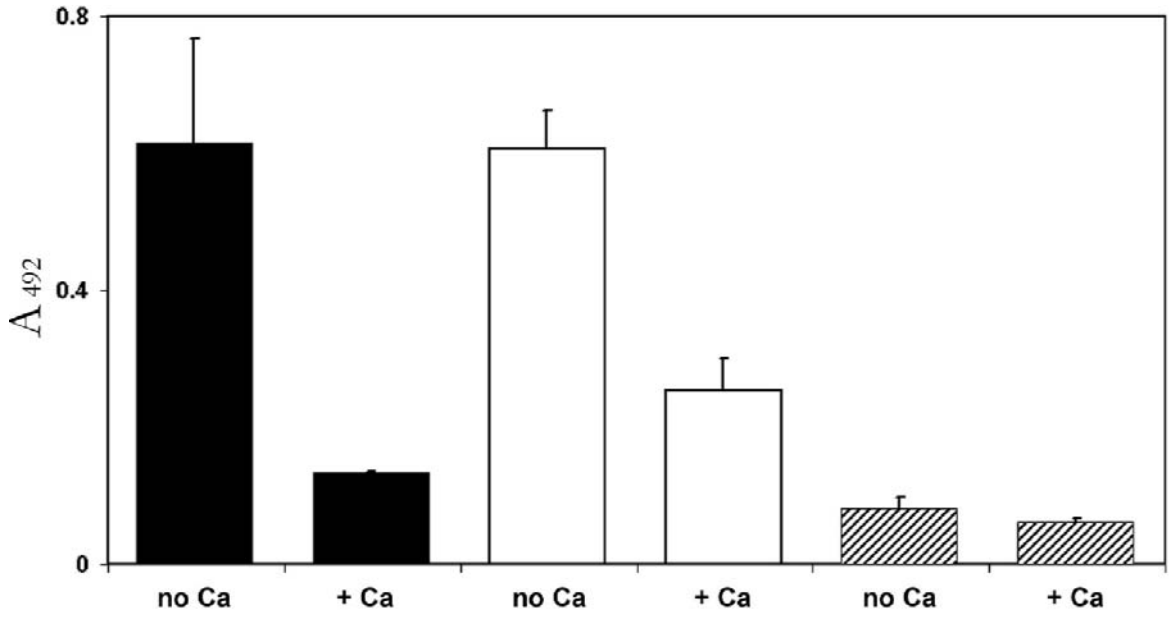

Figure 5.15. Solid phase binding assay showing milk solution gives lowest background binding of r-LTBP-2 to the plastic wells. Individual wells of microtitre plates were coated with BSA (400ng/well) and were blocked in 3% BSA (*black columns*), 3% ovalbumin (*white columns*) or 3% dutch jug milk solution (*cross-hatched columns*) in TBS buffer. r-LTBP-2 (400ng/well) was added in the absence or presence of 2mM $CaCl_2$ and left to incubate for 3 hrs at 37°C. After washing, anti-[tetrahis] antibody (1:2000 dilution) was added to wells and incubated for 2 hrs at 37°C. After washing specific binding of the anti-[tetrahis] antibody was detected at 492nm using peroxidase-conjugated secondary antibody and colour development for 30 minutes. Means ± S.D. and binding of triplicate determinations are shown.

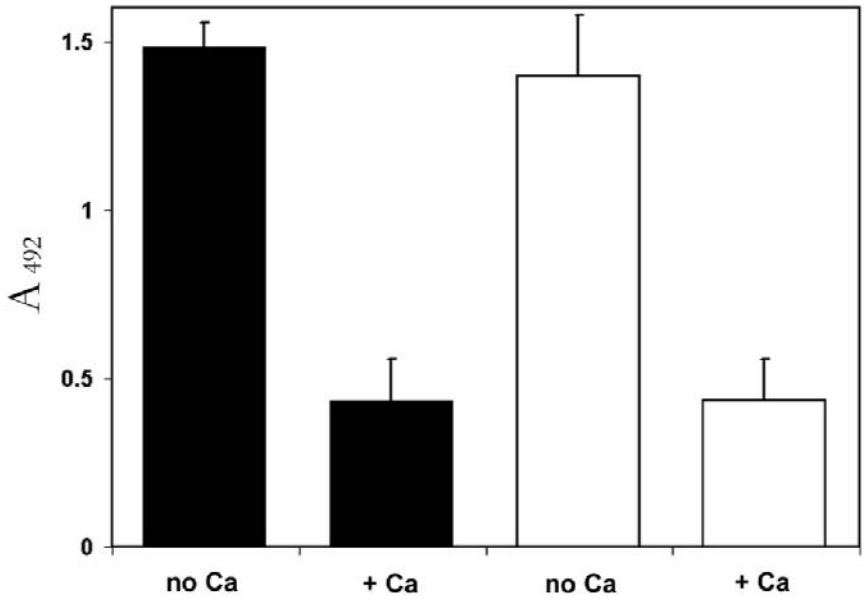

Figure 5.16. Solid phase binding assay showing tween-20 and collagen-I do not block background binding of r-LTBP-2 to the plastic. Individual wells of microtitre plates were blocked in 1% tween-20 (*black columns*) and 1% collagen-I solution (*white columns*) in TBS buffer. r-LTBP-2 (400ng/well) was added to wells in the absence or presence of 2mM $CaCl_2$ and incubated for 3 hrs at 37°C. After washing, anti-[tetrahis] antibody (1:2000 dilution) was added to wells and incubated for 2 hrs at 37°C. After washing, specific binding of the anti-[tetrahis] antibody was detected at 492nm using peroxidase-conjugated secondary antibody and colour development for 30 minutes. Means ± S.D. and binding of triplicate determinations are shown.

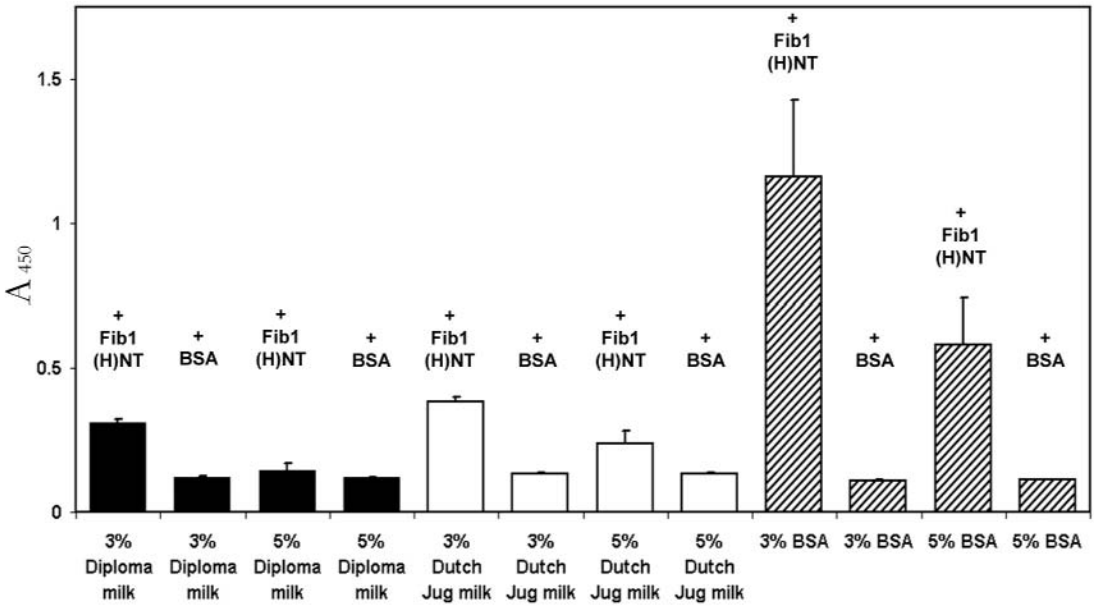

Figure 5.17. Solid phase binding assay showing 5% (w/v) diploma brand milk solution gives optimal blocking. Individual wells of microtitre plates were blocked in Diploma brand milk solution (*black columns*), dutch jug brand milk solution (*white columns*) and BSA (*cross-hatched columns*) in 3% and 5% (w/v) concentrations in TBS/2mM $CaCl_2$ buffer. Fib1(H)NT (280ng/well) or BSA (247ng/well), diluted in TBS/2mM $CaCl_2$ buffer, was added to appropriate wells and incubated for 3 hrs at 37°C. After washing, anti-[fibrillin-1] antibody, MAB2502 (1:2000 dilution) was added to wells and incubated for 2 hrs at 37°C. After washing, specific binding of the MAB2502 antibody was detected at 450nm using peroxidase-conjugated secondary antibody and colour development for 30 minutes. Means ± S.D. and binding of triplicate determinations are shown.

^{125}I-labelled [Fib1N(H)], [Fib2NT(H)] or [Fib2C(H)] fragments in solution (**figure 5.18**). This finding indicates that LTBP-2 interacts exclusively with fibrillin-1 and that the binding region is located at the N-terminus (**figure 5.5**).

To confirm the interaction between LTBP-2 and Fib1(H)NT, another solid phase binding assay was conducted with the recombinant fibrillin fragments coated on the well and ^{35}S-labelled r-LTBP-2 in solution. r-LTBP-2 was labelled with ^{35}S since in some cases it is possible that synthetic radiolabelling of recombinant proteins with ^{125}I could mask potential binding sites through conformational changes or steric hinderance. ^{35}S is advantageous since this radiolabel is added to culture medium during protein production and incorporates biosynthetically in place of cysteine and methionine residues. A solid phase binding assay conducted with ^{35}S-labelled r-LTBP-2 in solution and Fib1(H)NT coated on the well verified the exclusive interaction between fibrillin-1 and LTBP-2. No significant interactions above background levels were found between ^{35}S-labelled r-LTBP-2 and the other fibrillin fragments tested [Fib1N(H)], [Fib1C(H)], [Fib1(H)CT] and [Fib2C(H)] (**figure 5.19**). However, it should be noted that in most cases when r-LTBP-2 was used in liquid phase it was found a large amount of non-specific background binding to the plastic wells interfered with the differential binding signal between positive interactions and BSA control wells (an example can be found in **figure 9.1**).

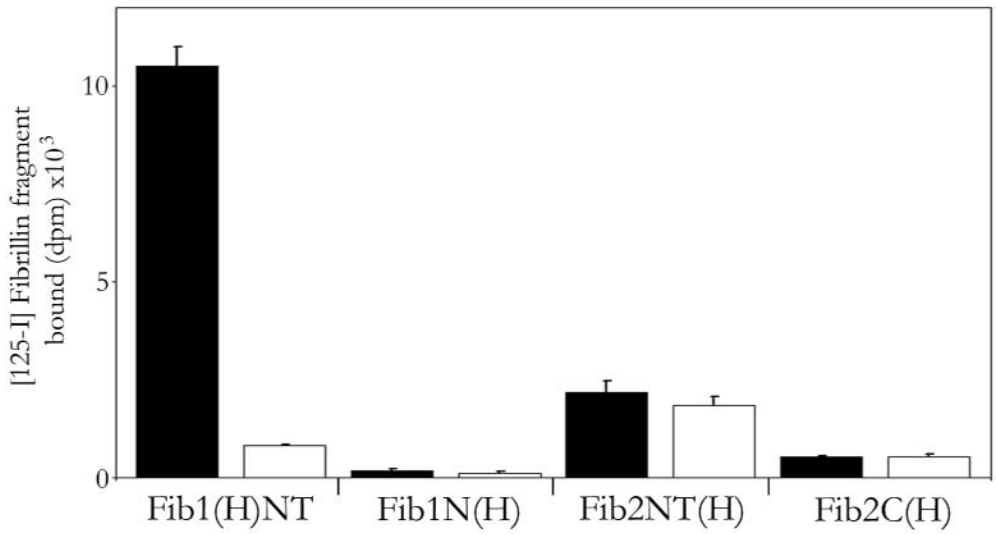

Figure 5.18. Solid phase binding assay showing that the ^{125}I-labelled N-terminal recombinant fragment of fibrillin-1 [Fib1(H)NT] interacts with r-LTBP-2. Individual wells of microtitre plates were coated with r-LTBP-2 (200ng/well, *black columns*) in TBS/2mM $CaCl_2$. Control wells were coated with the molar equivalent of BSA (62ng/well, *white columns*). After blocking with 3% milk/TBS, $8x10^5$dpm of ^{125}I-labelled Fib1(H)NT, Fib1N(H), Fib2NT(H) and Fib2C(H) (each of specific activity $1.28x10^7$dpm/μg) was added to wells and incubated for 3 hrs at 37°C. After washing, binding of the radioligand was measured by direct γ counting. Means ± S.D. and binding of triplicate determinations are shown.

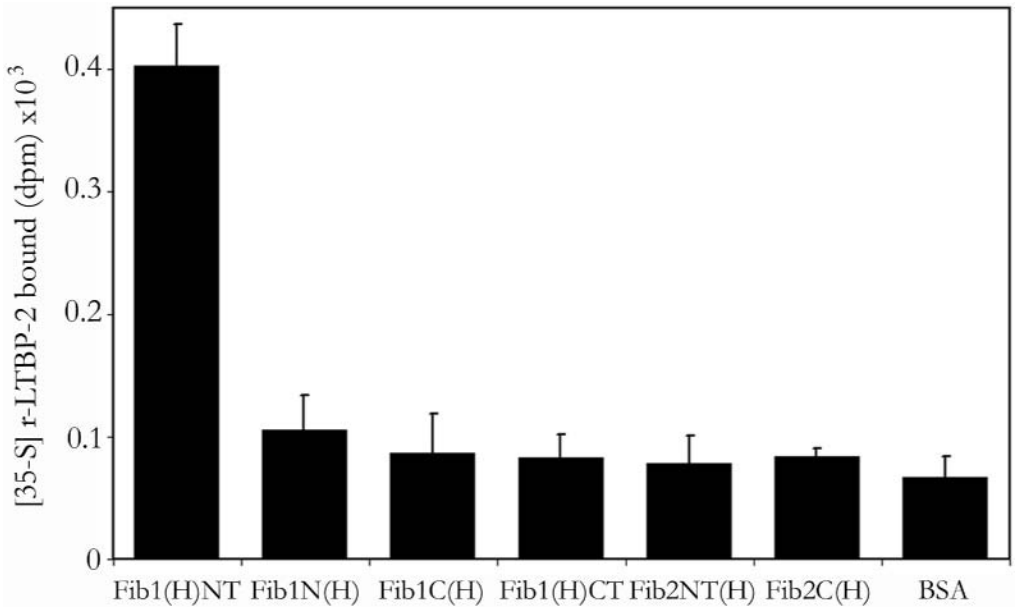

Figure 5.19. Solid phase binding assay showing ^{35}S-labelled r-LTBP-2 interacts exclusively with Fib1(H)NT. Individual wells of microtitre plates were coated with molar equivalents of the following recombinant fibrillin fragments, [Fib1(H)NT] (50ng/well), [Fib1N(H)] (120ng/well), [Fib1C(H)] (120ng/well), [Fib1(H)CT] (60ng/well), [Fib2NT(H)] (125ng/well), [Fib2C(H)] (170ng/well) or BSA (62ng/well) in TBS/2mM $CaCl_2$ buffer. After blocking with 3% milk/TBS, $1.28x10^4$dpm of ^{35}S-labelled r-LTBP-2 (specific activity $1.28x10^5$dpm/μg) was added to wells and incubated for 3 hrs at 37°C. After washing, binding of the radioligand was measured by scintillation counting. Means ± S.D. and binding of triplicate determinations are shown.

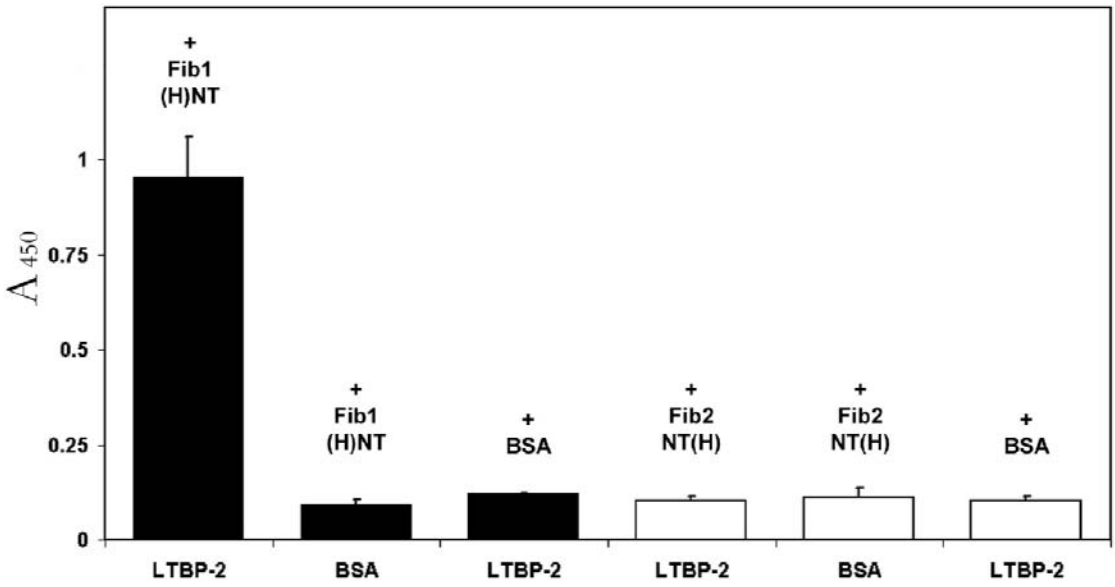

Figure 5.20. Solid phase binding assay to show the interaction between r-LTBP-2 and unlabelled Fib1(H)NT can be detected using anti-[fibrillin-1] antibody, MAB2502. Individual wells of microtitre plates were coated with r-LTBP-2 (400ng/well) in TBS/2mM $CaCl_2$. Control wells were coated with the molar equivalent of BSA (124ng/well). After blocking with 5% diploma milk/TBS, Fib1(H)NT (290ng/well, *black columns*) and Fib2NT(H) (500ng/well, *white columns*) were added to wells and incubated for 3 hrs at 37°C. After washing, anti-[fibrillin-1] antibody, MAB2502 (1:5000 dilution, *black columns*) and anti-[fibrillin-2] antibody, 16E12 (1:100 dilution, *white columns*) was added to wells and incubated for 2 hrs at 37°C. After washing, specific binding of the MAB2502 or 16E12 antibody was detected at 450nm using peroxidase-conjugated secondary antibody and colour development for 60 minutes. Means ± S.D. of triplicate determinations are shown.

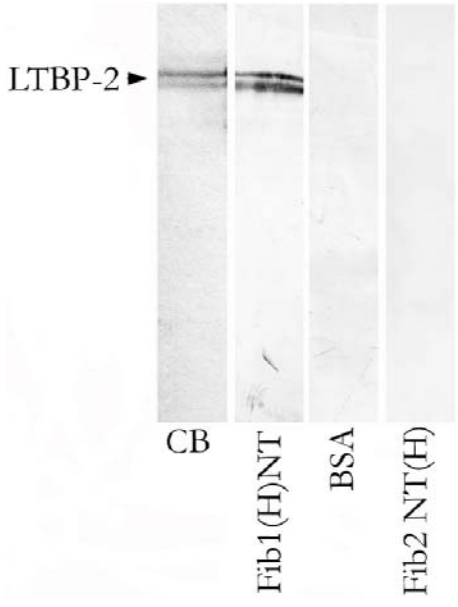

Figure 5.21. Overlay immunoblot to confirm interaction between r-LTBP-2 and Fib1(H)NT. r-LTBP-2 (1µg/lane) was resolved by SDS-PAGE on a 8% gel under reducing conditions and stained with Coomassie Blue (*CB*) or transferred onto PVDF membrane. After equilibration in binding buffer (TBS containing 2mM $CaCl_2$, see section 5.2.3 for explanation on adding calcium) and blocking with 3% milk/TBS, duplicate blots were incubated with 5µg/mL Fib1(H)NT or BSA for 8 hours at 4°C. Specific binding of Fib1(H)NT to r-LTBP-2 (~200kDa) was detected with anti-[fibrillin-1] antibody, MAB2502 (1:2000 dilution). A further blot was incubated with 5µg/mL Fib2NT(H) followed by the anti-[fibrillin-2] antibody, 16E12 (1:100 dilution) and showed no binding of Fib2NT(H) to r-LTBP-2.

Thus, subsequent binding assays for further analysis of the interaction between LTBP-2 and fibrillin-1 were conducted with the recombinant fibrillin-1 fragment in solution.

The specific interaction between r-LTBP-2 and the N-terminal region of fibrillin-1 [Fib1(H)NT] was again confirmed using a solid phase binding assay where binding between r-LTBP-2 and unlabelled r-Fib1(H)NT was detected using the monoclonal anti-[fibrillin-1] antibody, MAB2502 (**figure 5.20**, *black columns*). It was also verified that r-LTBP-2 does not interact with the analogous N-terminal region of fibrillin-2 [Fib2NT(H)] detected using the monoclonal anti-[fibrillin-2] specific antibody, 16E12 (**figure 5.20**, *white columns*). Control wells conducted where the BSA was used as a substitution for the r-fibrillin fragments in solution confirmed that the positive signal was not due to cross-reaction between r-LTBP-2 and antibody MAB2502 (**figure 5.20**).

Overlay immunoblots were used as an alternate technique to confirm protein-protein interactions detected in the solid phase binding experiments. This procedure involved the blotting of one protein [such as r-LTBP-2] onto PVDF membrane and after blocking, incubating the blot with the second test protein [such as Fib1(H)NT] in solution. Binding was detected using an antibody specific to the protein added in solution. If an interaction occurred between the immobilised protein and the protein in solution then a band(s) should appear at the expected size of the immobilised protein after colour detection. To determine if non-specific binding of the primary or secondary antibodies occurred a further control blot was carried out with BSA added in solution.

Overlay immunoblots were carried out to confirm the interaction of r-LTBP-2 with fibrillin-1. r-LTBP-2 was resolved on 8% SDS-PAGE followed by blotting onto PVDF membrane. After blocking, r-LTBP-2 blots were incubated with the recombinant N-terminal fragments of fibrillin-1 and -2. It was found that the blot strip incubated with Fib1(H)NT showed two bands, which matched in molecular size to the r-LTBP-2 standard stained with Coomassie Blue (**figure 5.21**). However, no bands appeared on an analogous blot incubated with Fib2NT(H) and no bands were detected in the BSA control, thus indicating that there was no cross-reaction between r-LTBP-2 and antibody MAB2502 or the phosphatase-conjugated secondary antibody (**figure 5.21**). These western overlay blots corroborated the results of the solid phase binding assay in that there was an interaction of LTBP-2 with fibrillin-1 but not with fibrillin-2.

5.2.3 The Interaction Between LTBP-2 and Fibrillin-1 is Cation Dependent

Both LTBP-2 and fibrillin-1 have a large number of calcium binding-EGF domains, and the conformation of these proteins is dependent on the presence of cations most likely to be Ca^{2+}

(see **figure 2.6**) (Corson *et al.*, 1993; Morén *et al.*, 1994). Therefore, it was strongly suspected that Ca^{2+} ions could directly or indirectly influence the binding between LTBP-2 and fibrillin-1. Solid phase binding assays were conducted between r-LTBP-2 and Fib1(H)NT in the presence of a range of concentrations of Ca^{2+} ions (0.1mM-2mM), and EDTA, a chemical which chelates Ca^{2+} ions. 0.1mM to 2mM Ca^{2+} ion concentrations were chosen since they are commonly used in published literature for interaction studies (Hanssen *et al.*, 2004; Isogai *et al.*, 2003; Reinboth *et al.*, 2002). It was found that the addition of 2mM Ca^{2+} ions gave interaction levels that were marginally higher than those without calcium added or for the other concentrations of $CaCl_2$ tested (**figure 5.22**). Consequently, 2mM Ca^{2+} ions was added to all subsequent solid phase assays. However, it was also shown that in the presence of 5mM EDTA the interaction between r-LTBP-2 to Fib1(H)NT was almost completely abolished (**figure 5.22**). EDTA is a chemical known to chelate divalent cations and since the interaction between r-LTBP-2 and Fib1(H)NT is abolished in the presence of EDTA, this indicates that this interaction requires divalent cations to be present and most likely the cations involved would be calcium due to the large number of cbEGF domains within the two molecules. If the interaction of r-LTBP-2 with fibrillin-1 were not dependant on cations (calcium) then the presence of added EDTA would have had minimal impact on the binding levels. Thus, the above findings indicate that the interaction between r-LTBP-2 and Fib1(H)NT is most likely directly or indirectly dependant on the presence of calcium ions.

5.2.4 Kinetic Analysis between LTBP-2 and Fibrillin-1

To determine the strength of the association between LTBP-2 and fibrillin-1 the dissociation constant was calculated. To determine the dissociation constant of protein-protein interactions, BIAcore™ technology is commonly utilised and although this approach was initially investigated for the analysis of the interaction between r-LTBP-2 and fibrillin-1 several problems to this approach were encountered. Firstly, BIAcore™ technology also requires the use of an optimised buffer for the mobile phase. However this buffer contains EDTA. Since the interaction between fibrillin and LTBP-2 is cation dependent, the presence of EDTA will abolish the protein-protein interaction. Thus, an EDTA-free buffer would be required. Furthermore, coupling of proteins to the standard BIAcore™ amine CM5 chip requires buffers that did not contain primary amine groups, such as tris or sodium azide, and which contain low salt concentrations to allow for critical ion exchange reactions with the carboxy-methyl groups of the chip. The manufacturers of BIAcore™ technology suggested the optimal pH range is 4.0-5.5 with a buffer containing 10mM acetate. However, when r-LTBP-2 was dialysed into this buffer it was found that the protein was no longer in solution indicating it was not soluble in the lower salt

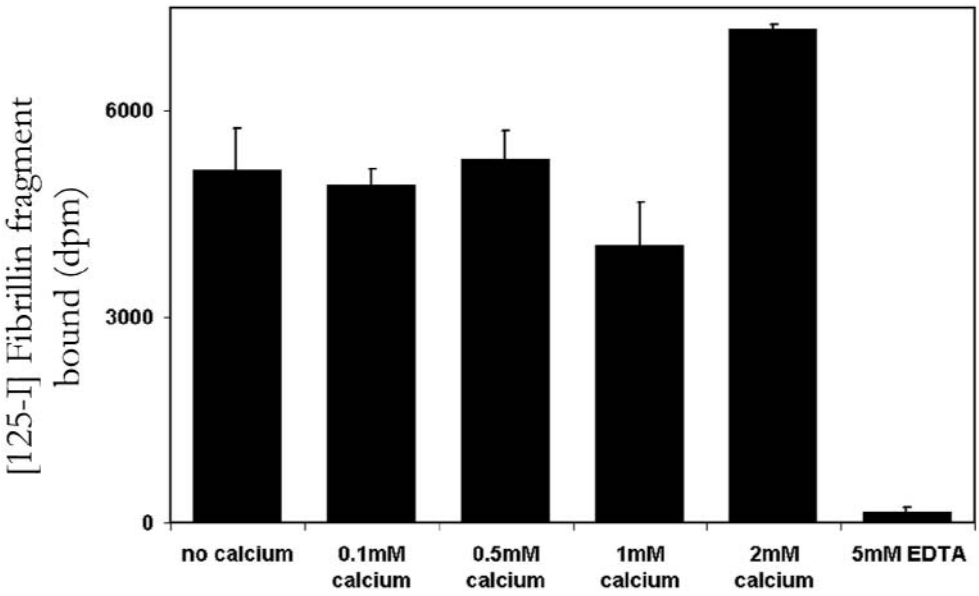

Figure 5.22. Solid phase binding assay showing that the interaction between r-LTBP-2 and Fib1(H)NT is marginally enhanced by the presence of 2mM Ca^{2+} ions and abolished in the presence of EDTA. Individual wells of microtitre plates were coated with r-LTBP-2 (200ng/well) in TBS buffer containing no added $CaCl_2$, 0.1mM, 0.5mM, 1mM, 2mM $CaCl_2$ or 5mM EDTA. After blocking with 5% milk/TBS, 25000dpm of Fib1(H)NT (specific activity of $1.28x10^7$dpm/µg) was added to wells after dilution using the appropriate TBS buffer with no added $CaCl_2$, 0.1mM, 0.5mM, 1mM or 2mM $CaCl_2$, or 5mM EDTA and incubated for 3 hrs at 37°C. After washing, specific binding of the radioligand was measured by γ counting. Means ± S.D. and specific binding of the Fib1(H)NT bound to r-LTBP-2-coated wells minus that bound to the corresponding BSA-coated wells of triplicate determinations is shown.

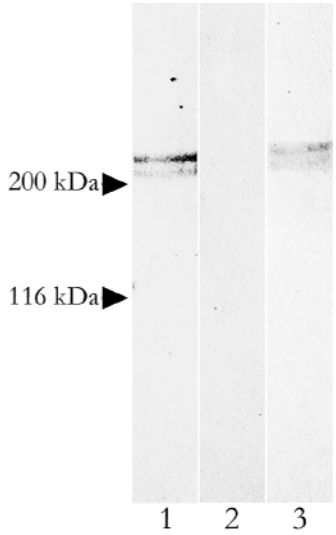

Figure 5.23. r-LTBP-2 is insoluble in low salt, low pH buffer solutions. r-LTBP-2 sample was dialysed into 10mM sodium acetate pH 4.5 buffer. After dialysis, the sample was centrifuged at maximum speed for 10 minutes prior to analysis of the supernatant and residual pellet. r-LTBP-2 was resolved using 8% SDS-PAGE under reducing conditions and stained with Coomassie Blue. *Lane 1*, r-LTBP-2 standard sample before dialysis into 10mM sodium acetate pH 4.5 buffer. *Lane 2*, supernatant sample after dialysis showing no r-LTBP-2 is present in solution. *Lane 3*, sample of the residual pellet after dialysis showing r-LTBP-2 was present in the pellet and had not remained soluble in the low salt buffer. The *arrowheads* indicate the relative mobilities of concurrently run protein standards.

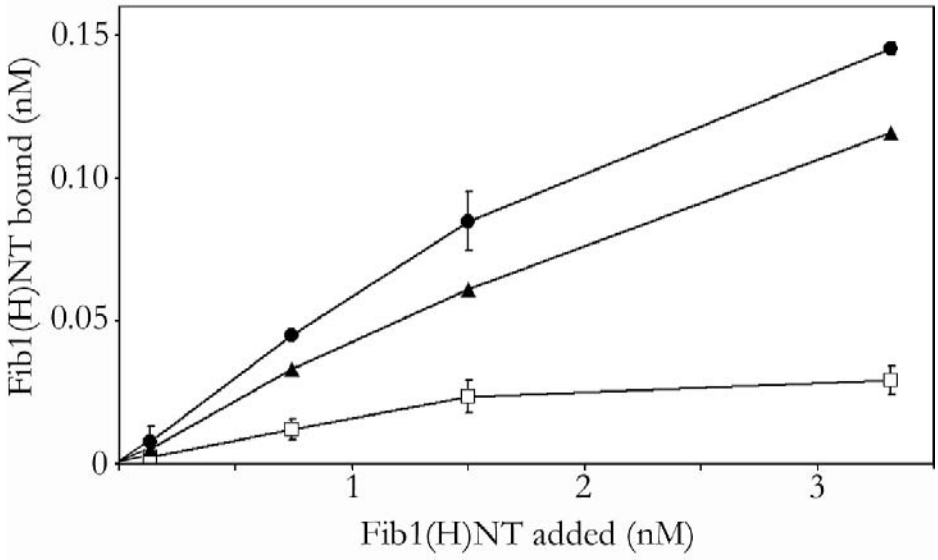

Figure 5.24. Saturation curve for determining the K_d value for the interaction of Fib1(H)NT with LTBP-2**.** Individual wells of microtitre plates were coated with r-LTBP-2 (75ng/well) (*black circles*) or BSA (20ng/well) (*open squares*). After blocking with 5% milk/TBS ^{125}I-labelled Fib1(H)NT at concentrations of 0-40ng/well (specific activity of 1.28×10^7dpm/μg) was added to wells and incubated for 3 hrs at 37°C. The liquid phase was then removed, the wells were washed and the amount of bound and unbound radioactivity in each well was determined by γ counting. Specific binding (*black triangles*) was calculated as the amount of Fib1(H)NT bound to r-LTBP-2-coated wells minus that bound to the corresponding BSA-coated wells. The K_d was calculated as 9.4nM using non-linear regression analysis of the specific binding curve. Means ± S.D. of triplicate determinations are shown.

concentrations with low pH (**figure 5.23**).

In cases of insolubility in low salt buffer the manufacturers of BIAcore™ suggested adding 0.0005% tween-20 to coupling buffer solutions but when tested this did not improve solubility (data not shown). Thus, high salt concentrations are required for r-LTBP-2 solubility but these could not be used for coupling to CM5 amine chips. An alternative to the CM5 amine chip is the Ni-coated chip, which binds his_6-tags. However, the Ni-coated chip could not be used for these studies since both the r-LTBP-2 and r-fibrillin fragments contain his_6-tags. Thus, it could not be guaranteed that the [his_6-tag]-containing protein in the mobile phase would not exchange with Ni^{2+} ions coated on the chip in a non-specific manner even after blocking the chip in a solution of imidazole. One feasible solution to the above problems would be to re-engineer the construct to contain a biotin tag for coupling onto the BIAcore™ strepavidin chip, which would allow coupling to be conducted in buffers with high salt concentration and neutral pH. However, after time and cost considerations for re-engineering the recombinant proteins it was decided to perform the initial measurements of the dissociation constant between r-LTBP-2 and fibrillin-1 using solid phase binding assays with radiolabelled recombinant proteins.

Using solid phase binding assays for kinetic analysis of the interaction between LTBP-2 and fibrillin-1 proved to be challenging. The analysis entailed using increasing amounts of radiolabelled protein in solution to achieve saturated binding to the protein coated on the well

and measuring the number of counts bound verses those remaining in solution (free). An estimate of the dissociation constant was calculated using non-linear regression analysis available on the GraphPad Prism version 4.02 software (GraphPad Software, San Diego CA, www.graphpad.com). This software analyses the slope of the line, after background subtraction, through a specific algorithm and equation to obtain an estimate of the dissociation constant (K_d).

It was found that saturation curves of the interaction between r-LTBP-2 and fibrillin-1 were uninformative when Fib1(H)NT was used at high concentrations (above 5nM) probably due to the aggregation of the protein in solution. When lower concentrations (less than 5nM) of Fib1(H)NT were used the dissociation constant (K_d) was estimated as 9.4×10^{-9}M (**figure 5.24**), indicating that r-LTBP-2 and Fib1(H)NT have reasonably strong avidity for binding to each other.

6 The C-terminal region of LTBP-2 contains the interacting domains for fibrillin-1

Evidence presented in chapter 5 indicates that LTBP-2 interacts with the N-terminal region of fibrillin-1, but not with the analogous region of fibrillin-2. Thus LTBP-2 appears to have a function associated specifically with fibrillin-1-containing microfibrils. In addition, previous studies within this research field have shown that LTBP-1 interacts with fibrillins-1 and -2 and LTBP-4 interacts with the fibrillin-1 and in those studies the binding sites were identified to the N-terminal region of fibrillins-1 and -2 and the C-terminal region of LTBPs-1 and -4 (Isogai *et al.*, 2003). Since the findings reported in chapter 5 have indicated that the N-terminal region of fibrillin-1 interacts with the full-length recombinant LTBP-2 protein, the following studies were conducted to determine if the analogous C-terminal region of LTBP-2 has similar fibrillin binding properties to LTBP-1.

6.1 Expression and purification of the C-terminal region of LTBP-2 [LTBP-2CT(H)]

A cDNA encoding the C-terminal region of LTBP-2 (bases 5089-5847 of the published LTBP-2 sequence with Genbank™ accession number NM_000428) was made from the full-length LTBP-2 cDNA using the specific primers, LTBP-2CT(H)F and LTBP-2CT(H)R (**appendix A**). These primers flanked the region of the cDNA encoding the last 8-Cys repeat through to the unique C-terminal region of LTBP-2 (**figure 6.1**) and PCR amplification resulted in a cDNA product of expected size (758bp) (**figure 6.2*A***), which was cloned into the mammalian expression vector pCEP-4 as described in section **4.2** of materials and methods.

Since all of the recombinant proteins produced for these studies contained the his_6-tag, this proved to be a disadvantage in situations where the anti-[his_6-tag] specific antibodies are the only antibodies available to detect binding in the solid phase assays. In an attempt to resolve this complication the pCEP-4 cassette vector was re-engineered to introduce a cDNA sequence coding for a protease site, which would facilitate the removal of the his_6-tag (**figure 6.1**). After specificity considerations, the protease chosen was enterokinase (EK), which cleaves after a unique recognition sequence consisting of Asp-Asp-Asp-Asp-Lys (DDDDK) (**figure 6.1** and **appendix D**).

The production of the recombinant C-terminal LTBP-2 fragment proved to be less difficult than that of the full-length protein. Transfection of 293-EBNA cells was conducted with 5µg of purified pCEP-4:LTBP-2CT(H) plasmid. Recombinant LTBP-2CT(H) protein was purified from serum-free DMEM media with yields of approximately 30mg/L. Confluent flasks

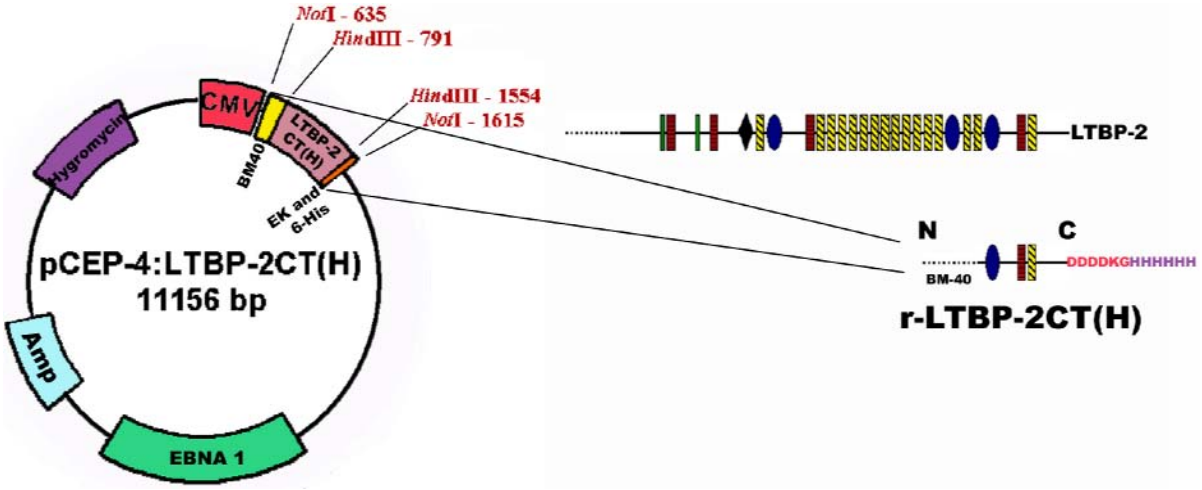

Figure 6.1. Schematic representation of the r-LTBP-2CT(H) expression construct and the encoded recombinant LTBP-2CT(H) fragment. The cDNA encoding LTBP-2CT(H) was inserted using the *Not*I restriction site of the pCEP-4 vector. The cytomegalovirus (CMV) promoter drives expression of the r-LTBP-2CT(H) protein modified to contain the sequence for the BM-40 signal peptide, enterokinase site and 6-histidine-tag. The full-length LTBP-2 domain structure is shown on the right to indicate the domains expressed within the r-LTBP-2CT(H) protein. The N-terminus (*N*) of r-LTBP-2CT(H) contains the BM-40 signal peptide and the C-terminus (*C*) region contains the enterokinase cleavage site (*pink*) and his_6-tag (*purple*). *green rectangles*, 4-cys motif; *red rectangles*, EGF-like domain; *black diamond*, hybrid region; *yellow cross-hatched rectangles*, calcium-binding EGF-like domains; *blue ovoid*, 8-Cys containing motif.

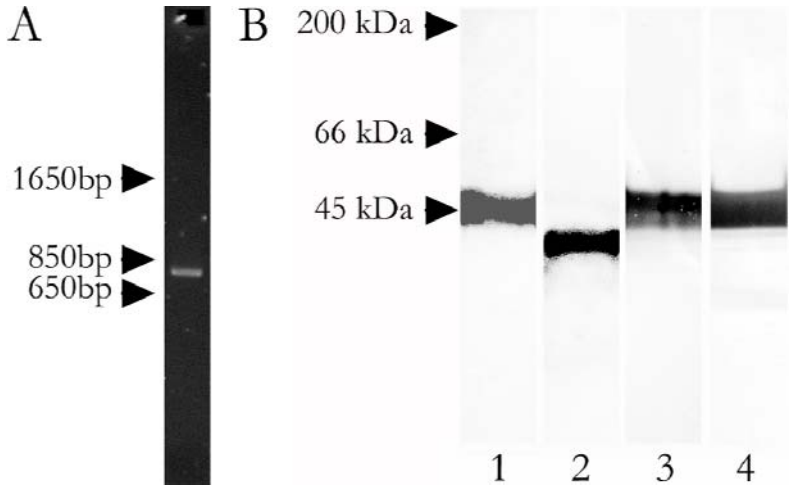

Figure 6.2. PCR amplification of a cDNA encoding for r-LTBP-2CT(H) and analysis of purified recombinant protein. *A*, LTBP-2CT(H) PCR product analysed on 1% (w/v) agarose gel and stained with ethidium bromide, indicating the presence of a single band of expected product size (758bp). *B*, r-LTBP-2CT(H) resolved on 12% SDS-PAGE after being purified from conditioned serum-free DMEM. The Coomassie Blue stained gel indicates a contaminant-free protein band of 45kDa when sample is reduced (*lane 1*) and 35kDa when non-reduced (*lane 2*). The identity of r-LTBP-2CT(H) was confirmed after transfer of the protein band onto PVDF membrane and probing with anti-[his_6-tag] antibody, tetrahis (1:2000 dilution, *lane 3*) and anti-[LTBP-2 peptide] antibody, LTBP-2C (1:500 dilution, *lane 4*). The *arrowheads* indicate the relative mobilities of concurrently run protein standards.

of expressing cells were incubated with two-rounds of serum-free media before deterioration of yield and protein quality occurred. However, it is noted that in contrast to the full-length LTBP-2 protein, little or no LTBP-2CT(H) protein was produced when expressing cells were incubated with Excell 293 serum-free media instead of DMEM (data not shown).

r-LTBP-2CT(H) was resolved using 12% SDS-PAGE as a single band of 45kDa when reduced (**figure 6.2*B***, *lane 1*) and 35kDa when non-reduced (**figure 6.2*B***, *lane 2*). This was larger than the predicted molecular weight of 31.5kDa. This discrepancy between the apparent and expected molecular weights of r-LTBP-2CT(H) has an unknown cause but has also been found to occur with other recombinant proteins including some of the fibrillin fragments. It is most likely the differences occur due to various post-translational modifications. LTBP-2CT(H) was analysed for glycosylation and it was found that N-glycosylation accounted for a 6kDa difference between the predicted and actual molecular weights (data not shown) but there may also be other forms of post-translational modifications accounting for the remaining 7.5kDa difference in molecular weight. It is also common for many proteins to appear larger or smaller than expected on SDS-PAGE, an example includes MAGP-1 which appears at 31kDa on SDS-PAGE but should appear as 20kDa. These discrepancies are likely to occur due to protein conformation where they may be more or less folded than expected and thus travel differently through the acrylamide pores during electrophoresis, resulting in the protein appearing larger or smaller than predicted.

The authenticity of the 45kDa recombinant protein was confirmed as a fragment of the C-terminal region of LTBP-2 using the rabbit polyclonal anti-[LTBP-2 peptide] antibody, LTBP-2C (**figure 6.2*B***, *lane 4*). Anti-[LTBP-2 peptide] antibody, LTBP-2C, was raised specifically to recognise the C-terminal region of LTBP-2 and as expected had a strong immunoreaction with r-LTBP-2CT(H) (**figure 5.13**). Antibody LTBP-2C was used to detect r-LTBP-2CT(H) at similar titre dilution as determined for the full-length LTBP-2 protein (1:10000-1:64000) (**figure 5.11**). Once the identity of r-LTBP-2CT(H) had been confirmed the protein was dialysed into TBS/0.5M NaCl and stored exactly as stated for the full-length LTBP-2 in section **4.3**.

6.1.1 Digestion of LTBP-2CT(H) with the Enterokinase Enzyme

Samples of purified r-LTBP-2CT(H) were digested with enterokinase to determine if the his_6-tag could be removed. 0.5µg of protein was digested with 0.2U of enterokinase for between 8-16 hours at various temperatures from room temperature to 37°C. **Figure 6.3** shows an example of r-LTBP-2CT(H) digestion with enterokinase, *lane 1* shows the undigested protein analysed on 12% SDS-PAGE stained with coomassie blue, the protein size and integrity is exactly

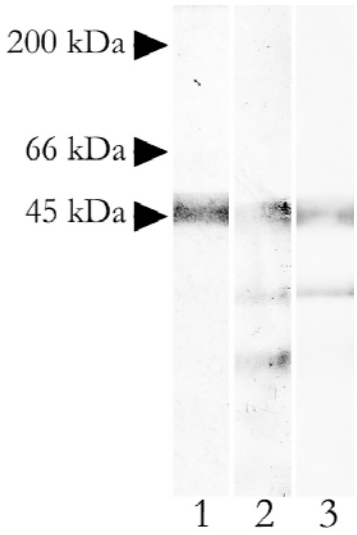

Figure 6.3. Digestion of purified r-LTBP-2CT(H) with enterokinase. r-LTBP-2CT(H) was resolved on 12% SDS-PAGE and stained with Coomassie Blue (*lane 1*). After digestion of r-LTBP-2CT(H) with 0.2U of recombinant enterokinase (Novagen) for 16 hrs at room temperature, protein was transferred onto PVDF membrane and was probed with anti-[LTBP-2 peptide] antibody, LTBP-2C (1:500 dilution, *lane 2*) and anti-[his-tag] antibody, tetrahis (1:2000 dilution, *lane 3*). The results indicate that the r-LTBP-2CT(H) protein still contained the his_6-tag and was also that there was some evidence for non-specific degradation by the enzyme. The *arrowheads* indicate the relative mobilities of concurrently run protein standards.

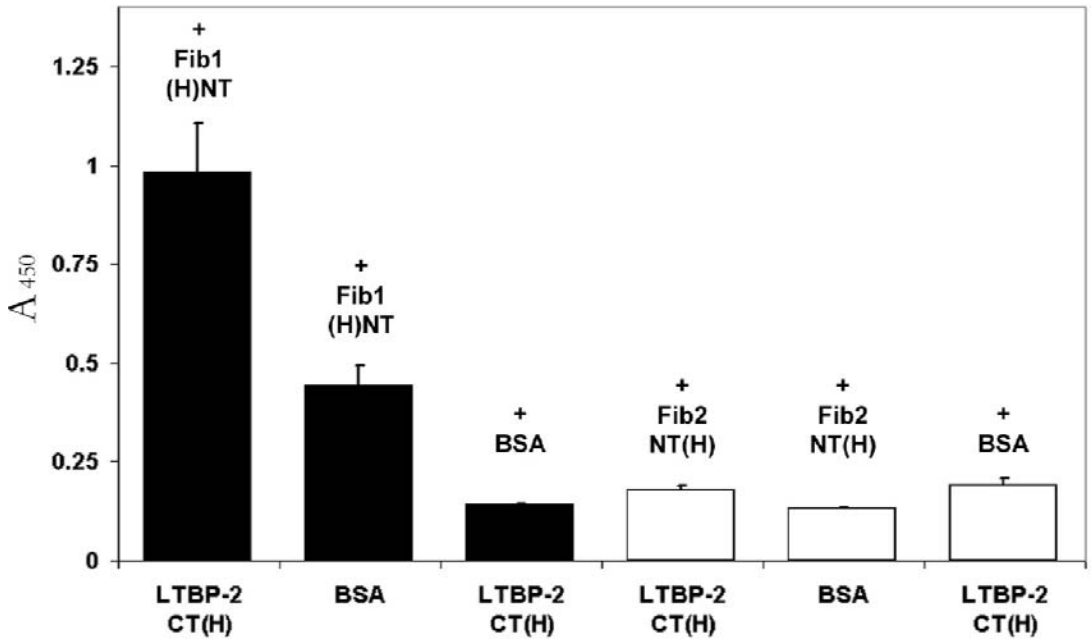

Figure 6.4. The C-terminal region of r-LTBP-2 interacts with the N-terminal region of fibrillin-1 but not fibrillin-2. Individual wells of microtitre plates were coated with r-LTBP-2CT(H) (100ng/well) in TBS/2mM $CaCl_2$. Control wells were coated with the molar equivalent of BSA (32ng/well). After blocking with 5% milk/TBS, Fib1(H)NT (200ng/well), Fib2NT(H) (348ng/well) or BSA (176ng/well) was added to the wells and incubated for 3 hrs at 37°C. After washing, anti-[fibrillin-1] antibody, MAB2502 (1:2000 dilution, *black columns*) or anti-[fibrillin-2] antibody 16E12 (1:400 dilution, *white columns*) was added to wells and incubated for 2 hrs at 37°C. After washing, specific binding of the MAB2502 or 16E12 antibody was detected at 450nm using peroxidase-conjugated secondary antibody and colour development for 35 minutes. Means ± S.D. of triplicate determinations are shown.

as expected. Following digestion the protein was found to have been degraded when analysed by western immunoblot probed with the anti-[LTBP-2 peptide] specific antibody, LTBP-2C (**figure 6.3**, *lane 2*). However, when the digested protein was analysed using the anti-[his_6-tag] specific antibody to determine if the his_6-tag had been successfully removed it was found that some intact protein containing the his_6-tag was still present (**figure 6.3**, *lane 3*). The degradation was not caused by the presence of other cleavage kit components, as a control reaction was performed where the enterokinase enzyme was replaced with ddH_2O. The r-LTBP-2CT(H) in this control was found to be of the expected size (~45kDa) with no evidence of degradation when analysed with the anti-[LTBP-2 peptide] antibody, LTBP-2C (data not shown). Degradation of the r-LTBP-2CT(H) was an unexpected effect of using the EK enzyme to remove the his_6-tag and this precluded its use for his_6-tag removal. However, it was subsequently determined that the polyclonal anti-[LTBP-2 peptide] antibody, LTBP-2C could be used to uniquely identify LTBP-2CT(H) in solid phase binding assays so that the cleavage of the his_6-tag proved to be unnecessary.

6.2 The C-terminal region of LTBP-2 contains the major binding site for fibrillin-1

Solid phase binding assays were conducted to determine if the C-terminal region of LTBP-2 contained the binding site for the interaction between LTBP-2 and the N-terminal region of fibrillin-1. It was shown that r-LTBP-2CT(H) did interact with Fib1(H)NT (**figure 6.4**) but not with Fib2NT(H). Using controls where BSA was substituted for Fib1(H)NT in solution it was determined there was no cross-reaction between r-LTBP-2CT(H) and the mouse monoclonal anti-[fibrillin] specific antibodies, MAB2502 (used to detect [Fib1(H)NT]) and 16E12 (used to detect [Fib2NT(H)]) (**figure 6.4**). These results are consistent to those reported by Isogai *et al.* (2003), where the analogous C-terminal regions of LTBP-1 and -4 were found to contain the binding site for fibrillin-1. However, in contrast to the above findings, Isogai *et al.* (2003) also reported the interaction between the C-terminal regions of LTBP-1 with the N-terminal region of fibrillin-2. Findings presented in chapter 5 showed that full-length LTBP-2 did not interact with the N-terminal region of fibrillin-2 [Fib2NT(H)] (**figure 5.18**) and the lack of interaction between LTBP-2 and fibrillin-2 was confirmed here, since the C-terminal fragment of LTBP-2 also did not interact with the N-terminal region of fibrillin-2 [Fib2NT(H)] (**figure 6.4**). This suggests that LTBP-2 has an exclusive role with fibrillin-1-containing microfibrils.

The interaction between r-LTBP-2CT(H) and Fib1(H)NT was found to be specific since the level of interaction between the two proteins was proportional to the amount of LTBP-2CT(H) coated on the well and was saturable as the amount of LTBP-2CT(H) coated on the well increased (**figure 6.5**). The binding signal strength between r-LTBP-2CT(H) and Fib1(H)NT was specific, however, it was not as extensive as for the equimolar quantity

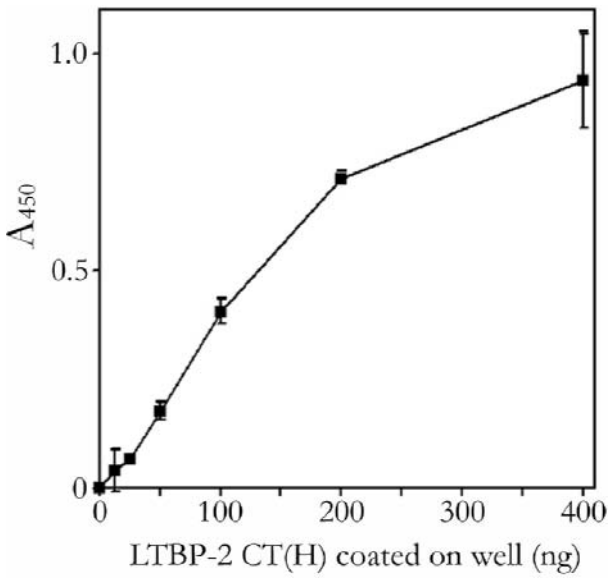

Figure 6.5. The interaction of r-LTBP-2CT(H) with Fib1(H)NT is proportional to the amount of solid phase ligand**.** Individual wells of microtitre plates were coated with r-LTBP-2CT(H) (0-400ng) in TBS/2mM $CaCl_2$. Control wells were coated with the molar equivalent of BSA. After blocking with 5% milk/TBS, Fib1(H)NT (250ng/well) was added to each well and incubated for 3 hrs at 37°C. After washing, anti-[fibrillin-1] antibody, MAB2502 (1:2000 dilution) was added to wells and incubated for 2 hrs at 37°C. After washing, specific binding of the MAB2502 antibody was detected at 450nm using peroxidase-conjugated secondary antibody and colour development for 45 minutes. Means ± S.D. and specific binding of the Fib1(H)NT bound to r-LTBP-2CT(H)-coated wells minus that bound to the corresponding BSA-coated wells of triplicate determinations is shown.

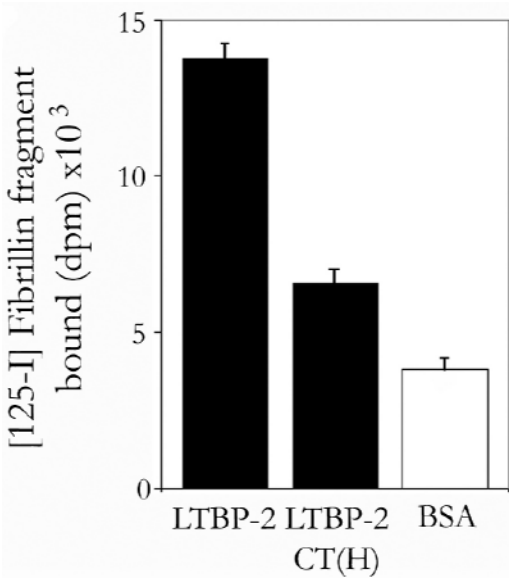

Figure 6.6. The C-terminal region of LTBP-2 contains a binding site(s) for fibrillin-1**.** Individual wells of microtitre plates were coated with r-LTBP-2 (200ng/well) or a molar equivalent of r-LTBP-2CT(H) (43ng/well) in TBS/2mM $CaCl_2$. Control wells were coated with a molar equivalent of BSA (62ng/well, *white column)*. After blocking with 5% milk/TBS, $6.4x10^4$dpm of ^{125}I-labelled Fib1(H)NT (specific activity $1.28x10^7$dpm/μg) was added to each well and incubated for 3 hrs at 37°C. After washing, specific binding of the radioligand was measured by direct γ counting. Means ± S.D. of quadruplicate determinations are shown.

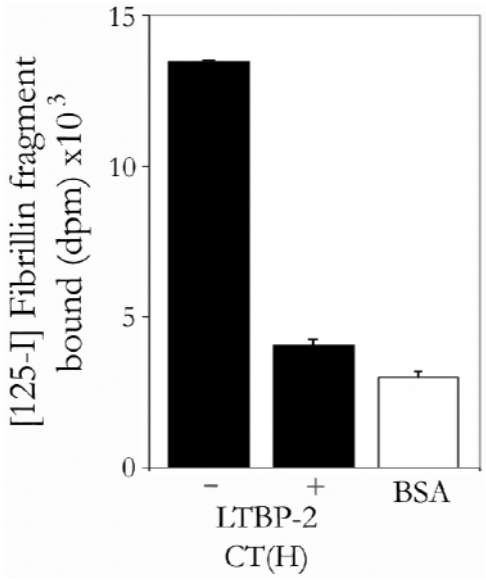

Figure 6.7. The C-terminal region of r-LTBP-2 contains the only major binding site for fibrillin-1. Individual wells of microtitre plates were coated with r-LTBP-2 (200ng/well, *black columns*) in TBS/2mM $CaCl_2$. Control wells were coated with a molar equivalent of BSA (62ng/well, *white column)*. After blocking with 5% milk/TBS, $6.4x10^4$dpm of ^{125}I-labelled Fib1(H)NT (specific activity $1.28x10^7$dpm/µg), which had been pre-treated overnight at 37°C with either 7 molar equivalents of BSA (-) or r-LTBP-2CT(H) (+), was added to appropriate wells and incubated for 3 hrs at 37°C. After washing, binding of the radiolabelled ligand was measured by direct γ counting. Means ± S.D. of quadruplicate determinations are shown.

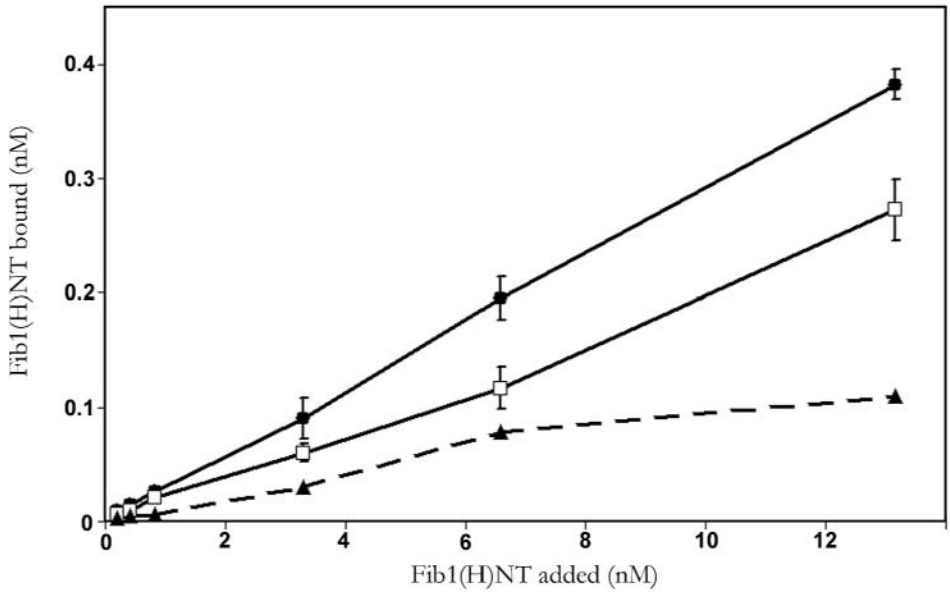

Figure 6.8. Binding curve for determining K_d values for the interaction of fibrillin-1 with LTBP-2CT(H)**.** Individual wells of microtitre plates were coated with r-LTBP-2CT(H) (50ng/well, *black circles*) or BSA (60ng/well, *open squares*) in TBS/2mM $CaCl_2$. After blocking with 5% milk/TBS, ^{125}I-labelled Fib1(H)NT (0-100ng/well, specific activity of 1 x 10^7dpm/µg) was added to wells and incubated for 3 hrs at 37°C. The liquid phase was then removed, the wells were washed and the amount of bound and unbound radioactivity in each well was determined by γ counting. Specific binding (*black triangles with dashed line*) was calculated as the amount of Fib1(H)NT bound to r-LTBP-2CT(H)-coated wells minus that bound to the corresponding BSA-coated wells. The K_d was calculated as 22nM using non-linear regression analysis of the specific binding curve. The means ± S.D. of triplicate determinations are shown.

of full-length r-LTBP-2 with Fib1(H)NT (**figure 6.6**). Two possible reasons for this result at the time were, a) there may be multiple binding regions for fibrillin-1 upon LTBP-2 or b) coating on the well could reduce access of the fibrillin-1 binding site on the smaller LTBP-2 C-terminal fragment coated on the plastic wells. An experiment was conducted to determine if LTBP-2 contained more than one binding region for fibrillin-1. Fib1(H)NT was pre-treated with 7-fold molar excess of r-LTBP-2CT(H) and was then incubated with full-length r-LTBP-2 coated onto individual microtitre wells. If multiple binding regions for fibrillin-1 are present on full-length LTBP-2 then pre-treatment of fibrillin-1 with r-LTBP-2CT(H) would not completely block the interaction between fibrillin-1 and r-LTBP-2. If pre-treatment of fibrillin-1 resulted in the complete abolishment of the interaction this would indicate that the C-terminal domains of LTBP-2 contain the single major binding site for fibrillin-1.

It was found that pre-treating fibrillin-1 with LTBP-2CT(H) resulted in the blocking of the interaction between fibrillin-1 and r-LTBP-2 completely to background levels when compared to the positive control (**figure 6.7**). The positive control was conducted where Fib1(H)NT had been pre-treated with BSA as a substitute for r-LTBP-2CT(H). BSA acts as a non-specific protein and does not prevent the specific binding of Fib1(H)NT to the full-length r-LTBP-2 coated on the well. This result demonstrates that the C-terminal domains of LTBP-2 [r-LTBP-2CT(H)] contains the single major binding site for fibrillin-1 (**figure 6.7**).

6.2.1 Kinetic Analysis Between LTBP-2CT(H) and Fibrillin-1

To determine the strength of the interaction between the C-terminal fragment of LTBP-2 with fibrillin-1, kinetic analysis was conducted. This information would be useful in determining if LTBP-2 has the potential to compete with other members of the LTBP family, specifically LTBP-1, for binding to fibrillin-1 (see chapter 7 for further detail). As for the interaction between the full-length LTBP-2 and fibrillin-1, kinetic analysis of the LTBP-2CT(H)/fibrillin-1 interaction was difficult to obtain from solid phase assays. After a number of attempts it was found that the best estimate of the dissociation constant was calculated as 22×10^{-9}M using the GraphPad prism software (**figure 6.8**). This result indicates that the strength of the association between LTBP-2CT(H) and fibrillin-1 is similar in strength to the LTBP-2/fibrillin-1 interaction, which was calculated as 9.4×10^{-9}M (**figure 5.24**). The small difference seen between the estimated binding strengths of the full-length LTBP-2 and the C-terminal fragment to fibrillin-1 is most probably due to reduced accessibility of the fibrillin binding site on the recombinant fragment.

7 LTBP-2 competes with LTBP-1 for binding to fibrillin-1

The novel findings presented in chapters 5 and 6 suggest that the C-terminal domains of LTBP-2 contain the major binding sequence for the N-terminal region of fibrillin-1. Previous studies (Isogai *et al.*, 2003) conducted in this field have also shown that the C-terminal domains of LTBP-1 contain the binding sequence for the N-terminal region of fibrillin-1. It is thus hypothesised that LTBP-1 and LTBP-2 compete for interaction with fibrillin-1. LTBP-1 covalently binds to latent forms of TGF-β, but LTBP-2 does not. Therefore, if competition between these LTBP family members is found, it could indicate a novel regulatory system for modulating latent TGF-β storage on fibrillin-1-containing microfibrils. To determine if LTBP-1 and -2 compete with each other for binding to fibrillin-1, a C-terminal fragment of LTBP-1 corresponding to that shown to bind fibrillin-1 by Isogai *et al.* (2003), was produced in the 293-EBNA cells. This fragment [LTBP-1CT(H)] was tested for competitive binding with LTBP-2CT(H) to fibrillin-1.

7.1 Expression and purification of the recombinant C-terminal region of LTBP-1 [LTBP-1CT(H)]

To make recombinant LTBP-1 a cDNA clone of LTBP-1 needed to be constructed. After several attempts, cDNA encoding for the full-length LTBP-1 protein could not be amplified from the human trabecular bone mRNA library. However, a partial cDNA (636bp) was amplified encoding the LTBP-1 region spanning the last 8-Cys repeat through to the unique C-terminal region of LTBP-1 (**figures 7.1** and **7.2*A***). For this, primer LTBP-1CT(H)F (**appendix A**), which compliments bases 3681-3700 of the published sequence (Genbank™ NM_000627) was used for first strand synthesis followed by subsequent PCR with the primers LTBP-1CT(H)F and LTBP-1CT(H)R (**appendix A**). Ligation of this cDNA fragment into the modified pGEM-T vector [pGEM-T:BM-40:his_6-tag:EK] containing the BM-40 signal peptide, enterokinase site and his_6-tag sequence proved to be difficult. It was attempted to digest the LTBP-1 cDNA product with the *Hin*dIII restriction enzyme prior to ligation into the *Hin*dIII site of the pGEM-T:BM-40:his_6-tag:EK vector using T4 DNA ligase (see section **4.2** for details). However, this approach was unsuccessful for ligating the LTBP-1 cDNA into the vector. It was considered that *Hin*dIII restriction enzyme efficiency would be improved if the cDNA product was directly ligated into pGEM-T-easy vector, prior to digestion with *Hin*dIII and ligating the insert into the pGEM-T:BM-40:his_6-tag:EK vector. However, this approach for ligating the LTBP-1 cDNA into the pGEM-T:BM-40:his_6-tag:EK vector was also unsuccessful.

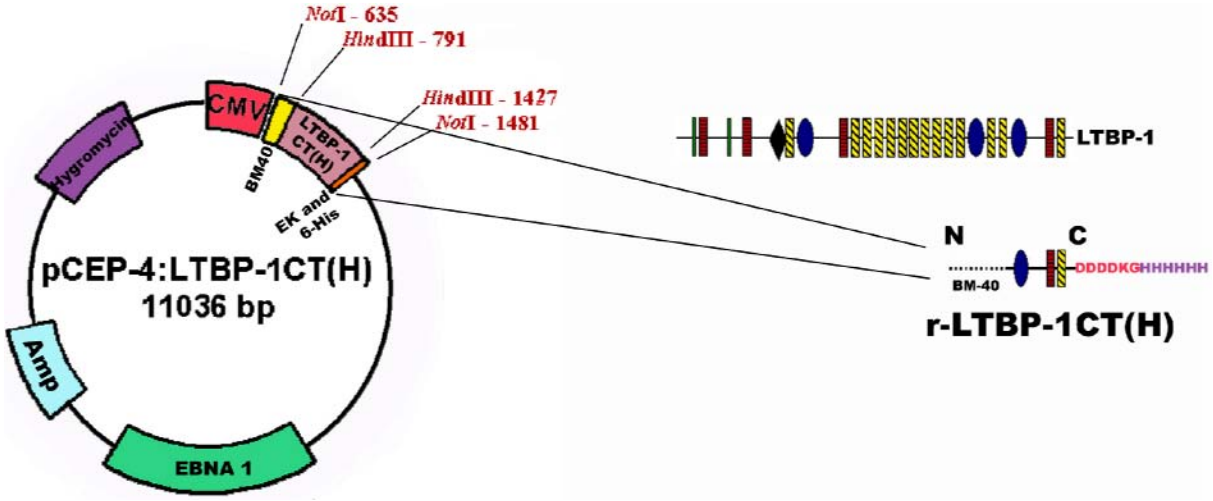

Figure 7.1. Schematic representation of the LTBP-1CT(H) expression construct and expressed recombinant fragment r-LTBP-1CT(H). The cDNA encoding for r-LTBP-1CT(H) was inserted using the *Not*I restriction site of the pCEP-4 vector. The cytomegalovirus (CMV) promoter drives expression of the r-LTBP-1CT(H) protein modified to contain the sequence for the BM-40 signal peptide, enterokinase site and 6-histidine tag. The full-length LTBP-1 domain structure is shown to indicate the domains expressed within the r-LTBP-1CT(H) fragment. The N-terminus (*N*) of r-LTBP-1CT(H) contains the BM-40 signal peptide and the C-terminus (*C*) region contains the enterokinase cleavage site (*pink*) and his_6-tag (*purple*). *green rectangles*, 4-cys motif; *red rectangles*, EGF-like domain; *black diamond*, hybrid region; *yellow cross-hatched rectangles*, calcium-binding EGF-like domains; *blue ovoid*, 8-Cys containing motif.

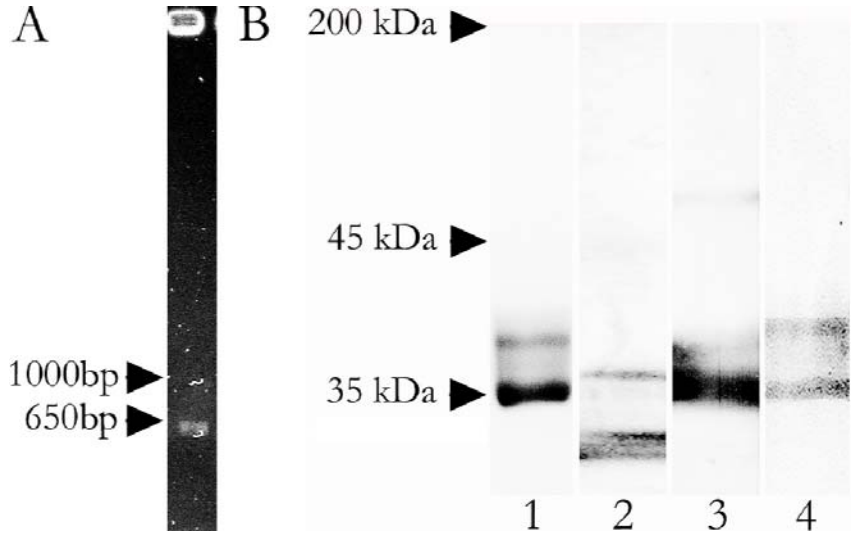

Figure 7.2. PCR amplification of the cDNA encoding the C-terminal region of LTBP-1 and analysis of the purified recombinant protein fragment. *A*, LTBP-1CT(H) PCR product analysed on 1% (w/v) agarose gel and stained with ethidium bromide, indicating a single band of expected product size (636bp). *B*, 12% SDS-PAGE of r-LTBP-1CT(H) purified from DMEM serum-free media. Coomassie Blue staining indicates a contaminant-free doublet band of 35 and 40kDa under reducing condition (*lane 1*) and 33 and 36kDa when non-reduced (*lane 2*). The purified protein was transferred onto PVDF membrane and immunoreacted with the anti-[his_6-tag] antibody, tetrahis (1:2000 dilution, *lane 3*). The identity of r-LTBP-1CT(H) was confirmed after probing the membrane with anti-[LTBP-1] antibody, MAB388 (1:250 dilution, *lane 4*). The *arrowheads* indicate the relative mobilities of concurrently run protein standards.

To resolve this problem a third ligation approach, Gateway® cloning, was employed. Gateway® technology uses the site-specific recombination properties of bacteriophage lambda. The cDNA insert was re-amplified to contain flanking recombination sequences (*att* sites) and was cloned into the sister sites within the pDONR™201 vector using the Clonase™ enzyme mix (see sections **4.1** and **4.2** for experimental details). Thus, in preparation for Gateway® cloning, the LTBP-1CT(H) cDNA product was further amplified using LTBP-1CT(H)gateF and LTBP-1CT(H)gateR (**appendix A**) to introduce the required *attB* recombination sites. The LTBP-1 cDNA was then recombined with the pDONR™201 vector. The cDNA encoding for the C-terminal region of LTBP-1 was then removed from the pDONR™ vector by restriction enzyme digest with *Hin*dIII and ligated into the pGEM-T:BM-40:his_6-tag:EK vector to form the pGEM-T:LTBP-1CT(H) plasmid. Digestion of this plasmid with *Not*I liberated the final LTBP-1CT(H) insert for ligation into pCEP-4 (**figure 7.1**; see sections **4.1** and **4.2** for experimental details).

The transfection and expression of the LTBP-1 C-terminal clone proved to be uncomplicated. r-LTBP-1CT(H) was easily expressed in 293-EBNA cells using DMEM serum-free media and purified with Ni-chelate chromatography. An abundant yield of pure recombinant protein of approximately 40mg per litre of serum-free media was routinely obtained. As for r-LTBP-2CT(H) but in contrast to r-LTBP-2, little or no protein was produced when LTBP-1CT(H)-expressing cells were incubated with Excell 293 serum-free media in place of DMEM. r-LTBP-1CT(H) was analysed using SDS-PAGE, which resulted in a doublet protein band of size 35 and 40kDa when reduced and 33 and 36kDa when non-reduced (**figure 7.2*B***, *lane 1* and *lane 2*), which was slightly larger than the expected protein size of 28kDa. To explore this discrepancy in size, LTBP-1CT(H) was digested with N- and O-glycosidase enzymes, however no change in molecular weight was found with either enzyme (data not shown). Thus, it is most likely that the size discrepancy could occur due to the manner in which the protein separated during SDS-PAGE as discussed in section **6.1**. The purified recombinant protein immunoreacted with anti-[his_6-tag] specific antibodies (**figure 7.2*B***, *lane 3*) and the identity of the protein was confirmed by probing immunoblots with an anti-[LTBP-1] specific antibody, MAB388 (**figure 7.2*B***, *lane 4*).

A sample of purified r-LTBP-1CT(H) was then digested with enterokinase to determine if the his_6-tag could be removed when required. **Figure 7.3** shows the r-LTBP-1CT(H) digested with enterokinase, *lane 1* shows the undigested protein analysed on a 12% gel and stained with Coomassie Blue. Following digestion, r-LTBP-1CT(H) was analysed by western immunoblot with anti-[LTBP-1] specific antibody, MAB388. The results showed that the protein had been degraded to small fragments migrating close to the dye-front of the SDS gel (**figure 7.3**, *lane 2*).

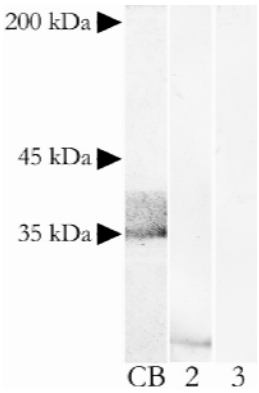

Figure 7.3. Digestion of the purified r-LTBP-1CT(H) with enterokinase. r-LTBP-1CT(H) was resolved on a 12% gel and stained with Coomassie blue (*CB*). r-LTBP-1CT(H) was then digested with 0.2U of recombinant enterokinase (Novagen) for 16 hrs at room temperature, the digestion product was resolved using 12% SDS-PAGE and transferred onto PVDF membrane. The membrane was probed with anti-[LTBP-1] antibody, MAB388 (1:250 dilution, *lane 2*) or anti-[his_6-tag] antibody, tetrahis (1:2000 dilution, *lane 3*). The *arrowheads* indicate the relative mobilities of concurrently run protein standards.

There was no immunoreaction of this digested r-LTBP-1CT(H) with the anti-[his_6-tag] specific antibody (**figure 7.3**, *lane 3*). However, since all the recombinant protein was degraded into very small fragments it was difficult to determine if the his_6-tag had been removed by enzymatic digestion or if small degradation products containing the his_6-tag had migrated with the dye front so they could no longer be detected. A control reaction where the enterokinase enzyme was replaced with ddH_2O showed no digestion of LTBP-1CT(H) indicating that no enterokinase kit components contributed to the degradation process (data not shown). Thus, degradation was only found in the presence of the recombinant enterokinase enzyme. This degradation of the recombinant protein with the enterokinase enzyme was unexpected. However, the removal of the his_6-tag proved to be unnecessary since the anti-[LTBP-1] antibody, MAB388 was shown to react strongly and specifically against the C-terminal region of LTBP-1 and could be used to detect r-LTBP-1CT(H) in the required binding assays (see section below).

7.1.1. LTBP-1CT(H) Antibodies

It was found using ELISAs and western immunoblots (with the antibody used at a 1:250 dilution; **figure 7.2*B***, *lane 4*) that r-LTBP-1CT(H) was strongly detected using the anti-[LTBP-1] antibody, MAB388. The titre dilution for use of the antibody was chosen as 1:6400 for economic considerations and this dilution could detect a minimum of 12.5ng of r-LTBP-1CT(H) (**figures 7.4** and **7.5**).

The MAB388 antibody was tested for cross-reaction against a myriad of extracellular proteins and was found to have a minimal reaction with fibrillin-2 [Fib2NT(H)] (**figure 7.6**),

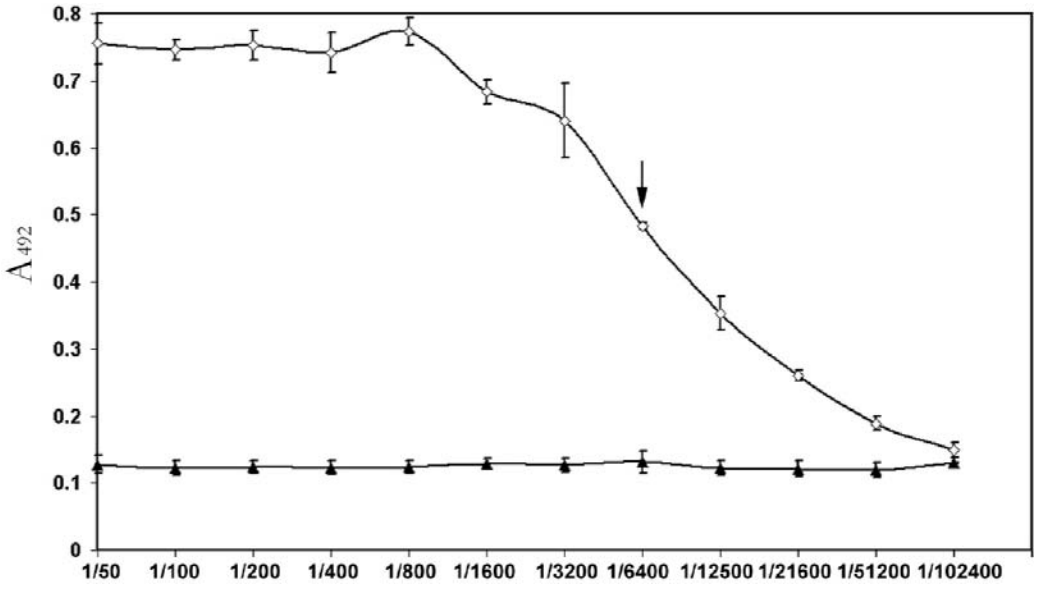

Figure 7.4. ELISA to determine the titre of the anti-LTBP-1 antibody, MAB388. Individual wells of microtitre plates were coated with r-LTBP-1CT(H) (100ng/well, *open diamonds*) or the molar equivalent of BSA (188ng/well, *black triangles*) in TBS/2mM $CaCl_2$ buffer. After blocking wells with 5% milk/TBS, a serial dilution of the anti-[LTBP-1] antibody, MAB388 (1:50 to 1:1024000), was added to the wells and incubated for 3 hrs at 37°C. After washing, specific binding of MAB388 was detected at 492nm using peroxidase-conjugated secondary antibody and colour development for 10 minutes. *Arrow* indicates a chosen optimal dilution of 1:6400. Means ± S.D. of triplicate determinations shown.

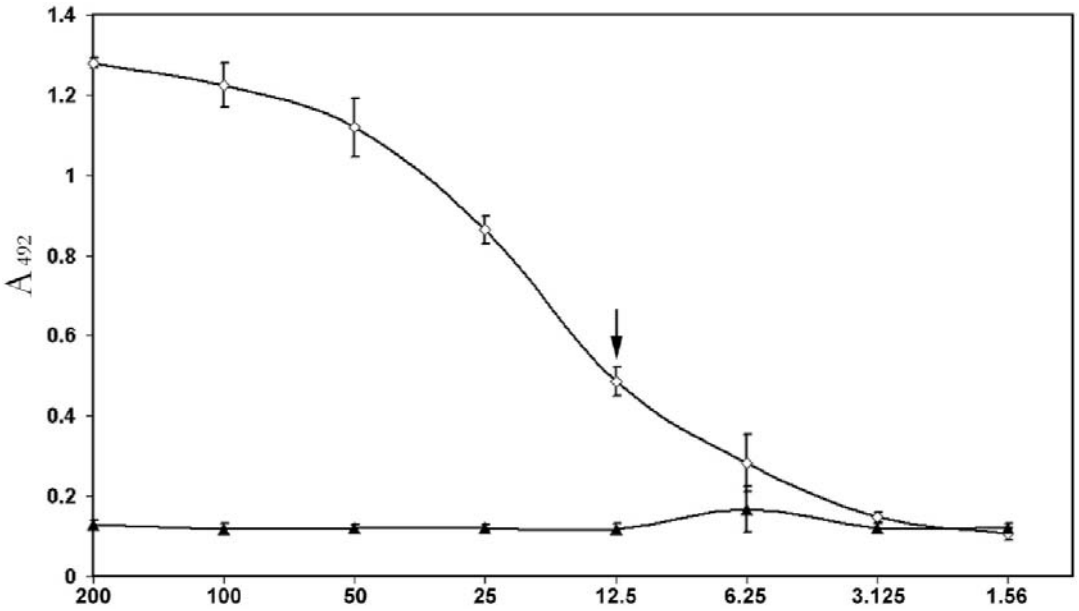

Figure 7.5. ELISA to determine the minimum amount of r-LTBP-1CT(H) detectable with a 1:6000 dilution of the anti-[LTBP-1] specific antibody, MAB388. Individual wells of microtitre plates were coated with a serial dilution of r-LTBP-1CT(H) (200ng-1.56ng/well, *open diamonds*) in TBS/2mM $CaCl_2$. Control wells were coated with a molar equivalent of BSA (388ng-3ng/well, *black triangles*). After blocking with 5% milk/TBS, MAB388 (1:6000 dilution) was added to wells and incubated for 3 hrs at 37°C. After washing, specific binding of MAB388 was detected at 492nm using peroxidase-conjugated secondary antibody and colour development for 20 minutes. *Arrow* indicates that 12.5ng of r-LTBP-1CT(H) can be detected using a 1:6000 dilution of MAB388. Means ± S.D. of triplicate determinations are shown.

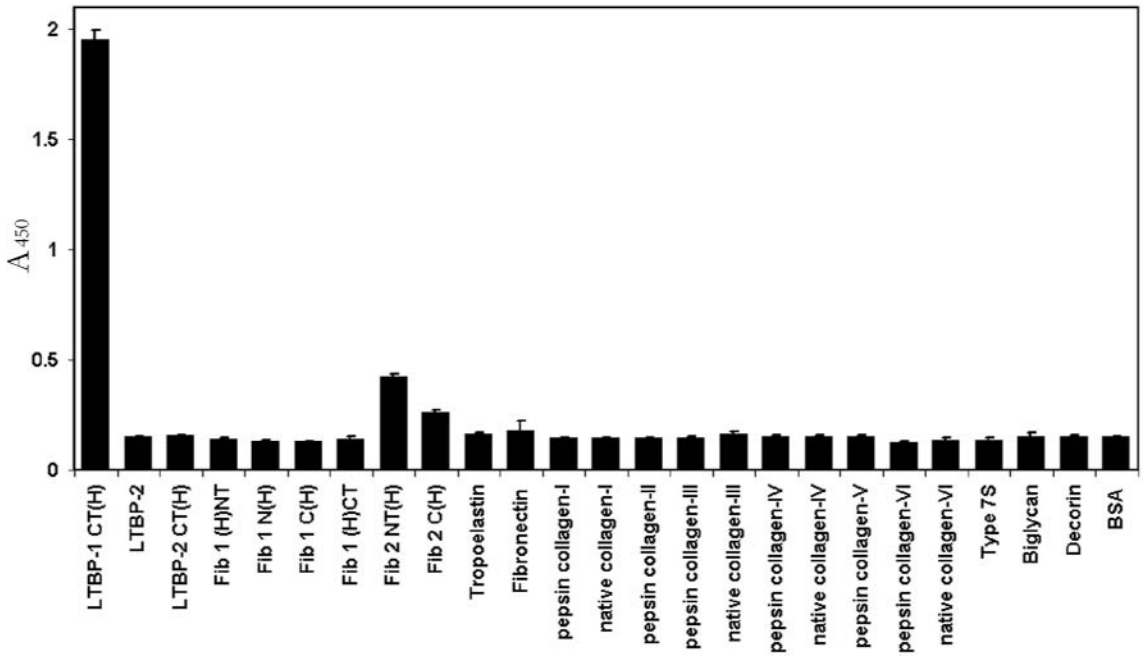

Figure 7.6. ELISA to screen antibody MAB388 for cross-reactivity with a range of extracellular molecules. Individual wells of microtitre plates were coated with extracellular macromolecules (200ng/well) and r-LTBP-1CT(H) (100ng/well) in TBS/2mM $CaCl_2$. Control wells were coated with BSA (200ng/well). After blocking using 5% milk/TBS, anti-[LTBP-1] antibody, MAB388 (1:6000 dilution) was added to wells and incubated for 3 hrs at 37°C. After washing, specific binding of MAB388 was detected at 450nm using peroxidase-conjugated secondary antibody and colour development for 10 minutes. Means ± S.D. and binding of triplicate determinations are shown.

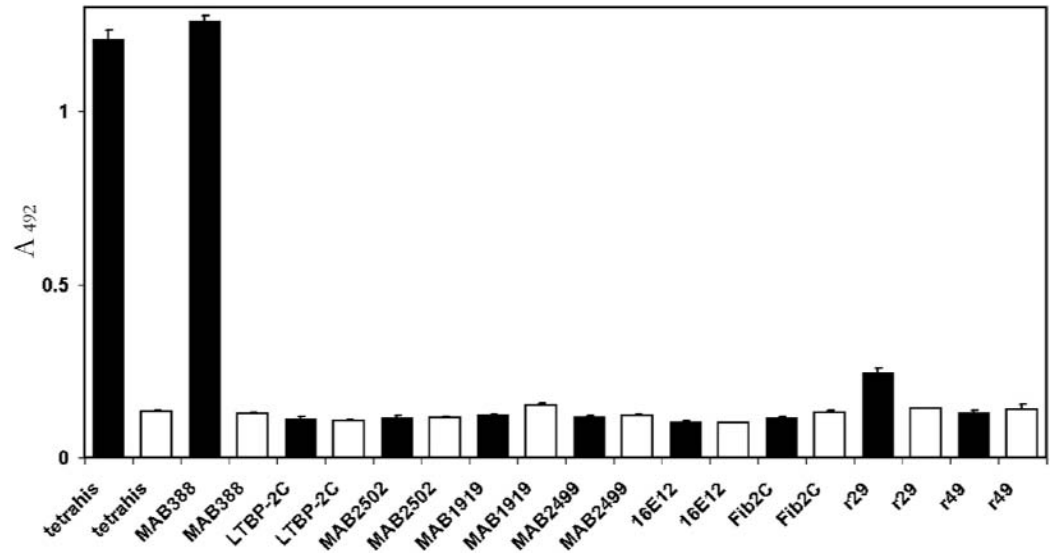

Figure 7.7. ELISA to determine cross-reactivity of r-LTBP-1CT(H) with a range of antibodies raised to detect other extracellular matrix macromolecules. Individual wells of microtitre plates were coated with r-LTBP-1CT(H) (400ng/well, *black columns*) in TBS/2mM $CaCl_2$. Control wells were coated with a molar equivalent BSA (750ng/well, *white columns*). After blocking using 5% milk/TBS, the various test antibodies were added to wells using the dilutions stated in **appendix C** and incubated for 3 hrs at 37°C. After washing, specific binding of each test antibody was detected at 492nm using the corresponding peroxidase-conjugated secondary antibody and colour development for 10 minutes. Means ± S.D. and binding of triplicate determinations are shown.

where the antibody reacted at least four times stronger with r-LTBP-1CT(H) than with fibrillin-2. The fibrillin-2 activity was successfully absorbed out by incubating 500ng of purified r-Fib2NT(H) for 5 hours at 37°C with gentle shaking, followed by centrifugation to remove any immunoprecipitate. Immunoblots and ELISAs confirmed the removal of fibrillin-2 activity, without affecting reactivity to r-LTBP-1CT(H) (data not shown). r-LTBP-1CT(H) was found not to cross-react with a range of antibodies to LTBP-2, fibrillins-1 and -2 and other extracellular matrix macromolecules (**figure 7.7**). Furthermore, since r-LTBP-1CT(H) contained a his_6-tag, the protein was immunoreactive to the anti-[his_6-tag] antibody, tetrahis which could be used at dilutions as stated in **appendix C** to detect the recombinant protein (**figures 7.2*B*,** *lane 3* and **7.7**).

7.2 LTBP-1 and LTBP-2 compete for binding to fibrillin-1

7.2.1 LTBP-1CT(H) Interacts with the N-terminal Region of Fibrillin-1

r-LTBP-1CT(H) was tested for binding to Fib1(H)NT to confirm that it contained a fibrillin-1 binding site as anticipated from the studies of Isogai *et al.* (2003). Indeed, a strong interaction was found between Fib1(H)NT and r-LTBP-1CT(H), which was shown to be concentration dependant (**figure 7.8**). However, in contrast to the results reported by Isogai *et al.* (2003), no binding could be demonstrated between r-LTBP-1CT(H) and the N-terminal region of fibrillin-2 (**figure 7.9**). The lack of an interaction between r-LTBP-1CT(H) and fibrillin-2 was consistent with our binding studies using full-length r-LTBP-2 and r-LTBP-2CT(H), which also did not interact with this fibrillin.

7.2.2 Kinetic Analysis of the Interaction Between LTBP-1 and Fibrillin-1

Isogai *et al.* reported an interaction between fibrillin-1 and LTBP-1, however the strength of this binding was not investigated (Isogai *et al.*, 2003). Since knowledge of the strength of binding between LTBP-1 and fibrillin-1 could have important implications for any potential competitive binding of LTBP-1 and LTBP-2 to fibrillin-1, kinetic analysis of the interaction between fibrillin-1 and LTBP-1 was conducted. As for LTBP-2CT(H), accurate kinetic analysis of the LTBP-1 and fibrillin-1 interaction was difficult to obtain from solid phase binding assays. A number of analyses were conducted and the best estimate of the dissociation constant was calculated as 17 x 10^{-9}M using the GraphPad Prism version 4.02 (**figure 7.10**) (GraphPad Software, San Diego CA, www.graphpad.com). The result indicates that the LTBP-1/fibrillin-1 interaction is of similar strength to the LTBP-2/fibrillin-1 interaction, which was calculated as 9.4 x 10^{-9}M (**figure 5.24**) and LTBP-2CT(H)/fibrillin-1 interaction, which was calculated as 20 x 10^{-9}M (**figure 6.8**).

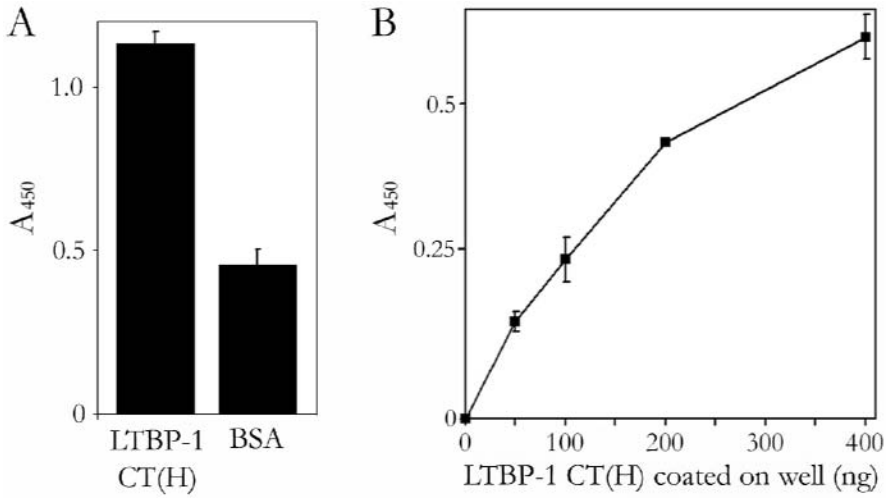

Figure 7.8. r-LTBP-1CT(H) interacts specifically with Fib1(H)NT**.** *A*, individual wells of microtitre plates were coated with r-LTBP-1CT(H) (400ng/well) in TBS/2mM $CaCl_2$ buffer. Control wells were coated with a molar equivalent of BSA (125ng/well). After blocking with 5% milk/TBS, Fib1(H)NT (280ng/well) was added to wells and incubated for 3 hrs at 37°C. *B,* individual wells of microtitre plates were coated with a serial dilution of r-LTBP-1CT(H) (0-400ng/well) in TBS/2mM $CaCl_2$. Control wells were coated with a molar equivalent of BSA. After blocking, Fib1(H)NT (200ng/well) was added wells and incubated for 3 hrs at 37°C. After washing, anti-[fibrillin-1] antibody, MAB2502 (1:2000 dilution) was added to wells and incubated for 2 hrs at 37°C. After washing, specific binding of MAB2502 was detected at 450nm using peroxidase-conjugated secondary antibody and colour development for 20 minutes (*A*) or 10 minutes (*B*). For *B,* specific binding of the Fib1(H)NT bound to r-LTBP-1CT(H)-coated wells minus that bound to the corresponding BSA-coated wells is displayed. Means ± S.D. of triplicate determinations are shown.

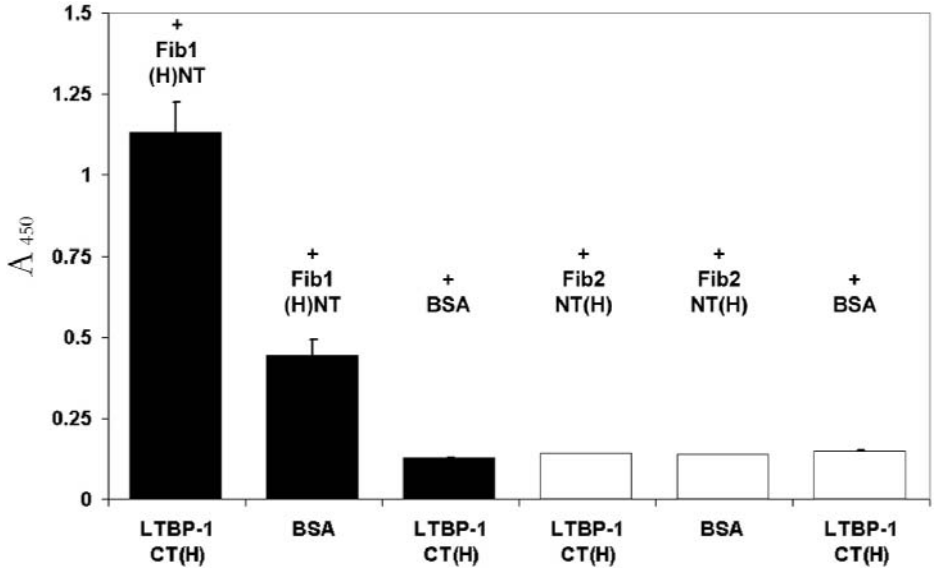

Figure 7.9. r-LTBP-1CT(H) does not interact with the N-terminal region of fibrillin-2**.** Individual wells of microtitre plates were coated with r-LTBP-1CT(H) (280ng/well) in TBS/2mM $CaCl_2$. Control wells were coated with a molar equivalent of BSA (132ng/well). After blocking with 5% milk/TBS, a molar equivalent of Fib1(H)NT (200ng/well), Fib2NT(H) (348ng/well) or BSA (176ng/well) was added to wells and incubated for 3 hrs at 37°C. After washing, anti-[fibrillin-1] antibody, MAB2502 (1:2000 dilution, *black columns*) or anti-[fibrillin-2] antibody, 16E12 (1:400 dilution, *white columns*) was added to wells and incubated for 2 hrs at 37°C. After washing, specific binding of MAB2502 or 16E12 was detected at 450nm using peroxidase-conjugated secondary antibody and colour development for 35 minutes. Means ± S.D. of triplicate determinations are shown.

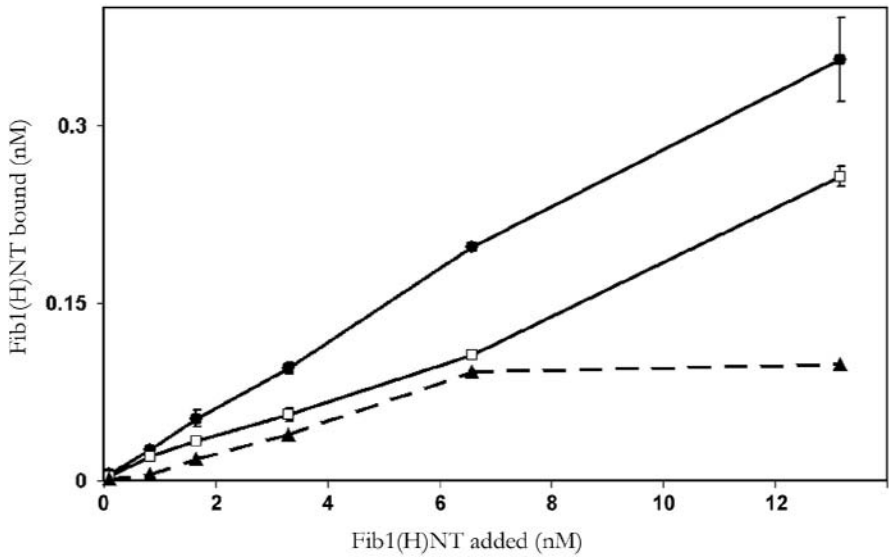

Figure 7.10. Binding curve for determining K_d values for the interaction of fibrillin-1 with LTBP-1**.** Individual wells of microtitre plates were coated with r-LTBP-1CT(H) (32ng/well, *black circles*) or BSA (60ng/well, *open squares*) in TBS/2mM $CaCl_2$. After blocking with 5% milk/TBS, ^{125}I-labelled Fib1(H)NT (0-100ng/well, specific activity of 1 x 10^7dpm/µg) was added to wells and incubated for 3 hrs at 37°C. The liquid phase was then removed, the wells were washed and the amount of bound and unbound radioactivity in each well was determined by γ counting. Specific binding (*black triangles with dashed line*) was calculated as the amount of Fib1(H)NT bound to r-LTBP-1CT(H)-coated wells minus that bound to the corresponding BSA-coated wells. The K_d was calculated as 17nM using non-linear regression analysis of the specific binding curve. The means ± S.D. of triplicate determinations are shown.

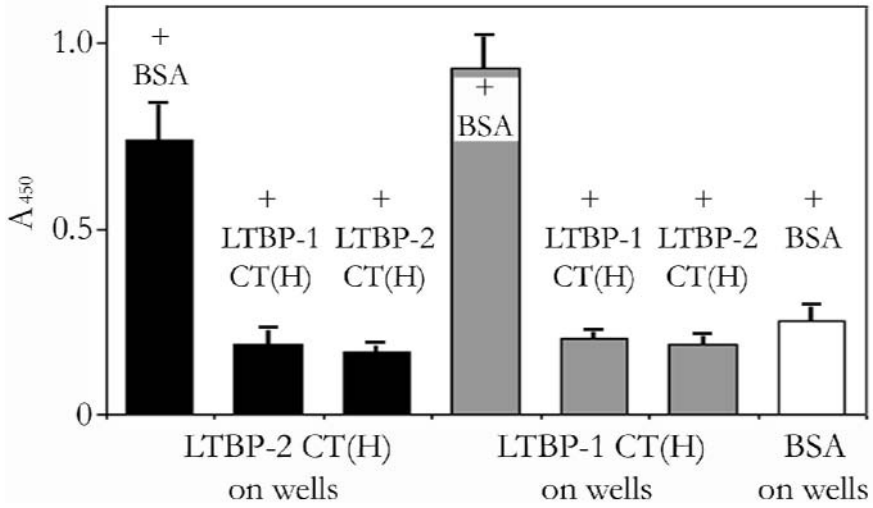

Figure 7.11. r-LTBP-1CT(H) and r-LTBP-2CT(H) compete for binding to Fib1(H)NT**.** Individual wells of microtitre plates were coated with r-LTBP-2CT(H) (400ng/well, *black columns),* r-LTBP-1CT(H) (400ng/well, *grey columns)* or a molar equivalent of BSA (125ng/well, *white columns)* in TBS/2mM $CaCl_2$. After blocking with 5% milk/TBS, Fib1(H)NT (280ng/well), which had been pre-treated either with 10-fold molar equivalents of r-LTBP-2CT(H) or r-LTBP-1CT(H) overnight at 37°C in the presence of 2mM $CaCl_2$, was added to wells and incubated for 3 hrs at 37°C. After washing, anti-[fibrillin-1] antibody, MAB2502 (1:2000 dilution) was added to wells and incubated for 2 hrs at 37°C. After washing, specific binding of MAB2502 was detected at 450nm using peroxidase-conjugated secondary antibody and colour development for 30 minutes. Means ± S.D. of quadruplicate determinations are shown.

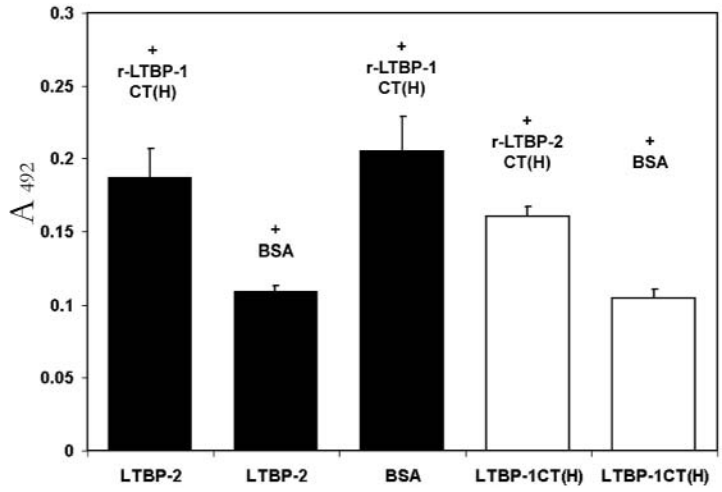

Figure 7.12. r-LTBP-1CT(H), r-LTBP-2 and r-LTBP-2CT(H) do not interact with each other**.** Individual wells of microtitre plates were coated with r-LTBP-2 (400ng/well), r-LTBP-1CT(H) (400ng/well) or BSA (400ng/well) in TBS/2mM $CaCl_2$. After blocking with 5% milk/TBS, r-LTBP-1CT(H) (63ng/well), r-LTBP-2 (2545ng/well), r-LTBP-2CT(H) (545ng/well) or BSA (125ng/well for *black column* and 799ng/well for *white column*) was added to appropriate wells and incubated for 3 hrs at 37°C. After washing, anti-[LTBP-1] antibody, MAB388 (1:250 dilution, *black columns*) or anti-[LTBP-2 peptide] antibody, LTBP-2C (1:5000 dilution, *white columns*) was added to wells and incubated for 2 hrs at 37°C. After washing, specific binding of MAB388 or LTBP-2C was detected at 492nm using peroxidase-conjugated secondary antibody and colour development for 10 minutes. Means ± S.D. of quadruplicate determinations are shown.

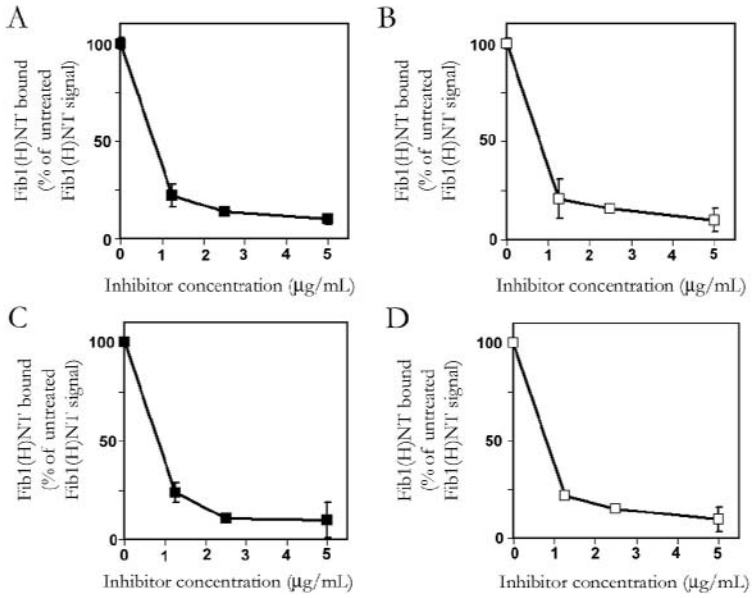

Figure 7.13. Competition inhibition curves for the LTBP-1CT(H) and LTBP-2CT(H) interactions with fibrillin-1. Individual wells of microtitre plates were coated with r-LTBP-1CT(H) (100ng/well) for experiments *A* and *B* and r-LTBP-2CT(H) (140ng/well) for experiments *C* and *D* in TBS/2mM $CaCl_2$. Control wells were coated with a molar equivalent of BSA (188ng/well). After blocking with 5% milk/TBS, Fib1(H)NT (280ng/well), which had been pre-treated with r-LTBP-1CT(H) (0-500ng/well) (*black squares*) or a molar equivalent of r-LTBP-2CT(H) (0-710ng/well) (*open squares*) overnight at 37°C in the presence of 2mM $CaCl_2$, was added to wells and incubated for 3 hrs at 37°C. After washing, anti-[fibrillin-1] antibody, MAB2502 (1:2000 dilution) was added to wells and incubated for 2 hrs at 37°C. After washing, specific binding of the MAB2502 antibody was detected at 450nm using peroxidase-conjugated secondary antibody and colour development for 10 minutes. Means ± S.D. and specific binding of the Fib1(H)NT bound to r-LTBP-fragment-coated wells minus that bound to the corresponding BSA-coated wells of triplicate determinations is shown.

7.2.3 LTBP-1 and LTBP-2 Compete for Binding to Fibrillin-1

It has been shown in section **7.2.1** that the C-terminal regions of LTBP-2 and LTBP-1 bind to the same N-terminal region of fibrillin-1. However it was yet to be determined if they had the same binding site on fibrillin-1 or if they had distinct binding sites. To determine if the binding sites for LTBP-1 and LTBP-2 are close together on Fib1(H)NT, a competitive solid phase binding assay was performed. Each LTBP fragment was coated onto the surface of the plastic well, with BSA as a negative control, and was then incubated with Fib1(H)NT which had been pre-treated with a 10-fold molar excess of r-LTBP-1CT(H), r-LTBP-2CT(H) or BSA (as positive interaction control). Specific binding of Fib1(H)NT was detected using the anti-[fibrillin-1] specific antibody, MAB2502. It was found that in each case the pre-treatment of Fib1(H)NT with either C-terminal LTBP fragment blocked the interactions of this Fib1(H)NT with the LTBP fragment coated on the well. As expected BSA did not block the binding of Fib1(H)NT to either LTBP fragment (**figure 7.11**). Importantly, it was shown in a separate experiment that neither LTBP fragment interacted with itself or with the other LTBP (**figure 7.12**). Thus LTBP-LTBP interactions were not a factor for the observed blocking of the interaction with fibrillin-1 (**figure 7.11**). This finding indicates that the binding site for LTBP-1 and -2 upon fibrillin-1 are the same or are in close proximity.

It remained to be determined which LTBP was most effective at blocking LTBP/fibrillin-1 interactions. In an attempt to obtain this information competition binding curves were conducted between the LTBPs and fibrillin-1 (**figure 7.13**). Solid phase binding assays were conducted where Fib1(H)NT in the liquid phase was pre-treated with increasing amounts of each LTBP fragment, prior to testing for binding to either LTBP fragment coated on the well. The curve with the steepest drop to background levels would indicate the stronger interaction. Preliminary data indicated that binding strengths of both LTBPs were very similar (**figure 7.13**). It was found that the binding of fibrillin-1 to the fragment coated on the well was almost completely blocked in the presence of 1 molar equivalent (1μg/mL) of LTBP fragment in solution and went to basal levels when 4 molar equivalents (5μg/mL) of LTBP fragment was added in solution (**figure 7.13**). Since this was the case for each individual blocking curve it was not possible to conclude which LTBP was best at blocking the LTBP/fibrillin-1 interactions. This finding was consistent with the analysis of the dissociation constants, which indicated that both the LTBP-1 and –2 C-terminal fragments had similar K_d values of 17nM and 22nM respectively. These competition curves are only preliminary and further analysis would require more points to be performed between the 0 and 1μg/mL inhibitor concentrations to determine which LTBP fragment has the steepest curve towards background levels to determine which has the strongest binding. However, these experiments could not be conducted within the scope of

this thesis due to constraints on the amount of fibrillin fragment available, time and cost considerations for production of further fibrillin material.

8 Immunohistochemical analysis of human foetal aorta indicates LTBP-2 has a distinct but partially overlapping distribution with LTBP-1

Chapter 7 of this thesis presented data to shown that LTBP-1 and LTBP-2 compete for binding to fibrillin-1 with similar avidities. However, this may not be the case *in vivo*. If LTBP-1 and -2 are not expressed in the same tissues at the similar developmental stages, then they would not be able to compete for binding to fibrillin-1-containing microfibrils. Previously it has been shown that LTBP-2 has widespread localisation with fibrillin-containing microfibrils in bovine nuchal ligament and aorta (Gibson *et al.*, 1995) and LTBP-1 has been shown to localise with some fibrillin-containing microfibrils in foetal bovine aorta (Isogai *et al.*, 2003). However, there has been little analysis on the tissue localisations of members of the LTBP family with relation to each other and fibrillin-1. In this thesis immunohistochemical analysis of bovine tissues was primarily performed to determine if the antibodies were immunoreactive when using frozen cryostat tissues sections. This was followed by analysis of the developing human throracic aorta. This tissue was selected for its importance in relation to the Marfan phenotype but also since, as mentioned above, some analysis of the distribution of LTBPs in this tissue had been carried out previously (Gibson *et al.*, 1995; Isogai *et al.*, 2003).

8.1 LTBP-2 has a distinct but partially overlapping tissue-localisation pattern from that of LTBP-1

8.1.1 Analysis of Bovine Tissues

Bovine nuchal ligament, foetal kidney and foetal aorta were analysed with antibodies raised against fibrillin-1, LTBP-2 and LTBP-1. Bovine nuchal ligament was chosen since this is a highly characterised tissue within the literature and has a high content of elastic fibres and fibrillin-containing microfibrils. Cryostat sections of nuchal ligament from 210-230 day bovine were incubated with the monoclonal anti-[fibrillin-1] antibody, MAB1919, affinity purified polyclonal anti-[LTBP-2 peptide] antibody, LTBP-2C and monoclonal anti-[LTBP-1] antibody, MAB388 (**appendix C** outlines the appropriate dilution for each antibody). A control section incubated with mouse IgG was used to give a general idea of non-specific background staining. Anti-[fibrillin-1] antibody, MAB1919 gave strong and specific staining of fibrillar structures within the nuchal ligament, most likely to be elastic fibres, which is expected since these fibres are rich in fibrillin-containing microfibrils (**figure 8.1*A***) (Sakai *et al.*, 1986; Zhang *et al.*, 1994). Anti-[LTBP-2 peptide] specific antibody, LTBP-2C also showed widespread strong and specific

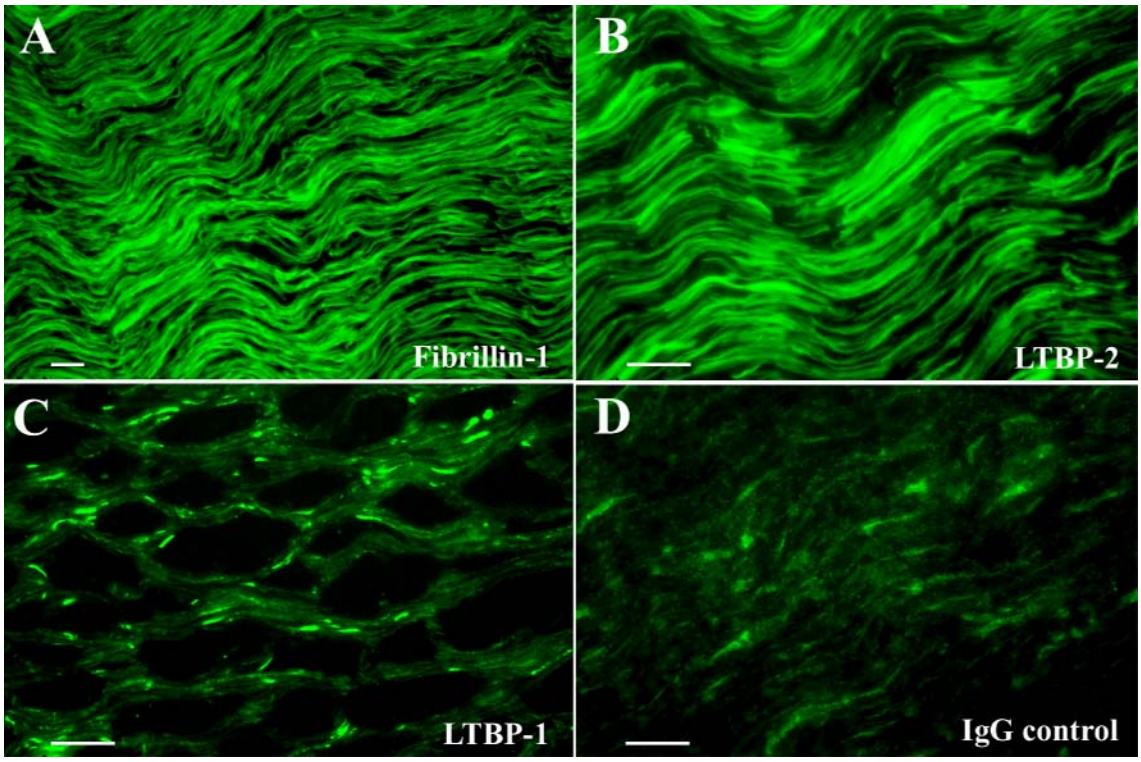

Figure 8.1. Fibrillin-1 and LTBP-2 co-localise on elastic fibres in bovine nuchal ligament. Cryostat sections (5µm) of bovine nuchal ligament from a 210-230 day foetal calf were incubated with antibodies to fibrillin-1, LTBP-1, and LTBP-2 diluted in PBS as indicated below. Primary antibody binding was detected using an appropriate secondary antibody conjugated to flurophore FITC, prior to analysis on the Nikon-FXa microscope. *A*, mouse monoclonal anti-[fibrillin-1] antibody, MAB1919 (5µg/mL), 20x objective with 1.97 second exposure. *B*, rabbit polyclonal anti-[LTBP-2 peptide] antibody, LTBP-2C (10µg/mL), 40x objective with 1.8 second exposure; *C*, mouse monoclonal anti-[LTBP-1] antibody, MAB388 (10µg/ml), 40x objective with 42.5 second exposure; *D*, mouse IgG control (10µg/ml), 40x objective with 42.5 second exposure. Magnification bars = 50µm.

staining of elastic fibres indicating LTBP-2 is present in association with elastic fibres. This antibody showed a pattern consistent with that demonstrated using the anti-[fibrillin-1] antibody, MAB1919 (**figure 8.1*B***). Thus, LTBP-2 and fibrillin-1 appear to be found in the same structures at the same developmental stage, indicating that the spatiotemporal patterns are consistent with the potential for the molecular interaction of LTBP-2 with fibrillin-1. This finding correlates with studies previously conducted by Gibson *et al.* where it was shown using antibodies raised to two different bovine LTBP-2 peptide sequences that LTBP-2 localised to fibrillin-containing microfibrillar component of elastic fibres in nuchal ligament and aorta, indicating that LTBP-2 was associated with these structures (Gibson *et al.*, 1995). In contrast, staining of the bovine nuchal ligament with the anti-[human LTBP-1] antibody, MAB388, was very similar to the IgG control since much of the staining was punctate cellular staining (**figure 8.1*C*** and ***D***). It was expected that LTBP-1 would be present within these structures since previous research has indicated there is a strong association of LTBP-1 with elastic fibres (Isogai *et al.*, 2003). Thus, it appears that the anti-[human LTBP-1] antibody, MAB388 is unreactive with bovine tissues.

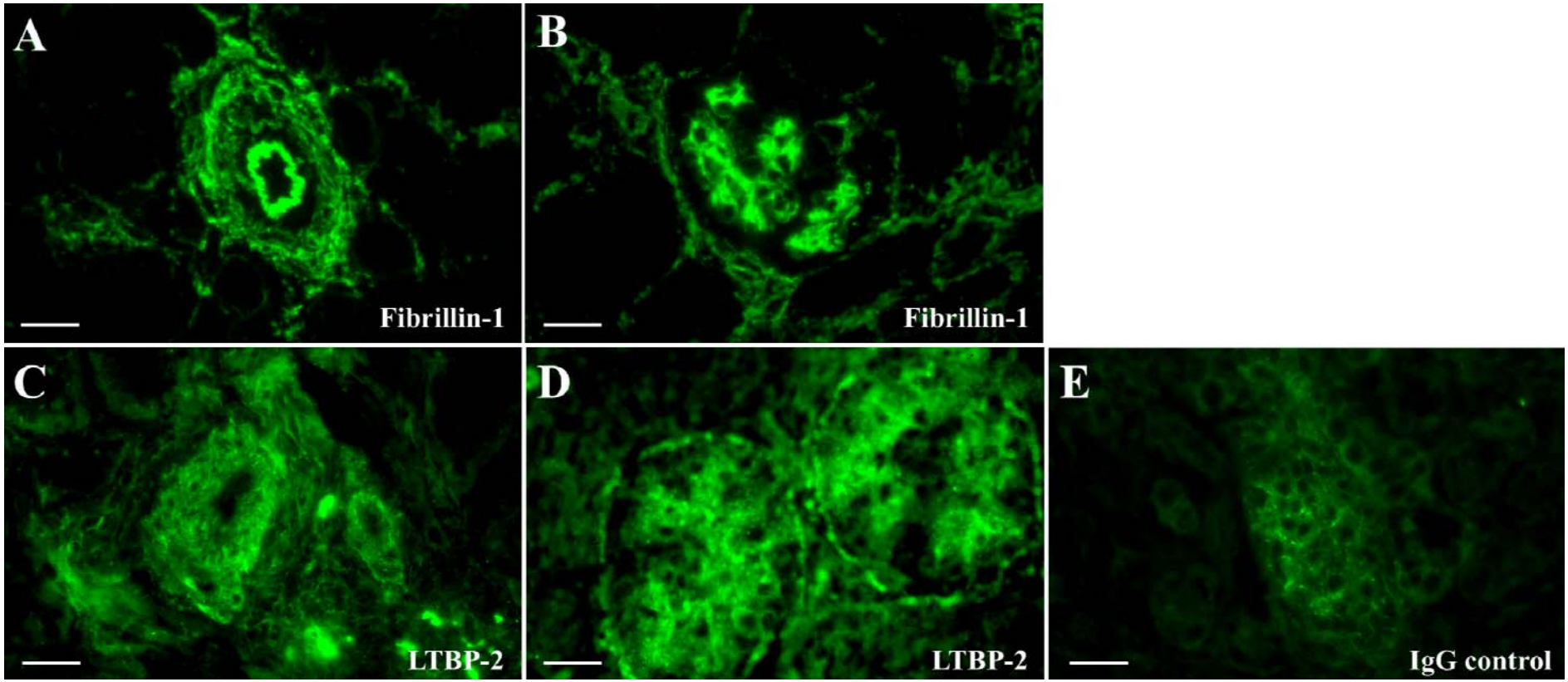

Figure 8.2. Fibrillin-1 and LTBP-2 localisation within foetal bovine kidney. Cryostat sections (5µm) of kidney tissue from a 200 day foetus were incubated with antibodies to fibrillin-1 and LTBP-2 diluted in PBS as indicated below. Primary antibody binding was detected using an appropriate secondary antibody conjugated to the flurophore FITC, prior to analysis on the Nikon-FXa microscope. *A* and *B,* mouse monoclonal anti-[fibrillin-1] antibody, MAB1919 (5µg/mL), 40x objective with 0.75 and 1.53 second exposure, respectively. *C* and *D,* rabbit polyclonal anti-[LTBP-2 peptide] antibody, LTBP-2C (10µg/mL), 40x objective with 7.15 and 7.51 second exposure, respectively. *E*, rabbit IgG (10µg/ml) control, 40x objective with 7.51 second exposure. Magnification bars = 50µm.

The tissue localisation studies of LTBP-1 with foetal bovine kidney and aorta tissues gave a similar result. Since the antibody, MAB388 was raised against the human LTBP-1 sequence it seemed likely that immunohistochemical analysis of LTBP-1 would be more successful in human tissues. Analysis of the staining of the remaining bovine tissues were continued using anti-[LTBP-2 peptide] and anti-[fibrillin-1] specific antibodies only.

As will be described in chapters 9 and 10, LTBP-2 has a potential interaction with collagen-IV or another potential basement membrane protein. Foetal bovine kidney tissues, rich in basement membranes, were chosen for analysis of the localisation of fibrillin-1 and LTBP-2 to determine a) if LTBP-2 is localised to basement membrane structures and b) if this localisation is close to fibrillin-1-containing structures. Foetal (200 day) bovine kidney sections were incubated with anti-[fibrillin-1] specific antibody, MAB1919 and it was shown that there was staining of blood vessels and glomeruli (**figure 8.2*A*** and ***B***). The anti-[LTBP-2 peptide] antibody, LTBP-2C gave a general and mostly non-specific staining pattern, which made it difficult to determine which structures of the tissue, if any, actually contained LTBP-2 (**figure 8.2*C*** and ***D***). Thus, these preliminary results indicated that there is little correlation between the distributions of fibrillin-1 and LTBP-2 in this tissue.

Since examination of basement membrane containing kidney proved to be uninformative, it was decided to focus the tissue localisation studies of LTBP-2 using tissues mainly composed of elastic fibres. Another tissue with high presence of elastic fibres and which is also strongly pertinent to Marfan syndrome patients is aorta. Foetal bovine aorta was examined for the presence of fibrillin-1 and LTBP-2. It was found that both fibrillin-1 and LTBP-2 stained elastic fibres strongly and could be easily distinguished from background non-specific staining (**figure 8.3**). The LTBP-2 staining of the elastic fibres was more indistinct than seen for fibrillin-1 but this was attributed to the higher level of non-specific background from the normal rabbit serum (**figure 8.3*D***). Since this tissue gave an excellent result for both the LTBP-2 and fibrillin antibodies, and was available within the human tissue library, human foetal aorta was chosen to continue localisation studies of LTBP-1 and LTBP-2 in relation to fibrillin-containing microfibrils. Furthermore, since a human tissue was to be utilised for these studies it was likely that the anti-[LTBP-1] antibody, MAB388, would be functional.

8.1.2 Analysis of Foetal Human Aorta

In some patients with MFS, the deadly aspect of the disease is the rupture of thoracic aortic aneurysms. To determine if LTBP-2 competes with LTBP-1 for binding to fibrillin-1-containing microfibrils in a similar region at a similar developmental time, a suitable tissue to study would be aorta for its relevance to MFS patients.

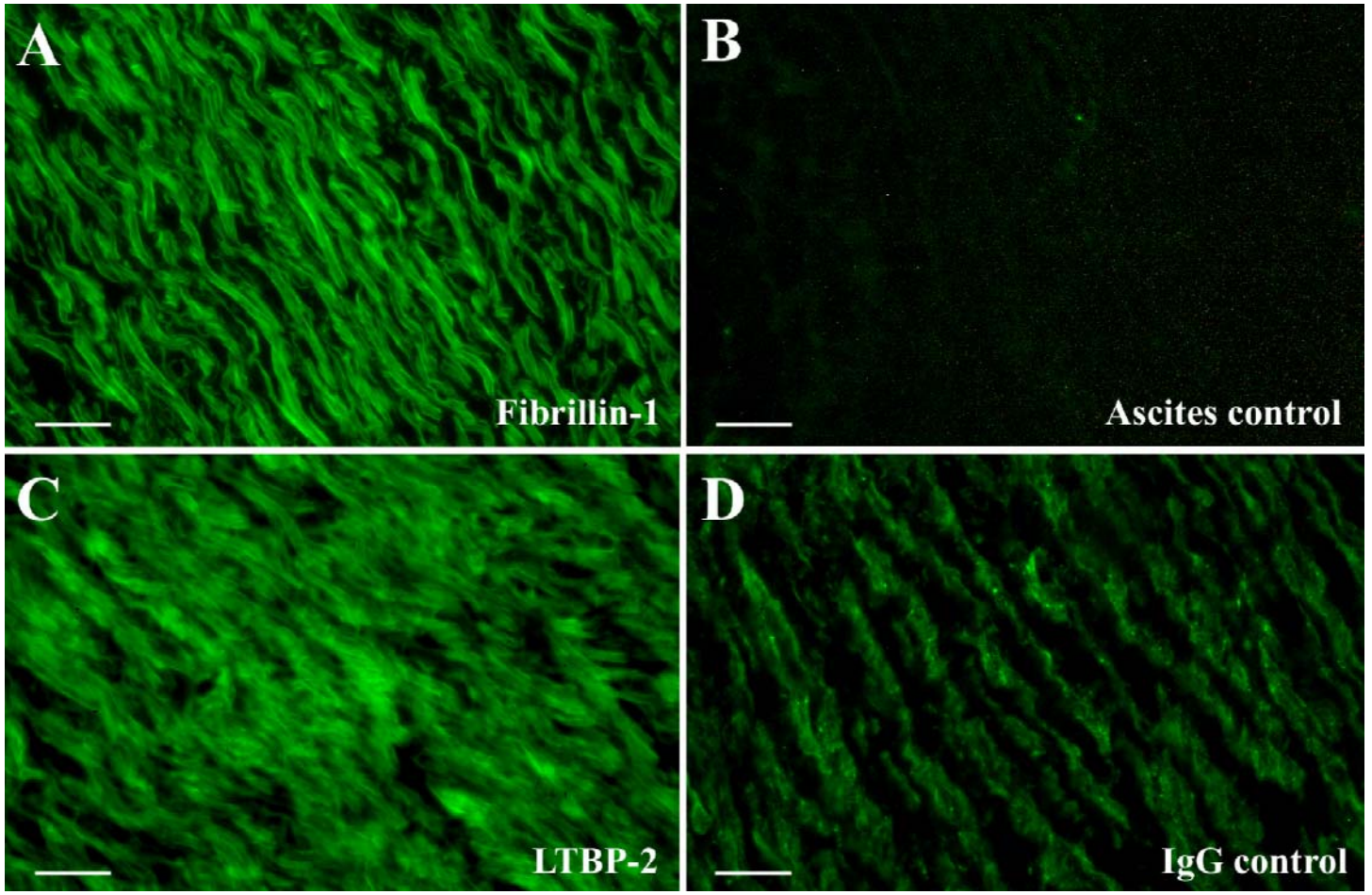

Figure 8.3. Fibrillin-1 and LTBP-2 staining within foetal bovine aorta. Cryostat sections (5 µm) from foetal (200 day) aorta tissue were incubated with antibodies to fibrillin-1 and LTBP-2 diluted in PBS as indicated below. Primary antibody binding was detected using an appropriate secondary antibody conjugated to the flurophore FITC, prior to analysis on the Nikon-FXa microscope. *A,* mouse monoclonal anti-[fibrillin-1] antibody, MAB1919 (5µg/mL), 40x objective with 0.29 second exposure. *B,* mouse ascites control (5µg/mL), 40x objective with 0.29 second exposure. *C,* rabbit polyclonal anti-[LTBP-2 peptide] antibody, LTBP-2C (10µg/mL), 40x objective with 0.86 second exposure. *D*, rabbit IgG (10µg/ml) control, 40x objective with 0.86 second exposure. Magnification bars = 50 µm.

Since the tissue sections were to be dual labelled for fibrillin-1 and LTBPs, all specific antibodies first had to be checked for cross-reaction. LTBP antibodies had already been analysed for cross-reactivity prior to use in solid phase binding assays (**figure 5.13** and **7.6**). However, a polyclonal anti-[fibrillin-1-peptide] antibody, Fib1A, was needed for dual-labelling experiments with the monoclonal anti-[LTBP-1] antibody, MAB388. Antibody Fib1A was tested for cross-reactivity with LTBPs using a solid phase screen. Antibody Fib1A was found to react with the N-terminal fragment of fibrillin-1 [Fib1(H)NT] as expected and did not cross react with fibrillin-2, LTBP-2 or the C-terminal region of LTBP-1 (**figure 5.14**). Incubation of Fib1(H)NT with the anti-[fibrillin-1] antibody, MAB2502 was performed as a positive control for the experiment.

Sections of third trimester human foetal aorta was stained with antibodies to LTBP-1, LTBP-2 and fibrillin-1 and areas of the tissue staining most strongly with each antibody were analysed as described below. As anticipated, the anti-[LTBP-1] specific antibody, MAB388 was found to be immunoreactive within human tissues (**figures 8.4, 8.5*A*** and ***I*** and **8.6*A*** and ***I***).

Initially, cryostat sections of human aorta incubated with antibodies to LTBP-1 or LTBP-2 was analysed using the Nikon FXa microscope and the 10x objective (**figure 8.4**). It was found that for LTBP-1, the distribution was of a gradient nature, with most staining occurring at the junction between the adventitia and the outer media and then petering out towards the inner media only to be strong once again in the internal elastic lamina and intima (**figure 8.4*A***). Staining was absent within the adventitia itself (**figure 8.4*A***). In contrast, the distribution of LTBP-2 was evenly spread throughout the media but the protein was largely absent from the adventitia and intima (**figure 8.4*B***). There was no strong staining of the outer media observed. This pattern of distribution for each LTBP is consistent with the potential for competitive binding of each LTBP to fibrillin-1. In general, it is observed that in regions where there is strong staining of LTBP-2, LTBP-1 is relatively weak and vice versa. To examine this pattern in more detail and confirm that both LTBP proteins were localised on fibrillin-containing microfibrils of elastic fibres, confocal analysis was conducted with cryostat sections incubated with dual combinations of antibodies raised to LTBP-1, LTBP-2 and fibrillin-1. It was chosen to analyse the junction between the adventitia and outer media (**figure 8.5**) and the junction between the intima and inner media, since these regions contain the strongest staining for LTBP-1 (**figure 8.6**).

For confocal microscopy of human aorta tissues, the secondary flurophores were Alexa488 and Cy5. This change from FITC was necessary since the filters used to excite these flurophores are the furthest apart in the emission spectrum to maximise differential staining and the distinct visualisation of the LTBPs, fibrillins and elastin autofluorescence with minimal bleed-through of the fluorescent signal between the individual channels used for analysis.

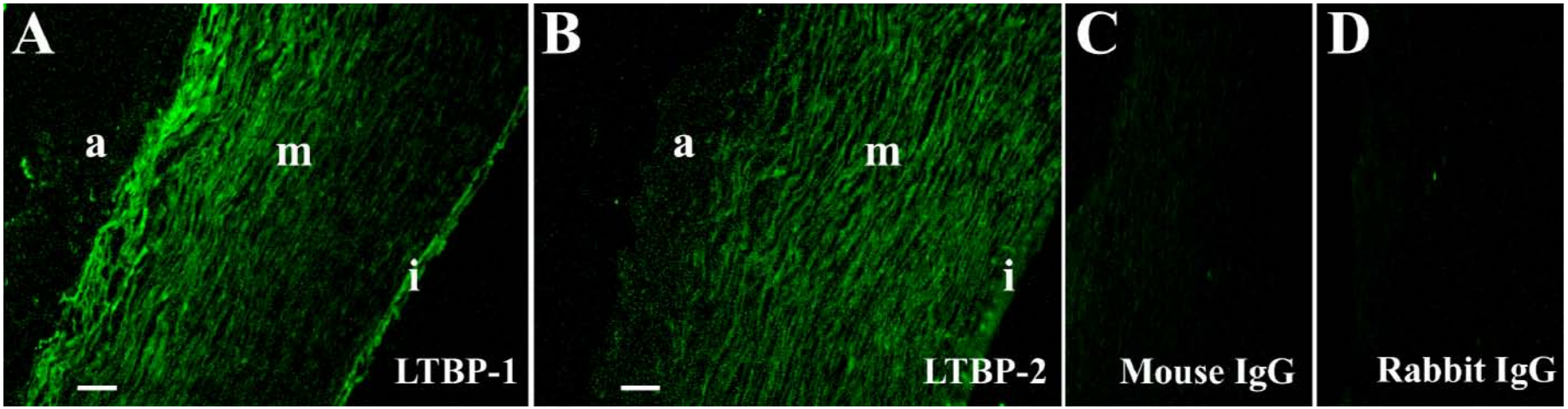

Figure 8.4. Distributions of LTBP-1 and LTBP-2 staining within human foetal aorta. Cryostat sections (5 μm) from third trimester human aorta tissue were incubated with antibodies to LTBP-1 and LTBP-2 diluted in PBS as indicated below. Primary antibody binding was detected using an appropriate secondary antibody conjugated to the flurophore FITC, prior to analysis on the Nikon-FXa microscope. *A,* mouse monoclonal anti-[LTBP-1] antibody, MAB388 (10μg/mL), 10x objective with 40.68 second exposure. *B,* rabbit polyclonal anti-[LTBP-2 peptide] antibody, LTBP-2C (10μg/mL), 10x objective with 48.7 second exposure. *C,* mouse IgG (10μg/mL) control, 10x objective with 40.68 second exposure. *D*, rabbit IgG (10μg/ml) control, 10x objective with 48.7 second exposure. *a,* adventitia; *m*, medial layer; *I*, intima. Magnification bars = 300μm.

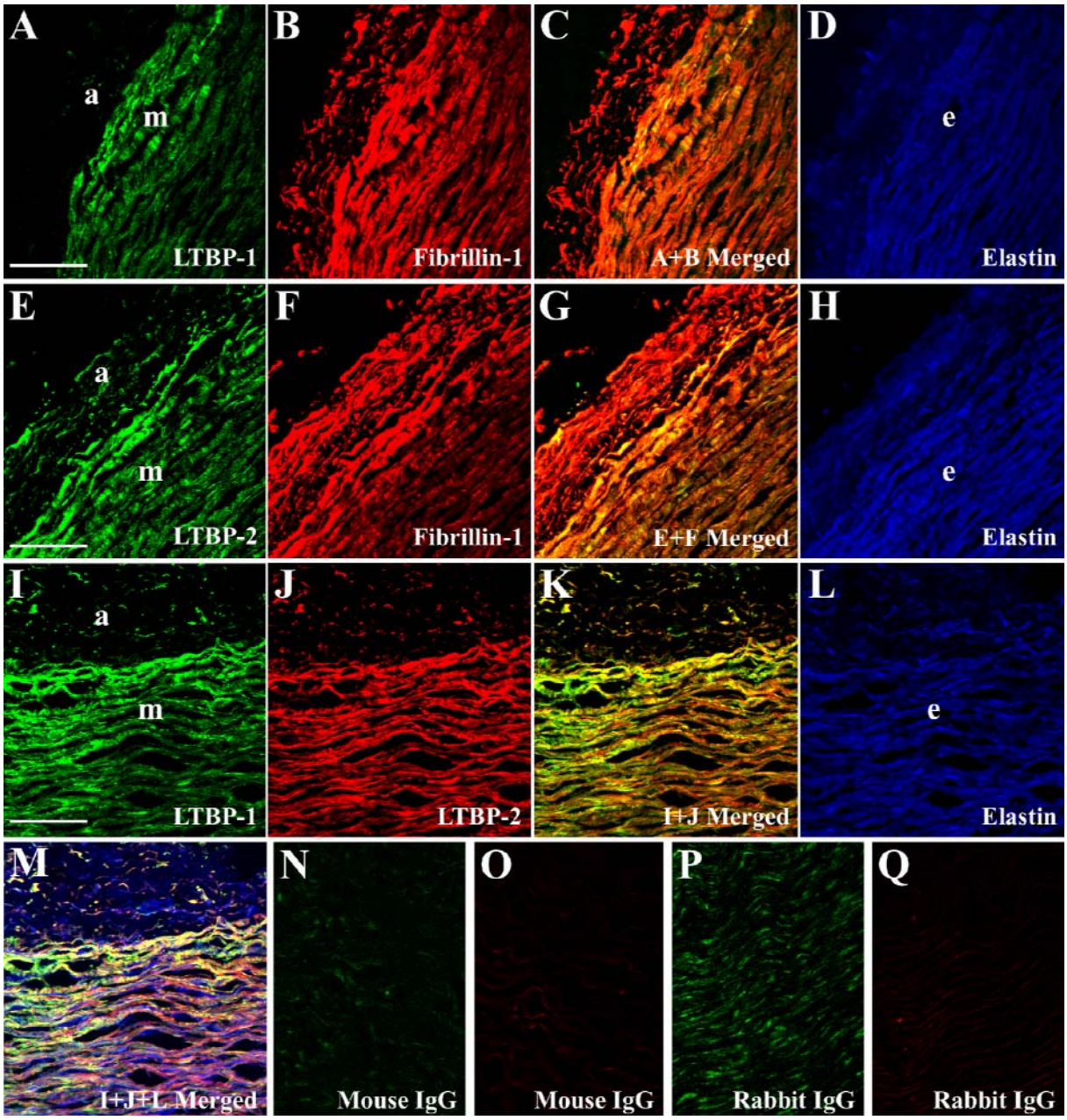

Figure 8.5. The distinct localisation of LTBP-1 and LTBP-2 within the adventitial and medial layers of human foetal aorta. Cryostat sections (5µm) from human trimester foetal aorta tissue was incubated with antibodies to fibrillin-1, LTBP-1 and LTBP-2 diluted in PBS as indicated below. Primary antibody binding was detected using an appropriate secondary antibody conjugated to flurophore Alexa488 or Cy5, prior to analysis on the BioRad scanning confocal microscope equipped with a 40x objective and a 1.5x zoom. *A* and *I,* mouse monoclonal anti-[LTBP-1] specific antibody, MAB388 (10µg/mL); *B*, rabbit polyclonal anti-[fibrillin-1 peptide] specific antibody, Fib1A (1:10 dilution of serum); *C*, A and B merged; *D, H* and *L,* elastin autofluorescence analysed under distinct channel; *E* and *J,* rabbit polyclonal anti-[LTBP-2 peptide] specific antibody LTBP-2C (10µg/mL); *F*, mouse monoclonal anti-[fibrillin-1] specific antibody, MAB1919 (5µg/mL); *G*, E and F merged; *K*, I and J merged; *M*, I, J and L merged; *N,* mouse IgG (10µg/mL) control for A and I*; O*, Mouse IgG (10µg/mL) control for F; *P*, rabbit IgG (10µg/ml) control for E; *Q*, rabbit IgG (10µg/mL) control for B and J. *a*, adventitia; *e*, elastic lamellae; *m*, medial layer. Magnification bars = 50µm.

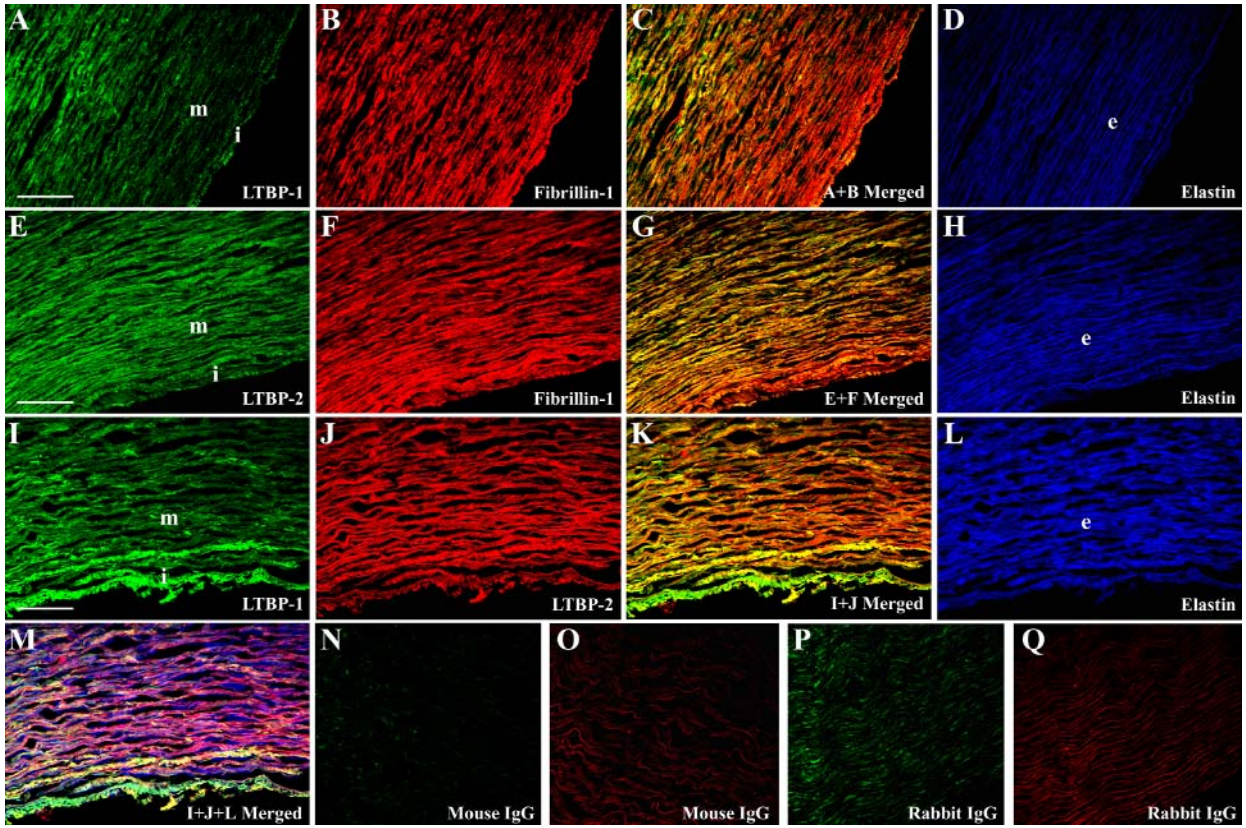

Figure 8.6. LTBP-1 and LTBP-2 have minimal co-localisation within the intimal and medial layers of human foetal aorta. Cryostat sections (5 μm) from human trimester foetal aorta tissue was incubated with antibodies to fibrillin-1, LTBP-1 and LTBP-2 diluted in PBS as indicated below. Primary antibody binding was detected using an appropriate secondary antibody conjugated to flurophore Alexa488 or Cy5, prior to analysis on the BioRad scanning confocal microscope equipped with a 40x objective and a 1.5x zoom. *A* and *I,* mouse monoclonal anti-[LTBP-1] specific antibody, MAB388 (10μg/mL); *B*, rabbit polyclonal anti-[fibrillin-1 peptide] specific antibody, Fib1A (1:10 dilution of serum); *C*, A and B merged; *D, H* and *L,* elastin autofluorescence analysed under distinct channel; *E* and *J,* rabbit polyclonal anti-[LTBP-2 peptide] specific antibody LTBP-2C (10μg/mL); *F*, mouse monoclonal anti-[fibrillin-1] specific antibody, MAB1919 (5μg/mL); *G*, E and F merged; *K*, I and J merged; *M*, I, J and L merged; *N,* mouse IgG (10μg/mL) control for A and I*; O*, Mouse IgG (10μg/mL) control for F; *P*, rabbit IgG (10μg/ml) control for E; *Q*, rabbit IgG (10μg/mL) control for B and J. *a*, adventitia; *e*, elastic lamellae; *m*, medial layer. Magnification bars = 50μm.

Control sections were incubated with the appropriate pre-immune mouse or rabbit IgG and were visualised under the same excitation channels to indicate the level of background staining for each antibody. It was shown that only minimal non-specific cellular staining and/or elastin autofluorescence was visualised (**figures 8.5*N-Q*** and **8.6*N-Q***).

Confocal analysis confirmed that LTBP-1 was localised most intensely in patches of the outer medial region and within the media generally (**figure 8.5*A*** and ***I***). Signal was further intensified again in the intimal regions (**figure 8.6*A*** and ***I***). Fibrillin-1 showed patchy staining within the adventitial region but had strong and continual signal throughout the media (**figure 8.5*B*** and ***F***) and intima regions of the aorta (**figure 8.6*B*** and ***F***). Where staining for LTBP-1 occurred in the outer medial region it coincided with that of fibrillin-1 in most instances (visualised as yellow areas within **figure 8.5*C***). Interestingly, some staining for LTBP-1 occurred independently of fibrillin-1 within the inner medial region (visualised in **figure 8.6*C***, where green staining indicates LTBP-1, red staining indicates fibrillin-1 and yellow/orange indicates co-localisation of the two proteins). However, this independent staining of LTBP-1 is most likely attributed to non-specific background cellular staining of the antibody, which is also seen within the mouse IgG control section (**figure 8.6*N***). This staining pattern indicates that most of the LTBP-1 is localised on fibrillin-containing microfibrils associated with elastic lamellae, with elastin autofluorescence visualised as blue staining (**figures 8.5*D, H*** and ***L*** and **8.6*D, H*** and ***L***).

In contrast to LTBP-1, LTBP-2 showed some punctate localisation within the adventitial and intimal regions but was uniformly and strongly localised within the medial region (**figures 8.5*E*** and ***J*** and **8.6*E*** and ***J***). This staining extensively co-localised with fibrillin-1 (visualised as yellow/orange staining in **figures 8.5*G*** and **8.6*G***) and elastin (**figures 8.5*H*** and **8.6*H***). In further co-localisation studies the two LTBPs were shown to have mostly distinct localisation patterns with some areas of balanced co-localisation evident (visualised in **figures 8.5*K*** and **8.6*K***, where green staining indicates LTBP-1, red staining indicates LTBP-2 and yellow staining indicates strong co-localisation of the two proteins) and the LTBPs staining patterns also localised with the surfaces of elastin lamellae (visualised in **figures 8.5*M*** and **8.6*M***, pink areas indicates the co-localisation of LTBP-2 with elastic lamellae).

Of particular note is that the distribution of LTBP-1 (visualised as the green staining) in the outer medial region (**figure 8.5*K***) and within the intima (**figure 8.6*K***), which is stronger relative to LTBP-2 in these regions. Thus, confocal analysis confirms that the distribution patterns for each LTBP seems to have a general trend whereby areas that are stained strongly for LTBP-2, have LTBP-1 staining which is relatively weak and *vice versa*. This pattern is consistent with the idea that LTBPs-1 and –2 compete for binding onto fibrillin-containing microfibrils throughout the aortic wall but particularly in the outer medial region where the LTBP-1 is predominantly located. Consequently, the high levels of LTBP-2 expression within the medial

region of the aorta may be responsible for the relatively low levels of matrix-associated LTBP-1. Thus, this higher level of LTBP-2 associated with fibrillin-1-containing microfibrils could prevent the binding of latent forms of TGF-β to this region of the tissue. Conversely, in the outer medial and intimal regions of the aorta where LTBP-1 expression is high, there may be reduced attachment of LTBP-2 and thus more latent forms of TGF-β may be available for subsequent activation upon these specific structures. Therefore, even though LTBP-2 does not covalently bind to latent forms of TGF-β, the findings presented within chapters 5-8 of this thesis indicate that LTBP-2 could have a major role in modulating the storage of the growth factor on fibrillin-1-containing microfibrils.

9 Analysis of interactions between LTBP-2 and other extracellular matrix macromolecules

In the chapters 5-8 of this thesis the novel interaction between r-LTBP-2 and the N-terminal region of fibrillin-1 was explored in detail. However, it is still possible that LTBP-2 has the potential to interact with other extracellular matrix macromolecules. In this chapter the potential interactions between r-LTBP-2 and MAGPs, proteoglycans, tropoelastin, fibronectin and collagen were explored. If potential interactions were to be established this would offer further clues to the role(s) of LTBP-2 within the matrix and in relation to its role with fibrillin-1 containing microfibrils.

9.1 LTBP-2 and MAGPs

The possible interaction of r-LTBP-2 with microfibril associated glycoprotein (MAGP)-1 and -2 was investigated using detection with specific antibodies or radiolabelled proteins. No significant interaction was detected between MAGP-1 and r-LTBP-2, with either protein coated in solid phase on the well and the other protein added in solution (**figure 9.1**). Neither MAGP-1 nor LTBP-2 cross-reacted with specific antibodies used to detect potential protein-protein interactions, which was tested by substituting BSA in the solution phase. The lack of interaction between MAGP-1 and r-LTBP-2 was further confirmed by using ^{125}I-labelled r-LTBP-2 in the liquid phase (**figure 9.2**).

Since LTBP-2 has a large number of calcium-binding EGF-like repeats, it is possible that protein-protein interactions between r-LTBP-2 and extracellular matrix macromolecules could be enhanced by the presence of Ca^{2+} ions within buffering solutions. Thus, in another set of experiments conducted between MAGP-2 and r-LTBP-2, Ca^{2+} ions were added to the buffers to determine if potential interactions could be Ca^{2+} ion dependent. To test for interactions between r-LTBP-2 and MAGP-2, solid phase binding assays were conducted both in the presence of 5mM $CaCl_2$ and without added Ca^{2+} ions (**figure 9.3**). In the case of MAGP-2 and LTBP-2 no significant protein-protein interactions were detected with or without added Ca^{2+} ions (**figure 9.3**). MAGP-2 did not cross-react with the anti-[tetrahis] antibody since the addition of BSA in solution gave minimal signal (**figure 9.3**). The reverse interaction with r-LTBP-2 coated on the well was tested with ^{125}I-labelled MAGP-2 and no significant binding above background levels was again detected (**figure 9.4*A***). This lack of interaction was also checked using ^{125}I-labelled r-LTBP-2 with consistent results (**figure 9.4*B***). This data indicates that LTBP-2 does not interact with MAGPs-1 or –2.

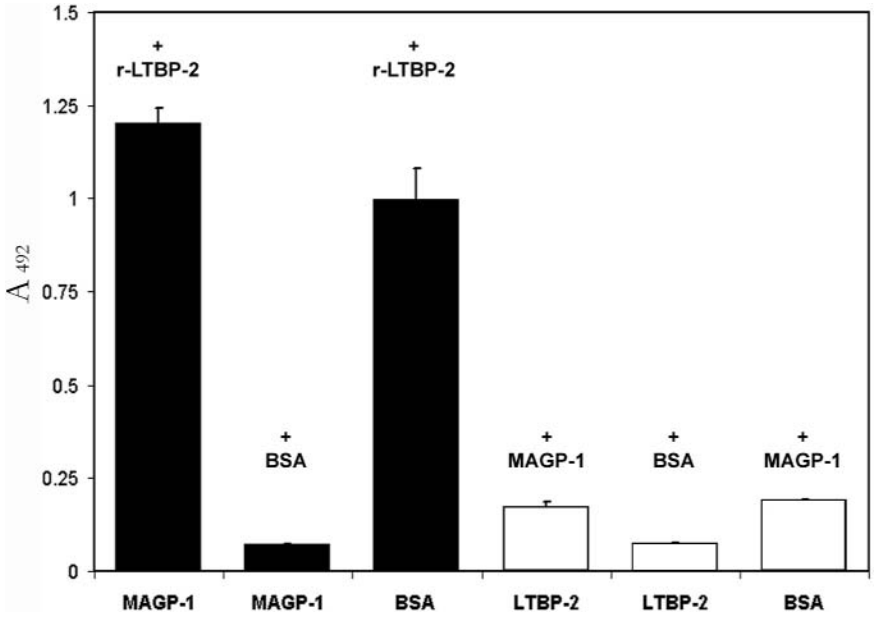

Figure 9.1. Solid phase binding assay to determine possible interactions between r-LTBP-2 and tissue-extracted MAGP-1. Individual wells of microtitre plates were coated with tissue-extracted MAGP-1 (200ng/well, *black columns*) or r-LTBP-2 (200ng/well, *white columns*) in TBS buffer. Control wells were coated with BSA (16ng/well). After blocking with 3% BSA/TBS (*black columns*) or 3% milk/TBS (*white columns*), MAGP-1 (400ng/well, *white columns*), r-LTBP-2 (400ng/well, *black columns*) or BSA (400ng/well) were added to wells and incubated for 3 hrs at 37°C. After washing, anti-[tetrahis] antibody (1:2000 dilution) was added to wells of *black columns* and anti-[MAGP-1] antibody, rabbit 18 (1:1000 dilution) was added to wells of *white columns* and left to incubate for 2 hrs at 37°C. After washing, specific binding of the anti-[tetrahis] or anti-[MAGP-1] antibodies were detected at 492nm using peroxidase-conjugated secondary antibody and colour development for 30 minutes. Means ± S.D. and binding of triplicate determinations are shown.

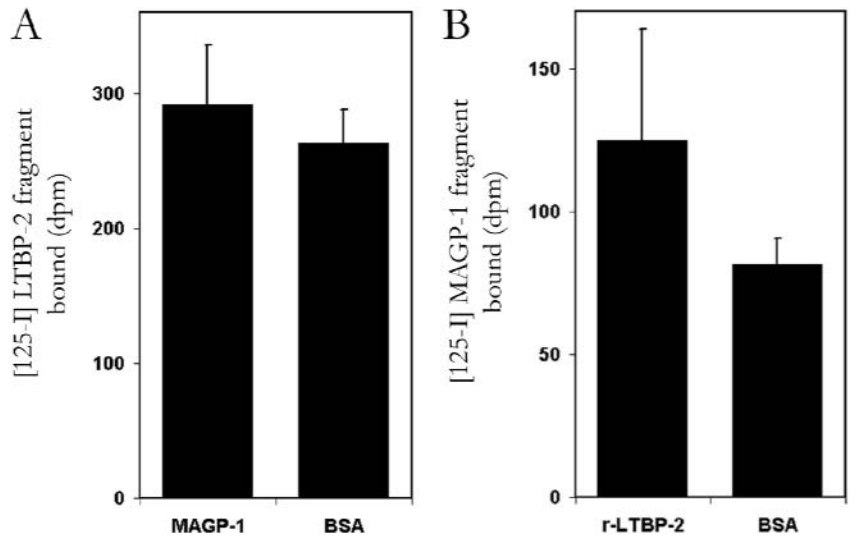

Figure 9.2. Solid phase binding assays showing r-LTBP-2 does not interact with MAGP-1. *A,* individual wells of microtitre plates were coated with tissue-extracted MAGP-1 (100ng/well) or BSA (366ng/well) in TBS buffer. After blocking with 3% milk/TBS, 6500dpm of ^{125}I-labelled r-LTBP-2 (specific activity 1.8×10^5/μg) was added to each well and incubated for 3 hrs at 37°C. *B,* individual wells of microtitre wells were coated with r-LTBP-2 (200ng/well) and BSA (62ng/well) in TBS buffer. After blocking, 1.28×10^5 dpm of ^{125}I-labelled MAGP-1 (specific activity 1.5×10^7dpm/μg) was added to each well and incubated for 3 hrs at 37°C. After washing, binding of radioligand was measured by γ counting. Means ± S.D. and binding of triplicate determinations are shown.

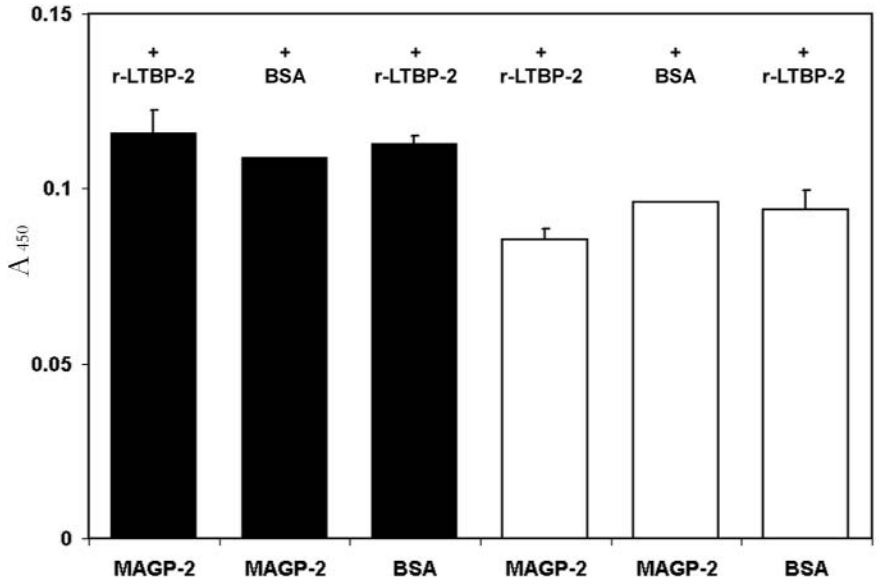

Figure 9.3. Solid phase binding assay to test for potential interactions between r-LTBP-2 and tissue-extracted MAGP-2. Individual wells of microtitre plates were coated with tissue-extracted MAGP-2 (200ng/well) without $CaCl_2$ (*black columns*) or with 5mM $CaCl_2$ (*white columns*) in TBS buffer. Control wells were coated with a molar equivalent of BSA (350ng/well). After blocking with 3% milk/TBS, r-LTBP-2 (400ng/well) or BSA (124ng/well) was added to wells and incubated for 3 hrs at 37°C. After washing, anti-[tetrahis] antibody (1:2000 dilution) was added to wells and incubated for 2 hrs at 37°C. After washing, specific binding of the anti-[tetrahis] antibody was detected at 450nm using peroxidase-conjugated secondary antibody and colour development for 60 minutes. Means ± S.D. and binding of triplicate determinations are shown.

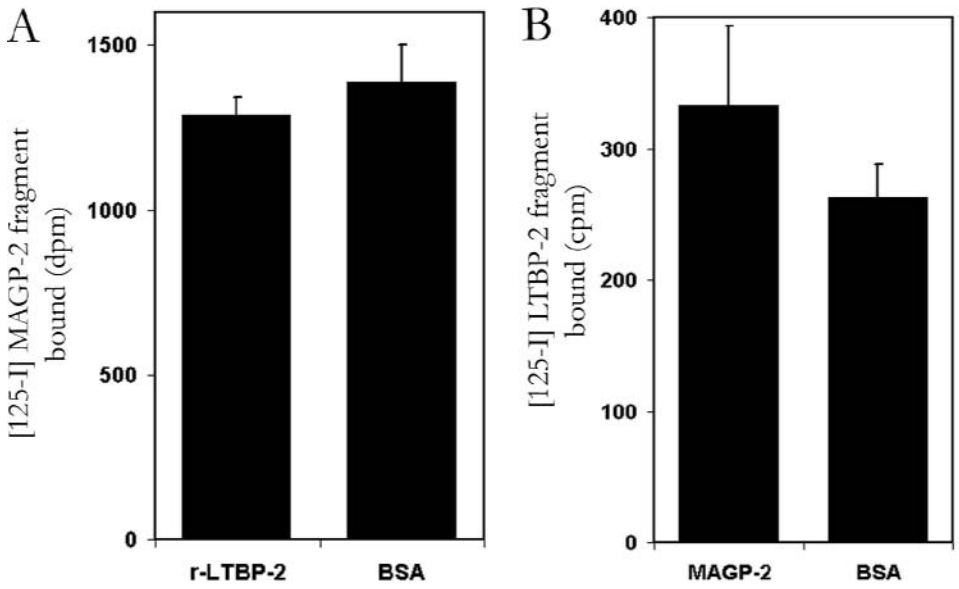

Figure 9.4. Solid phase binding assay showing r-LTBP-2 does not interact with MAGP-2. *A,* individual wells of microtitre plates were coated with r-LTBP-2 (200ng/well) or BSA as a control (62ng/well) in TBS buffer. After blocking with 3% milk/TBS, $2x10^5$dpm of ^{125}I-labelled MAGP-2 (specific activity $1.28x10^7$dpm/μg) was added to each well and incubated for 3 hrs at 37°C. *B,* individual wells of microtitre plates were coated with tissue-extracted MAGP-2 (100ng/well) or BSA as a control (366ng/well) in TBS buffer. After blocking, 6500dpm of ^{125}I-labelled r-LTBP-2 (specific activity $1.8x10^5$dpm/μg) was added to each well and incubated for 3 hrs at 37°C. After washing, binding of the radioligand was measured by γ counting. Means ± S.D. and binding of triplicate determinations are shown.

9.2 LTBP-2 and laminin, proteoglycans, fibronectin and tropoelastin

r-LTBP-2 was tested for interaction with laminin and was not found to have a significant interaction above background levels. Laminin did not cross-react with the specific anti-[LTBP-2 peptide] antibody, LTBP-2C, since the signal detected was similar to that for when BSA was added in solution (**figure 9.5**).

For some of the interaction studies between r-LTBP-2 and MAGPs, the r-LTBP-2 was radiolabelled with $Na^{125}I$, however in some cases this radiolabel could result in conformation changes within the protein and mask potential binding regions. To ensure that the ^{125}I radiolabel was not interfering with potential extracellular macromolecule binding sites upon r-LTBP-2, it was chosen to radiolabel r-LTBP-2 with ^{35}S for subsequent binding assays for reasons as described in section **5.2.1**. ^{35}S-labelled r-LTBP-2 was tested for interaction with decorin and biglycan and no significant interaction was detected with either the mature proteoglycans containing the glycosaminoglycan (GAG) chains or with the protein core alone (**figure 9.6**).

^{35}S-labelled r-LTBP-2 was also screened for interaction with tropoelastin (**figure 9.7*A***) and fibronectin (**figure 9.7*B***) and again no significant interaction was seen with either protein.

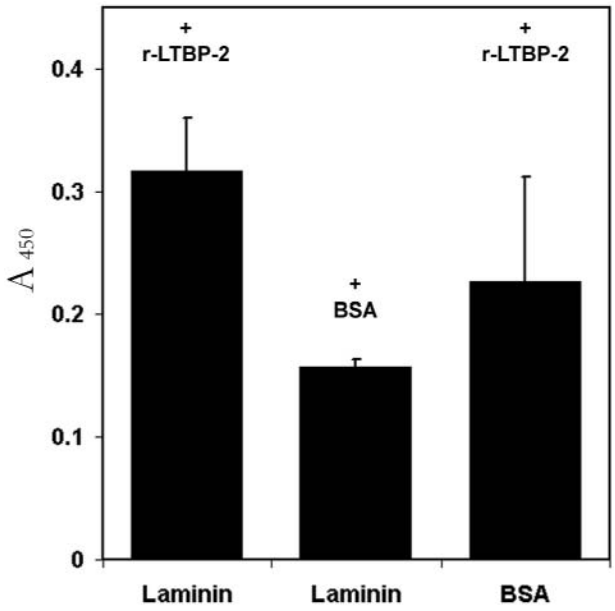

Figure 9.5. Solid phase binding assay showing r-LTBP-2 does not interact with laminin. Individual wells of microtitre plates were coated with laminin (400ng/well) in TBS/2mM $CaCl_2$ buffer. Control wells were coated with a molar equivalent of BSA (150ng/well). After blocking with 3% BSA/TBS, r-LTBP-2 (400ng/well) was added to wells and incubated for 3 hrs at 37°C. After washing, anti-[tetrahis] antibody (1:2000 dilution) was added to each well and incubated for 2 hrs at 37°C. After washing, specific binding of the anti-[tetrahis] antibody was detected at 450nm using peroxidase-conjugated secondary antibody and colour development for 30 minutes. Means ± S.D. and binding of triplicate determinations are shown.

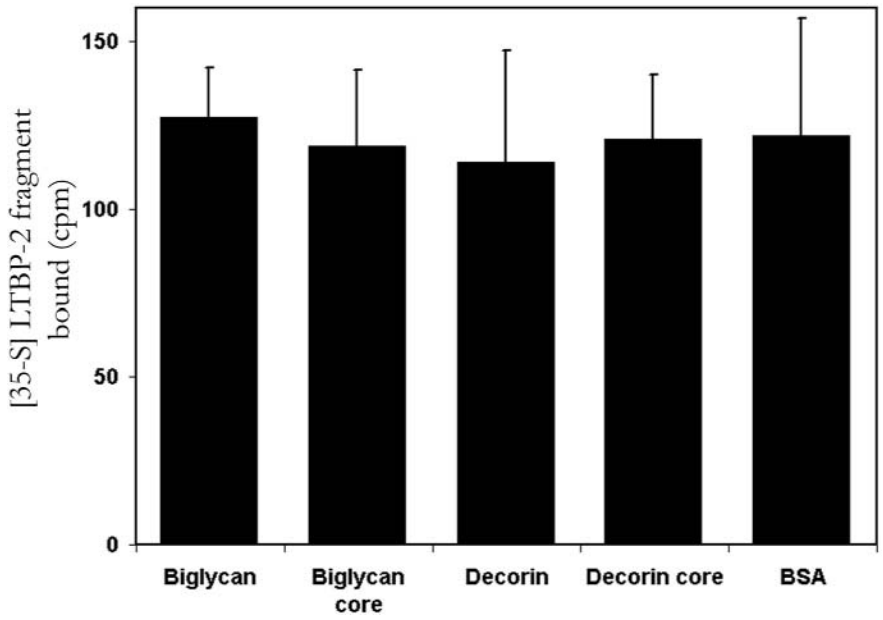

Figure 9.6. Solid phase binding assay showing r-LTBP-2 does not interact with biglycan or decorin. Individual wells of microtitre plates were coated with mature or core proteoglycans (200ng/well) in TBS/2mM $CaCl_2$. Control wells were coated with BSA (200ng/well). After blocking with 3% milk/TBS, 12800dpm of ^{35}S-labelled r-LTBP-2 (specific activity $1x10^6$dpm/µg) was added to each well and incubated for 3 hrs at 37°C. After washing, binding of the radioligand was measured by scintillation counting. Means ± S.D. and binding of triplicate determinations are shown.

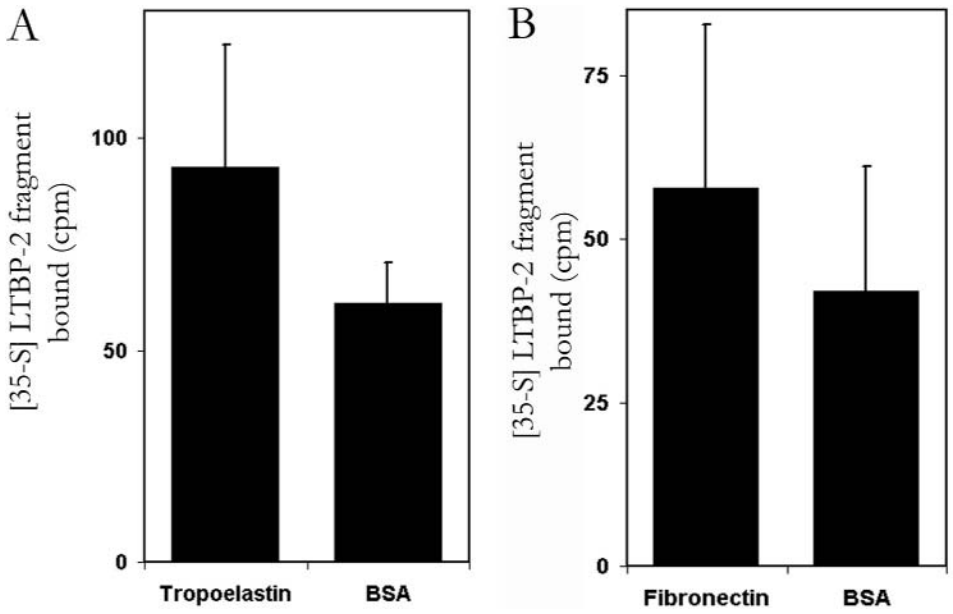

Figure 9.7. Solid phase binding assay showing r-LTBP-2 does not interact with tropoelastin or fibronectin. *A,* individual wells of microtitre plates were coated with tropoelastin (200ng/well) in TBS/2mM $CaCl_2$. Control wells were coated with BSA (200ng/well). After blocking with 3% milk/TBS, 6500dpm of ^{35}S-labelled r-LTBP-2 (specific activity $1x10^6$dpm/µg) was added to wells and incubated for 3 hrs at 37°C. *B,* individual wells of microtitre plates were coated with fibronectin (200ng/well) in TBS/2mM $CaCl_2$. Control wells were coated with BSA (200ng/well). After blocking, 12800dpm of ^{35}S-labelled r-LTBP-2 (specific activity $1x10^6$dpm/µg) was added to wells and incubated for 3 hrs at 37°C. After washing, specific binding of the radioligand was measured by scintillation counting. Means ± S.D. and binding of triplicate determinations are shown.

9.3 LTBP-2 and collagens

r-LTBP-2 was screened against a variety of collagen preparations, both native (salt-extracted) or pepsin-digested. Some of these preparations were commercial, however the majority had been prepared in the Gibson laboratory by salt extraction from bovine tissues (see section **4.6** of materials and methods for details). No significant interaction above background levels was detected between r-LTBP-2 and bovine pepsin-collagens-I, -II, -III, -V, -VI or native collagens-I, -III and -VI. However, it was found that r-LTBP-2 reacted strongly to a crude bovine collagen-IV preparation (**figure 9.8**) and further investigation of this interaction will be discussed in chapter 10.

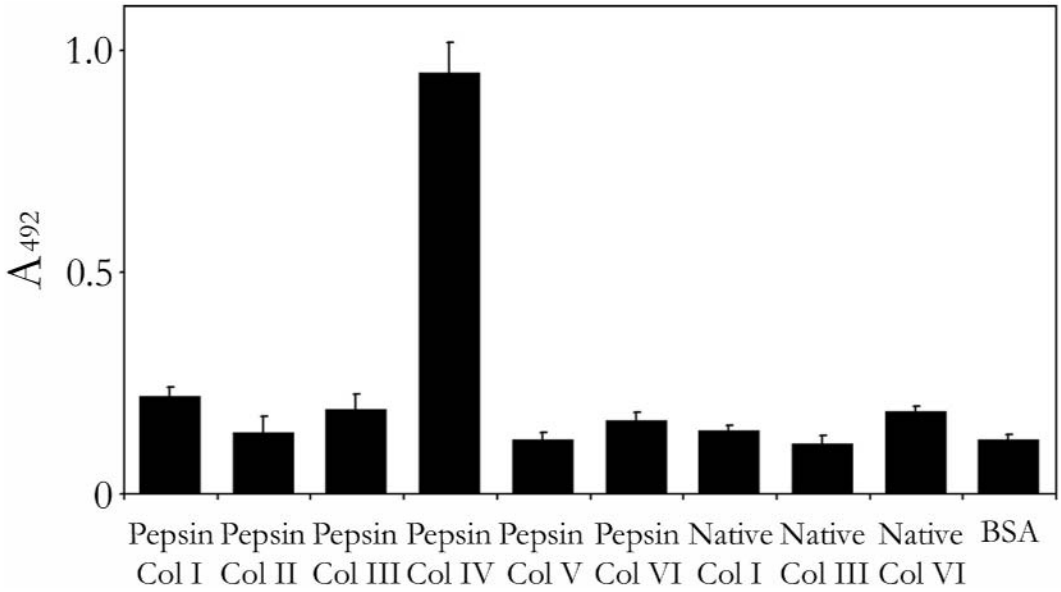

Figure 9.8. r-LTBP-2 interacts with a crude bovine collagen-IV preparation**.** Individual wells of microtitre plates were coated with collagen preparations, both native and pepsin treated (400ng/well) in TBS/2mM $CaCl_2$ buffer. Control wells were coated with BSA (400ng/well). After blocking with 5% milk/TBS/2mM $CaCl_2$, r-LTBP-2 (400ng/well) was added to wells and incubated for 3 hrs at 37°C. After washing, anti-[tetrahis] antibody (1:2000 dilution) was added to wells and incubated for 2 hrs at 37°C. After washing, specific binding of the anti-[tetrahis] antibody was detected at 492nm using peroxidase-conjugated secondary antibody and colour development for 30 minutes. Means ± S.D. of sextuplet determinations are shown.

10 LTBP-2 interactions with a crude salt-fractionated pepsin-collagen-IV preparation

10.1 r-LTBP-2 interactions with bovine collagen-IV enriched pepsin extract

As mentioned in chapter 9, r-LTBP-2 was screened for interaction with a myriad of collagens, both native and pepsin-treated. Solid phase binding assays indicated an interaction occurred between r-LTBP-2 and a crude bovine preparation enriched with basement membrane collagen-IV (**figure 9.8**). This crude bovine collagen-IV extract used within this assay was prepared by differential salt precipitation from bovine placental tissue as described by Abedin *et al.*, 1982. It was determined that the interaction between r-LTBP-2 and the crude collagen-IV preparation was specific since it was concentration dependent (**figure 10.1**). For the interaction between LTBP-2 and fibrillin-1 reported in chapters 5 and 6, it was determined that the C-terminal region of LTBP-2 contained the specific binding sequence for fibrillin-1. To determine whether this region of the molecule of LTBP-2 interacts with the crude collagen-IV preparation, the C-terminal fragment [LTBP-2CT(H)] was tested for binding with the collagen-IV enriched extract. The C-terminal fragment of r-LTBP-2 was found not to interact with this collagen-IV preparation, indicating the binding site was located in the central or N-terminal region of r-LTBP-2 (**figure 10.2**).

10.1.1 The Interaction Between r-LTBP-2 and the Crude Bovine Collagen-IV Preparation is not Ca^{2+} Ion Dependant

As reported in section **5.2.3**, the interaction between LTBP-2 and fibrillin-1 was shown to have dependence on the presence of Ca^{2+} ions. To determine if the interaction between r-LTBP-2 and the crude collagen-IV preparation required the presence of Ca^{2+} ions, a solid phase binding assay was conducted with calcium ion concentrations of 2mM and 5mM and EDTA of 5mM concentration was added to some wells to chelate Ca^{2+} ions from the protein. It was found that the interaction between r-LTBP-2 and the collagen-IV preparation was not abolished by the presence of EDTA in binding solutions, indicating it was not directly Ca^{2+} ion dependant (**figure 10.3**). However, as seen for the interaction between LTBP-2 and fibrillin-1, there was some enhancement of the interaction in the presence of 2mM Ca^{2+} ions, which possibly acts to ensure the correct tertiary structure of r-LTBP-2 (**figure 10.3**).

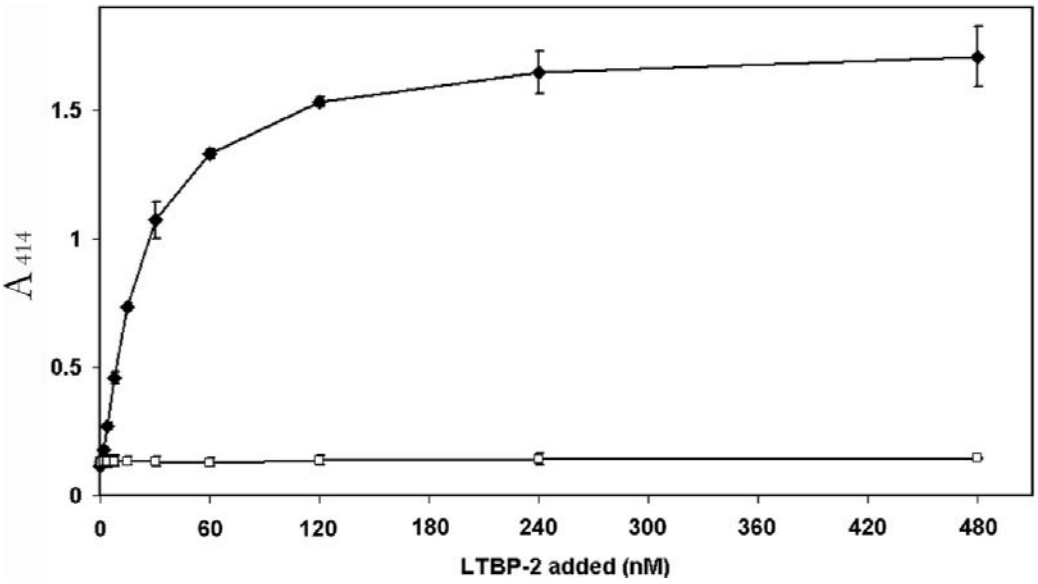

Figure 10.1. Solid phase binding assay to show that the interaction between r-LTBP-2 and the crude bovine collagen-IV preparation is concentration dependant. Individual wells of microtitre plates were coated with the crude collagen-IV preparation (200ng/well, *black diamonds*) in TBS/2mM $CaCl_2$. Control wells were coated with BSA (200ng/well, *open squares*). After blocking with 3% BSA/TBS, a serial dilution of r-LTBP-2 (0-480nM/well) was added to wells and left to incubate for 3 hrs at 37°C. After washing, anti-[his_6-tag] antibody, tetrahis (1:2000 dilution) was added to wells and incubated for 2 hrs at 37°C. After washing, specific binding of the anti-[tetrahis] antibody was detected at 414nm using peroxidase-conjugated secondary antibody and colour development for 10 minutes. Means ± S.D. of triplicate determinations shown.

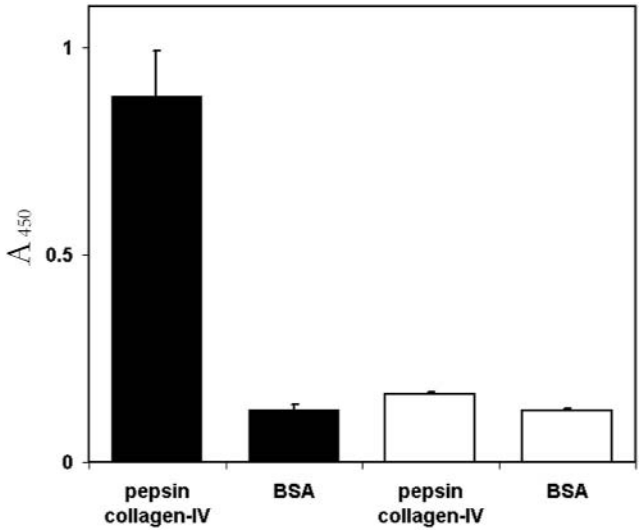

Figure 10.2. r-LTBP-2CT(H) does not interact with the crude bovine collagen-IV preparation. Individual wells of microtitre plates were coated with the collagen-IV preparation (400ng/well) or BSA (400ng/well) in TBS/2mM $CaCl_2$. After blocking with 5% milk/TBS, r-LTBP-2 (400ng/well, *black columns*) or r-LTBP-2CT(H) (400ng/well, *white columns*) were added to wells and incubated for 3 hrs at 37°C. After washing, anti-[LTBP-2 peptide] specific antibody, LTBP-2C (1:10000 dilution) was added to wells and incubated for 2 hrs at 37°C. After washing, specific binding of the LTBP-2C antibody was detected at 450nm using peroxidase-conjugated secondary antibody and colour development for 30 minutes. Means ± S.D. of triplicate determinations are shown.

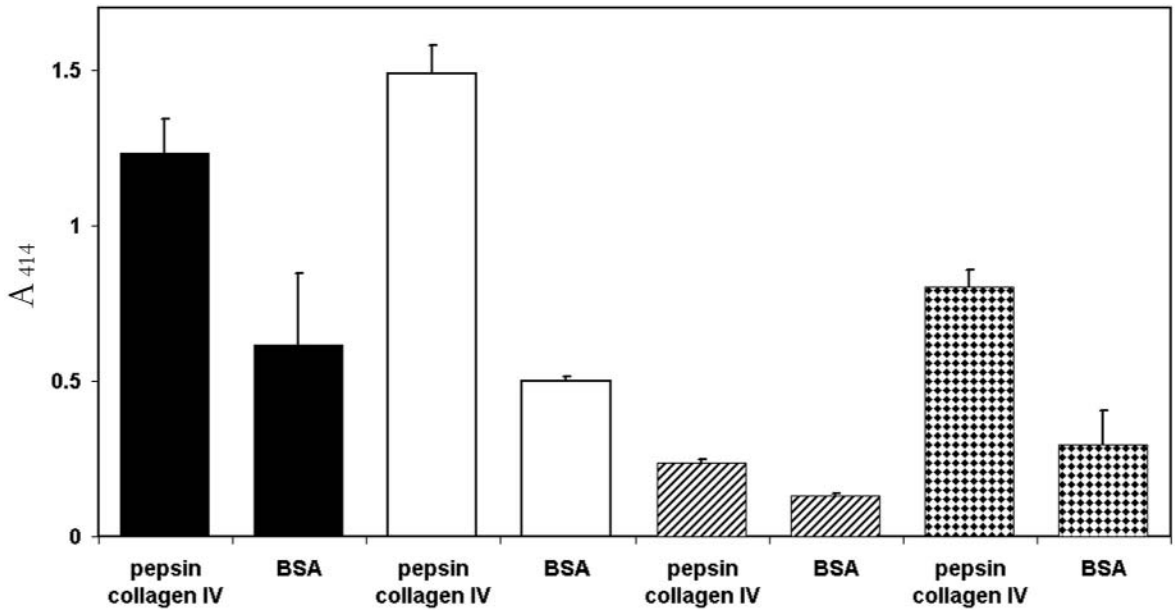

Figure 10.3. The interaction between r-LTBP-2 and the crude bovine collagen-IV preparation is not dependant on the presence of calcium ions. Individual wells of microtitre plates were coated with the collagen-IV preparation (100ng/well) in TBS without added $CaCl_2$ (*black columns*) or containing 2mM $CaCl_2$ (*white columns*), 5mM $CaCl_2$ (*cross-hatched columns*) or 5mM EDTA (*chequered columns*). Control wells were coated with BSA (400ng/well). After blocking with 3% BSA/TBS, r-LTBP-2 (200ng/well) was added to the wells diluted in the appropriate TBS buffer and incubated for 3 hrs at 37°C. After washing, anti-[his_6-tag] antibody, tetrahis (1:2000 dilution) was added to wells and incubated for 2 hrs at 37°C. After washing, specific binding of the anti-[tetrahis] antibody was detected at 414nm using peroxidase-conjugated secondary antibody and colour development for 30 minutes. Means ± S.D. of triplicate determinations are shown.

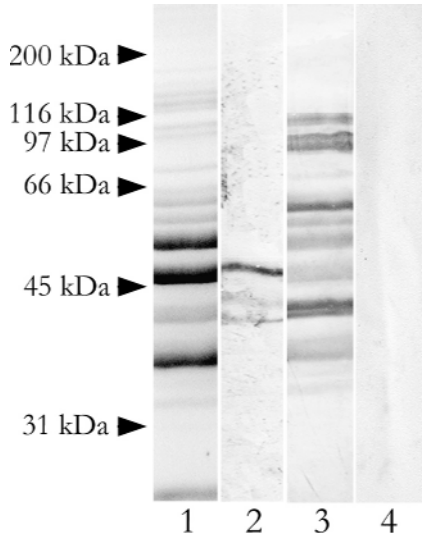

Figure 10.4. Overlay western blot to identify the r-LTBP-2 interactive bands of the crude collagen-IV preparation. The collagen-IV preparation (1µg/lane) was resolved by SDS-PAGE using a 12% gel under reducing conditions and was stained with Coomassie Blue (*lane 1*) or transferred onto PVDF membrane. After equilibration in binding buffer (TBS/2mM $CaCl_2$) and blocking with 3% milk, duplicate blots were incubated with 5µg/mL of r-LTBP-2 (*lane 2*) or BSA (*lane 4*) for 8 hours at 4°C. Specific binding to protein bands within the bovine collagen-IV preparation (~35-40kDa) was detected using anti-[his_6-tag] antibody, tetrahis (1:2000 dilution). A further blot was incubated with anti-[collagen-IV] antibody, r29 (1:50 dilution) as a positive control (*lane 3*). The *arrowheads* indicate the relative mobilities of concurrently run protein standards.

10.1.2 Mass Spectrometric Analysis of the Interacting Protein Within the Crude Collagen-IV Preparation

When this crude bovine collagen-IV preparation was analysed on SDS-PAGE a number of bands were present and the majority, but not all, of these immunoreacted to a rabbit polyclonal anti-[collagen-IV] antibody, rabbit 29 (r29) (**figure 10.4**, *lanes 1* and *3*). Thus, it is possible that proteins unrelated to collagen-IV chains are present within this crude pepsin extract that may be responsible for the interaction with r-LTBP-2. Thus it was pertinent to confirm the identity of the LTBP-2 interacting protein. Western blot overlay assays were performed to identify the interacting protein band, which could then be isolated and subjected to mass spectrometric analysis for identification. Western overlay blots conducted between r-LTBP-2 and the crude collagen-IV preparation resulted in three specific bands of sizes 42, 42.5 and 45.5kDa (**figure 10.4**).

These interacting bands were subjected to mass spectrometric analysis for identification. The top most band was determined to contain the peptide sequence of AADPGPEGLPLVVLGSLGFQGPQGDR, which was found to match NCBI#33859528 (Swissprot:CA14_MOUSE, Collagen alpha 1 IV chain precursor), followed by manual inspection of the peptide fragment indicating a likely peptide sequence of VVPLLGPLGAEGLLGSLGFQGPQGDR which strongly matched the tryptic peptide VVPLPGPPGAEGLPGSPGFPGPQGDR of XP_509730 (Collagen alpha 1 IV from Pan troglodytes). The two closely spaced bands identified to interact with r-LTBP-2 from the western overlay blot were analysed with mass spectrometry together and most likely had a peptide sequence of {DG}PGPPGPPPLLEPGmK (where {DG} = DG or GD and m = methionine sulphoxide) which was identified to match NCBI#115349 (Swissprot:CA24_HUMAN, Collagen alpha 2 IV chain precursor). Other peptides analysed from the sample were found to be rich in glycine, proline, leucine and serine with evidence for hydroxylation of the proline residues and glycosylation, which is indicative of amino acid compositions typical for collagen proteins.

Mass spectrometric analysis indicated that LTBP-2 appeared to bind two separate chains (α1 and α2) of collagen-IV. This seemed unusual since most binding sites occur on only one collagen chain due to the complex triple helical complex of the collagen-IV molecule. This indicated the potential for the interaction between r-LTBP-2 and the crude bovine collagen-IV preparation to be due to non-specific binding. To determine if the binding between collagen-IV and LTBP-2 occurs in a biological situation, interactions between r-LTBP-2 and commercial preparations of human basement membrane collagen-IV were analysed (see section below).

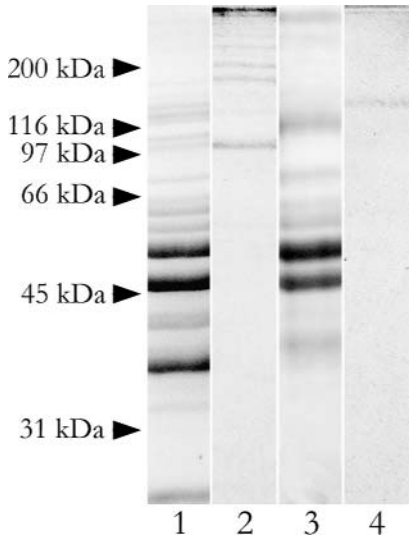

Figure 10.5. Comparison of the protein bands present between the crude collagen-IV and the commercial human placenta collagen-IV preparations. The collagen-IV protein bands were resolved on 12% SDS-PAGE and stained with Coomassie Blue. *Lane 1,* the crude collagen-IV preparation (1µg/lane) under reducing conditions. *Lane 2*, human placenta native collagen-IV (1µg/lane) under reducing conditions. *Lane 3,* the crude collagen-IV preparation (1µg/lane) under non-reducing conditions. *Lane 4,* human placenta native collagen-IV (1µg/lane) under non-reducing conditions. The commercial collagen-IV preparation contains a large number of high molecular weight bands when compared with the crude bovine collagen-IV preparation. The *arrowheads* indicate the relative mobilities of concurrently run protein standards.

10.1.3. r-LTBP-2 does not Interact with Commercial Human Preparations of Collagen-IV

To confirm an interaction occurs between LTBP-2 and the basement membrane collagen-IV itself, a preparation of human placenta basement membrane collagen-IV was obtained from commercial sources (Sigma-Aldrich catalogue number C5533) and tested for interaction with r-LTBP-2. This commercial collagen-IV preparation had been prepared by salt-fractionation and had been only mildly digested with pepsin. When analysed on SDS-PAGE the commercial collagen-IV preparation was composed of a number of high molecular weight bands (of a range of sizes upwards of 97kDa), which differed from the crude bovine collagen-IV preparation where protein bands of numerous sizes could be seen (upwards of 33kDa) (**figure 10.5**). These differences in the number of protein bands is most likely due to the duration of pepsin treatment. Solid phase binding assays were used to test for an interaction between r-LTBP-2 and the commercial collagen-IV preparation and it was found that there was little significant signal above background levels (for this control, BSA was coated on the well in place of collagen-IV), indicating no interaction had occurred (**figure 10.6**). This interaction was also tested using an alternate preparation of human placental collagen type-IV available from Sigma-Aldrich (catalogue number C7521). It was also found that there was no interaction between LTBP-2 and collagen type-IV (C7521) and this was found to be consistent with the preparation under the catalogue number C5533 used in **figure 10.6** (data not shown).

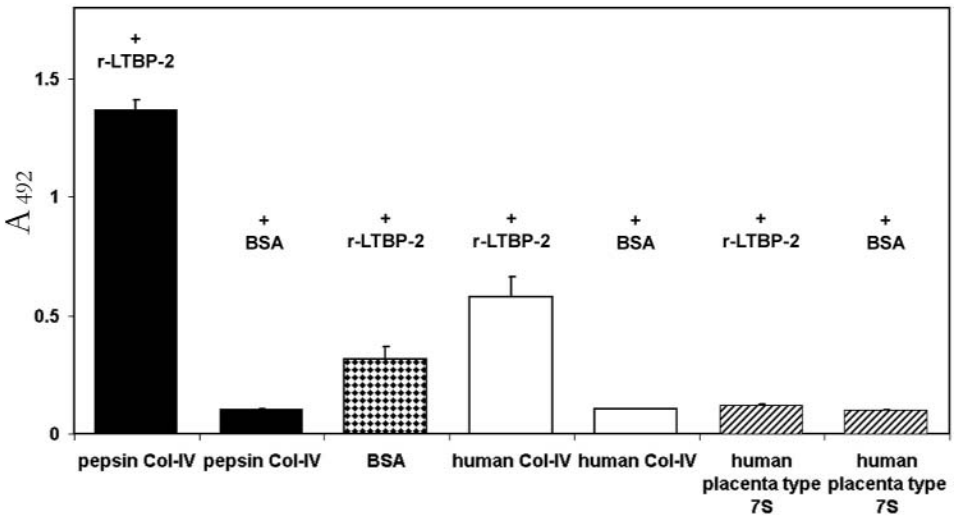

Figure 10.6. r-LTBP-2 does not interact with the commercial human placenta collagen-IV preparation. Individual wells of microtitre plates were coated with the crude bovine collagen-IV preparation (400ng/well, *black columns*), BSA (400ng/well, *chequered column*), commercial collagen-IV (400ng/well, *white columns*) or human placenta type 7S preparation (400ng/well, *cross-hatched columns*) in TBS/2mM $CaCl_2$. After blocking with 3% BSA/TBS, r-LTBP-2 (400ng/well) or a molar equivalent of BSA (125ng/well) was added to wells as indicated and incubated for 3 hrs at 37°C. After washing, anti-[his_6-tag] antibody, tetrahis (1:2000 dilution) was added to wells and incubated for 2 hrs at 37°C. After washing, specific binding of the tetrahis antibody was detected at 492nm using peroxidase-conjugated secondary antibody and colour development for 30 minutes. Means ± S.D. of triplicate determinations are shown.

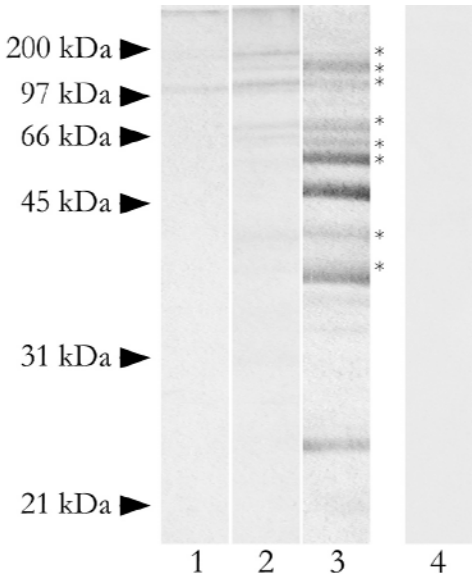

Figure 10.7. Analysis of the commercial native human placenta collagen-IV preparation following pepsin-digestion. The collagen-IV protein bands (~1µg/lane) were resolved under reducing conditions on 15% SDS-PAGE and stained with Coomassie Blue. Commercial collagen-IV (*lane 1*) was digested with 20mg of pepsin for 72 hours at 4°C (*lane 2*). After pepsin-digestion, some of the bands (*) present within the commercial collagen-IV sample matched bands present within the crude bovine collagen-IV preparation (*lane 3*). Pepsin enzyme (MW 35kDa) nor buffer solution contributed to the presence of any bands present within the pepsin-treated commercial collagen-IV sample (*lane 4*). The 20mg of pepsin enzyme which should be present could not be seen in *lane 4* thus it seems most likely the enzyme had degraded during the 72 hour incubation period. The *arrowheads* indicate the relative mobilities of concurrently run protein standards.

A further solid phase binding assay was conducted with type 7S domains. Type 7S domains are the cross-linked ends of collagen-IV molecules that are cleaved off by pepsin. Since these domains have unique binding properties when compared with the pepsin-collagen-IV chains, it was pertinent to test these domains for interaction with r-LTBP-2. When a preparation of human placenta type 7S was tested for interaction with r-LTBP-2 there was no significant interaction above BSA background levels (**figure 10.6**).

It is possible that the interaction site is buried within the triple helical structure of the collagen chains and may only be exposed after pepsin treatment. Even though pepsin-treated collagen-IV is not present within biological systems it would explain the larger interaction level between the crude bovine pepsin-collagen-IV alpha chains and r-LTBP-2 when compared with the commercial human collagen-IV preparation. To determine if the interaction site is recoverable after disrupting the triple helical conformation of collagen-IV with pepsin enzyme digestion, commercial collagen-IV was digested to completion with pepsin and tested for interaction. It was found that digesting the commercial human collagen-IV preparation did result in some bands that were at a common molecular weight to those found within the crude bovine collagen-IV extract and these are marked with an asterix (*) in **figure 10.7**. However, no interaction was found between r-LTBP-2 and the commercial collagen-IV preparation following pepsin treatment (**figure 10.8**) nor did the pepsin enzyme interfere with the solid phase binding assay. Thus, r-LTBP-2 did not react with the commercial preparation of human collagen-IV before or after pepsin treatment.

It was possible that the crude bovine collagen-IV preparation contained pepsin-resistant fragments of other extracellular matrix macromolecules. Since it was shown in chapter 5 that LTBP-2 and fibrillin-1 interact strongly and the N-terminal region of fibrillin-1 has been shown to be pepsin resistant (Maddox *et al.*, 1989), it was possible that the interaction between r-LTBP-2 and the crude collagen-IV preparation could occur due to residual fibrillin protein. To determine if pepsin-resistant fragments of fibrillin-1 are present within the crude bovine collagen-IV preparation, a sample of the preparation was transferred onto PVDF membrane and immunoblotted with the rabbit polyclonal anti-[fibrillin-1 peptide] specific antibody, Fib1A. Antibody Fib1A was raised to a sequence in the pepsin resistant N-terminal region of fibrillin-1. The antibody was analysed for reactivity to Fib1(H)NT and cross-reactivity with the other fibrillin fragments [Fib1N(H); Fib1C(H); Fib1(H)CT; Fib2NT(H) or Fib2N(H)] and LTBP-2 and the C-terminal region of LTBP-1. It was found the Fib1A specifically reacted with the Fib1(H)NT fragment (**figure 5.14**). After transfer of the crude bovine collagen-IV extract onto PVDF and probing the membrane with antibody Fib1A, it was determined that some bands from the preparation did immunoreact with this antibody (**figure 10.9**). These bands, sized at 40 and 40.5kDa, were close to those that interacted with r-LTBP-2 on the western blot overlay assay,

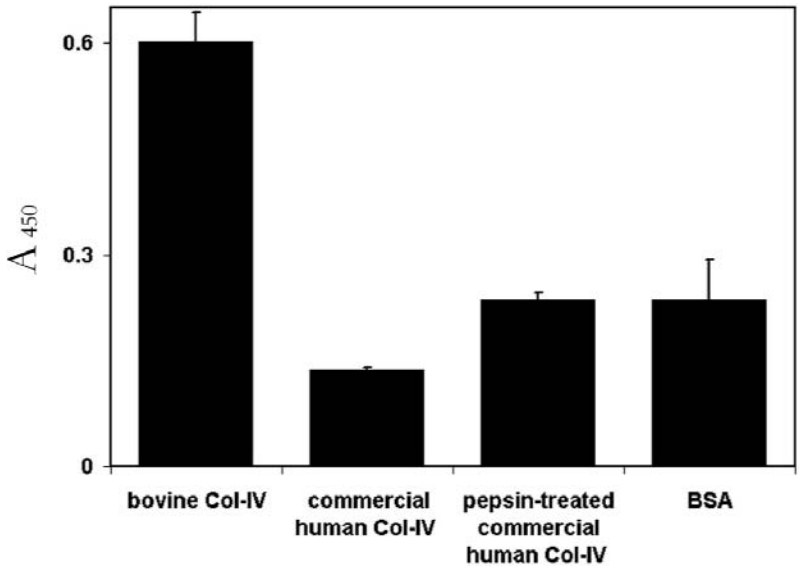

Figure 10.8. r-LTBP-2 does not interact with the commercial human placenta collagen-IV preparation that has been pepsin-treated. Individual wells of microtitre plates were coated with the crude bovine collagen-IV preparation (400ng/well), commercial human placenta collagen-IV (400ng/well), commercial human collagen-IV that had been treated with pepsin for 72 hours at 37°C (400ng/well) or BSA (400ng/well) in TBS/2mM $CaCl_2$. After blocking with 5% milk/TBS, r-LTBP-2 (200ng/well) was added to wells and incubated for 3 hrs at 37°C. After washing, anti-[LTBP-2 peptide] specific antibody, LTBP-2C (1:5000 dilution) was added to wells and incubated for 2 hrs at 37°C. After washing, specific binding of LTBP-2C was detected at 450nm using peroxidase-conjugated secondary antibody and colour development for 30 minutes. Means ± S.D. of triplicate determinations are shown.

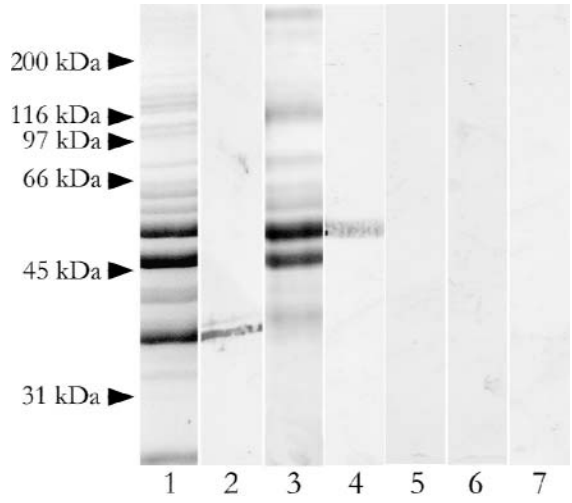

Figure 10.9. Proteins within the crude bovine collagen-IV preparation immunoreacts with anti-[fibrillin-1] antibody. The crude collagen-IV preparation (1µg/lane) was resolved by SDS-PAGE on a 12% gel and was stained with Coomassie Blue under reducing (*lane 1*) or non-reducing conditions (*lane 3*) or was transferred onto PVDF membrane. After blocking the membrane with 3% milk/TBS, each lane was incubated with anti-[fibrillin-1] specific antibody, Fib1A at a 1:100 dilution. After washing, specific binding of the Fib1A antibody was detected with phosphatase-conjugated secondary antibody. Under reducing conditions two bands of ~40kDa are detected from the crude bovine collagen-type IV preparation (*lane 2*) and under non-reducing conditions a single band of ~50kDa was observed (*lane 4*). Commercial human placenta collagen-IV both untreated (*lane 5*) and pepsin-treated (*lane 6*) did not react with the Fib1A antibody. Pepsin enzyme (control for lane 6) also did not immunoreact to the antibody (*lane 7*). The *arrowheads* indicate the relative mobilities of concurrently run protein standards.

which had molecular weight of 42, 42.5 and 45.5kDa (**figure 10.4**). However, mass spectrometric analysis of these bands did not result in a fibrillin-1 peptide being detected.

To further test if r-LTBP-2 was interacting with a fibrillin-1 fragment present within the crude bovine collagen-IV preparation, the collagen-IV sample was coated onto microtitre wells and blocked with milk. The wells were then treated with the rabbit polyclonal anti-[fibrillin-1 peptide] specific antibody, Fib1A overnight, prior to adding r-LTBP-2 in the liquid phase. If there was an interaction between the fibrillin-1 present in the collagen-IV extract and r-LTBP-2, treatment of the well with the anti-[fibrillin-1 peptide] antibody, Fib1A should block access of the r-LTBP-2 to the fibrillin-1 and thus the binding signal should be reduced. However, when the assay was performed it was found that there was no significant reduction in the binding signal between the crude bovine collagen-IV extract and r-LTBP-2 after blocking with the anti-[fibrillin-1 peptide] antibody (**figure 10.10**). Controls showed that there was no cross-reaction between the anti-[his_6-tag]-specific antibody or the corresponding goat anti-mouse secondary antibody and the crude collagen-IV preparation or the normal rabbit serum used to produce the anti-[fibrillin-1 peptide] antibody. Normal rabbit serum was also used to indicate that no protein inherently present within the rabbit serum was contributing to the experimental outcome. This finding suggests that the interaction between r-LTBP-2 and the crude bovine collagen-IV preparation was not due to an interaction with fibrillin-1.

10.2 Further attempts to identify the protein interacting with r-LTBP-2 present within the crude bovine collagen-IV extract

The above findings suggest the presence of an unknown r-LTBP-2-interacting protein within the crude bovine collagen-IV preparation. To determine the identity of this protein co-affinity purification was attempted. Since, r-LTBP-2 contains a his_6-tag, Ni-chelate chromatography was employed to capture any complex of r-LTBP-2 and the unknown binding protein, which would be eluted from the column using 500mM imidazole. The complexes would be analysed under reducing conditions on SDS-PAGE, where each protein band would be resolved individually to identify unique proteins bound to r-LTBP-2. However, since Ni-chelate chromatography requires the use of sepharose beads, which could bind proteins non-specifically, a control column was also be required with which the crude collagen-IV extract would be incubated with Ni-chelate sepharose in the absence of r-LTBP-2. Protein bands eluted from the experimental and control columns would then be analysed for differences. If any unique bands could be identified they would be submitted to mass spectrometric analysis for identification.

r-LTBP-2 was incubated with the crude collagen-IV extract overnight at room temperature and then applied to the Ni-sepharose column. When imidazole eluants were analysed on 12% SDS-PAGE and stained using coomassie blue, faint bands could be seen within

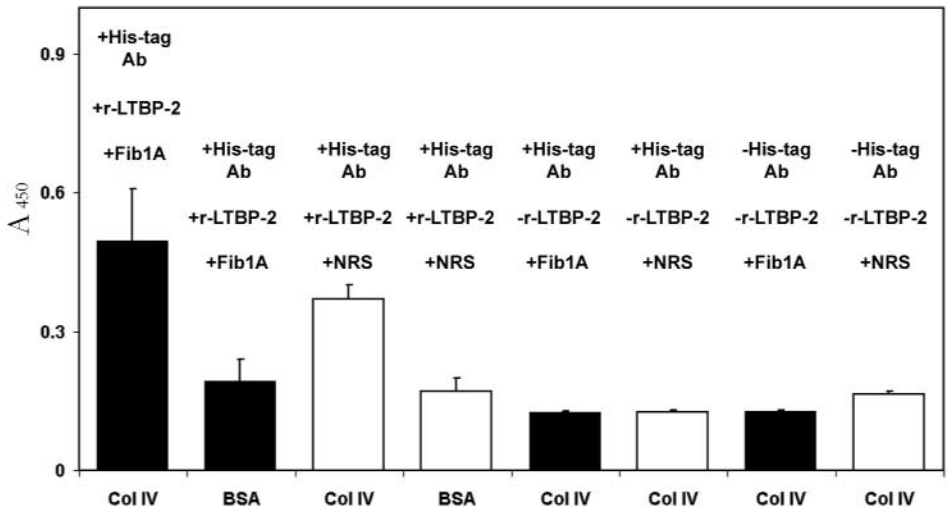

Figure 10.10. r-LTBP-2 interacts with the crude bovine collagen-IV preparation after blocking with anti-[fibrillin-1 peptide] antibody, Fib1A. Individual wells of microtitre plates were coated with the crude collagen-IV preparation (400ng/well) or BSA (400ng/well) in TBS/2mM $CaCl_2$. After blocking with 3% BSA/TBS, anti-[fibrillin-1 peptide] antibody, Fib1A (*black columns*, 1:10 dilution) or normal rabbit serum (*white columns*, 1:10 dilution) was added to appropriate wells as indicated and incubated overnight at room temperature. After washing, r-LTBP-2 (400ng/well) or TBS was added to appropriate wells as indicated and incubated for 3 hrs at 37°C. After washing, anti-[his_6-tag] antibody, tetrahis (1:2000 dilution) or TBS was added to appropriate wells as indicated and incubated for 2 hrs at 37°C. After washing, specific binding of the tetrahis antibody was detected at 450nm using peroxidase-conjugated secondary antibody (added to all individual wells), and colour development for 5 minutes. Means ± S.D. of triplicate determinations are shown.

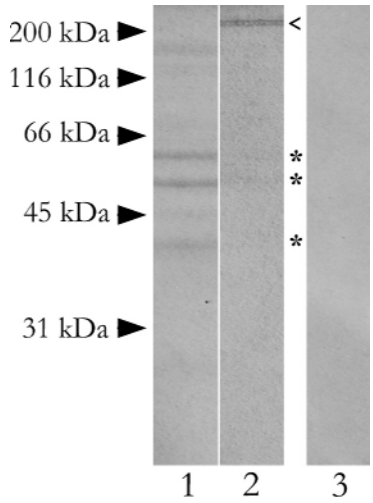

Figure 10.11. Proteins within the crude bovine collagen-IV preparation form a complex with r-LTBP-2. Collagen-IV (2µg) was incubated with r-LTBP-2 (1µg) overnight at room temperature. Protein complexes were captured by Ni-chelate chromatography and resolved by SDS-PAGE under reducing conditions on a 12% gel stained with coomassie blue. *Lane 1*, flow-through of bovine collagen-IV post-incubation with Ni-sepharose column. *Lane 2*, 500mM imidazole eluant showing r-LTBP-2 (<) and potential bound protein bands from the crude collagen-IV preparation (*). *Lane 3*, background binding of bovine collagen-IV sample to Ni-charged sepharose. The *arrowheads* indicate the relative mobilities of concurrently run protein standards.

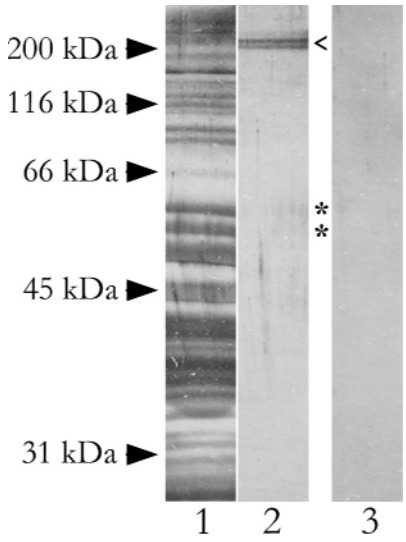

Figure 10.12. Silver stained gel of complexes between the crude bovine collagen-IV preparation and r-LTBP-2. Collagen-IV (2µg) was incubated with r-LTBP-2 (1µg) overnight at room temperature. Protein complexes were captured by Ni-chelate chromatography and resolved using 12% SDS-PAGE under reducing conditions stained with silver nitrate. *Lane 1*, flow-through of collagen-IV post-incubation with Ni-sepharose. *Lane 2*, 500mM imidazole eluant showing r-LTBP-2 (<) and potential bound protein bands from the crude collagen-IV preparation (*). *Lane 3*, background binding of the collagen-IV preparation to Ni-charged sepharose, indicating bands similar to those found in lane 2 can also be detected in background sample (*). The *arrowheads* indicate the relative mobilities of concurrently run protein standards.

the 500mM imidazole fractions which co-migrated with the r-LTBP-2 standard (**figure 10.11**). However, the bands were so faint it was difficult to distinguish if these were specific or whether they represented background binding. To increase sensitivity of the system it was decided to analyse the complexes by silver nitrate staining of the SDS gel, which is a more sensitive staining method than Coomassie Blue but is not quantitative (see section 4.4 for procedural details). With silver staining, it was found that the binding pattern of protein bands within the r-LTBP-2/bovine collagen-IV imidazole eluants were very similar to those of the collagen-IV only control column (**figure 10.12**). Even with silver staining the bands were still very faint which precluded mass spectrometric analysis without greater amounts of material. Since this method of Ni-chelate chromatography did not aid in distinguishing the r-LTBP-2 interacting protein present within the crude collagen-IV preparation, another approach would be needed. One tactic would be to sub-fractionate the collagen-IV preparation using HPLC technology and screening separate size fractions for interaction with r-LTBP-2 followed by protein identification by mass spectrometric analysis. This experiment could not be conducted within the scope of this PhD project due to time constraints.

The novel findings presented in this thesis indicate that LTBP-2 has some intriguing potential to be an important molecule for the function of elastic fibres. The significance of the

interactions found between r-LTBP-2 and fibrillin-1 and a basement membrane components are discussed in further detail in the following chapter.

11 Discussion and perspectives

LTBP-2 is a matrix protein of unknown function and findings presented within this thesis give a unique insight into potential roles for LTBP-2 within the extracellular matrix. The domain structure of LTBP-2 clearly places this protein in the LTBP family. However, LTBP-2 is the LTBP family member most structurally similar to the fibrillins and differs from the other LTBPs in that it does not form covalent complexes with latent TGF-β, since it lacks the required TGF-β-binding consensus sequence within its third 8-Cys motif (Saharinen and Keski-Oja, 2000; Saharinen *et al.*, 1996). Since LTBP-2 is an integral component of the extracellular matrix but lacks the ability to associate with TGF-β, it has been suggested that LTBP-2 maybe more functionally related to the fibrillin proteins rather than to the other LTBPs (Gibson *et al.* 1995).

LTBP-2 has been shown to be abundantly associated with the elastic fibres of some developing bovine elastic tissues indicating the potential for LTBP-2 to have a role within, or associated with, these structures (Gibson *et al.*, 1995; Hyytiäinen *et al.*, 1998). LTBP-2 also appears to have an important developmental role since *Ltbp-2*$^{-/-}$ null mice do not survive past the implantation stage of embryogenesis (Shipley *et al.*, 2000). This phenotype largely differs with those of gene knockout animals for other LTBPs (Colarossi *et al.*, 2005; Dabovic *et al.*, 2002a; Dabovic *et al.*, 2002b; Dabovic *et al.*, 2005; Koli *et al.*, 2004; Sterner-Kock *et al.*, 2002), fibrillins (Carta *et al.*, 2006; Chaudhry *et al.*, 2001) or TGF-β (Kaartinen *et al.*, 1995; Kulkarni *et al.*, 1993; Sanford *et al.*, 1997), where the phenotypes become evident at later stages of development.

Further studies have showed that LTBP-1 and LTBP-2 partially co-immunolocalise with fibrillin-1 in the wall of porcine coronary arteries. The intensity of the staining for LTBP-1, TGF-β and LTBP-2 increased following angioplasty-induced injury to the arteries, suggesting that LTBP-2 may have a role in tissue repair (Sinha *et al.*, 2002). LTBP-2 has also been shown to function in cell adhesion, where it acts as an anti-adhesive matrix component for embryonic lung fibroblasts (Hyytiäinen and Keski-Oja, 2003) or a pro-adhesive for melanoma cells with the adhesive domains being in the N-terminal region of LTBP-2 (Vehviläinen *et al.*, 2003). Despite the above studies, the function and molecular binding partners for LTBP-2 within ECM structures are still unclear. In order to determine more about the function of LTBP-2, the experiments conducted within this thesis screened a range of well-characterised elastic fibre components and other ECM macromolecules for potential binding partners of LTBP-2.

The first proteins to be analysed were the major structural components of fibrillin-containing microfibrils, the fibrillin proteins. Fibrillins were primarily chosen since LTBP-2 has been localised to fibrillin-containing microfibrils in developing elastic tissues such as bovine aorta and nuchal ligament (Gibson *et al.*, 1995) and they share a large degree of structural

homology with the LTBPs. Members of both protein families contain unique 8-cysteine motifs and thus form a superfamily of proteins (reviewed by Kielty *et al.*, 2002a). Some members of this superfamily have been shown to bind with each other, for example, LTBP-1 interacts with the N-terminal domains of fibrillins-1 and –2 and LTBP-4 has been shown to interact with the N-terminal domains of fibrillin-1 (Isogai *et al.*, 2003). Furthermore, since LTBPs-1, -3 and –4 covalently bind to latent forms of TGF-β, it has been suggested that one role of LTBPs is to localise the latent cytokine to specific extracellular matrix structures, such as fibrillin-containing microfibrils (reviewed by Todorovic *et al.*, 2005).

To determine if LTBP-2 and fibrillins-1 and -2 interact, solid phase binding assays were conducted. Firstly, recombinant human LTBP-2 protein was successfully produced using a mammalian-based cell culture expression system and it correlated well in size with tissue-extracted LTBP-2 protein when analysed by SDS-PAGE (**figure 5.2**). The use of mammalian cells to produce human recombinant proteins was necessary to ensure correct folding and disulphide bond formation of the protein. Recombinant LTBP-2 protein appeared to contain authentic post-translational modifications as determined by digesting the protein with N- and O-glycosidase enzymes (**figure 5.4**). A direct protein-protein interaction between r-LTBP-2 and the N-terminal region of fibrillin-1 was detected, but the analogous region of fibrillin-2 did not interact (**figures 5.18** and **5.19**). The finding that LTBP-2 interacts only with fibrillin-1 indicates that any potential roles of LTBP-2, related to fibrillin-1 function, could be restricted to tissues containing fibrillin-1-containing microfibrils.

The direct interaction between r-LTBP-2 and fibrillin-1 was found to be of high affinity since the estimated dissociation constant (K_d) was calculated as 9.4nM (**figure 5.24**). Furthermore, the binding between LTBP-2 and fibrillin-1 was also found to be dependant on calcium since the interaction level was enhanced by the presence of up to 2mM Ca^{2+} ions in solution but was completely abolished in the presence of 5mM EDTA, which is a chemical known to chelate divalent cations, including Ca^{2+} (**figure 5.22**). It is not surprising that Ca^{2+} ions are required for the interaction between LTBP-2 and fibrillin-1 since both proteins contain a large number of calcium binding EGF-like repeats, which require bound calcium to perform key structural roles including; protection from protease targeting, restricting interdomain flexibility as well as facilitating protein-protein interactions (Downing *et al.*, 1996; Handford *et al.*, 1991; Werner *et al.*, 2000).

Thus, as previously reported for LTBPs-1 and –4 (Isogai *et al.* 2003), LTBP-2 also interacts with the N-terminal region of fibrillin-1. However the interaction characterised within this thesis differs from the findings of Isogai *et al.* (2003) in that the interaction of LTBP-2 with fibrillin-1 was found to be Ca^{2+} ion dependant. Isogai *et al.* (2003) had documented that the interaction between LTBP-1 and fibrillin-1 was not Ca^{2+} ion dependant but the data for this

conclusion was not shown within the publication. Isogai *et al.* (2003) had determined that the binding site for the interaction between LTBP-1 and the N-terminal region of the fibrillin proteins was located to the C-terminal region of LTBP-1. This was confirmed by solid phase binding assays conducted with LTBP-1 within this thesis, but one difference was noted in that the C-terminal region of LTBP-1 did not interact with fibrillin-2 (**figure 7.9**). This difference between the studies was surprising, since Isogai *et al.* (2003) had used a similar expression system to produce their recombinant LTBP-1. However, they reported the interaction between LTBP-1 and fibrillin-2 to be relatively weak when compared with the LTBP-1/fibrillin-1 interaction. It is possible that the solid phase detection system used for detecting protein-protein interactions described in this thesis may not be sensitive enough to detect such weaker interactions. Furthermore, it is possible there are subtle differences in the binding characteristics of the individual fibrillin-2 fragments used in each study. Further investigation of the LTBP-1 and fibrillin-2 interaction were outside the scope of this thesis, which focuses on LTBP-2.

To determine if the C-terminal region of LTBP-2, analogous to that of LTBP-1, bound to the N-terminal region of fibrillin-1, a recombinant fragment of the carboxyl-terminal region of LTBP-2 [LTBP-2CT(H)] was produced using 293-EBNA mammalian cells (**figures 6.1** and **6.2**). This fragment of LTBP-2 interacted with the N-terminal fragment of fibrillin-1, [Fib1(H)NT] (**figure 6.6**). However, it was found that the interaction level between the LTBP-2CT(H) and Fib1(H)NT was lower than that observed when using a equimolar amount of full-length LTBP-2 protein (**figure 6.6**). It needed to be determined whether LTBP-2 contained multiple fibrillin-1 binding sites upon the length of the protein. It was shown by pre-incubating the N-terminal fragment of fibrillin-1 with LTBP-2CT(H) that the interaction between the pre-treated fibrillin-1 fragment and the full-length LTBP-2 coated on the well was completely abolished (**figure 6.7**). This finding indicated the presence of a single major binding site for fibrillin-1 within the C-terminal domains of LTBP-2, the exact sequence of which is yet to be established. If pre-treatment of fibrillin-1 with LTBP-2CT(H) had not completely abolished the interaction of fibrillin-1 with the full-length LTBP-2 coated on the well then it would have indicated the presence of more than one binding site within LTBP-2 for fibrillin-1. Thus, the lower interaction level seen for the interaction between LTBP-2CT(H) and fibrillin-1 was most likely attributable to reduced accessibility of the interacting sequence with the smaller LTBP-2CT(H) fragment coated on the well, in comparison to the full-length LTBP-2.

LTBP-2 does not covalently bind to latent forms of TGF-β but interacts with fibrillin-1 *via* a region analogous to that used by LTBP-1. Recent evidence indicates that the interaction between TGF-β-bound LTBPs-1 and -4 and fibrillins facilitates the attachment and storage of latent TGF-β molecules on the fibrillin-containing microfibrils, which in the correct molecular environment would allow the later release of the active growth factor (Isogai *et al.*, 2003). If this

interaction is disrupted then it has been shown that the resultant aberrant activation of TGF-β can result in some aspects of the Marfan syndrome phenotype (Nataatmadja *et al.* 2006; Neptune *et al.* 2003). Thus, it seems conceivable that LTBP-1 and -2 may compete for binding to fibrillin-1-containing microfibrils, which could potentially influence the regulation of latent TGF-β storage upon these structures. To determine if LTBP-1 and -2 compete for binding to fibrillin-1 *in vitro*, the C-terminal region of LTBP-1 [LTBP-1CT(H)] (corresponding to the LTBP-1 C-terminal fragment described by Isogai *et al.*, (2003)) was successfully produced using the 293-EBNA mammalian expression system (**figures 7.1** and **7.2**). Isogai *et al.* (2003) had not determined the avidity of the binding between LTBP-1 and fibrillin-1. Using the radiolabelled N-terminal fragment of fibrillin-1 and non-linear regression analysis software, an estimate of the dissociation constant (K_d) for the interaction between LTBP-1 and fibrillin-1 was found to be 17nM (**figure 7.10**). This value was very similar to that for the LTBP-2/fibrillin-1 and LTBP-2CT(H)/fibrillin-1 interactions, which were estimated at 9.4nM and 22nM, respectively (**figures 5.24** and **6.8**). Since these dissociation constants were so similar it was likely that LTBP-1 and –2 could compete for binding to fibrillin-1 *in vivo* with the assumption that no other extraneous factors are involved.

When the C-terminal fragments of LTBPs-1 and -2 were analysed for competitive interaction with fibrillin-1 in solid phase, it was shown that either LTBP fragment could equally block the binding of fibrillin-1 to the other fragment (**figure 7.11**). Further confirmation that LTBP-2CT(H) and LTBP-1CT(H) have similar binding affinities was shown using the analysis of competition binding curves, which indicated that the two LTBPs were equally effective at inhibiting the interaction of the other with fibrillin-1 (**figure 7.13**). If one LTBP had had a greater affinity for fibrillin-1 than the other it would have been expected that inhibition experiments would have shown differences between the effectiveness of one fragment when compared to the other. Competition binding curves would have shown the strongest binding LTBP fragment to have a steeper slope than the other. These experiments all indicated that LTBPs-1 and -2 appear to bind fibrillin-1 with similar avidities, thus it is seems highly possible that one LTBP may be able to modulate the other LTBP for fibrillin binding through changes in the concentration gradients at different developmental stages within a particular tissue.

To investigate if such distribution gradients may possibly exist for LTBPs-1 and –2 in tissues, immunohistochemical analysis was conducted to determine the tissue distribution of the LTBPs in relation to each other and fibrillin. Human foetal aorta was the tissue chosen for this analysis since LTBP-2 has been extensively co-localised with microfibrils in developing bovine aorta (Gibson *et al.*, 1995) and LTBP-1 had been located ultrastructurally to some microfibrils in foetal human aorta (Isogai *et al.*, 2003). However, combined studies of the co-distribution of LTBPs-1 and –2 with fibrillin-1 have not previously been conducted. Furthermore human aorta

is a tissue particularly pertinent for Marfan syndrome patients, since the deadliest aspect of the syndrome is the rupture of aortic aneurysms. If significant biochemical interactions could be characterised, this could lead to the eventual development of therapeutic agents to correct or prevent aortic defects in these patients.

Tissue localisation studies of LTBPs within human foetal aorta using low-power magnification showed that the LTBPs have distinct but partially overlapping distribution patterns (**figure 8.4**). LTBP-1 has a definite distribution gradient. Staining was most strongly seen in the outer media and this petered out towards the inner media, only to became much stronger again within the intima (**figure 8.4*A***). LTBP-2 had a relatively even distribution throughout the media and was not particularly strong within the outer medial regions or the intima (**figure 8.4*B***). Neither protein was prominent within the adventitia. These distribution patterns indicated that the local concentration of each LTBP was consistent with the concept that competitive binding of LTBPs to the ECM were possible.

Confocal microscopy was then used to analyse in more detail the distribution of each LTBP in relation to fibrillin-1, elastin and with each other. Both LTBPs co-distributed with particular populations of elastic fibres. It was found that both LTBPs partially co-localised with fibrillin-1 in the medial layer and intima but were substantially absent from the fibrillin-staining structures in the adventitia (**figures 8.5** and **8.6**). When compared with each other the LTBPs did have distinct distribution within the tissue and showed very little co-localisation. Again LTBP-2 was strongly present throughout the medial layer whereas, strong signal for LTBP-1 was localised more intensely in patches of the outer medial layer and was weaker within the media generally until signal intensified once again at the intima. When merged together the images for LTBP-1 and –2 had very few areas of strong co-localisation. In most cases it was found that where LTBP-2 was detected strongly, LTBP-1 had only weak staining and vice versa. This tissue-localisation pattern indicates that the two LTBPs are present within the aorta at similar developmental stages but bind to fibrillin-1-containing microfibrils with overlapping but distinct distributions. Since the TGF-β-binding LTBP-1 is mainly localised on the outer medial regions and the internal elastic lamina, it can be inferred that these regions of the aorta are likely to be TGF-β-rich. The distinct staining patterns indicate that if LTBP-2 competes with LTBP-1 for binding to fibrillin-1-containing microfibrils to regulate the levels of TGF-β available in particular regions of the aorta, then it is likely to occur through a gradient system, as commonly found in other regulatory systems, for example, *Drosophila Melanogaster* embryos expressing the morphogenic developmental gene *sonic hedgehog* (reviewed by Tickle, 2006).

The differences in the expression of LTBP-2 compared to LTBP-1 could affect the amount of growth factor available for activation upon fibrillin-1-containing microfibrils and its release into the ECM environment. If LTBP-2 expression is higher than LTBP-1 at a given

region of the tissue or at a particular developmental stage, then more active TGF-β could be released, affecting downstream signalling pathways. However, if LTBP-1 expression is higher more TGF-β would be stored on the microfibrils and thus less would be available for activation, affecting intracellular signalling and ECM function. The release of TGF-β could also affect the expression levels of LTBPs within certain ECM structures. LTBP-3 regulates the bioavailability of TGF-β especially in the bone and recently it has been shown that TGF-β1 stimulates the activity of the LTBP-3 promoter and increases mRNA levels accordingly, when compared to other bone-derived growth factors and hormones (Kantola *et al.*, 2005). Thus, if expression of LTBP-2 is higher, more TGF-β will be available to stimulate the activity of the other LTBP promoters and conversely where less LTBP-2 is expressed, more TGF-β is stored upon the fibrillin-containing microfibrils, resulting in reduced expression of the other LTBP promoters. Such regulatory feedback mechanisms within groups of related proteins are not uncommon within biological systems, an example includes the metabolic pathway for regulating protein kinase enzyme activity (reviewed by Papin *et al.*, 2005).

It seems most likely that LTBP-2 would influence TGF-β availability in tissues through indirect mechanisms like those listed above. However, further immunohistochemical and ultrastructural tissue analyses need to be conducted to establish protein distributions of LTBPs-1 and -2, fibrillin-1, latent TGF-β and active TGF-β in relation to each other using appropriate tissue types over a number of developmental time points. This would allow comparisons of the dynamic distribution patterns of each protein, which could then be related to mRNA expression levels using *in situ* hybridisation and quantitative techniques such as real time-PCR. It would also be optimal to study tissue samples from MFS patients in a similar manner to determine the dynamic relationship between the proteins when compared with tissue samples from normal individuals. It has already been shown that MFS mouse models display altered levels of active TGF-β in lung (Neptune *et al.*, 2003). Immunohistochemical analysis of tissue samples from such model systems could provide information on whether TGF-β dysregulation can occur due to interruptions of the dynamic equilibrium between the LTBPs upon fibrillin-containing microfibrils.

It also remains to be elucidated if LTBP-2 has other functions in the ECM. Within this thesis a small number of prominent extracellular macromolecules were screened for interaction with LTBP-2. When analysed for direct protein-protein interaction r-LTBP-2 was found not to have significant binding with MAGPs (**figures 9.1, 9.2, 9.3** and **9.4**); laminin (**figure 9.5**); tropoelastin (**figure 9.7*A***); biglycan or decorin (**figure 9.6**); fibronectin (**figure 9.7*B***) or collagen types-I-III, -V and –VI (**figure 9.8**). However, all possible interactions with extracellular matrix macromolecules have not been explored within this study. It remains to be determined if LTBP-2 associates with fibronectin in a transitory manner as seen for LTBP-1 (Taipale *et al.*,

1996). It also has not been established if LTBP-2 interacts with EMILINS, fibulins, thromobospondin and many other extracellular macromolecules.

It also still remains unclear as to whether LTBP-2 does in fact have some non-covalent association with latent forms of TGF-β or related growth factors. If LTBP-2 binds non-covalently to latent TGF-β then the role for LTBP-2 in relation to growth factor storage upon fibrillin-1-containing microfibrils would be much more complex. If a non-covalent association between LTBP-2 and TGF-β is established this would indicate that the bioavailability of each molecule within specific stages of development is important and that could mean LTBP-2 has a role as a negative regulator of TGF-β in some tissues or cell types as well as a positive regulator of TGF-β availability in other tissues/developmental stages or cell types, such as has been shown for its cell adhesion role described above (Hyytiäinen and Keski-Oja, 2003; Sinha *et al.*, 2002).

LTBP-2 may also interact with other unidentified growth factors or may be involved in growth factor processing and activation. A potential family of growth factors to study in relation to LTBP-2 would be the bone morphogenetic proteins (BMPs) since recently a non-covalent interaction has been demonstrated between fibrillin-1 and the prodomain of BMP-7 (Gregory *et al.*, 2005). BMPs are structurally similar to TGF-β and thus it follows that fibrillin-containing microfibrils may act as stores for BMP-7, other BMPs and potentially other growth factors. It is possible that LTBP-2 and other members of the LTBP family, may also bind BMPs and this may be linked with regulating the role of BMP storage upon fibrillin-containing microfibrils.

LTBP-2 could also influence growth factor activation by acting as a mediating protein for other matrix macromolecules. Several matrix proteins have been shown to be involved with latent TGF-β activation and processing, such as thrombospondin, which directly activates TGF-β (Souchelnitskiy *et al.*, 1995) and fibronectin, which is essential for integrin-mediated latent TGF-β activation (Fontana *et al.*, 2005). It is possible LTBP-2 could modulate the function of these proteins and thus indirectly activate TGF-β. Interestingly, thrombospondin-1 null mice demonstrate a partial phenotypic overlap with TGF-β1 null animals, indicating the importance of thrombospondin for the activation of TGF-β (Crawford *et al.*, 1998). More recently, it has been shown that emilin-1 inhibits TGF-β signalling by binding to the pro-TGF-β precursor and preventing its maturation to the SLC by furin convertases in the ECM (Zacchigna *et al.*, 2006). This regulation by emilin-1 appears to be essential for modulating TGF-β signalling within the vascular wall and maintaining blood pressure homeostasis. Genetic inactivation of *Emilin1* causes increased TGF-β signalling in the vascular wall and high blood pressure. The normal phenotype can be rescued by the activation of a single TGF-β allele (Zacchigna *et al.*, 2006). If interactions occur between LTBP-2 and any of the above proteins then it is possible that an indirect regulation of TGF-β activity could occur through LTBP-2. In addition, a direct role of LTBP-2

in TGF-β storage and activation cannot be dismissed since non-covalent interactions between LTBP-2 and latent forms of TGF-β have not been fully explored.

Also reported within this thesis is an interaction between LTBP-2 and an unidentified component of a bovine collagen-IV-enriched pepsin extract of placenta (**figure 9.8**). The unidentified interacting protein within this extract could be a protein closely associated with the basement membrane protein collagen-IV and thus purified alongside the collagen during salt fractionation. It was determined that the interacting component of this extract was not the major collagen-IV itself since commercial preparations of human placenta collagen-IV did not interact with LTBP-2 (**figure 10.6**). Further studies would need to be conducted to identify this unknown protein component within this salt-fractionated extract. One approach would be to separate the various components of the pepsin collagen-IV extract by using high-pressure liquid chromatography. Once groups of proteins of a particular size have been separated, each fraction can be analysed for interaction with LTBP-2, using both solid phase binding assays and blot overlay assays. Protein bands found to interact with LTBP-2 could then be identified using mass spectrometric analysis. Interestingly, collagen-IV is one of the few extracellular matrix proteins expressed in pre-implantation embryos (Sherman *et al.*, 1980). Since *LTBP-2*$^{-/-}$ null mice die prior to implantation it is possible that an interaction between LTBP-2 and collagen-IV (or a protein very closely associated with it) may be particularly important in early development (Kadler, 2004; Sherman *et al.*, 1980).

It is conceivable that if the LTBP-2 interacting protein within the collagen-IV-enriched pepsin extract was identified to be closely associated with basement membrane structures, LTBP-2 could then be implicated in basement membrane function possibly as a molecular bridge between fibrillin-1-containing microfibrils and basement membranes. Perlecan, an extracellular matrix proteoglycan, has recently been shown to interact with fibrillin-1 at the dermal-epidermal junction and it was postulated that perlecan acts as a molecular bridge to join microfibrils and the basement membrane (Tiedemann *et al.*, 2005). LTBP-2 could be involved in this complex either by interacting directly with perlecan or indirectly through other molecular complexes. Interactions between perlecan and LTBPs have not been analysed within the study presented in this thesis, however this could be an interesting area for future investigation.

Bovine kidney was analysed within this thesis to determine if LTBP-2 was localised to basement membranes within this tissue but it was found that there was only a general non-specific staining. Since basement membrane composition varies between different tissue types, further immunohistochemical and ultrastructural analyses of other tissues for localisation of LTBP-2 in relation to a range of basement membranes could also be informative. In particular, the potential role for LTBP-2 in fibrillin-containing microfibril/basement membrane interactions possibly *via* collagen-IV or perlecan should be investigated. Such studies could be

extended to candidate tissues from human sources of normal tissues and diseased tissues from MFS patients and/or mice models of microfibrillar pathologies.

LTBP-2 appears to have an early developmental role, as indicated by the *Ltbp-2*$^{-/-}$ knockout mouse, which does not correlate with the phenotypes of the knockout mice of fibrillins-1 and –2 that manifest at much later stages of development (Atteaga-Solis *et al.* 2001; Carta *et al* 2006; Pereira *et al.* 1997). Thus, examination of early embryonic tissue may also be informative to determine the important developmental roles of LTBP-2, which seem to be independent of its potential function with fibrillin-containing microfibrils. Such a role could still involve modulation of TGF-β activity. The first differentiation event occurring in the preimplantation mouse blastocyst is the formation of inner cell mass (ICM) derived primitive endoderm (PrE) cells, some of which migrate over the inner surface of the trophectoderm to establish the parietal endoderm layer. TGF-β appears to influence the establishment of the parietal endoderm cell layer, formed within the inner cell mass of the mouse blastocyst by reducing the extent of laminin deposition in Reichert's membrane, which is a type of basement membrane, during endoderm cell migration (Tonary and Carnegie, 1996). One potential developmental function of LTBP-2 may involve this pre-implantation system of TGF-β-induced cell differentiation, possibly *via* influencing the location of latent TGF-β or having another unidentified non-TGF-β-related roles. Furthermore, if an interaction between LTBP-2 and a basement membrane protein could be established, this could bring together the function of LTBP-2 with regard to TGF-β regulation, pre-implantation embryogenesis and as a structural protein linking to basement membrane structures.

In conclusion, findings presented within this thesis show that the C-terminal region of LTBP-2 interacts with the N-terminal region of fibrillin-1, but not to the analogous region of fibrillin-2, indicating a role for LTBP-2 exclusively involving fibrillin-1-containing microfibrils. LTBP-1 and LTBP-2 bind to fibrillin-1 with similar avidities but localise to distinct regions within human foetal aorta with few areas of strong co-localisation. Since LTBP-1 is complexed with latent forms of TGF-β and LTBP-2 does not form covalent complexes with latent-TGF-β, LTBP-2 could have a unique role within fibrillin-1-rich tissues, such as aorta, to indirectly regulate the amount of TGF-β stored upon fibrillin-containing microfibrils. Furthermore, LTBP-2 has been shown to interact with a protein component of bovine collagen-IV-enriched pepsin extract and if verified could indicate a structural role in linking fibrillin-containing microfibrils, either directly or indirectly, with basement membrane structures.

Overall, the findings presented within this thesis have introduced LTBP-2 as an intriguing extracellular matrix macromolecule. LTBP-2 has been largely ignored through previous studies of the LTBP family since it does not covalently bind to latent forms of TGF-β. However, LTBP-2 could have a more crucial role in TGF-β biology than initially anticipated. If further

confirmation can be achieved of its influence on TGF-β regulation within major extracellular matrix structures, such as fibrillin-containing microfibrils, this would indicate an extremely novel, complex and intricate regulatory system for growth factor storage and activation. It would provide a further example of how the intricate balance between different proteins can influence major aspects of tissue biology and function. If this potential regulatory role of LTBP-2 can be extended to other TGF-β-related growth factors or to other structures, such as basement membranes, this would place LTBP-2 in an extremely important, if not crucial, role in elastic fibre biology. Further studies into LTBP-2 and its biological role is a new and exciting area of research, with the potential for a number of unique and intriguing outcomes.

12 Bibliography

Abedin, M. Z., Ayad, S. and Weiss, J. B. (1982). Isolation and native characterization of cysteine-rich collagens from bovine placental tissues and uterus and their relationship to types IV and V collagens. *Biosci Rep* **2**, 493-502.

Abrams, W. R., Ma, R-I., Kucich, U., Bashir, M. M., Decker, S., Tsipouras, P., McPherson, J. D., Wasmuth, J. J. and Rosenbloom, J. (1995). Molecular cloning of the microfibrillar protein MFAP3 and assignment of the gene to human chromosome 5q32-q33.2. *Genomics* **26**, 47-54.

Anderson, R. A., Koch, S. and Camerini-Otero, R. D. (1984). Cardiovascular findings in congenital contractural arachnodactyly: Report of an affected kindred. *Am J Med Genet* **18**, 265-271.

Annes, J. P., Chen, Y., Munger, J. S. and Rifkin, D. B. (2004). Integrin αVβ6-mediated activation of latent TGF-β requires the latent TGF-β binding protein-1. *J Cell Biol* **165**, 723-734.

Annes, J. P., Munger, J. S. and Rifkin, D. B. (2003). Making sense of latent TGF-β activation. *J Cell Sci* **116**, 217-224.

Annes, J. P., Rifkin, D. B. and Munger, J. S. (2002). The integrin αVβ6 binds and activates latent TGF-β3. *FEBS Lett* **511**, 65-68.

Argraves, W. S., Tran, H., Burgess, W. H. and Dickerson, K. (1990). Fibulin is an extracellular matrix and plasma glycoprotein with repeated domain structures. *J Cell Biol* **111**, 3155-3164.

Ashworth, J. L., Kelly, V., Rock, M. J., Shuttleworth, C. A. and Kielty, C. M. (1999a). Regulation of fibrillin carboxy-terminal furin processing by N-glycosylation, and association of amino- and carboxy-terminal sequences. *J Cell Sci* **112**, 4163-4171.

Ashworth, J. L., Kelly, V., Wilson, R., Shuttleworth, C. A. and Kielty, C. M. (1999b). Fibrillin assembly: dimer formation mediated by amino-terminal sequences. *J Cell Sci* **112**, 3549-3558.

Ashworth, J. L., Kielty, C. M. and McLeod, D. (2000). Fibrillin and the eye. *Br J Ophthalmol* **84**, 1312-1317.

Atteaga-Solis, E., Gayraud, B., Lee, S. Y., Shum, L., Sakai, L. and Ramirez, F. (2001). Regulation of limb patterning by extracellular microfibrils. *J Cell Biol* **154**, 275-281.

Aumailley, M., El Khal, A., Knoss, N. and Tunggal, L. (2003). Laminin 5 processing and its integration into the ECM. *Matrix Biol.* **22**, 49-54.

Aumailley, M. and Gayraud, B. (1998). Structure and biological activity of the extracellular matrix. *J Mol Med* **76**, 253-265.

Baccarani-Contri, M., Fornieri, C. and Pasquali-Ronchetti, I. (1985). Elastin-proteoglycans association revealed by cytochemical methods. *Connect Tissue Res* **13**, 237-249.

Baccarani-Contri, M., Vincenzi, D., Cicchetti, F. and Mori, G. (1990). Immunocytochemical localization of proteoglycans within normal elastin fibers. *Eur J Cell Biol* **53**, 305-312.

Baldock, C., Koster, A. J., Ziese, U., Rock, M. J., Sherratt, M. J., Kadler, K. E., Shuttleworth, C. A. and Kielty, C. M. (2001). The Supramolecular Organization of Fibrillin-rich Microfibrils. *J Cell Biol* **152**, 1045-1056.

Bartholomew, J. S. and Anderson, J. C. (1983). Investigation of relationships between collagens, elastin and glycosaminoglycans in bovine thoracic aorta by immunofluorescence techniques. *Histochem J* **15**, 1177-1190.

Bashir, M. M., Abrams, W. R., Rosenbloom, J., Kucich, U., Bacarra, M., Han, M. D., Brown-Augsberger, P., Mecham, R. and Rosenbloom, J. (1994). Microfibril-associated glycoprotein: Characterization of the bovine gene and of the recombinantly expressed protein. *Biochem* **33**, 593-600.

Bashir, M. M., Han, M.-D., Abrams, W. R., Tucker, T., Ma, R.-I., Gibson, M., Ritty, T., Mecham, R. and Rosenbloom, J. (1996). Analysis of the human gene encoding latent transforming growth factor-β-binding protein-2. *Int J Biochem Cell Biol* **28**, 531-542.

Bateman, J. F., Lamande, S. R. and Ramshaw, J. A. M. (1996). Extracellular Matrix, vol. 2 (ed. W. D. Comper), pp. 95-140. Amsterdam: Harwood Academic Publishers.

Bax, D. V., Bernard, S. E., Lomas, A., Morgan, A., Humphries, J., Shuttleworth, C. A., Humphries, M. J. and Kielty, C. M. (2003). Cell adhesion to fibrillin-1 molecules and microfibrils is mediated by αvβ1 and αvβ3 integrins. *J Biol Chem* **278**, 34605-34616.

Beals, R. K. and Hecht, F. (1971). Congenital contractural arachnodactyly: a heritable disorder of connective tissue. *J Bone Joint Surg* **53A**, 987-993.

Bernfield, M., Gotte, M., Park, P. W., Reizes, O., Fitzgerald, M. L. and Lincecum, J. (1999). Functions of cell surface heparan sulfate proteoglycans. *Annu Rev Biochem* **68**, 729-777.

Bidanset, D. J., Guidry, C., Rosenberg, L. C., Choi, H. U., Timpl, R. and Hook, M. (1992). Binding of the Proteoglycan Decorin to Collagen Type VI. *J Biol Chem* **267**, 5250-5256.

Bissell, M. J. and Barcellos-Hoff, M. H. (1987). The influence of extracellular matrix on gene expression: Is structure the message? *J Cell Sci Suppl.* **8**, 327-343.

Boak, A. M., Roy, R., Berk, J., Taylor, L., Polgar, P., Goldstein, R. H. and Kagan, H. M. (1994). Regulation of lysyl oxidase expression in lung fibroblasts by transforming growth factor-β1 and prostaglandin E2. *Am J Respir Cell Mol Biol.* **11**, 751-5.

Booms, P., Pregla, R., Ney, A., Barthel, F., Reinhardt, D. P., Pletschacher, A., Mundlos, S. and Robinson, P. N. (2005). RGD-containing fibrillin-1 fragments upregulate matrix metalloproteinase expression in cell culture: A potential factor in the pathogenesis of the Marfan syndrome. *Hum Genet* **116**, 51-61.

Border, W. A., Okuda, S., Languino, L. R. and Ruoslahti, E. (1990). Transforming growth factor-β regulates production of proteoglycans by mesangial cells. *Kidney Int* **37**, 689-695.

Bosman, F. T. and Stamenkovic, I. (2003). Functional structure and composition of the extracellular matrix. *J Pathol* **200**, 423-428.

Broek, D. L., Madri, J., Eikenberry, E. F. and Brodsky, B. (1985). Characterization of the tissue form of type V collagen from chick bone. *J Biol Chem* **260**, 555-562.

Brown, P. L., Mecham, L., Tisdale, C. and Mecham, R. P. (1992). The cysteine residues in the carboxy terminal domain of tropoelastin form an intrachain disulfide bond that stabilizes a loop structure and positively charged pocket. *Biochem Biophys Res Commun* **186**, 549-555.

Brown-Augsburger, P., Broekelmann, T., Mecham, L., Mercer, R., Gibson, M. A., Cleary, E. G., Abrams, W. R., Rosenbloom, J. and Mecham, R. P. (1994). Microfibril-associated glycoprotein binds to the carboxyl-terminal domain of tropoelastin and is a substrate for transglutaminase. *J Biol Chem* **269**, 28443-28449.

Cain, S. A., Baldock, C., Gallagher, J., Morgan, A., Bax, D. V., Weiss, A. S., Shuttleworth, C. A. and Kielty, C. M. (2005). Fibrillin-1 Interactions with Heparin: implications for microfibril and elastic fiber assembly. *J Biol Chem* **280**, 30526-30537.

Carta, L., Pereira, L., Arteaga-Solis, E., Lee-Arteaga, S. Y., Lenart, B., Starcher, B., Merkel, C. A., Sukoyan, M., Kerkis, A., Hazeki, N. and Keene, D. R., Sakai, L. Y. and Ramirez, F. (2006). Fibrillins 1 and 2 perform partially overlapping functions during aortic development. *J Biol Chem* **281**, 8016-8023.

Chan, F. L. and Choi, H. L. (1995). Proteoglycans associated with the ciliary zonule of the rat eye: a histochemical and immunocytochemical study. *Histochem Cell Biol* **104**, 369-381.

Chan, F. L., Choi, H. L. and Underhill, C. B. (1997). Hyaluronan and chondroitin sulfate proteoglycans are colocalized to the ciliary zonule of the rat eye: histochemical and immunocytochemical study. *Histochem Cell Biol* **107**, 289-301.

Charbonneau, N. L., Dzamba, B. J., Ono, R. N., Keene, D. R., Corson, G. M., Reinhardt, D. P. and Sakai, L. Y. (2003). Fibrillins can co-assemble in fibrils, but fibrillin fibril composition displays cell-specific differences. *J Biol Chem* **278**, 2740-2749.

Charbonneau, N. L., Ono, R. N., Corson, G. M., Keene, D. R. and Sakai, L. Y. (2004). Fine tuning of growth factor signals depends on fibrillin microfibril networks. *Birth Defects Res (Part C)* **72**, 37-50.

Chaudhry, S. S., Gazzard, J., Baldock, C., Dixon, J., Rock, M. J., Skinner, G. C., Steel, K. P., Kielty, C. M. and Dixon, M. J. (2001). Mutation of the gene encoding fibrillin-2 results in syndactyly in mice. *Hum Mol Genet* **10**, 835-843.

Chen, E., Larson, J. D. and Ekker, S. C. (2006). Functional analysis of zebrafish Microfibril-Associated Glycoprotein-1 (MAGP-1) in vivo reveals roles for microfibrils in both vascular development and function. *Blood* **107**, 4364-4374.

Chen, R. and Doolittle, R. F. (1971). γ-γ cross-linking sites in human and bovine fibrin. *Biochem* **10**, 4486-4491.

Chen, Y., Dabovic, B., Colarossi, C., Santori, F. R., Lilic, M., Vukmanovic, S. and Rifkin, D. B. (2003). Growth retardation as well as spleen and thymus involution in latent TGF-β binding protein (Ltbp)-3 null mice. *J Cell Physiol* **196**, 319-325.

Christ, M., McCartney-Francis, N. L., Kulkarni, A. B., Ward, J. M., Mizel, D. E., Mackall, C. L., Gress, R. E., Hines, K. L., Tian, H., Karlsson, S. and Wahl, S. M. (1994). Immune dysregulation in TGF-β1-deficient mice. *J Immunol* **153**, 1936-1946.

Christiano, A. M. and Uitto, J. (1994). Molecular pathology of the elastic fibers. *J Invest Dermatol* **103**, 53S-57S.

Chu, M. L., Conway, D., Pan, T. C., Baldwin, C., Mann, K., Deutzmann, R. and Timpl, R. (1988). Amino acid sequence of the triple-helical domain of human collagen type VI. *J Biol Chem* **263**, 18601-18606.

Clarke, A. W. and Weiss, A. S. (2004). Microfibril-associated glycoprotein-1 binding to tropoelastin. *Eur J Biochem* **271**, 3085-3090.

Cleary, E. G. and Gibson, M. A. (1983). Elastin-associated microfibrils and microfibrillar proteins (ed D. A. Hall and D. S. Jackson), pp. 97-209. New York: Academic press.

Cleary, E. G. and Gibson, M. A. (1996). Elastic tissue, elastin and elastin-associated microfibrils, vol. 2, (ed. W. D. Comper), pp. 95-140. Amsterdam: Harwood Academic Publishers.

Colarossi, C., Chen, Y., Obata, H., Jurukovski, V., Fontana, L., Dabovic, B. and Rifkin, D. B. (2005). Lung alveolar septation defects in *Ltbp-3*-null mice. *Am J Pathol* **167**, 419-428.

Colombatti, A., Bonaldo, P., Volpin, D. and Bressan, G. M. (1988). The elastin associated glycoprotein gp115: Synthesis and secretion by chick cells in culture. *J Biol Chem* **263**, 17534-17540.

Colombatti, A., Doliana, R., Bot, S., Canton, A., Mongiat, M., Mungiguerra, G., Paron-Cilli, S. and Spessotto, P. (2000). The EMILIN protein family. *Matrix Biol* **19**, 289-301.

Colosetti, P., Hellman, U., Heldin, C. H. and Miyazono, K. (1993). Ca^{2+} binding of latent transforming growth factor-β1 binding protein. *FEBS Lett* **320**, 140-144.

Comings, D. E. (1972). Evidence for ancient tetraploidy and conservation of linkage groups in mammalian chromosomes. *Nature* **238**, 455-457.

Corson, G. M., Chalberg, S. C., Dietz, H. C., Charbonneau, N. L. and Sakai, L. Y. (1993). Fibrillin binds calcium and is coded by cDNAs that reveal a multidomain structure and alternatively spliced exons at the 5' end. *Genomics* **17**, 476-484.

Corson, G. M., Charbonneau, N. L., Keene, D. R. and Sakai, L. Y. (2004). Differential expression of fibrillin-3 adds to microfibril variety in human and avian, but not rodent, connective tissues. *Genomics* **83**, 461-72.

Crawford, S. E., Stellmach, V., Murphy-Ullrich, J. E., Ribeiro, S. M., Lawler, J., Hynes, R. O., Boivin, G. P. and Bouck, N. (1998). Thrombospondin-1 is a major activator of TGF-β1 in vivo. *Cell* **93**, 1159-1170.

Dabovic, B., Chen, Y., Colarossi, C., Obata, H., Zambuto, L., Perle, M. A. and Rifkin, D. B. (2002a). Bone abnormalities in latent TGF-β binding protein (Ltbp)-3-null mice indicate a role for Ltbp-3 in modulating TGF-β bioavailability. *J Cell Biol* **156**, 227-232.

Dabovic, B., Chen, Y., Colarossi, C., Zambuto, L., Obata, H. and Rifkin, D. B. (2002b). Bone defects in latent TGF-β binding protein (Ltbp)-3 null mice; a role for Ltbp in TGF-β presentation. *J Endocrinol* **175**, 129-141.

Dabovic, B., Levasseur, R., Zambuto, L., Chen, Y., Karsenty, G. and Rifkin, D. B. (2005). Osteopetrosis-like phenotype in latent TGF-β binding protein 3 deficient mice. *Bone* **37**, 25-31.

Dallas, S. L., Keene, D. R., Bruder, S. P., Saharinen, J., Sakai, L. Y., Mundy, G. R. and Bonewald, L. F. (2000). Role of the latent transforming growth factor-β binding protein 1 in fibrillin-containing microfibrils in bone cells in vitro and in vivo. *J Bone Miner Res* **15**, 68-81.

Danielson, K. G., Baribault, H., Holmes, D. F., Graham, H., Kadler, K. E. and Iozzo, R. V. (1997). Targeted disruption of decorin leads to abnormal collagen fibril morphology and skin fragility. *J Cell Biol* **136**, 729-743.

Davis, E. C. (1994). Immunolocalization of microfibril and microfibril-associated proteins in the subendothelial matrix of the developing mouse aorta. *J Cell Sci* **107**, 727-736.

Dickson, M. C., Matrin, J. S., Cousins, F. M., Kulkarni, A. B., Karlsson, S. and Ackhurst, R. J. (1995). Defective hematopoiesis and vasculogenesis in transforming growth factor-β1 knockout mice. *Development* **121**, 1845-1854.

Diebold, R. J., Eis, M. J., Yin, M., Ormsby, I., Boivin, G. P., Darrow, B. J., Saffitz, J. E. and Doetschman, T. (1995). Early-onset multifocal inflammation in the transforming growth factor β1-null mouse is lymphocyte mediated. *Proc Natl Acad Sci USA* **92**, 12215-12219.

Dietz, H. C., Cutting, G. R., Pyeritz, R. E., Maslen, C. L., Sakai, L. Y., Corson, G. M., Puffenberger, E. G., Hamosh, A., Nanthakumar, E. J. and et al. (1991). Marfan syndrome caused by a recurrent de novo missense mutation in the fibrillin gene. *Nature* **352**, 337-339.

Dietz, H. C., Valle, D., Francomano, C. A., Kendzior, R. J. J., Pyeritz, R. E. and Cutting, G. R. (1993). The skipping of constitutive exons *in vivo* induced by nonsense mutations. *Science* **259**, 680-683.

Disabella, E., Grasso, M., Marziliano, N., Ansaldi, S., Lucchelli, C., Porcu, E., Tagliani, M., Pilotto, A., Diegoli, M., Lanzarini, L. *et al.* (2006). Two novel and one known mutation of the *TGFBR2* gene in Marfan syndrome not associated with FBN1 gene defects. *Eur J Hum Genet* **14**, 34-38.

Doliana, R., Mongiat, M., Bucciotti, F., Giacomello, E., Deutzmann, R., Volpin, D., Bressan, G. M. and Colombatti, A. (1999). EMILIN, a component of the elastic fiber and a new member of the C1q/tumor necrosis factor superfamily of proteins. *J Biol Chem* **274**, 16773-16781.

Downing, A. K., Knott, V., Werner, J. M., Cardy, C. M., Campbell, I. D. and Handford, P. A. (1996). Solution structure of a pair of calcium binding epidermal growth factor-like domains: implications for the Marfan syndrome and other genetic disorders. *Cell* **85**, 597-605.

Dubois, C. M., Laprise, M.-H., Blanchette, F., Gentry, L. E. and Leduc, R. (1995). Processing of transforming growth factor-β1 precursor by human furin convertase. *J Biol Chem* **270**, 10618-10624.

Fahrenbach, W. H., Sandberg, L. B. and Cleary, E. G. (1966). Ultrastructural studies on early elastinogenesis. *Anat Rec* **155**, 563-576.

Faivre, L., Gorlin, R. J., Wirtz, M. K., Godfrey, M., Dagoneau, N., Samples, J. R., Le Merrer, M., Collod-Beroud, G., Boileau, C., Munnich, A. and Cormier-Daire, V. (2003). In frame fibrillin-1 gene deletion in autosomal dominant Weill- Marchesani syndrome. *J Med Genet* **40**, 34-36.

Faivre, L., Megarbane, A., Alswaid, A., Zylberberg, L., Aldohayan, N., Campos-Xavier, B., Bacq, D., Legeai-Mallet, L., Bonaventure, J., Munnich, A. and Cormier-Daire, V. (2002). Homozygosity mapping of a Weill-Marchesani syndrome locus to chromosome 19p13.3-p13.2. *Hum Genet* **110**, 366-370.

Fang, J., Li, X., Smiley, E., Francke, U., Mecham, R. P. and Bonadio, J. (1997). Mouse latent TGF-β binding protein-2: Molecular cloning and developmental expression. *Biochim Biophys Acta* **1354**, 219-230.

Faraco, J., Bashir, M., Rosenbloom, J. and Francke, U. (1995). Characterization of the Human Gene for Microfibril-Associated Glycoprotein (MFAP2), Assignment to Chromosome 1p36.1-p35, and Linkage to D1S170. *Genomics* **25**, 630-637.

Finnis, M. L. and Gibson, M. A. (1997). Microfibril-associated glycoprotein-1 (MAGP-1) binds to the pepsin-resistant domain of the α3(VI) chain of type VI collagen. *J Biol Chem* **272**, 22817-22823.

Flaumenhaft, R., Abe, M., Sato, Y., Miyazono, K., Harpel, J., Heldin, C.-H. and Rifkin, D. B. (1993). Role of the latent TGF-β binding protein in the activation of latent TGF-β by co-cultures of endothelial and smooth muscle cells. *J Cell Biol* **120**, 995-1002.

Fontana, L., Chen, Y., Prijatelj, P., Sakai, T., Fässler, R., Sakai, L. Y. and Rifkin, D. B. (2005). Fibronectin is required for integrin αvβ6-mediated activation of latent TGF-β complexes containing LTBP-1. *Faseb J* **19**, 1798-1808.

Fornieri, C., Baccarani-Contri, M., Quaglino, D. J. and Pasquali-Ronchetti, I. (1987). Lysyl oxidase activity and elastin/glycosaminoglycan interactions in growing chick and rat aortas. *J Cell Biol* **105**, 1463-1469.

Frankfater, C., Maus, E., Gaal, K., Segade, F., Copeland, N. G., Gilbert, D. J., Jenkins, N. A. and Shipley, J. M. (2000). Organization of the mouse microfibril-associated glycoprotein-2 (MAGP-2) gene. *Mamm Genome* **11**, 191-195.

Freeman, L. J., Lomas, A., Hodson, N., Sherratt, M. J., Mellody, K. T., Weiss, A. S., Shuttleworth, C. A. and Kielty, C. M. (2005). Fibulin-5 interacts with fibrillin-1 molecules and microfibrils. *Biochem J* **388**, 1-5.

Giannelli, F., Green, P. M., Sommer, S. S., Poon, M. C., Ludwig, M., Schwaab, A., Reitsma, P. H., Goossens, M., Yoshioka, A., Figueiredo, M. S. *et al.* (1998). Haemophilia B: database of point mutations and short additions and deletions—eighth edition. *Nucleic Acids Res* **26**, 265-268.

Gibson, M. A. (1996). Extracellular Matrix, vol. 2 (ed. W. D. Comper), pp. 95-140. Amsterdam: Harwood Academic Publishers.

Gibson, M. A. (2004). Marfan Syndrome: A Primer for Clinicians and Scientists, (ed. P. N. Robinson and M. Godfrey), pp. 161-178. Kluwer Academic/Plenum.

Gibson, M. A. and Cleary, E. G. (1987). The immunohistochemical localization of microfibril-associated glycoprotein (MAGP) in elastic and non-elastic tissues. *Immunol Cell Biol* **65**, 345-356.

Gibson, M. A., Finnis, M. L., Kumaratilake, J. S. and Cleary, E. G. (1998). Microfibril-associated glycoprotein-2 (MAGP-2) is specifically associated with fibrillin-containing microfibrils but exhibits more restricted patterns of tissue localization and developmental expression than its structural relative MAGP-1. *J Histochem Cytochem* **46**, 871-885.

Gibson, M. A., Hatzinikolas, G., Davis, E. C., Baker, E., Sutherland, G. R. and Mecham, R. P. (1995). Bovine latent transforming growth factor-β1-binding protein 2: Molecular cloning, identification of tissue isoforms, and immunolocalization to elastin-associated microfibrils. *Mol Cell Biol* **15**, 6932-6942.

Gibson, M. A., Hatzinikolas, G., Kumaratilake, J. S., Sandberg, L. B., Nicholl, J. K., Sutherland, G. R. and Cleary, E. G. (1996). Further characterization of proteins associated with elastic fiber microfibrils including the molecular cloning of MAGP-2 (MP25). *J Biol Chem* **271**, 1096-1103.

Gibson, M. A., Hughes, J. L., Fanning, J. C. and Cleary, E. G. (1986). The major antigen of elastin-associated microfibrils is a 31-kDa glycoprotein. *J Biol Chem* **261**, 11429-11436.

Gibson, M. A., Kumaratilake, J. S. and Cleary, E. G. (1989). The protein components of the 12-nanometer microfibrils of elastic and nonelastic tissue. *J Biol Chem* **264**, 4590-4598.

Gibson, M. A., Leavesley, D. I. and Ashman, L. K. (1999). Microfibril-associated glycoprotein-2 specifically interacts with a range of bovine and human cell types via αvβ3 integrin. *J Biol Chem* **274**, 13060-13065.

Gibson, M. A., Sandberg, L. B., Grosso, L. E. and Cleary, E. G. (1991). Complementary DNA cloning establishes microfibril-associated glycoprotein (MAGP) to be a discrete component of the elastin-associated microfibrils. *J Biol Chem* **266**, 7596-7601.

Giltay, R., Kostka, G. and Timpl, R. (1997). Sequence and expression of a novel member (LTBP-4) of the family of latent transforming growth factor-β binding proteins. *FEBS Lett* **411**, 164-168.

Giltay, R., Timpl, R. and Kostka, G. (1999). Sequence, recombinant expression and tissue localization of two novel extracellular matrix proteins, fibulin-3 and fibulin-4. *Matrix Biol* **18**, 469-480.

Gleizes, P. E., Beavis, R. C., Mazzieri, R., Shen, B. and Rifkin, D. B. (1996). Identification and characterization of an eight-cysteine repeat of the latent transforming growth factor-β binding protein-1 that mediates bonding to the latent transforming growth factor-β1. *J Biol Chem* **271**, 29891-29896.

Greenlee, T. K. J., Ross, R. and Hartman, J. L. (1966). The fine structure of elastic fibers. *J Cell Biol* **30**, 59-71.

Gregory, K. E., Ono, R. N., Charbonneau, N. L., Kuo, C. L., Keene, D. R., Bachinger, H. P. and Sakai, L. Y. (2005). The prodomain of BMP-7 targets the BMP-7 complex to the extracellular matrix. *J Biol Chem* **280**, 27970-27980.

Gullberg, D. E. and Lundgren-Akerlund, E. (2002). Collagen-binding I domain integrins--what do they do? *Prog Histochem Cytochem*. **37**, 3-54.

Gupta, P. A., Putnam, E. A., Carmical, S. G., Kaitila, I., Steinmann, B., Child, A., Danesino, C., Metcalfe, K., Berry, S. A., Chen, E. *et al.* (2002). Ten novel FBN2 mutations in congenital contractural arachnodactyly: Delineation of the molecular pathogenesis and clinical phenotype. *Hum Mutat* **19**, 39-48.

Handford, P. A., Mayhew, M., Baron, M., Winship, P. R., Campbell, I. D. and Brownlee, G. (1991). Key residues involved in calcium-binding motifs in EGF-like domains. *Nature* **351**, 164-167.

Hanssen, E., Hew, F. H., Moore, E. and Gibson, M. A. (2004). MAGP-2 has multiple binding regions on fibrillins and has covalent periodic association with fibrillin-containing microfibrils. *J Biol Chem* **279**, 29185-29194.

Hanssen, E., Reinboth, B. and Gibson, M. A. (2003). Covalent and Non-covalent Interactions of βig-h3 with Collagen VI: βig-h3 is covalently attached to the amino-terminal region of collagen VI in tissue microfibrils. *J Biol Chem* **278**, 24334-24341.

Hatzinikolas, G. and Gibson, M. A. (1998). The exon structure of the human MAGP-2 gene: Similarity with the MAGP-1 gene is confined to two exons encoding a cysteine-rich region. *J Biol Chem* **273**, 29309-29314.

Hecht, F. and Beals, R. K. (1972). "New" syndrome of congenital contractural arachnodactyly originally described by Marfan in 1896. *Pediatrics* **49**, 574-579.

Henderson, M., Polewski, R., Fanning, J. C. and Gibson, M. A. (1996). Microfibril-associated glycoprotein-1 (MAGP-1) is specifically located on the beads of the beaded-filament structure for fibrillin-containing microfibrils as visualized by the rotary shadowing technique. *J Histochem Cytochem* **44**, 1389-1397.

Hinck, A. P., Archer, S. J., Qian, S. W., Roberts, A. B., Sporn, M. B., Weatherbee, J. A., Tsang, M. L., Lucas, R., Zhang, B. L., Wenker, J. and Torchia, D. A. (1996). Transforming growth factor-β1: three-dimensional structure in solution and comparison with the X-ray structure of transforming growth factor-β2. *Biochem* **35**, 8517-8534.

Hinek, A. (1996). Biological roles of the non-integrin elastin/laminin receptor. *Biol Chem Hoppe Seyler* **377**, 471-480.

Horrigan, S. K., Rich, C. B., Streeten, B. W., Li, Z. Y. and Foster, J. A. (1992). Characterization of an associated microfibril protein through recombinant DNA techniques. *J Biol Chem* **267**, 10087-10095.

Horton, R. M., Ho, S. N., Pullen, J. K., Hunt, H. D., Cai, Z. and Pease, L. R. (1993). Gene splicing by overlap extension. *Methods Enzymol* **217**, 270-279.

Huang, X. Z., Wu, J. F., Cass, D., Erle, D. J., Corry, D., Young, S. G., Farese, R. V., Jr. and Sheppard, D. (1996). Inactivation of the integrin β6 subunit gene reveals a role of epithelial integrins in regulating inflammation in the lung and skin. *J Cell Biol* **133**, 921-928.

Hubmacher, D., Tiedemann, K., Bartels, R., Brinckmann, J., Vollbrandt, T., Bätge, B., Notbohm, H. and Reinhardt, D. (2005). Modification of the structure and function of fibrillin-1 by homocysteine suggests a potential pathogenetic mechanism in homocystinuria. *J Biol Chem* **280**, 34946–34955.

Hudson, B. G., Reeders, S. T. and Tryggvason, K. (1993). Type IV collagen: structure, gene organization, and role in human diseases. Molecular basis of Goodpasture and Alport syndromes and diffuse leiomyomatosis. *J Biol Chem.* **268**, 26033-26036.

Hutchinson, S., Aplin, R. T., Webb, H., Kettle, S., Timmermans, J., Boers, G. H. and Handford, P. A. (2005). Molecular effects of homocysteine on cbEGF domain structure: insights into the pathogenesis of homocystinuria. *J Mol Biol* **346**, 833-844.

Hynes, R. O. (1992). Integrins: versatility, modulation, and signaling in cell adhesion. *Cell* **69**, 11-25.

Hynes, R. O. (2002). Integrins: bidirectional, allosteric signaling machines. *Cell* **110**, 673-687.

Hyytiäinen, M. and Keski-Oja, J. (2003). Latent TGF-β binding protein LTBP-2 decreases fibroblast adhesion to fibronectin. *J Cell Biol* **163**, 1363-1374.

Hyytiäinen, M., Taipale, J., Heldin, C. H. and Keski-Oja, J. (1998). Recombinant latent transforming growth factor-β-binding protein 2 assembles to fibroblast extracellular matrix and is susceptible to proteolytic processing and release. *J Biol Chem* **273**, 20669-20676.

Ignotz, R. A. and Massague, J. (1986). Transforming growth factor-β stimulates the expression of fibronectin and collagen and their incorporation into the extracellular matrix. *J Biol Chem* **261**, 4337-4345.

Indik, Z., Yeh, H., Ornstein, G. N., Kucich, U., Abrams, W., Rosenbloom, J. C. and Rosenbloom, J. (1989). Structure of the elastin gene and alternative splicing of elastin mRNA: implications for human disease. *Am J Med Genet* **34**, 81-90.

Iozzo, R. V. (2005). Basement membrane proteoglycans: from cellar to ceiling. *Nat Rev Mol Cell Biol.* **6**, 646-656.

Isogai, Z., Aspberg, A., Keene, D. R., Ono, R. N., Reinhardt, D. P. and Sakai, L. Y. (2002). Versican interacts with fibrillin-1 and links extracellular microfibrils to other connective tissue networks. *J Biol Chem* **277**, 4565-4572.

Isogai, Z., Ono, R. N., Ushiro, S., Keene, D. R., Chen, Y., Mazzieri, R., Charbonneau, N. L., Reinhardt, D. P., Rifkin, D. B. and Sakai, L. Y. (2003). Latent transforming growth factor-β-binding protein 1 interacts with fibrillin and is a microfibril-associated protein.*J Biol Chem* **278**, 2750-2757.

Jensen, S. A., Reinhardt, D. P., Gibson, M. A. and Weiss, A. S. (2001). Protein interaction studies of MAGP-1 with tropoelastin and fibrillin-1. *J Biol Chem* **276**, 39661-39666.

Johnstone, B., Markopoulos, M., Neame, P. J. and Caterson, B. (1993). Identification and characterization of glycanated and nonglycanated forms of biglycan and decorin in the human intervertebral disc. *Biochem J* **292**, 661-666.

Judge, D. P. and Dietz, H. C. (2005). Marfan's syndrome. *Lancet* **366**, 1965-1976.

Kaartinen, V., Voncken, J. W., Shuler, C., Warburton, D., Bu, D., Heisterkamp, N. and Groffen, J. (1995). Abnormal lung development and cleft palate in mice lacking TGF-β3 indicates defects of epithelial-mesenchymal interaction. *Nat Genet* **11**, 415-421.

Kadler, K. (2004). Matrix loading: assembly of extracellular matrix collagen fibrils during embryogenesis. *Birth Defects Res (Part C)* **72**, 1-11.

Kagan, H. M., Vaccaro, C. A., Bronson, E., Tang, S.-S. and Brody, J. S. (1986). Ultrastructural immunolocalisation of lysyl oxidase in vascular connective tissue. *J Cell Biol* **103**, 1121-1128.

Kainulainen, K., Karttunen, L., Puhakka, L., Sakai, L. and Peltonen, L. (1994). Mutations in the fibrillin gene responsible for dominant ectopia lentis and neonatal Marfan syndrome. *Nat Genet* **6**, 64-69.

Kantola, A. K., Keski-Oja, J. and Koli, K. (2005). Induction of human LTBP-3 promoter activity by TGF-β1 is mediated by Smad3/4 and AP-1 binding elements. *Gene* **363**, 142-150.

Kanzaki, T., Olofsson, A., Morén, A., Wernstedt, C., Hellman, U., Miyazono, K., Claesson-Welsh, L. and Heldin, C.-H. (1990). TGF-β1 binding protein: a component of the large latent complex of TGF-β1 with multiple repeat sequences. *Cell* **61**, 1051-1061.

Keene, D. R., Maddox, B. K., Kuo, H.-J., Sakai, L. Y. and Glanville, R. W. (1991). Extraction of extendable beaded structures and their identification as fibrillin-containing extracellular matrix microfibrils. *J Histochem Cytochem* **39**, 441-449.

Keene, D. R., Sakai, L. Y., Lunstrum, G. P., Morris, N. P. and Burgeson, R. E. (1987). Type VII collagen forms an extended network of anchoring fibrils. *J Cell Biol.* **104**, 611-21.

Kefalides, N. A. (1973). Structure and biosynthesis of basement membranes. *Int rev connect tissue res* **6**, 63-104.

Kidd, S., Kelley, M. R. and Young, M. W. (1986). Sequence of the notch locus of Drosophila melanogaster: relationship of the encoded protein to mammalian clotting and growth factors. *Mol Cell Biol* **6**, 3094-3108.

Kielty, C. M., Baldock, C., Lee, D., Rock, M. J., Ashworth, J. L. and Shuttleworth, C. A. (2002a). Fibrillin: From microfibril assembly to biomechanical function. *Philos Trans R Soc Lond B Biol Sci* **357**, 207-217.

Kielty, C. M. and Grant, M. E. (2002). The Collagen family: structure, assembly, and organization in the extracellular matrix. "Connective tissue and its heritable disorders" (ed. Royce, P. M. and Steinmann, B.), second edition, 585-626, Wiley-Liss Inc. New York.

Kielty, C. M., Sherratt, M. J. and Shuttleworth, C. A. (2002b). Elastic fibres. *J Cell Sci* **115**, 2817-2828.

Kielty, C. M., Whittaker, S. P. and Shuttleworth, C. A. (1996). Fibrillin: evidence that chondroitin sulphate proteoglycans are components of microfibrils and associate with newly synthesised monomers. *FEBS Lett* **386**, 169-173.

Kim, J.-E., Jeong, H.-W., Nam, J.-O., Lee, B.-H., Choi, J.-Y., Park, R.-W., Park, J. Y. and Kim, I.-S. (2002). Identification of motifs in the fasciclin domains of the transforming growth factor-β-induced matrix protein βig-h3 that interact with the αvβ5 integrin. *J Biol Chem* **277**, 46159-46165.

Kingsley, D. M. (1994). The TGF-β superfamily: new members, new receptors, and new genetic tests of function in different organisms. *Genes Dev* **8**, 133-146.

Kitahama, S., Gibson, M. A., Hatzinikolas, G., Hay, S., Kuliwaba, J. L., Evdokiou, A., Atkins, G. J. and Findlay, D. M. (2000). Expression of fibrillins and other microfibril-associated proteins in human bone and osteoblast-like cells. *Bone* **27**, 61-67.

Kluge, M., Mann, K., Dziadek, M. and Timpl, R. (1990). Characterisation of a novel calcium-binding 90-kDa glycoprotein (BM-90) shared by basement membranes and serum. *Eur J Biochem* **193**, 651-659.

Kobayashi, R., Mizutani, A. and Hidaka, H. (1994). Isolation and characterization of a 36-kDa microfibril-associated glycoprotein by the newly synthesized isoquinolinesulfonamide affinity chromatography. *Biochem Biophys Res Commun* **198**, 1262-1266.

Kobayashi, R., Tashima, Y., Masuda, H., Shozawa, T., Numata, Y., Miyauchi, K.-I. and Hayakawa, T. (1989). Isolation and characterization of a new 36-kDa microfibril-associated glycoprotein from porcine aorta. *J Biol Chem* **264**, 17437-17444.

Kojima, S., Kiyomitsu, N. and Rifkin, D. B. (1993). Requirement of transglutaminase in the activation of transforming growth factor-β in bovine endothelial cells. *J Cell Biol* **121**, 439-448.

Koli, K., Wempe, F., Sterner-Kock, A., Kantola, A., Komor, M., Hofmann, W.-K., von Melchner, H. and Keski-Oja, J. (2004). Disruption of LTBP-4 function reduces TGF-β activation and enhances BMP-4 signaling in the lung. *J Cell Biol* **167**, 123-133.

Koski, C., Saharinen, J. and Keski-Oja, J. (1999). Independent promoters regulate the expression of two amino terminally distinct forms of latent transforming growth factor-β binding protein-1 (LTBP-1) in a cell type-specific manner. *J Biol Chem* **274**, 32619-32630.

Kostka, G., Giltay, R., Bloch, W., Addicks, K., Timpl, R., Fässler, R. and Chu, M. L. (2001). Perinatal lethality and endothelial cell abnormalities in several vessel compartments of fibulin-1-deficient mice. *Mol Cell Biol* **21**, 7025-7034.

Kozel, B. A., Wachi, H., Davis, E. C. and Mecham, R. P. (2003). Domains on tropoelastin that mediate elastin deposition in vitro and in vivo. *J Biol Chem* **278**, 18491-18498.

Kramer, K. L. and Yost, H. J. (2003). Heparan sulfate core proteins in cell-cell signaling. *Annu Rev Genet* **37**, 461-484.

Kucich, U., Rosenbloom, J. C., Abrams, W. R. and Rosenbloom, J. (2002). Transforming growth factor-β stabilizes elastin mRNA by a pathway requiring active Smads, protein kinase C-delta, and p38. *Am J Respir Cell Mol Biol* **26**, 183-188.

Kulkarni, A. B., Huh, C.-G., Becker, D., Geiser, A., Lyght, M., Flanders, K. C., Roberts, A. B., Sporn, M. B., Ward, J. M. and Karlsson, S. (1993). Transforming growth factor-β1 null mutation in mice causes excessive inflammatory response and early death. *Proc Natl Acad Sci USA* **90**, 770-774.

Lack, J., O'Leary, J. M., Knott, V., Yuan, X., Rifkin, D. B., Handford, P. A. and Downing, A. K. (2003). Solution Structure of the Third TB Domain from LTBP1 Provides Insight into Assembly of the Large Latent Complex that Sequesters Latent TGF-β. *J Mol Biol* **334**, 281-291.

Laemmli, U. K. (1970). Cleavage of structural proteins during the assembly of the head of bacteriophage T4. *Nature* **227**, 680-685.

Lawler, J. and Hynes, R. (1986). The structure of human thrombospondin, an adhesive glycoprotein with multiple calcium-binding sites and homologies with several different proteins. *J Cell Biol* **103**, 1635-1648.

Lee, B., Godfrey, M., Vitale, E., Hori, H., Mattei, M. G., Sarfarazi, M., Tsipouras, P., Ramirez, F. and Hollister, D. W. (1991). Linkage of Marfan syndrome and a phenotypically related disorder to two different fibrillin genes. *Nature* **352**, 330-334.

Lee, S. S., Knott, V., Jovanovic, J., Harlos, K., Grimes, J. M., Choulier, L., Mardon, H. J., Stuart, D. I. and Handford, P. A. (2004). Structure of the integrin binding fragment from fibrillin-1 gives new insights into microfibril organization. *Structure* **12**, 717-729.

Li, D. Y., Brooke, B., Davis, E. C., Mecham, R. P., Sorensen, L. K., Boak, B. B., Eichwald, E. and Keating, M. T. (1998). Elastin is an essential determinant of arterial morphogenesis. *Nature* **393**, 276-280.

Lin, G., Tiedemann, K., Vollbrandt, T., Peters, H., Bätge, B., Brinckmann, J. and Reinhardt, D. P. (2002). Homo- and heterotypic fibrillin-1 and -2 interactions constitute the basis for the assembly of microfibrils. *J Biol Chem* **277**, 50795-50804.

Liu, W. G., Qian, C. P. and Francke, U. (1997). Silent mutations induce exon skipping of fibrillin-1 gene in Marfan syndrome. *Nat Genet* **16**, 328-329.

Lu, M., Munger, J. S., Steadele, M., Busald, C., Tellier, M. and Schnapp, L. M. (2002). Integrin α8β1 mediates adhesion to LAP-TGFβ1. *J Cell Sci* **115**, 4641-4648.

Lu, Y., Holmes, D. F. and Baldock, C. (2005). Evidence for the intramolecular pleating model of fibrillin microfibril organisation from single particle image analysis. *J Mol Biol* **349**, 73-85.

Lui, W., Faraco, J., Qian, C. and Francke, U. (1997). The gene for microfibril-associated protein-1 (MFAP1) is located several megabases centromeric to FBN1 and is not mutated in Marfan syndrome. *Hum Genet* **99**, 578-584.

Maddox, B. K., Sakai, L. Y., Keene, D. R. and Glanville, R. W. (1989). Connective tissue microfibrils. Isolation and characterization of three large pepsin-resistant domains of fibrillin. *J Biol Chem* **264**, 21381-21385.

Magenis, R. E., Maslen, C. L., Smith, L., Allen, L. and Sakai, L. Y. (1991). Localization of the fibrillin (FBN) gene to chromosome 15, band q21.1. *Genomics* **11**, 346-351.

Majors, A. K. and Pyeritz, R. E. (2000). A deficiency of cysteine impairs fibrillin-1 deposition: Implications for the pathogenesis of cystathionine β-synthase deficiency. *Mol Genet Metab* **70**, 252-260.

Marfan, A. B. (1896). Un cas de déformation congénitate des quatre membres plus prononcée aux estrémites charactérisée par l'allongement des os auvec un certain degré d'amincissement. *Bull. Mem. Soc. Méd Hôp* **13**, 220-226.

Marigo, V., Volpin, D. and Bressan, G. M. (1993). Regulation of the human elastin promoter in chick embryo cells. Tissue specific effect of TGF-β. *Biochim Biophys Acta* **1172**, 31-36.

Marigo, V., Volpin, D., Vitale, G. and Bressan, G. M. (1994). Identification of a TGF-β responsive element in the human elastin promoter. *Biochem Biophys Res Commun* **199**, 1049-1056.

Marson, A., Rock, M. J., Cain, S. A., Freeman, L. J., Morgan, A., Mellody, K., Shuttleworth, C. A., Baldock, C. and Kielty, C. M. (2005). Homotypic fibrillin-1 interactions in microfibril assembly. *J Biol Chem* **280**, 5013-5021.

Maslen, C. L., Corson, G. M., Maddox, B. K., Glanville, R. W. and Sakai, L. Y. (1991). Partial sequence of a candidate gene for the Marfan syndrome. *Nature* **352**, 334-337.

Maslen, C. L. and Glanville, R. W. (1993). The molecular basis of Marfan syndrome. *DNA Cell Biol* **12**, 561-572.

Massague, J. (1990). The transforming growth factor-β family. *Annu Rev Cell Biol* **6**, 597-641.

Matsudaira, P. T. and Burgess, D. R. (1978). SDS microslab linear gradient polyacrylamide gel electrophoresis. *Anal Biochem* **87**, 386-396.

Mayne, R. (2002). Morphology and chemical composition of connective tissue: the eye. "Connective tissue and its heritable disorders" (ed. Royce, P. M. and Steinmann, B.), second edition, 585-626, Wiley-Liss Inc. New York.

Mecham, R. P., Whitehouse, L. A., Hay, M., Hinek, A. and Sheetz, M. (1991). Ligand affinity of the 67 kDa elastin/laminin binding protein is modulated by the protein's lectin domain: visualisation of elastin/laminin receptor complexes with gold tagged ligands. *J Cell Biol* **113**, 187-194.

Milewicz, D. M., Urban, Z. and Boyd, C. (2000). Genetic disorders of the elastic fiber system. *Matrix Biol* **19**, 471-480.

Miyamoto, A., Lau, R., Hein, P. W., Shipley, J. M. and Weinmaster, G. (2006). Microfibrillar Proteins MAGP-1 and MAGP-2 Induce Notch1 Extracellular Domain Dissociation and Receptor Activation. *J Biol Chem* **281**, 10089-10097.

Miyazono, K., Hellman, U., Wernstedt, C. and Heldin, C.-H. (1988). Latent high molecular weight complex of transforming growth factor-β1. Purification from human platelets and structural characterisation. *J Biol Chem* **263**, 6407-6415.

Miyazono, K., Olofsson, A., Colosetti, P. and Heldin, C.-H. (1991). A role of the latent TGF-β1-binding protein in the assembly and secretion of TGF-β1. *EMBO J* **10**, 1091-1102.

Miyazono, K., Thyberg, J. and Heldin, C.-H. (1992). Retention of the transforming growth factor-β1 precursor in the Golgi complex in a latent endoglycosidase H-sensitive form. *J Biol Chem* **267**, 5668-5675.

Mizuguchi, T., Collod-Beroud, G., Akiyama, T., Abifadel, M., Harada, N., Morisaki, T., Allard, D., Varret, M., Claustres, M., Morisaki, H. *et al.* (2004). Heterozygous TGFBR2 mutations in Marfan syndrome. *Nat Genet* **36**, 855-860.

Morén, A., Olofsson, A., Stenman, G., Sahlin, P., Kanzaki, T., Claesson-Welsh, L., ten Dijke, P., Miyazono, K. and Heldin, C.-H. (1994). Identification and characterization of LTBP-2, a novel latent transforming growth factor-β-binding protein. *J Biol Chem* **269**, 32469-32478.

Mu, D., Cambier, S., Fjellbirkeland, L., Baron, J. L., Munger, J. S., Kawakatsu, H., Sheppard, D., Broaddus, V. C. and Nishimura, S. L. (2002). The integrin αvβ8 mediates epithelial homeostasis through MT1-MMP-dependent activation of TGF-β1. *J Cell Biol* **157**, 493-507.

Munger, J., Huang, X., Kawakatsu, H., Griffiths, M., Dalton, S., Wu, J., Pittet, J. F., Kaminski, N., Garat, C., Matthay, M. *et al.* (1999). The integrin αvβ6 binds and activates latent TGF-β1: a mechanism for regulating pulmonary inflammation and fibrosis. *Cell* **96**, 319-328.

Munger, J. S., Harpel, J. G., Giancotti, F. G. and Rifkin, D. B. (1998). Interactions between growth factors and integrins: Latent forms of transforming growth factor-β are ligands for the integrin αvβ1. *Mol Biol Cell* **9**, 2627-2638.

Nagase, T., Nakayama, M., Nakajima, D., Kikuno, R. and Ohara, O. (2001). Prediction of the coding sequences of unidentified human genes. XX. The complete sequences of 100 new cDNA clones from brain which code for large proteins in vitro. *DNA Res* **8**, 85-95.

Nakamura, T., Lozano, P. R., Ikeda, Y., Iwanaga, Y., Hinek, A., Minamisawa, S., Cheng, C.-F., Kobuke, K., Dalton, N., Takada, Y. *et al.* (2002). Fibulin-5/DANCE is essential for elastinogenesis in vitro. *Nature* **415**, 171-175.

Nataatmadja, M., West, J. and West, M. (2006). Overexpression of transforming growth factor-β is associated with increased hyaluronan content and impairment of repair in Marfan syndrome aortic aneurysm. *Circulation* **114**, I371-1377.

Nehring, L. C., Miyamoto, A., Hein, P. W., Weinmaster, G. and Shipley, J. M. (2005). The extracellular matrix protein MAGP-2 interacts with jagged1 and induces its shedding from the cell surface. *J Biol Chem* **280**, 20349-20355.

Neptune, E. R., Frischmeyer, P. A., Arking, D. E., Myers, L., Bunton, T. E., Gayraud, B., Ramirez, F., Sakai, L. Y. and Dietz, H. C. (2003). Dysregulation of TGF-β activation contributes to pathogenesis in Marfan syndrome. *Nat Genet* **33**, 407-411.

Ng, C. M., Cheng, A., Myers, L. A., Martinez-Murillo, F., Jie, C., Bedja, D., Gabrielson, K. L., Hausladen, J. M., Mecham, R. P., Judge, D. P. and Dietz, H. C. (2004). TGF-β-dependent pathogenesis of mitral valve prolapse in a mouse model of Marfan syndrome. *J Clin Invest* **114**, 1586-1592.

Nischt, R., Pottgiesser, J., Krieg, T., Mayer, U., Aumailley, M. and Timpl, R. (1991). Recombinant expression and properties of the human calcium-binding extracellular matrix protein BM-40. *Eur J Biochem* **200**, 529-536.

Nishio, E. and Wantanabe, Y. (1997). Transforming growth factor-β is a modulator of platelet-derived growth factor action in vascular smooth muscle cells: a possible role for catalase activity and glutathione peroxidase activity. *Biochem Biophys Res Commun* **232**, 1-4.

Nunes, I., Gleizes, P. E., Metz, C. N. and Rifkin, D. B. (1997). Latent transforming growth factor-β binding protein domains involved in activation and transglutaminase-dependent cross-linking of latent transforming growth factor-β. *J Cell Biol* **136**, 1151-1163.

Öklü, R. and Hesketh, R. (2000). The latent transforming growth factor-β binding protein (LTBP) family. *Biochem J* **352**, 601-610.

Pan, T.-C., Sasaki, T., Zhang, R.-Z., Fässler, R., Timpl, R. and Chu, M.-L. (1993). Structure and expression of fibulin-2, a novel extracellular matrix protein with multiple EGF-like repeats and consensus for calcium binding. *J Cell Biol* **123**, 1269-1277.

Papin, J. A., Hunter, T., Palsson, B. O. and Subramaniam, S. (2005). Reconstruction of cellular signalling networks and analysis of their properties. *Nat Rev Mol Cell Biol* **6**, 99-111.

Park, E. S., Putnam, E. A., Chitayat, D., Child, A. and Milewicz, D. M. (1998). Clustering of FBN2 mutations in patients with congenital contractural arachnodactyly indicates an important role of the domains encoded by exons 24 through 34 during human development. *Am J Med Genet* **78**, 350-355.

Pasquali-Ronchetti, I. and Baccarani-Contri, M. (1997). Elastic fiber during development and aging. *Microsurgical research techniques* **38**, 428-435.

Penttinen, C., Saharinen, J., Weikkolainen, K., Hyytiäinen, M. and Keski-Oja, J. (2002). Secretion of human latent TGF-β-binding protein-3 (LTBP-3) is dependent on co-expression of TGF-β. *J Cell Sci* **115**, 3457-3468.

Pereira, L., Andrikopoulos, K., Tian, J., Lee, S. Y., Keene, D. R., Ono, R. N., Reinhardt, D. P., Sakai, L. Y., Biery, N. J., Bunton, T. E., Dietz, D. C. and Ramirez, F. (1997). Targeting of the gene encoding fibrillin-1 recapitulates the vascular aspect of Marfan syndrome. *Nat Genet* **17**, 218-222.

Pereira, L., D'Alessio, M., Ramirez, F., Lynch, J. R., Sykes, B., Pangilinan, T. and Bonadio, J. (1993). Genomic organization of the sequence coding for fibrillin, the defective gene product in Marfan syndrome. *Hum Mol Genet* **2**, 961-968.

Pereira, L., Lee, S. Y., Gayraud, B., Andrikopoulos, K., Shapiro, S. D., Bunton, T., Biery, N. J., Dietz, H. C., Sakai, L. Y. and Ramirez, F. (1999). Pathogenetic sequence for aneurysm revealed in mice underexpressing fibrillin-1. *Proc Natl Acad Sci USA* **96**, 3819-3823.

Pierschbacher, M. D. and Ruoslahti, E. (1984). Cell attachment activity of fibronectin can be duplicated by small synthetic fragments of the molecule. *Nature* **309**, 30-33.

Piez, K. A., Eigner, E. A. and Lewis, M. S. (1963). The chromatographic separation and amino acid composition of the subunits of several collagens. *Biochem* **2**, 58-66.

Pinnell, S. R. and Martin, G. R. (1968). The cross-linking of collagen and elastin: Enzymatic conversion of lysine in peptide linkage to a α-aminoadipic-Δ-semialdehyde (allysine) by an extract from bone. *Proc Natl Acad Sci USA* **61**, 708-716.

Porst, M., Daniel, C., Plank, C., Schocklmann, H. O., Reinhardt, D. P. and Hartner, A. (2005). Induction and Coexpression of Latent Transforming Growth Factor-β-Binding Protein-1 and Fibrillin-1 in Experimental Glomerulonephritis. *Nephron Exp Nephrol* **102**, e99-e104.

Proetzel, G., Pawlowski, S. A., Wiles, M. V., Yin, M., Boivin, G. P., Howles, P. N., Ding, J., Ferguson, M. W. and Doetschman, T. (1995). Transforming growth factor-β3 is required for secondary palate fusion. *Nat Genet* **11**, 409-414.

Putnam, E. A., Cho, M., Zinn, A. B., Towbin, J. A., Byers, P. H. and Milewicz, D. M. (1996). Delineation of the Marfan phenotype associated with mutations in exons 23-32 of the FBN1 gene. *Am J Med Genet* **62**, 233-242.

Putnam, E. A., Zhang, H., Ramirez, F. and Milewicz, D. M. (1995). Fibrillin-2 (FBN2) mutations result in the Marfan-like disorder, congenital contractural arachnodactyly. *Nat Genet* **11**, 456-458.

Pyeritz, R. E. and Dietz, H. C. (2002). Marfan Syndrome and other microfibrillar disorders. "Connective tissue and its heritable disorders" (ed. Royce, P. M. and Steinmann, B.), second edition, 585-626, Wiley-Liss Inc. New York.

Pytela, R., Pierschbacher, M. D. and Ruoslahti, E. (1985). Identification and isolation of a 140 kd cell surface glycoprotein with properties expected of a fibronectin receptor. *Cell* **40**, 191-198.

Qian, R.-Q. and Glanville, R. W. (1997). The alignment of fibrillin molecules in elastic microfibrils is defined by transglutaminase derived cross links. *Biochem* **36**, 15841-15847.

Quaglino, D. J., Nanney, L. B., Ditesheim, J. A. and Davidson, J. M. (1991). Transforming growth factor-β stimulates wound healing and modulates extracellular matrix gene expression in pig skin: Incisional wound model. *J Invest Dermatol* **97**, 34-42.

Quondamatteo, F., Reinhardt, D. P., Charbonneau, N. L., Pophal, G., Sakai, L. Y. and Herken, R. (2002). Fibrillin-1 and fibrillin-2 in human embryonic and early fetal development. *Matrix Biol* **21**, 637-46.

Ramirez, F., Gayraud, B. and Pereira, L. (1999). Marfan syndrome: New clues to genotype-phenotype correlations. *Ann Med* **31**, 202-207.

Ramirez, F. and Pereira, L. (1999). The fibrillins. *Int J Biochem Cell Biol* **31**, 255-259.

Ramirez, F. and Rifkin, D. B. (2003). Cell signalling events: a view from the matrix. *Matrix Biol* **22**, 101-107.

Ramos-Arroyo, M. A., Weaver, D. D. and Beals, R. K. (1985). Congenital contractural arachnodactyly: Report of four additional families and review of literature. *Clin Genet* **27**, 570-581.

Rappolee, D. A., Brenner, C. A., Schultz, R., Mark, D. and Werb, Z. (1988). Developmental expression of PDGF, TGF-alpha, and TGF-beta genes in preimplantation mouse embryos. *Science* **241**, 1823-1825.

Rapraeger, A. C. (2002). Heparan sulfate-growth factor interactions. *Methods Cell Biol* **69**, 83-109.

Reinboth, B., Hanssen, E., Cleary, E. G. and Gibson, M. A. (2002). Molecular interactions of biglycan and decorin with elastic fiber components. Biglycan forms a ternary complex with tropoelastin and microfibril-associated glycoprotein 1. *J Biol Chem* **277**, 3950-3957.

Reinboth, B. J., Finnis, M. L., Gibson, M. A., Sandberg, L. B. and Cleary, E. G. (2000). Developmental expression of dermatan sulfate proteoglycans in the elastic bovine nuchal ligament. *Matrix Biol* **19**, 149-162.

Reinhardt, D. P., Gambee, J. E., Ono, R. N., Bachinger, H. P. and Sakai, L. Y. (2000). Initial steps in assembly of microfibrils: formation of disulfide-cross linked multimers containing fibrillin-1. *J Biol Chem* **275**, 2205-2210.

Reinhardt, D. P., Keene, D. R., Corson, G. M., Poschl, E., Bachinger, H. P., Gambee, J. E. and Sakai, L. Y. (1996a). Fibrillin-1: Organisation in microfibrils and structural properties. *J Mol Biol* **258**, 104-116.

Reinhardt, D. P., Ono, R. N., Notbohm, H., Mueller, P. K., Bachinger, H. P. and Sakai, L. Y. (2000). Mutations in calcium-binding epidermal growth factor modules render fibrillin-1 susceptible to proteolysis. A potential disease-causing mechanism in Marfan syndrome. *J Biol Chem* **275**, 12339-12345.

Reinhardt, D. P., Ono, R. N. and Sakai, L. Y. (1997). Calcium stabilizes fibrillin-1 against proteolytic degradation. *J Biol Chem* **272**, 1231-1236.

Reinhardt, D. P., Sasaki, T., Dzamba, B. J., Keene, D. R., Chu, M. L., Goehring, W., Timpl, R. and Sakai, L. Y. (1996b). Fibrillin-1 and fibulin-2 interact and are colocalized in some tissues. *J Biol Chem* **271**, 19489-19496.

Rich, A. and Crick, F. H. C. (1961). The molecular structure of collagen. *J Mol Biol* **3**, 483-506.

Rifkin, D. B. (2004). Latent TGF-β binding proteins: Orchestrators of TGF-β availability. *J Biol Chem* **280**, 7409-7412.

Roark, E. F., Keene, D. R., Haudenschild, C. C., Godyna, S., Little, C. D. and Argraves, W. S. (1995). The Association of Human Fibulin-1 with Elastic Fibers: An Immunohistological, Ultrastructural, and RNA Study. *J Histochem Cytochem* **43**, 401-411.

Roberts, A. B., Sporn, M. B., Assoian, R. K., Smith, J. M., Roche, N. S., Wakefield, L. M., Heine, U. I., Liotta, L. A., Falanga, V., Kehrl, J. H. *et al.* (1986). Transforming growth factor type β: rapid induction of fibrosis and angiogenesis *in vivo* and stimulation of collagen formation *in vitro*. *Proc Natl Acad Sci USA* **83**, 4167-4171.

Robinson, P. N. and Godfrey, M. (2000). The molecular genetics of Marfan syndrome and related microfibrillopathies. *J Med Genet* **37**, 9-25.

Rock, M. J., Cain, S. A., Freeman, L. J., Morgan, A., Mellody, K., Marson, A., Shuttleworth, C. A., Weiss, A. S. and Kielty, C. M. (2004). Molecular basis of elastic fiber formation. Critical interactions and a tropoelastin-fibrillin-1 cross-link. *J Biol Chem* **279**, 23748-23758.

Rosenbloom, J. and Abrams, W. R. (2002). Elastin and the microfibrillar apparatus. "Connective tissue and its heritable disorders" (ed. Royce, P. M. and Steinmann, B.), second edition, 249-269, Wiley-Liss Inc. New York.

Rosso, F., Giordano, A., Barbarisi, M. and Barbarisi, A. (2004). From cell-ECM interactions to tissue engineering. *J Cell Physiol* **199**, 174-180.

Roy, R., Polgar, P., Wang, Y., Goldstein, R. H., Taylor, L. and Kagan, H. M. (1996). Regulation of lysyl oxidase and cyclooxygenase expression in human lung fibroblasts: interactions among TGF-β, IL-1 β, and prostaglandin E. *J Cell Biochem* **62**, 411-417.

Saharinen, J. and Keski-Oja, J. (2000). Specific sequence motif of 8-Cys repeats of TGF-β binding proteins, LTBPs, creates a hydrophobic interaction surface for binding of small latent TGF-β. *Mol Biol Cell* **11**, 2691-2704.

Saharinen, J., Taipale, J. and Keski-Oja, J. (1996). Association of the small latent transforming growth factor-β with an eight cysteine repeat of its binding protein LTBP-1. *EMBO J* **15**, 245-253.

Saharinen, J., Taipale, J., Monni, O. and Keski-Oja, J. (1998). Identification and characterization of a new latent transforming growth factor-β-binding protein, LTBP-4. *J Biol Chem* **273**, 18459-18469.

Sakai, L., Keene, D. R., Glanville, R. W. and Bachinger, H. P. (1991). Purification and partial characterisation of fibrillin, a cysteine-rich structural component of connective tissue microfibrils. *J Biol Chem* **266**, 14763-14770.

Sakai, L. Y., Keene, D. R. and Engvall, E. (1986). Fibrillin, a new 350-kD glycoprotein, is a component of extracellular microfibrils. *J Cell Biol* **103**, 2499-2509.

Sakamoto, H., Broekelmann, T., Cheresh, D. A., Ramirez, F., Rosenbloom, J. and Mecham, R. P. (1996). Cell-type Specific Recognition of RGD- and Non-RGD-containing Cell Binding Domains in Fibrillin-1. *J Biol Chem* **271**, 4916-4922.

Sandberg, L. B., Soskel, N. T. and Leslie, J. B. (1981). Elastin structure, biosynthesis and relation to disease states. *N Engl J Med* **304**, 566-579.

Sanford, L. P., Ormsby, I., Gittenberger-de Groot, A. C., Sariola, H., Friedman, R., Boivin, G. P., Cardell, E. L. and Doetschman, T. (1997). TGF-β2 knockout mice have multiple developmental defects that are non-overlapping with other TGF-β knockout phenotypes. *Dev* **124**, 2659-2670.

Sasaki, T., Göhring, W., Miosge, N., Abrams, W. R., Rosenbloom, J. and Timpl, R. (1999). Tropoelastin binding to fibulins, nidogen-2 and other extracellular matrix proteins. *FEBS Lett* **460**, 280-284.

Schiemann, W. P., Blobe, G. C., Kalume, D. E., Pandey, A. and Lodish, H. F. (2002). Context-specific effects of fibulin-5 (DANCE/EVEC) on cell proliferation, motility, and invasion. Fibulin-5 is induced by transforming growth factor-β and affects protein kinase cascades. *J Biol Chem* **277**, 27367-27377.

Schlessinger, J., Plotnikov, A. N., Ibrahimi, O. A., Eliseenkova, A. V., Yeh, B. K. and Yayon, A. (2000). Crystal structure of a ternary FGF–FGFR–heparin complex reveals a dual role for heparin in FGFR binding and dimerization. *Mol Cell* **6**, 743-750.

Segade, F., Broekelmann, T. J., Pierce, R. A. and Mecham, R. P. (2000). Revised genomic structure of the human MAGP1 gene and identification of alternate transcripts in human and mouse tissues. *Matrix Biol* **19**, 671-682.

Shanley, C. J., Gharaee, K. M., Sarkar, R., Welling, T. H., Kriegel, A., Ford, J. W., Stanley, J. C. and Phan, S. H. (1997). Transforming growth factor-β1 increases lysyl oxidase enzyme activity and mRNA in rat aortic smooth muscle cells. *J Vasc Surg* **25**, 446-452.

Sherman, M. I., Gay, R., Gay, S. and Miller, E. J. (1980). Association of collagen with preimplantation and peri-implantation mouse embryos. *Dev Biol* **74**, 470-478.

Sherratt, M. J., Wess, T. J., Baldock, C., Ashworth, J. L., Purslow, P. P., Shuttleworth, C. A. and Kielty, C. M. (2001). Fibrillin-rich microfibrils of the extracellular matrix: Ultrastructure and assembly. *Micron* **32**, 185-200.

Shipley, J. M., Mecham, R. P., Maus, E., Bonadio, J., Rosenbloom, J., McCarthy, R. T., Baumann, M. L., Frankfater, C., Segade, F. and Shapiro, S. D. (2000). Developmental expression of latent transforming growth factor-β binding protein 2 and its requirement early in mouse development. *Mol Cell Biol* **20**, 4879-4887.

Shull, M. M., Ormsby, I., Kier, A. B., Pawlowski, S., Diebold, R. J., Yin, M., Allen, R., Sidman, C., Proetzel, G., Calvin, D. *et al.* (1992). Targeted disruption of the mouse transforming growth factor-β1 gene results in multifocal inflammatory disease. *Nature* **359**, 693-699.

Siese, A., Jaros, P. P. and Willig, A. (1999). Analysis of interleukin (IL)-1β and transforming growth factor (TGF)-β-induced signal transduction pathways in IL-2 and TGF-β secretion and proliferation in the thymoma cell line EL4.NOB-1. *Scand J Immunol* **49**, 139-148.

Sinha, S., Heagerty, A. M., Shuttleworth, C. A. and Kielty, C. M. (2002). Expression of latent TGF-β binding proteins and association with TGF-β1 and fibrillin-1 following arterial injury. *Cardiovasc Res* **53**, 971-983.

Skinner, M. K. and Moses, H. L. (1989). Transforming growth factor gene expression and action in seminiferous tubule: peritubular cell-sertoli cell interactions. *Mol Endocrinol* **3**, 625-634.

Smallridge, R. A., Whiteman, P., Doering, K., Handford, P. A. and Downing, A. K. (1999). EGF-like domain calcium affinity modulated by N-terminal domain linkage in human fibrillin-1. *J Mol Biol* **286**, 661-668.

Smith-Mungo, L. I. and Kagan, H. M. (1998). Lysyl oxidase: Properties, regulation and multiple functions in biology. *Matrix Biol* **16**, 387-398.

Souchelnitskiy, S., Chambaz, E. M. and Feige, J. J. (1995). Thrombospondins selectively activate one of the two latent forms of transforming growth factor-β present in adrenocortical cell-conditioned medium. *Endocrinology* **136**, 5118-5126.

Stenman, G., Sahlin, P., Olofsson, A., Geurts van Kessel, A. and Miyazono, K. (1994). Assignment of the gene encoding the latent TGF-β1-binding protein (LTBP1) to human chromosome 2, region p12-->q22. *Cytogenet Cell Genet* **66**, 117-119.

Sterner-Kock, A., Thorey, I. S., Koli, K., Wempe, F., Otte, J., Bangsow, T., Kuhlmeier, K., Kirchner, T., Jin, S., Keski-Oja, J. *et al.* (2002). Disruption of the gene encoding the latent transforming growth factor-β binding protein 4 (LTBP-4) causes abnormal lung development, cardiomyopathy, and colorectal cancer. *Genes Dev* **16**, 2264-2273.

Strausberg, R. L., Feingold, E. A., Grouse, L. H., Derge, J. G., Klausner, R. D., Collins, F. S., Wagner, L., Shenmen, C. M., Schuler, G. D., Altschul, S. F. *et al.* (2002). Generation and initial analysis of more than 15,000 full-length human and mouse cDNA sequences. *Proc Natl Acad Sci USA* **99**, 16899-16903.

Suk, J. Y., Jensen, S., McGettrick, A., Willis, A. C., Whiteman, P., Redfield, C. and Handford, P. A. (2004). Structural consequences of cysteine substitutions C1977Y and C1977R in calcium-binding epidermal growth factor-like domain 30 of human fibrillin-1. *J Biol Chem* **279**, 51258-51265.

Taipale, J., Koli, K. and Keski-Oja, J. (1992). Release of transforming growth factor-β1 from the pericellular matrix of cultured fibroblasts and fibrosarcoma cells by plasmin and thrombin. *J Biol Chem* **267**, 25378-25384.

Taipale, J., Lohi, J., Saarinen, J., Kovanen, P. T. and Keski-Oja, J. (1995). Human Mast Cell Chymase and Leukocyte Elastase Release Latent Transforming Growth Factor-1 from the Extracellular Matrix of Cultured Human Epithelial and Endothelial Cells. *J Biol Chem* **270**, 4689-4696.

Taipale, J., Miyazono, K., Heldin, C. H. and Keski-Oja, J. (1994). Latent transforming growth factor-β1 associates to fibroblast extracellular matrix via latent TGF-β binding protein. *J Cell Biol* **124**, 171-181.

Taipale, J., Saharinen, J., Hedman, K. and Keski-Oja, J. (1996). Latent transforming growth factor-β1 and its binding protein are components of extracellular matrix microfibrils. *J Histochem Cytochem* **44**, 875-889.

Tamkun, J. W., DeSimone, D. W., Fonda, D., Patel, R. S., Buck, C., Horwitz, A. F. and Hynes, R. O. (1986). Structure of integrin, a glycoprotein involved in the transmembrane linkage between fibronectin and actin. *Cell* **46**, 271-282.

Taylor, K. R. and Gallo, R. L. (2006). Glycosaminoglycans and their proteoglycans: host-associated molecular patterns for initiation and modulation of inflammation. *Faseb J.* **20**, 9-22.

Tickle, C. (2006). Making digit patterns in the vertebrate limb. *Nat Rev Mol Cell Biol.* **7**, 45-53.

Tiecke, F., Katzke, S., Booms, P., Robinson, P. N., Neumann, L., Godfrey, M., Mathews, K. R., Scheuner, M., Hinkel, G. K., Brenner, R. E. *et al.* (2001). Classic, atypically severe and neonatal Marfan syndrome: Twelve mutations and genotype-phenotype correlations in FBN1 exons 24-40. *Eur J Hum Genet* **9**, 13-21.

Tiedemann, K., Bätge, B., Müller, P. K. and Reinhardt, D. P. (2001). Interactions of fibrillin-1 with heparin/heparan sulfate, implications for microfibrillar assembly. *J Biol Chem* **276**, 36035-36042.

Tiedemann, K., Sasaki, T., Gustafsson, E., Göhring, W., Bätge, B., Notbohm, H., Timpl, R., Wedel, T., Schlötzer-Schrehardt, U. and Reinhardt, D. P. (2005). Microfibrils at basement membrane zones interact with perlecan via fibrillin-1. *J Biol Chem* **280**, 11404-11412.

Timpl, R. and Chu, M. L. (1994). Microfibrillar type VI. "Extracellular matrix assembly and structure", (ed. Yurchenco, P. D.), pp. 207-242. Orlando, FL: Academic Press.

Timpl, R., Sasaki, T., Kostka, G. and Chu, M.-L. (2003). Fibulins: a versatile family of extracellular matrix proteins. *Nat Rev Mol Cell Biol* **4**, 479-489.

Todorovic, V., Jurukovski, V., Chen, Y., Fontana, L., Dabovic, B. and Rifkin, D. B. (2005). Latent TGF-β binding proteins. *Int J Biochem Cell Biol* **37**, 38-41.

Tonary, A. M. and Carnegie, J. A. (1996). TGF-β1 regulation of laminin secretion by F9-derived primitive endoderm cells: a potential role in cell migration within the mouse blastocyst. *Can J Physiol Pharmacol* **74**, 940-948.

Toyoshima, T., Nishi, N., Kusama, H., Kobayashi, R. and Itano, T. (2005). 36-kDa microfibril-associated glycoprotein (MAGP-36) is an elastin-binding protein increased in chick aortae during development and growth. *Exp Cell Res* **307**, 224-230.

Toyoshima, T., Yamashita, K., Furuichi, H., Shishibori, T., Itano, T. and Kobayashi, R. (1999). Ultrastructural distribution of 36-kD microfibril-associated glycoprotein (MAGP-36) in human and bovine tissues. *J Histochem Cytochem* **47**, 1049-1056.

Trask, B. C., Trask, T. M., Broekelmann, T. and Mecham, R. P. (2000). The microfibrillar proteins MAGP-1 and fibrillin-1 form a ternary complex with chondroitin sulfate proteoglycan decorin. *Mol Biol Cell* **11**, 1499-1507.

Trask, T. M., Ritty, T. M., Broekelmann, T., Tisdale, C. and Mecham, R. P. (1999). N-terminal domains of fibrillin 1 and fibrillin 2 direct the formation of homodimers: A possible first step in microfibril assembly. *Biochem J* **340**, 693-701.

Tsuda, T., Wang, H., Timpl, R. and Chu, M. L. (2001). Fibulin-2 expression marks transformed mesenchymal cells in developing cardiac valves, aortic arch vessels, and coronary vessels. *Dev Dyn* **222**, 89-100.

Tsuji, T., Okada, F., Yamaguchi, K. and Nakamura, T. (1990). Molecular cloning of the large subunit of transforming growth factor type-β masking protein and expression of the mRNA in various rat tissues. *Proc Natl Acad Sci USA* **87**, 8835-8839.

Tsuruga, E., Yajima, T. and Irie, K. (2005). Microfibril-associated glycoprotein-1 and fibrillin-2 are associated with tropoelastin deposition in vitro. *Int J Biochem Cell Biol* **37**, 120-129.

Unsöld, C., Hyytiäinen, M., Bruckner, T. L. and Keski-Oja, J. (2001). Latent TGF-β binding protein LTBP-1 contains three potential extracellular matrix interacting domains. *J Cell Sci* **114,** 187-197

Uyeda, T., Takahashi, T., Eto, S., Sato, T., Xu, G., Kanezaki, R., Toki, T., Yonesaka, S. and Ito, E. (2004). Three novel mutations of the fibrillin-1 gene and ten single nucleotide polymorphisms of the fibrillin-3 gene in Marfan syndrome patients. *J Hum Genet* **49**, 404-407.

Vehviläinen, P., Hyytiäinen, M. and Keski-Oja, J. (2003). Latent TGF-β binding protein LTBP-2 mediates melanoma cell adhesion. *J Biol Chem* **278**, 24705-24713.

Verderio, E., Gaudry, C., Gross, S., Smith, C., Downes, S. and Griffin, M. (1999). Regulation of cell surface tissue transglutaminase: Effects on matrix storage of latent transforming growth factor-β binding protein-1. *J Histochem Cytochem* **47**, 1417-1432.

Vollbrandt, T., Tiedemann, K., El-Hallous, E., Lin, G., Brinckmann, J., John, H., Bätge, B., Notbohm, H. and Reinhardt, D. P. (2004). Consequences of cysteine mutations in calcium-binding epidermal growth factor modules of fibrillin-1. *J Biol Chem* **279**, 32924–32931.

Wallace, R., Streeten, B. W. and Hanna, R. (1991). Rotary shadowing of elastic system microfibrils in the ocular zonule, vitreous, and ligamentum nuchae. *Curr Eye Res* **10**, 99-109.

Weber, E., Rossi, A., Solito, R., Agliano, M., Sacchi, G. and Gerli, R. (2004). The pattern of fibrillin deposition correlates with microfibril-associated glycoprotein 1 (MAGP-1) expression in cultured blood and lymphatic endothelial cells. *Lymphology* **37**, 116-126.

Wiesmann, U. N. (2002). Disorders of lysosomal enzymes: General considerations. "Connective tissue and its heritable disorders" (ed. Royce, P. M. and Steinmann, B.), second edition, 585-626, Wiley-Liss Inc. New York.

Werneck, C. C., Trask, B. C., Broekelmann, T. J., Trask, T. M., Ritty, T. M., Segade, F. and Mecham, R. P. (2004). Identification of a major microfibril-associated glycoprotein-1-binding domain in fibrillin-2. *J Biol Chem* **279**, 23045-23051.

Werner, J. M., Knott, V., Handford, P. A., Campbell, I. D. and Downing, A. K. (2000). Backbone dynamics of a cbEGF domain pair in the presence of calcium. *J Mol Biol* **296**, 1065-1078.

Whiteman, P. and Handford, P. A. (2003). Defective secretion of recombinant fragments of fibrillin-1: implications of protein misfolding for the pathogenesis of Marfan syndrome and related disorders. *Hum Mol Genet* **12**, 727-37.

Wright, D. W., McDaniels, C. N. and Swasdison, S. (1994). Immunisation with undenatured bovine zonular fibrils results in monoclonal antibodies to fibrillin. *Matrix Biol* **14**, 41-49.

Wu, T. H. and Werb, Z. (2000). Matrix metalloproteinases effectors of development and normal physiology. *Genes and Development* **14**, 2123-2133.

Xu, T., Bianco, P., Fisher, L. W., Longenecker, G., Smith, E., Goldstein, S., Bonadio, J., Boskey, A., Heegaard, A.-M., Sommer, B. *et al.* (1998). Targeted disruption of the biglycan gene leads to an osteoporosis-like phenotype in mice. *Nat Genet* **20**, 78-82.

Yamaguchi, Y., Mann, K. and Ruoslahti, E. (1990). Negative regulation of TGF-β by the proteoglycan decorin. *Nature* **346**, 281-283.

Yamaguchi, N., Mayne, R. and Ninomiya, Y. (1991). The alpha 1 (VIII) collagen gene is homologous to the alpha 1 (X) collagen gene and contains a large exon encoding the entire triple helical and carboxyl-terminal non-triple helical domains of the alpha 1 (VIII) polypeptide. *J Biol Chem* **266**, 4508-4513.

Yanagisawa, H., Davis, E. C., Starcher, B. C., Ouchi, T., Yanagisawa, M., Richardson, J. A. and Olson, E. N. (2002). Fibulin-5 is an elastin-binding protein essential for elastic fibre development in vivo. *Nature* **415**, 168-171.

Yeh, H., Chow, M., Abrams, W. R., Fan, J., Foster, J., Mitchell, H., Muenke, M. and Rosenbloom, J. (1994). Structure of the human gene encoding the associated microfibrillar protein (MFAP1) and localization to chromosome 15q15-q21. *Genomics* **23**, 443-449.

Yin, W., Smiley, E., Germiller, J., Mecham, R. P., Florer, J. B., Wenstrup, R. J. and Bonadio, J. (1995). Isolation of a Novel Latent Transforming Growth Factor-β Binding Protein Gene (LTBP-3). *J Biol Chem* **270**, 10147-10160.

Young, M. F., Bi, Y., Ameye, L. and Chen, X. D. (2002). Biglycan knockout mice: new models for musculoskeletal diseases. *Glycoconj J* **19**, 257-262.

Yu, Q. and Stamenkovic, I. (2000). Cell surface-localised matrix metalloproteinase-9 proteolytically activates TGF-β and promotes tumour invasion and angiogenesis. *Genes Dev* **14**, 163-176.

Yuan, X., Downing, A. K., Knott, V. and Handford, P. A. (1997). Solution structure of the transforming growth factor β-binding protein-like module, a domain associated with matrix fibrils. *EMBO J* **16**, 6659-6666.

Yurchenco, P. D. and Schittny, J. C. (1990). Molecular architecture of basement membranes. *Faseb J.* **4**, 1577-1590.

Zacchigna, L., Vecchione, C., Notte, A., Cordenonsi, M., Dupont, S., Maretto, S., Cifelli, G., Ferrari, A., Maffei, A., Fabbro, C. *et al.* (2006). Emilin1 links TGF-β maturation to blood pressure homeostasis. *Cell* **124**, 929-942.

Zanetti, M., Braghetta, P., Sabatelli, P., Mura, I., Doliana, R., Colombatti, A., Volpin, D., Bonaldo, P. and Bressan, G. M. (2004). EMILIN-1 deficiency induces elastogenesis and vascular cell defects. *Mol Cell Biol* **24**, 638-650.

Zhang, H., Apfelroth, S. D., Hu, W., Davis, E. C., Sanguineti, C., Bonadio, J., Mecham, R. P. and Ramirez, F. (1994). Structure and expression of fibrillin-2, a novel microfibrillar component preferentially located in elastic matrices. *J Cell Biol* **124**, 855-863.

Zhang, H., Hu, W. and Ramirez, F. (1995). Developmental expression of fibrillin genes suggests heterogeneity of extracellular microfibrils. *J Cell Biol* **129**, 1165-1176.

Zhao, Z., Lee, C. C., Jiralerspong, S., Juyal, R. C., Lu, F., Baldini, A., Greenberg, F., Caskey, C. T. and Patel, P. I. (1995). The gene for a human microfibril-associated glycoprotein is commonly deleted in Smith-Magenis syndrome patients. *Hum Mol Genet* **4**, 589-597.

Zimmermann, D. R., Dours-Zimmermann, M. T., Schubert, M. and Bruckner-Tuderman, L. (1994). Versican is expressed in the proliferating zone in the epidermis and in association with the elastic network of the dermis. *J Cell Biol* **124**, 817-825.

13 Appendices

Appendix A

Primer sequences

The following table indicates the primer sequences used for cloning recombinant LTBP proteins. Primer sequences (written 5'-3') are based upon published sequence data from Genbank™ with accession numbers and base numbers as indicated.

	Sequence (5'-3')	Bases	Genbank™ accession code
M13F	GTTTTCCCAGTCACGAC		
M13R	CAGGAAACAGCTATGAC		
pCEPF	AGAGCTCGTTTAGTGAACCG	500-481	
pCEPR	GTGGTTTGACCAAACTCATC	367-387	
LTBP-2mRNA	TCAGGGCCCAGAACAGATTG	6373-6392	NM_000428
LTBP-2F	CGCGCAGCCCTCGTTCCG	212-229	NM_000428
LTBP-2R	CAGTCCAAGCTTCCCCAAATCCT	6331-6307	NM_000428
BM40F	GCCCGGAGAGCGCGCTCTG	5' UTR	Y00755
BM40R	CCACCACCTCTGTCTCATCAGGC	128-106	Y00755
BM40/LTBP-2F	TGGCCGGGAGGGCTCTGGCAGCCCCAAGCTTCCAAAGGGACCCCGTAGGGAG		
BM40/LTBP-2R	CTCCCTACGGGGTCCCTTTGGAAGCTTGGGGCTGCCAGAGCCCTCCCGGCCA		
LTBP-2R/His	CTAATGGTGATGGTGATGGTGAAGCTTGGCAGTGCAGTGGGGGGG		
LTBP-2CT(H)F	CCCCAAGCTTGAACAGCACCAGCAGCACGG	5089-5107	NM_000428
LTBP-2CT(H)R	TGGTGATGGTGAAGCTTGGCAGTGC	5847-5837	NM_000428
LTBP-2CT(H)EKF	CTGCCAAGCTTGATGACGATGACAAGGGACACCATCACCATCACCATTAG		
LTBP-2CT(H)EKR	CTAATGGTGATGGTGATGGTGTCCCTTGTCATCGTCATCAAGCTTGGCAG		
LTBP-1CT(H)F	GTATAAGCTTAGCTGAGTCAAACGAACAAA	3681-3700	NM_000627
LTBP-1CT(H)R	GTGAAGCTTCTCCAGGTCACTGTCTTTCTC	4317-4296	NM_000627
LTBP-1CT(H)gateF	GGGGACAAGTTTGTACAAAAAAGCAGGCTAAGCTTAGCTGAGTCAAACGAACAAA		
LTBP-1CT(H)gateR	GGGGACCACTTTGTACAAGAAAGCTGGGTAAGCTTCTCCAGGTCACTGTCTTTCTC		

Appendix B

Solution formulations

50x TAE
2M Tris base
57.1mL glacial acetic acid
0.1M $Na_2EDTA.2H_2O$
Adjust to 1L volume using ddH_2O

6x load buffer for DNA gels
5mL glyercol
2mL 50x TAE buffer (see above)
2mL Bromophenol Blue (saturated) (see below)
Adjust volume to 10mL using ddH_2O, aliquot and store at -20°C

Saturated Bromophenol Blue
0.1g Bromophenol Blue
Dissolve in 20 mL ddH_2O by stirring overnight at 37°C

Luria broth
10g Bacto-tryptone (BD Biosciences, Sparks, MD)
5g Bacto-yeast extract (BD Biosciences, Sparks, MD)
86mM NaCl
Dissolve in 1L ddH_2O, adjust pH to 7.5 with NaOH and autoclave to sterilise. For LB plates, include 15g bacto-agar (BD, Sparks, MD) prior to autoclaving. Allow solutions to cool to 55°C prior to adding ampicillin

Soc medium
2g bacto-tryptone
0.5g bacto yeast extract
10mM NaCl
2.5mM KCl
Dissolve in 100mL ddH_2O, autoclave and cool to room temperature. Add 20mM Mg^{2+} (1mL of 2M Mg^{2+} stock containing 1M $MgCl_2$ and 1M $MgSO_4$) and 20mM glucose. Filter through 0.2µm filter to sterilise store at room temperature in 25-50mL aliquots.

Dulbecco's Phosphate Buffered Saline (PBS)
Without Ca/Mg

137mM NaCl
2.7 mM KCl
3.2mM $Na_2HPO_4.12H_2O$
1.5mM KH_2PO_4
Dissolve in ddH_2O, adjust pH to 7.4 with HCl and filter sterilise using peristaltic pump and 0.2 µm bell filter, store at room temperature

8x Phosphate Buffer pH 7.4
80mM $Na_2HPO_4.12H_2O$
80mM $NaH_2PO_4.2H_2O$
4M NaCl
Dissolve in ddH_2O, adjust pH to 7.4 with HCl and filter through a 0.2µm bell filter

2M Imidazole pH 7.4
2M imidazole
Dissolve in ddH_2O, adjust pH to 7.4 with HCl and filter through a 0.2µm bell filter

0.1M $NiSO_4$ (nickel sulphate)
0.1M $NiSO_4.6H_2O$
Dissolve in ddH_2O and filter through a 0.2µm bell filter

500mM Imidazole
6.25mL 8x PO_4 buffer
12.5mL 2M imidazole buffer
Adjust to 50mL volume using ddH_2O

10mM Imidazole
6.25mL 8x PO_4 buffer
0.25mL 2M imidazole buffer
Adjust to 50mL volume using ddH_2O

Tris Buffered Saline (TBS)
20mM Tris
0.13M NaCl
0.005% (w/v) Thimerosal
Dissolve in ddH_2O, adjust pH to 7.4 with HCl and autoclave if sterile solution required

TBS/0.5M NaCl (sodium chloride)
20mM Tris
0.5M NaCl
0.005% (w/v) Thimerosal
Dissolve in ddH_2O, adjust pH to 7.4 with HCl and autoclave if sterile solution required

Sample Loading Buffer
10mL Glycerol *
25mL Stacking gel buffer (see below)
2M Urea
20mL of 10% (w/v) SDS solution
20mg phenylmethylsulphonyl fluoride (PMSF) (dissolved in 250µl of ethanol-add dropwise) (Sigma-Aldrich, St Louis, MO)
5mL Bromophenol Blue (saturated) (see above)
* Add glycerol last, dissolve in 100mL ddH_2O, stir until dissolved, aliquot and store at –20°C.

Stacking Gel Buffer
250mM Tris
7mM SDS
Dissolve in ddH_2O, adjust pH to 6.8 with HCl

Separating Gel Buffer
750mM Tris
7mM SDS
Dissolve in ddH_2O, adjust pH to 8.8 with HCl

Stock 30% Acrylamide Solution
4.22M (30%) acrylamide
52mM (0.8%) Bis-acrylamide
(N-N,Methylenebisacrylamide)
Dissolve in ddH_2O, filter using whatman paper, store in a dark bottle at 4°C

Seperating Gel
25mL Separating gel buffer
mL Stock 30 %acrylamide solution (amount depends on the strength of the separating gel, for example 20mL used for 12% SDS-PAGE)
10mg Ammonium persulphate
22.5µL TEMED (Sigma-Aldrich, St. Louis, MO)
Dissolve in ddH_2O to total volume of 50mL, the ammonium persulphate and TEMED should only be added just before gels are to be set

3% Stacking Gel
12.5mL Stacking Gel Buffer
2.5mL Stock acrylamide solution
18.8mg Ammonium Persulphate
11µL TEMED
Dissolve in ddH_2O to total volume of 25mL, the ammonium persulphate and TEMED should only be added just before gels are to be set

Chamber Buffer
25mM Tris
192mM Glycine
3.5mM SDS
Dissolve in ddH_2O, do not pH

Coomassie Brilliant Blue R-250
Dye content of Coomassie Blue should be ~ 50%

0.3% (w/v) Coomassie brilliant Blue R-250
45% (v/v) Methanol
9% (v/v) Acetic Acid.
Dissolve in ddH_2O, stir solution well, filter using Whatman paper before use

Destain 40% Methanol
40% (v/v) Methanol
7% (v/v) Acetic Acid
Dissolve in ddH_2O

Destain 7.5% Methanol
7.5% (v/v) Methanol
7% (v/v) Acetic Acid
Dissolve in ddH_2O

Immunoblot chamber buffer
6.23mM Tris
47.56mM Glycine
Dissolve in ddH_2O, prepare this solution on the day of the western blot

Tris/Tween-20/Triton X-100 (TTX)
20mM Tris
500mM NaCl
0.05% (v/v) Tween 20
0.2% (v/v) Triton X-100
0.005% Thimerosal
Dissolve Tris, NaCl & Thimerosal in dd H_20, then add tween 20 and triton X-100, adjust pH to 7.5

TE buffer
10mM Tris-HCl
1mM EDTA
Dissolve in ddH_2O, adjust pH to 8.0 using NaOH

Substrate Buffer
100mM Tris
100mM NaCl
50mM $MgCl_2$ (molecular weight of 203.3)
Dissolve in ddH_2O, adjust pH to 9.5 with HCl

Nitro Blue Tetrazolium (NBT) substrate (Sigma)
50 mg NBT
0.3mL H_2O
0.7 mL DMF (N, N-Dimethylformamide)
Aliquot and store at –20°C

5-Bromo-4-Chloro-3-indolyl -phosphate (BCIP) substrate (Sigma)
25mg BCIP
0.5mL H_2O
0.5 mL DMF (N, N-Dimethylformamide) * Toxic use in fumehood
Aliquot and store at –20°C

Colour Solution for revealing Western blot
10mL Substrate Buffer
100µL BCIP
100µL NBT
Mix and use immediately

Phosphate buffered saline (PBS)
20mM $NaH_2PO_42H_2O$
0.13M NaCl
0.005% (w/v) thimerosal
Dissolve in ddH_2O, adjust pH to 7.4 with NaOH

Sodium phosphate buffer
20mM sodium dihydrogen orthophosphate
Dissolve in ddH_2O, adjust pH to 7.2 with acetic acid

PBS/EDTA
137mM NaCl
2.7mM KCl
1.8mM KH_2PO_4
4mM Na_2HPO_4
0.2mL of 500mM EDTA solution (pH8.0)
Dissolve in ddH_2O, adjust pH to 7.4 with HCl and degas prior to use

Sodium acetate
0.1M CH_3COONa
Dissolve in ddH_2O, adjust pH to 4.5 with acetic acid and degas prior to use

Glycine
0.2M glycine
Dissolve in ddH_2O, adjust pH to 4.5 with HCl

Tris base
2M tris
Dissolve in ddH_2O, do not pH

NaCl
0.15M NaCl
0.005% (w/v) thimerosal
Dissolve in ddH_2O, do not pH

Appendix C

Antibody concentrations

Antibody concentrations for various experiments conducted are listed within this table. Concentrations for each antibody are indicated as working dilutions from stock antibody solution and are specified for western blots, ELISAs/solid phase assays and tissue section immunofluorescence.

Antigen	Antibody		Concentration for blot	Concentration for ELISA	Concentration for immuno-fluorescence
his_6-tag	**Tetrahis** at 100µg/mL (Qiagen)	Mouse ascites monoclonal	1:1000	1:2000	
LTBP-2	**FLP-E** (Gibson *et al*. 1995)	Rabbit polyclonal	1:10	1:20	
LTBP-2	**LTBP-2C** (affinity purified at 500µg/mL)	Rabbit polyclonal	1:500	1:5000-1:10000	Affinity purified used at 10µg/mL Serum used at 1:50
LTBP-2	**L9F** (Gibson *et al*. 1995)	Rabbit polyclonal	1:200	1:250	
Fibrillin-1	**MAB2502**-Fib1(H)NT 1mg/mL (Chemicon)	Mouse ascites monoclonal	1:2000	1:2000-1:5000	1:200
Fibrillin-1	**MAB1919**-Fib1N(H) 2mg/mL (Chemicon)	Mouse ascites monoclonal	1:2000	1:2000	1:400
Fibrillin-1	**MAB2499**-Fib1(H)CT 1mg/mL (Chemicon)	Mouse ascites monoclonal	1:2000		
Fibrillin-1	**Fib1A**-Fib1(H)NT	Mouse polyclonal	1:100	1:200	1:10
Fibrillin-2	**m16E12**-Fib2NT(H)	Mouse cell culture monoclonal	1:100	1:400	
Fibrillin-2	**Fib2C**-Fib2NT(H)	Rabbit polyclonal	1:100	1:200	
Collagen-IV	Col-IV rabbit 29 (**r29**)	Rabbit polyclonal	1:50	1:500	

Antigen	Antibody		Concentration for blot	Concentration for ELISA	Concentration for immuno-fluorescence
LTBP-1	**MAB388**-LTBP-1 500µg:mL (RnD systems)	Mouse ascites monoclonal	1:250	1:6000	1:50
MAGP-1	MAGP-1 rabbit 18 (**r18**)	Rabbit polyclonal		1:1000	
MAGP-2	MAGP-2 rabbit 49 (**r49**)	Rabbit polyclonal		1:500	
	Goat anti-rabbit conjugated to alkaline phosphatase or horseradish peroxidase (Bio-Rad)	Goat secondary	1:2000 (or 1:5000 for detecting 6His-specific antibodies)	1:2000	
	Goat anti-mouse conjugated to alkaline phosphatase or horseradish peroxidase (Bio-Rad)	Goat secondary	1:2000 (or 1:5000 for detecting 6His-specific antibodies)	1:2000	
	FITC 1.5mg/mL (Jackson Immuno-research)	Donkey secondary			1:25
	Alexa488 2mg/mL (Invitrogen)	Donkey secondary			1:25
	Cy5 1.5mg/mL (Jackson Immuno-research)	Donkey secondary			1:25

Appendix D

Amino acids changes within recombinant sequences

Amino acids introduced to the published human LTBP-2 sequence (Genbank™ accession number NM_000428) for the purposes of recombinant expression are indicated as follows. The LTBP-2 signal sequence (marked in red) was altered to that of BM-40 (marked in green). The remainder of the protein sequence was conserved (with exceptions listed below). Furthermore, glutamic acid (E) was replaced with leucine (L) for insertion of the *Hin*dIII restriction site (marked in blue). 6 histidine residues (marked in purple) were also added for protein purification.

```
                      1                                                  50
LTBP-2 NM_000428      MRPRTKARSPGRALRNPWRGFLPLTLALFVGAGHAQRDPVGRYEPAGGDAN.....
recombinant LTBP-2                  MRAWIFFLLCLAGRALAAPSFQRDPVGRYEPAGGDAN.....

.....sequence conserved as published.....
.....sequence conserved as published.....

                           1780                                       1821
LTBP-2 NM_000428      .....NGPAVLCVHGYCENTEGSYRCHCSPGYVAEAGPPHCTAKE*
recombinant LTBP-2    .....NGPAVLCVHGYCENTEGSYRCHCSPGYVAEAGPPHCTAKLHHHHHH*

Amino acid (aa) deviations from published sequence present in r-LTBP-2:
aa(439) P→L, aa(490) Q→P, aa(668) S→F, aa(1213) G→D

-------------------------------------------------------------------------
```

Published amino acid sequence was conserved during production of recombinant LTBP-1CT(H) and LTBP-2CT(H). Signal sequence BM-40 (marked in green) was added at the N-terminus and the glutamic acid (E) was changed into leucine (L) due to the introduction of the *Hin*dIII site (marked in blue) within r-LTBP-2CT(H). The enterokinase recognition site (marked in pink) and 6 histidine residues (marked in purple) were introduced to allow for protease digestion and protein purification.

```
                                    1183                               1212
LTBP-1 NM_000627                      AESNEQIEETDVYQDLCWEHLSDEYVCSRP.....
r-LTBP-1CT(H)         MRAWIFFLLCLAGRALAAPSLAESNEQIEETDVYQDLCWEHLSDEYVCSRP.....

.....sequence conserved as published.....
.....sequence conserved as published.....

                     1356                                  1394
LTBP-1 NM_000627     .....NTDGSYKCLCLPGYVPSKPNYCTPLNTALNLEKDSDLE
r-LTBP-1CT(H)        .....NTDGSYKCLCLPGYVPSKPNYCTPLNTALNLEKDSDLEKLDDDDKGHHHHHH*

-------------------------------------------------------------------------

                                    1568                               1597
LTBP-2 NM_000428                      NSTSSTEDLPDHDIHMDICWKKVTNDVCSE.....
r-LTBP-2CT(H)         MRAWIFFLLCLAGRALAAPSFNSTSSTEDLPDHDIHMDICWKKVTNDVCSE.....

.....sequence conserved as published.....
.....sequence conserved as published.....

                     1782                                  1821
LTBP-2 NM_000428     .....NGPAVLCVHGYCENTEGSYRCHCSPGYVAEAGPPHCTAKE*
r-LTBP-2CT(H)        .....NGPAVLCVHGYCENTEGSYRCHCSPGYVAEAGPPHCTAKLDDDDKGHHHHHH*
```